

**Design and development of a community
based micro-hydro turbine system with
hydrogen energy storage to supply
electricity for off-grid rural areas in
Tanzania**

Thesis by

Daniel H. Ngoma

In Partial Fulfilment of the Requirements
for the Degree
Doctor of Philosophy



Supervisors:

Dr. Yaodong Wang

Professor Tony Roskilly

25th June 2020

Abstract

Micro-hydropower plants are used to supply electricity to the rural and off-grid areas of most developing countries like Tanzania. Their power capacity ranges from 5 kW to 100 kW which is equivalent to supply electricity from few households to several villages. The challenges that have influenced to undertake this research project are centred on the possibility of designing and developing a cost effective micro-hydro turbine system that can meet the dynamic load demand from the rural off-grid users and at the same time achieve high energy utilization efficiency with minimum energy losses using integrated renewable energy storage technologies such as hydrogen energy storage. The methods used in this research study are based on the field work and site data measurements together with power and energy determination as inputs to system design, modelling and simulation which will determine system characteristics. The results from data analysis show that the feasible water flow discharge for the micro-hydropower plant is $0.45 \text{ m}^3/\text{s}$ with the gross head of 25m which gives a turbine power of 79.5 kW and generator power of 75.5 kW as a power supply. On the other hand, results of the demand power analysis from the case study village shows the load profile has a low demand power of 8.42 kW and high demand power with peak power of 101.8 kW during the evening hours with the daily average energy of 1,114.38 kWh/d while the micro-hydropower can produce a maximum energy supply of 1,812 kWh/day. When supplying power to the load demand, the results show that the micro-hydro system produces excess power of up to 60 kW during low demand hours. In addition to this excess power production, it is also noted that the power supply is not sufficient to supply power during the peak hours of the day. So, in order to supply this peak power deficit, an energy storage system is introduced to store the produced excess electrical energy from the micro-hydro turbine system during the off-peak hours and then export it during the peak hours. Several energy storage options have been studied and analysed and based on the optimization results, the following system has been selected, i.e. micro-hydro turbine system with an electrolyser system and hydrogen fuelled internal combustion engine-generator system. The use of excess electricity to supply to the electrolyser system reduces the excess power to the dump loads to a minimum which results to an increase in the plant capacity factor and make the micro-hydro turbine system more energy efficient.

Acknowledgement

First and foremost, I would like to thank my Lord JESUS for giving me life and good health throughout my study time without any major problem.

Secondly, I would like to thank my wife Gladyce A. Banzi, and my children, Miriam D. Ngoma, Nuru D. Ngoma and Elisha D. Ngoma for their encouragement, support and comfort throughout my study time which gave me a peace of mind to focus more on my studies and research work.

Thirdly, I would like to acknowledge Newcastle University - UK and Commonwealth Scholarship Commission - UK for giving the opportunity to study this course and support financial which resulted to complete this energy research study at the Doctorate level within the required time.

Fourthly, I would like to thank my Supervisors Dr. Yaodong Wang and Professor Tony Roskilly for their valuable knowledge support and advice throughout my research study which made me understand most of the important research information for my work.

Also, I would like to thank my employer, Arusha Technical College - Tanzania for giving me the chance to come to the UK to study which will be beneficial to the college as well as the country in large.

Lastly but not least, I would like to thank all the people who have helped me in one way or another from my fellow research students and staffs at SWAN Centre for Energy Research and also to my colleagues and friends.

May almighty GOD bless you all.

List of Figures

Figure 1.1: The National Grid System in Tanzania	4
Figure 1.2: General layout - micro hydro system	6
Figure 1.3: Outline of the research plan	14
Figure 2.1: Dam hydro storage scheme	22
Figure 2.2: Pumped hydro storage system	23
Figure 2.3: Available electrical energy storage technologies	29
Figure 2.4: Impulse Pelton turbine	30
Figure 2.5: Reaction Francis turbine	30
Figure 2.6: Mini/micro hydro turbine selection based on head and discharge value	33
Figure 2.7: Basic components of a micro-hydropower	35
Figure 3.1: Waterwheel layout	39
Figure 3.2: Water energy conversion to produce hydro power	40
Figure 3.3: Penstock pipe layout	41
Figure 3.4: Concrete weir	43
Figure 3.5: Side intake.....	43
Figure 3.6: Side intake with rectangular orifice	44
Figure 3.7: Trapezoidal shape canal	45
Figure 3.8: Longitudinal section of a spillway	46
Figure 3.9: Cross-section of a spillway	46
Figure 3.10: Fore-bay layout	47
Figure 3.11: Penstock pipe layout	48
Figure 3.12: Turbine-generator power and control system layout	49
Figure 4.1: Power and energy demand determination.....	52
Figure 4.2: Actual power demand curve for a single household.....	59
Figure 4.3: Power demand curve for the village study community.....	65
Figure 5.1: Village location in relation to the distance from the site area.....	69
Figure 5.2: Landscape of Hhaynu micro-hydro power site location	70
Figure 5.3: Resource assessment methods	71
Figure 5.4: River flow layout and site location	72
Figure 5.5: Penstock profile with site elevation	73
Figure 5.6: Water flow velocity profile across the river	74
Figure 5.7: A propeller type current meter	75
Figure 5.8: Flow velocity measurements depths	76
Figure 5.9: River cross-sectional area shape showing length and width.....	76
Figure 5.10: Model river sub-sections along the river cross-section area.....	77
Figure 5.11: Hhaynu river cross-section area measurement	77
Figure 5.12: Hhaynu river depth measurement	78
Figure 5.13: Hhaynu river depth profile and width sub-sections at the measurement location	79
Figure 5.14: Hhaynu river flow velocity and area calculations.....	79

Figure 5.15: A linear scale for the travelling distance of the floating object	81
Figure 5.16: Pre-defined flow channel dimensions	81
Figure 5.17: Pre-defined structure for flow velocity measurement.....	82
Figure 5.18: Hhaynu river water flow capacity - measured and historical flowrate	87
Figure 5.19: Annual Hhaynu river hydrograph	88
Figure 5.20: Hhaynu river flow duration curve.....	91
Figure 5.21: Micro-hydro turbine design discharge flow duration curve	93
Figure 5.22: Daily power supply and demand for the local community (Study area)	98
Figure 5.23: Power potential in relation to water flow discharge and system efficiency	99
Figure 6.1: Schematic layout diagram of the hydro turbine-generator system	101
Figure 6.2: Layout diagram of the hydro turbine-generator and load system	102
Figure 6.3: Systems design configuration	108
Figure 6.4: Hydro-turbine system configuration without storage	110
Figure 6.5: Micro-hydropower supply to the load demand without energy storage	113
Figure 6.7: Micro-hydro turbine with battery energy storage	118
Figure 6.8: System configuration for the hydro turbine with battery storage	119
Figure 6.9: Hydro turbine with a battery storage system	121
Figure 6.10: Micro-hydro turbine with an electrolyser and hydrogen engine.....	124
Figure 6.11: Micro-hydro turbine with an electrolyser and hydrogen engine-generator.....	125
Figure 6.12: Working of PEM electrolysis	126
Figure 6.13: Efficiency range with design flow discharge for different turbines [8]	142
Figure 7.1: Schematic diagram of a micro-hydropower plant	145
Figure 7.2: Hydropower plants functional block modelling diagrams.....	145
Figure 7.3: Components layout of a hydro turbine system	146
Figure 7.4: Micro-hydro power plant block diagram	146
Figure 7.5: Water flow discharge through a penstock pipe.....	148
Figure 7.6: Step signal input $Q(s)$ to the signal response $H(s)$	152
Figure 7.7: Formulation of hydraulic head H equation based on Q and G during modelling.....	153
Figure 7.8: Block diagram of $Q(s)$ signal input to $P(s)$ signal output	154
Figure 7.9: Penstock hydraulic model with power gain and efficient factor.....	156
Figure 7.10: Block diagram transfer function of the linearized turbine model	157
Figure 7.11: Stead state turbine-penstock transfer function block diagram.....	157
Figure 7.12: Block diagram for stead state turbine-penstock of a linearized micro hydro turbine model	158
Figure 7.13: Block diagram representing a generator model	160
Figure 7.14: Generator swing equation block diagram	161
Figure 7.15: Generator speed (RPM) to frequency (Hz) block diagram.....	162

Figure 7.16: Block diagram representing the turbine, generator and control system layout.....	163
Figure 7.17: General block diagram for the turbine and governor system.....	164
Figure 7.18: Block diagram of the turbine-generator system transfer function ...	164
Figure 7.19: Hydraulic turbine control model block diagram.....	166
Figure 7.20: Block diagram of a typical mechanical governor	168
Figure 7.21: Hydraulic mechanical governor model.....	169
Figure 7.22: PID controller parameters	170
Figure 7.23: A typical PID control governor block diagram.....	171
Figure 7.24: Tuned PID control governor block diagram	172
Figure 7.25: A model block diagram of a Pseudo-Derivative Feedback (PDF) control.....	173
Figure 7.26: Tuned PDF control governor block diagram	174
Figure 7.27: Load control governor layout.....	175
Figure 7.28: Schematic Block diagram of Load Frequency Control.....	175
Figure 7.29: Schematic Block diagram of Load Frequency Control.....	176
Figure 7.30: Tuned PID control governor model (PI controller)	179
Figure 7.31A: Final model diagram (Input and controls).....	180
Figure 7.31B: Final model diagram (Turbine and generator)	181
Figure 7.32: Optimized system model layout.....	185
Figure 7.33: Optimised system design layout	186
Figure 8.1: Signal response for input discharge $Q(s)$ with the output pressure head $H(s)$	189
Figure 8.2: Signal response for the input pressure head $H(s)$ to the output discharge $Q(s)$	191
Figure 8.3: Signal response for the input discharge $Q(s)$ with the output Power $P(s)$	192
Figure 8.4: Step signal response for gate position $G(s)$ with turbine Power P_m , pressure change ΔH and flow discharge $Q(s)$	193
Figure 8.5: Changes in mechanical power (P_m) with gate valve position (G_v)...194	
Figure 8.6: Improved signal responses for the power output in relation to the gate position	195
Figure 8.7: Turbine power and gross head variation at different water flow rate	196
Figure 8.8: Mechanical and electrical power output stability response time	197
Figure 8.9: Generator speed response to rated load power capacity and no-load power	199
Figure 8.10: Generator speed stability response time at the two power supply steps	200
Figure 8.11: Generator power stability response time at the two power supply steps	201
Figure 8.12: Generator frequency stability response time at the two power supply steps	202
Figure 8.13: Speed variations at a different water flow rate and head values.....	203
Figure 8.14: Turbine-generator system control modes of operation	204

Figure 8.15: Mechanical governor action for the step signal input p.u. value	206
Figure 8.16: PD controller action for the step signal input p.u. value.....	208
Figure 8.17: PI control governor response for the micro hydro turbine system design	210
Figure 8.18: PDF control governor response with step input p.u. value.....	211
Figure 8.19: PDF control governor response for the micro-hydro turbine system	212
Figure 8.20: Relationship between the load power and dumping coefficient	214
Figure 8.21: Responses of consumer load power in relation to dumping power .	215
Figure 8.22: Un-tuned control governor's responses to input set value.....	216
Figure 8.23: Tuned control governor comparison based on response to step input value	217
Figure 8.24: Simulated values for the power and load demand	218
Figure 8.25: Hourly AC primary load demand – Simulated values	222
Figure 8.26: Dynamic values of generator frequency during a typical day	225
Figure 8.27: Response of damping coefficient with load Power changes.....	230
Figure 8.28: Optimized power supply and demand from micro-hydro and engine	231
Figure 8.29: Simulated generator characteristic at 100% and 50% rated Power capacity with 5.44% speed droop	232
Figure A.1: Micro-hydro power plants project cost estimation	266

List of Tables

Table 1.1: Energy Resources Potentials – Tanzania	2
Table 1.2: Electricity generation capacity – Tanzania	2
Table 2.1: Small hydropower plant sites in Tanzania	37
Table 3.1: Commonly used penstock materials.....	47
Table 4.1: Domestic electricity allocated for a single household – Lighting.....	54
(actual values).....	54
Table 4.2: Domestic electricity allocated for a single household – Power (actual values).....	55
Table 4.3: Power and energy demand values for each household (actual consumption)	56
Table 4.4: Power and energy demand data for the community (actual values).....	61
Table 4.5: Hourly Power demand and daily energy demand values for the case study area	64
Table 4.6: Current monthly energy demand in the research study village community	67
Table 5.1: Evaluation of site head locations.....	73
Table 5.2: Hhaynu river flow velocity and flow discharge measured values.....	84
Table 5.3: Historical and site measured monthly discharge values.....	85
Table 5.4: Percentage of exceedance with river flowrate.....	89
Table 5.5: Standardised % of exceedance with river flowrate	90
Table 5.6: Available flow discharge for micro-hydro turbine.....	92
Table 5.7: Standardised design flow discharge for the micro-hydro turbine	93
Table 5.8: Typical optimal water flow values for mini and micro hydropower schemes.....	94
Table 5.9: Design flow values for hydropower schemes	95
Table 5.10: Hydro power and hydro energy potential.....	96
Table 5.11: Optimisation of power potential with the availability of water flow discharge.....	97
Table 6.1: Daily hours of Power deficit	116
Table 6.2: Power surplus with available AC charging current and battery charge	120
Table 6.3: Micro-hydro turbine with a battery storage system	122
Table 6.4: Battery parameters and energy storage capacity (simulation results) .	122
Table 6.5: Annual energy production and consumption.....	126
Table 6.6: Modelling parameter values for PEM electrolyser	128
Table 6.7: Power capacity for the electrolyser (simulation results)	129
Table 6.8: Hydrogen gas production and consumption (simulation results).....	129
Table 6.9: Commercial selected Electrolysis unit	130
Table 6.10: Electrolyser detailed technical specification	131
Table 6.11: Hydrogen storage tank capacity	132
Table 6.12: Hydrogen engine-generator system capacity (simulation results)	134

Table 6.13: Fuel consumption rates.....	135
Table 6.14: Gas and liquid fuel comparison	136
Table 6.15: Main turbine design values	138
Table 6.16: Penstock pipe design values	139
Table 6.18: Generator power and speed at different rated capacity	143
Table 7.1: Validated parameters used in the modelling	183
Table 8.1: PID Controller gain values with permanent droop and response time	209
Table 8.2: Relationship between load power, dumping coefficient and stability response	213
Table 8.3: Static simulations results at rated capacity/Full load condition	226
Table 8.4: Static simulations results at rated capacity/Full load condition	226
Table 8.5: Static simulations results at no load condition	228
Table 8.6: Dynamic simulations results at rated capacity/Full load condition.....	229
Table A.1: Summary of total capital cost.....	262
Table A.2: Revenue from hydrogen and oxygen production	264
Table A.3: Proposed tariff	264
Table A.4: Total annual costs	265
Table A.5: Cost-benefit analysis results	267
Table A.6: Sources of Finance	269

List of symbols

<i>Symbol</i>	Unit	Description	<i>Symbol</i>	Unit	Description
A	m ²	Area	$E_{D(monthly\ avg)}$	kWh	Monthly average energy demand
A_p	m ²	Area of penstock	$E_{D(monthly\ domestic)}$	kWh	Monthly domestic energy demand
A_T	kNm	Acceleration torque	$E_{D(daily\ domestic)}$	kWh	Daily domestic energy demand
A_{site}	m ²	Site area	$E_{D(deficit)}$	kWh	Energy demand deficit
$A_{catchment}$	m ²	Catchment area	$E_{MHP(g)}$	kWh	Electrical energy generated by micro hydropower plant
A_g	pu	Hydro turbine gain	$E_{REC-IN(t)}$	kWh	Hourly energy input to rectifier
$ASBI$	pu	Abstraction sensitivity band - 1	$E_{REC-OUT(t)}$	kWh	Hourly energy input from rectifier
A	m/s	Pressure wave speed in penstock pipe	$E_{D(load)}$	kWh	Load energy demand from consumers
a_{ij}	pu	Turbine characteristics coefficients	$E_{HEG(g)}$	kWh	Hourly energy generated by hydrogen engine generator
$B_{storage(c)}$	Ah	Battery storage capacity	$E_{D(daily\ domestic)}$	kWh	Daily domestic energy demand
$B_{storage(c/u)}$	Ah	Per unit battery storage capacity in Ah	$E_{D(monthly\ domestic)}$	kWh	Monthly domestic energy demand
C_{BAT}	£	Capital cost of battery system	$E_{BAT(t)}$	kWh	Energy stored in battery at time t
C_F	£	Total fixed cost	$E_{BAT(t-1)}$	kWh	Energy stored in battery at time t-1
C_{rate}	C	Charging rate	E_T	kNm	Electrical torque
$C_f (MHP)$	%	Macro-hydropower capacity factor	f	Hz	Frequency
CRF	pu	Capital recovery factor for the system with expected discount rate	F_d	kN	Driving force
D, d	m	Diameter	$G_{P(S)}$	pu	Power system dynamics
D_t	pu	Turbine damping	$G_{T(S)}$	pu	Turbine system dynamics
DoD	%	Depth of discharge	$G_{C(S)}$	pu	Governor system dynamics
$E_{D(hourly)}$	kWh	Hourly energy demand	g_t	pu	Real gate opening
$E_{D(hourly\ avg)}$	kWh	Hourly average energy demand	G	m/s ²	Acceleration due to gravity
$E_{D(daily\ avg)}$	kWh	Daily average energy demand	G	pu	Ideal gate open

<i>Symbol</i>	<i>Unit</i>	<i>Description</i>	<i>Symbol</i>	<i>Unit</i>	<i>Description</i>
<i>HOMER</i>	-	Hybrid optimization model for electrical renewables	<i>p</i>	N/m ²	Pressure
<i>HoF</i>	pu	Hands of flow	<i>P_{MHP(g)}</i>	kW	Micro-hydro generator power
<i>H, h</i>	m	Head (height)	<i>P_{dump}</i>	kW	Dump power
<i>I_g</i>	MW.s /MVA	Inertia time constant of governor	<i>P_{MHP(t)}</i>	kW	Micro-hydro turbine power
<i>I_(AC)</i>	A	AC current	<i>P_m</i>	kW	Mechanical power
<i>I_(DC)</i>	A	DC current	<i>P_h</i>	kW	Hourly power
<i>ICE</i>	-	Internal combustion engine	<i>P_{rated}</i>	kW	Rated power of electrical items
<i>J</i>	s	Inertia time constant of generator	<i>P_{D(hourly)}</i>	kW	Hourly power demand
<i>K_p</i>	pu	Proportional gain	<i>P_{D(load)}</i>	kW	Consumer load demand power
<i>K_i</i>	pu	Integral gain	<i>P_L</i>	kW	Load power
<i>K_s</i>	pu	Gain of servo system	<i>P_{stored}</i>	kW	Stored power
<i>K_d</i>	pu	Derivative gain	<i>P_{HEG(g)}</i>	kW	Rated power output of hydrogen engine generator
<i>K_D</i>	pu	Dumping coefficient	<i>P_F</i>	pu	Power factor
<i>K_{Dt}</i>	pu	Turbine dumping coefficient	<i>P_{D(deficit)}</i>	kW	Power demand deficit
<i>K_{Dg}</i>	pu	Generator dumping coefficient	<i>P_{avg}</i>	kW	Average power
<i>K_{pd}</i>	pu	Pseudo-derivative dumping f	<i>P_{max}</i>	kW	Maximum power
<i>K_G</i>	pu	Servo gain	<i>P_{h(avg)}</i>	kW	Average hydraulic power
<i>K_s</i>	pu	Secondary control gain	<i>P_{MHP(g)} [surplus]</i>	kW	Micro-hydro generator surplus power
<i>L_p</i>	m	Length of penstock pipe	<i>P_{inv/conv}</i>	kW	Inverter or converter power
<i>M_{Tq}</i>	Nm	Mechanical torque	<i>P_{Dump.}</i>	kW	Dump power
<i>m_c</i>	pu	Manning coefficient	<i>P_{MHP(excess)}</i>	kW	Excess power from the micro-hydro
<i>m</i>	kg	Mass	<i>P_{MHP(dump)}</i>	kW	Dumped power from the micro-hydro
<i>N</i>	RPM	Rotational speed	<i>P_{HP}</i>	kW	Hydro power capacity
<i>n_p</i>	pu	Number of poles	<i>P_e</i>	kW	Electrical power
<i>N_L</i>	pu	Subscript for no-load values	<i>P_T</i>	kW	Total belt power
<i>N_{battery}</i>	pcs	Number of batteries	<i>P_{c/b}</i>	kW	Correction power per belt
<i>n</i>	pcs	Number of items	<i>P_F</i>	pu	Power factor
<i>N_s</i>	RPM	Specific speed	<i>P</i>	kW	Power

<i>Symbol</i>	<i>Unit</i>	<i>Description</i>	<i>Symbol</i>	<i>Unit</i>	<i>Description</i>
$P(t)$	kW/s	Power per second	U_{water}	m/s	Water flow velocity
pu	-	Per unit	$V_{battery}$	volts	Battery nominal battery
Q	m ³ /s	Flow discharge	V_0	volts	Phase output voltage
Q_D	m ³ /s	Design flow discharge	v	m ³ /s	Volume
Q_{site}	m ³ /s	Site flow discharge	ω	Rad/se c	Angular velocity of the generator
$Q_{catchment}$	m ³ /s	Catchment flow discharge	ω_r	Rad/se c	Rated angular velocity
R	Ω	Resistance	ω_{nl}	Rad/ sec	No load angular velocity
R_T	pu	Temporary/transient droop	Z_p	pu	Normalized hydraulic surge impedance of the penstock
R_P	pu	Permanent droop	ρ_{water}	Kg/m ³	Density of water
R_g	pu	Governor droop value	η	%	Efficiency
RPM	pu	Revolutions per minute	$\eta_{turbine}$	%	Micro-hydro turbine efficiency
SoC	%	State of charge	$\eta_{generator}$	%	Generator efficiency
T or t	s	Time	η_{CHG}	%	Battery charging efficiency
TF	pu	Transfer function	η_{DCHG}	%	Battery discharging efficiency
$T_{MHP(t)}$	kNm	Mechanical torque	η_{REC}	%	Efficiency of rectifier
T_{ep}	s	Elastic time constant of penstock	η_{cc}	%	Efficiency of charge controller
T_M	s	Mechanical starting time of turbine	η_{DEG}	%	Hydrogen engine generator efficiency
T_P	s	Pilot valve time constant	η_{INV}	%	Efficiency of an inverter
T_G	s	Gate servo time constant	ϕ	$\frac{A}{m^2}$	Current density
T_R	s	Reset time	σ	pu	Gain value
T_q	Nm	Torque	δ	pu	Rotor angle
T_W	s	Water starting time	$\lambda(x)$	pu	PEM water content
t_p	mm	Penstock thickness	τ_s	N/m ²	Shear stress
U	m/s	velocity	β	pu	Frequency response coefficient

Note: Some of the symbols and mathematical variables are not listed here and have been explained within the text or equations

Glossary

Name	Description
Alternating Current	An electric current changing regularly from one direction to the opposite
Ampere	The common unit of measurement of electrical current
Baseload	The minimum constant amount of load connected to the power system over a given time period eg. daily or monthly
Ballast	Thermal loads supplied by excess electrical power
Capacity	The amount of electric power delivered or required for which a generator or turbine is rated by the manufacturer
Capacity factor/Load factor	The ratio of actual energy produced per year to the theoretical maximum energy production when the system runs at full rated capacity all the year round
Current	A flow of electrons in an electrical conductor
Dam	A massive wall or structure built across a valley or river for storing water
De-silting tank	A small tank that is used to silt sand and debris
Direct current	Electric current going in one direction only
Distribution system	The portion of an electric system that is dedicated to delivering electric energy to an end user
Diversion weir	A concrete wall on the river that restrict water flow to create sufficient upstream depth for the water intake
Dump load	Excess power produced and directed to the in the ballast
Energy	The capacity of doing work as measured by the capability of doing work (P.E.) or the conversion of this capability to motion (P.E.)
Energy demand	Power consumed at a certainly period of time (kWh)
Environmental flow	The amount of water discharge which must be left in the river flow at the point of abstraction in order to support ecological activities
Flow discharge	Amount of volumetric water flow in a river
Flow duration curve	A graph that shows the percentage of time that the river flow discharge at a particular gauging station equals or exceeds certain values
Forebay tank	A water tank at the end of the canal for slowing down the incoming flow and settling out silt and gravel before the flow passes into the penstock
Generation (Electricity)	The process of producing electric energy by transforming other forms of energy or the amount of electric energy produced
Generator	Electrical power unit that converts mechanical energy into electrical energy

Name	Description
Head	The difference in elevation between upstream (headwater) and downstream water (tailwater) flow levels
Headrace	The channel that forms the inlet to the turbine
Hydroelectric power	Electric current produced from water power
Installed capacity	The total maximum power output in kW of the generating units in a hydropower plant
Kilowatt (kW)	Unit of electric power which is equal to 1,000 watts
Kilowatt-hour (kWh)	Unit of electrical energy which is equivalent to the electricity supplied by 1 kW working for 1 hour (1 kWh = 3,6000 Joules)
Kinetic energy	Energy which a moving body has due to its motion and it depend on its mass and the rate at which it is moving
Load (Electric)	The amount of electric power delivered or required at any specific point on system
Megawatt	A unit of power equal to one million watts
Peak load	The greatest amount of power given out or taken by a machine or power distribution system in a given time
Penstock	A steel pipe that carries under pressure water flow discharge from the forebay to the turbine unit
Power	Rate at which work is done by a mechanical force/electric current of a turbine/generator system
Power house	Building at which hydro turbine and generator system are installed and operated
Power transmission	The distance on which power output have been transmitted
Pumped-storage hydroelectric plant	A plant that usually generates electric energy during peak-load periods by using water previously pumped into an elevated storage reservoir during off-peak periods when excess generating capacity is available to do so
Rated capacity	The capacity at which the hydro turbine delivers a nominal power or it is a nameplate rating of the turbine power
Reservoir	The water storage structure that is used to store large amount of water for future use
Spillway	A controlled discharge access point for extra flow discharge which is directed back into the river
Tailrace	The channel that takes flow away from the turbine outlet
Trash-rack	A protective metal screen that prevents tree branches and trunks and other debris from entering and damaging the turbine unit
Turbine	A mechanical machine that convert the kinetic energy of falling water to produce rotational speed that produce mechanical power
Volt	The unit of electromotive force or potential difference that will cause a current of one ampere to flow through a conductor

List of papers

Published peer review papers

Part of my research work has been published in the following research journals:

(a) **First paper article:** Hhaynu micro hydropower scheme: Mbulu – Tanzania comparative river flow velocity and discharge measurement methods.

Journal: Flow Measurement and Instrumentation Volume 62, August 2018, Pages 135-142.

The published materials for this journal article is extracted from Chapter 5 content on resource assessment for the case study site which include flow discharge measurements and analysis.

(b) **Second paper article:** Determination of design discharge and environmental flow in micro-hydropower plants based on flow duration curve in small rivers: A case study of Hhaynu River – Mbulu, Tanzania.

Journal: International Journal of Advanced Scientific Technologies in Engineering and Management Sciences (IJASTEMS - ISSN: 2454 - 356X) Volume.3, Issue.11, November 2017.

The content of this journal article is based on results from Chapter 5, resource assessment for the case study site which include river hydrology and water flow measurement data.

(c) **Third paper article:** Feasibility study of un-tapped small hydropower potential sites in Tanzania.

Journal: International Journal of Scientific Research Engineering & Technology (IJSRET), ISSN 2278 – 0882 Volume 7, Issue 6, June 2018.

The published material on this journal article is not included in the thesis but it is worth mentioning because it highlights the research objectives in terms of power and energy potential available for small hydropower in Tanzania and also the gives an overview of the cost analysis for such kinds of projects as it has been analysed in the economic analysis.

(d) **Fourth paper article:** Crossflow Turbine Design Specifications for Hhaynu Micro-Hydropower Plant - Mbulu, Tanzania

Journal: Innovative Energy and Research - ISSN: 2576-1463, Volume 8, Issue 2, April 2019.

The content of this journal article is extracted from Chapter 6 on System design and specifically in Section 6.5.4: Micro-hydro turbine design calculations.

Un-published papers

The following articles are being extracted from my research work and are expected to be published before the end of this year 2020

Article 1 Title:

Comparative turbine governing methods for frequency control in micro-hydropower plant system. A case study of Hhaynu micro-hydropower plant in Tanzania

Article 2 Title:

Theoretical analysis of micro-hydropower technology for electricity generation. A case study of Hhaynu micro-hydropower plant in Tanzania

Article 3 Title:

Dynamic modelling and simulation of a micro-hydro turbine system with hydrogen fuelled internal combustion engine for supplying electricity to off-grid rural community. A case study of Hhaynu micro-hydropower plant in Tanzania

Article 4 Title:

Optimization model of a micro-hydro turbine power supply to consumer load demand for off-grid rural community. A case study of Hhaynu micro-hydropower plant in Tanzania

Article 5 Title:

Design and simulation of a micro-hydro turbine system for electricity supply and hydrogen production in off-grid rural community of Tanzania

Article 6 Title:

Design and simulation of PID controller for a micro-hydropower plant

Table of Contents

Abstract.....	ii
Acknowledgement.....	iv
List of Figures.....	vi
List of Tables	x
List of symbols.....	xii
Glossary	xvi
List of papers	xviii
Published peer review papers.....	xviii
Un-published papers.....	xix
Table of Contents	xx
Chapter 1 Introduction	1
1.1 Research background	1
1.1.1 Hydro power	3
1.1.2 Micro-hydro power.....	5
1.1.3 Value of the research project.....	8
1.1.4 Problem statement	9
1.2 Aim and objects of the study.....	10
1.3 Introduction to research contribution and methodology	10
1.3.1 Research study rationale.....	10
1.3.2 Outline of the methodology.....	12
1.3.3 Research questions	16
1.4 Contribution and outline of the thesis	16
Chapter 2 Literature review	20
2.1 Introduction.....	20
2.2 Hydropower.....	21
2.3 Types of hydropower schemes.....	22
2.3.1 Reservoir (Dam) hydro storage scheme (Impoundment)	22
2.3.2 Pumped hydro storage scheme	23
2.3.3 Run-of-river scheme	25
2.4 Micro-hydropower scheme	26
2.4.1 Integrated micro-hydropower schemes	27
2.4.2 Classification of mini/micro-hydro turbine system.....	29
2.5 Technical aspects of micro-hydropower schemes.....	31
2.5.1. Role of micro-hydropower in development	31
2.5.2 Choice of the micro-hydropower scheme.....	32
2.5.3 Basic components of a micro-hydropower.....	34

2.5.4 Misconception on micro-hydropower technology.....	35
2.5.5 Survey of similar micro-hydropower scheme	35
2.6 Summary	38
Chapter 3 Theory of hydropower.....	39
3.1 Introduction.....	39
3.2 Hydro-power technology	39
3.3 Parts of a hydropower system	42
3.3.1 Hydraulic system components.....	42
3.3.2 The power and control system components	48
3.4 Advantages of hydropower plants.....	49
3.5 Summary	50
Chapter 4 Demand analysis	51
4.1 Introduction.....	51
4.2 Methodology	51
4.2.1 Energy demand determination methods	52
4.3 Power and energy demand determination.....	53
4.3.1 Household power and energy demand determination	53
4.3.2 Total energy demand in the village community	60
4.4 Summary	68
Chapter 5 Resources assessment for the case study site.....	69
5.1 Introduction.....	69
5.2 Methodology	71
5.3 Field work and data measurements	71
5.4 Site head measurement.....	72
5.5 Water resource measurement methods.....	74
5.5.1 Floating object flow discharge measurement method.....	74
5.5.2 Current meter method.....	74
5.6 River cross-section area measurement.....	76
5.8 Flow velocity and discharge measurement results.....	80
5.8.1 Floating method flow velocity measurement results.....	80
5.8.2 Current meter flow velocity measurement results.....	82
5.8.3 Flow discharge determination	82
5.8.4 Validation of flow discharge measurement values.....	85
5.8.5 Importance and limitations of flow discharge measurement methods	88
5.8.6 Water flow discharge duration curve determination	89
5.8.7 The accuracy of flow discharge measurement methods.....	91
5.9 Water flow discharge determination for hydropower potential	92
5.9.1 River flow discharge optimization	94
5.10 Power and energy potential assessment	95
5.10.1 Micro-hydro power potential.....	95
5.10.2 Power potential and water flow discharge optimization	97

5.11 Summary	100
Chapter 6 System design	101
6.1 Introduction	101
6.2 Design methodology	102
6.2.1 Micro-hydropower system.....	102
6.2.2 Energy storage	103
6.3 System design optimization using HOMER	106
6.4 System design configuration	107
6.5.1 Micro-hydro turbine system without energy storage.....	108
6.5.2 Micro-hydro-turbine system with battery storage	114
6.5.3 Micro-hydro turbine system with hydrogen storage	123
6.5.4 Micro-hydro turbine design calculations.....	136
6.7 Summary	143
Chapter 7 Modelling.....	144
7.1 Introduction	144
7.2 Hydro Turbine System Modelling	144
7.2.1 Hydraulic Turbine dynamics	146
7.2.2 Hydraulic Turbine transfer function.....	147
7.2.3 Penstock Pipe and Turbine system	147
5.3 Generator and Load Power System.....	159
5.4.1 Optimization for hydro control governors.....	162
5.4.2 Hydraulic Turbine control governor.....	163
5.4.3 Hydraulic – Mechanical governor	167
7.4.4 Electro-hydraulic (<i>PID</i>) governor	169
7.4.5 Pseudo-Derivative Feedback (<i>PDF</i>) control governor.....	173
5.4.6 Load control governor	174
7.5 Hydro-Turbine and Generator System.....	177
7.6 Model validation	182
7.7 Model optimization	185
Chapter 8 Results and discussion.....	187
8.1 Operational variables	187
8.2 Turbine performance.....	189
8.3 Generator system.....	196
8.4 Control action.....	203
8.4.1 Mechanical control governor response.....	205
8.4.2 <i>PID</i> control governor response (<i>PD</i> controller)	207
8.4.3 <i>PDF</i> control governor response.....	210
8.4.4 Load control governor system	212
8.5 Control governor choice for the system design	215
8.6 Power supply and load demand optimization	217
8.6.1 AC primary load	220

8.6.2 Electrolyser system.....	233
8.7 Summary	234
Chapter 9 Conclusions and Recommendations for further work	235
9.1 Introduction	235
9.2 Summary of the findings and the resulting conclusions	235
9.3 Recommendations for further work	241
9.4 Contributions to the knowledge	242
References.....	245
Appendices.....	256
Appendix A: Economic analysis	256
Appendix B: Detail drawings.....	271
Appendix C: Optimized energy utilization block diagram	278
Appendix D: Electrolyser system.....	279
Appendix E: Hydrogen gas Internal Combustion Engine.....	282
Appendix F: Typical electrical equipment’s power capacities	285

Chapter 1 Introduction

1.1 Research background

Tanzania is among the least developed country in the world, ranking almost at the bottom of the list and its energy sector is mainly dominated by traditional biomass for domestic uses mainly for cooking and especially in the rural areas [1]. Despite its large population of around 55 million people, the country has very low electricity access rate and in 2014 the access was only 36% of the population on and about 11% in the rural areas. On the other hand, electricity connection among the population is also very low and estimated to be around 24% nationally (mainly urban and semi-urban areas) and on which only around 11% is available in rural areas [2]. The low in electricity access and the connection is also highlighted in energy consumption among the population and in 2014 Tanzania per capita electricity consumption was 104.79 kWh on average per year which is very low and less than half of the consumption of low-income countries [3]. This low electricity consumption is resulting to the large population of people especially in rural and off-grid areas to rely heavily on expensive and dangerous energy alternatives like disposable batteries, charcoal, firewood, sawdust, kerosene and diesel-powered generators. This resulted in most of the people spent much of their income on buying kerosene/candle lamps for lighting purposes and charcoal/firewood for cooking.

There have been several improvements in terms of economic development and in the last five years, Tanzania economy has grown tremendously as stipulated by the growth in GDP and population has also increased in recent years [4]. Despite the economic growth in urban and semi-urban areas that Tanzania has developed in the last five years, but still, most of the population are still residing in rural areas on which adequate energy services are also vital importance.

On the other hand, despite the country's struggling on the economic development, Tanzania has a lot of energy resources and energy potential which include Hydropower, Solar, Wind, Geothermal, Natural gas and Coal. To date, medium size hydroelectric power plants account for around 35% of the electricity generation in Tanzania despite the huge hydropower potential which is estimated at 4.7 GW on which only 12% have been developed so far [5]. On the other hand, when combining renewable energy and excluding medium capacity hydro, they account for only about 4.9% of generation capacity [6]. Grid generation capacity is dominated by thermal on which 32% from natural gas and 29% from

oil. Small renewable energy technologies contribute only a small proportion of around 1% despite its huge potential, especially in rural and off-grid areas as shown in Table 1.1 and Table 1.2 below.

Table 1.1: Energy Resources Potentials – Tanzania [7]

Source	Resource potential estimated	Status of development
Hydro	4.7 GW	12%
Small Hydropower	485 MW	2%
Coal	1.2 Billion Tonnes	304 Million Tonnes are proven
Natural Gas		57.25 TCF Discovered; 10.17 TCF Onshore and 47.13 TCF Offshore (deep sea)
Biomass	More than 500 MW	24.3 Million m ³ per annum
Solar	>200 Watt peak per square metre	Average installation 215 W/m ²
Bio-Fuels	Tanzania has crops for ethanol and bio-diesel	
Wind Power	Wind Speed of more than 8 m/s in some places	

Note: TCF = Trillion cubic feet

Table 1.2: Electricity generation capacity – Tanzania [7]

Source	TANESCO	IPP	EPP	SPP	Total	Per cent
Hydropower	553	-	-	-	553	35%
Small<10MW	8.8	-	-	4	12.8	0.8%
Oil (Jet-A1 and Diesel)	88.3	163	205	-	456.3	29%
Gas	252	249	-	-	501	32%
Biomass	-	-	-	27	27	1.7%
Imports	14	-	-	-	14	0.9%
Total (MW)	916	412	205	31	1564.1	100%
Per cent	59%	26%	13%	2%	100%	

Note: TANESCO = Tanzania Electricity Supply Company, IPP = Independent Power

Producer, EPP = Emergency Power Producer, SPP = Small Power Producer

Most of electricity generation capacity from Table 1.2 above is supplied to the national grid and is distributed throughout the country. But due to the geographical locations of the large power plants in Tanzania, some of the regions that are very far from the existing hydropower plant due to their remoteness on which there is no grid connection. By referring to the national grid map for Tanzania Figure 1.1 below, it is shown that the national grid is only

concentrated in the north-west, north-east and some parts of central and south-west regions of the country with no grid connection to the western regions.

1.1.1 Hydro power

In Tanzania, there are several renewable energy technologies that can be developed to provide affordable and reliable village level energy needs. Among the sustainable renewable energy technologies, hydro-electric power which comes from the power of the flowing water provides the cost-effective energy solution to most African countries where water resources are available. This flowing water results in the formation of kinetic energy which turns the blades of the hydraulic turbine to form mechanical power (turbine power) that rotates the generator to produce electrical power. These kinds of systems that use water power to run the turbines and turns the generators to produce electricity are called hydro-electric power plants [8].

There are six main classifications of hydropower plants in the world based on the available power capacity they produce [9]. The first class is the large-scale hydropower plants which have the power capacity of large than 500 MW and according to IEA they currently supply about 16% of the world electricity. There is no such plants capacity in Tanzania, but recently new plans are underway to construct such kind of plant capacity at Stiegler's Gorge which will have a power capacity of 2,100 MW.

When the power capacity of the hydropower plants is reduced to a medium power range of 100 MW to 500 MW, the types of power plants class are called medium scale hydropower plants. Tanzania is having two hydropower station in this category, Kihansi (180 MW) and Kidatu (204 MW) and use stored water from huge reservoirs of Rifiiji river.

The third class of the hydropower plant have the reduced value of the power capacity and they are called small scale hydropower plants. They have the power capacity range from 1 MW to 100 MW and Tanzania has four hydropower plants of this category, i.e. Mtera (80 MW), New Pangani (68 MW), Hale (21 MW) and Nyumba ya Mungu (8 MW) which uses stored water from reservoirs along the Ruaha and Pangani rivers [10]. Most of the large, medium and small-scale hydropower plants are connected to the national grid as shown in Figure 1.1 below.

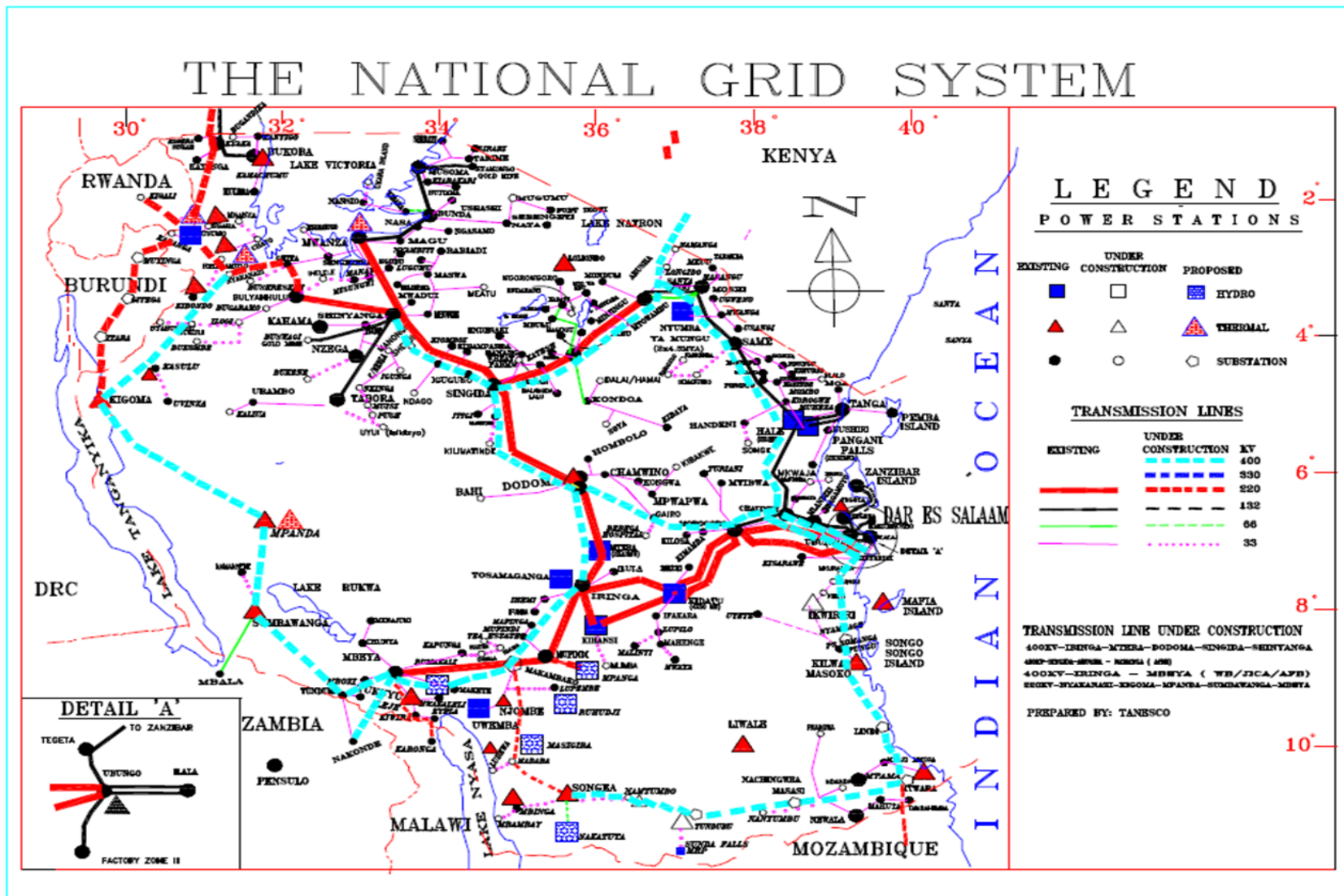


Figure 1.1: The National Grid System in Tanzania [2]

Despite the huge power production from these kind of power plants their developments require tremendous amount of land displacement and compensation, dam construction and flood control measures together with the detailed environmental impact assessments which increase the project investment costs and does not attract funds from private investors hence most of these kinds of hydropower plants are government funded and owned [11].

In the lower power capacity, there are two main classes of hydropower plants categories, i.e. the mini and micro class hydropower plants. Their power ranges from 100 kW to 1 MW for the mini hydropower plants and 5 kW to 100 kW for the micro hydropower plants. Most of these hydropower plants operate as run-of-river schemes which do not require the construction of the dam hence reduce the overall project investment cost. Also, in this category, the hydropower plants can operate in an islanding condition with the local grid hence they are suitable in off-grid and rural areas with no possibility of grid extension. Studies have shown that in mini and micro hydropower plants category have reduced investments costs compared to the large and medium plants and hence they are very attractive to private investors [12].

In a small rural and off-grid community with few villages, the type of hydropower plant that is suitable to supply electricity is the micro hydropower plant which utilizes a small amount of volumetric flow from the local river which also makes provision for environmental flow and water for irrigation activities and hence in this research study, this category of micro-hydropower plants have been studied and analysed based on the selected case study site information of Mbulu - Tanzania.

1.1.2 Micro-hydro power

Micro-hydropower energy resources are renewable energy technologies that have a large and sustainable potential for electricity and power generation in developing countries like Tanzania and especially in the rural village community areas where there is no electricity connection from the national grid [13]. The micro-hydro turbine technology can play a very important function by providing electrical power to the rural and off-grid areas in developing countries like Tanzania where there is no future for the grid extension. The technology is basically relying on a fast water flowing stream which has been channelled through a pipe (penstock) that is directed to a turbine which is connected to a generator and produce electricity as shown in Figure 1.2 below.

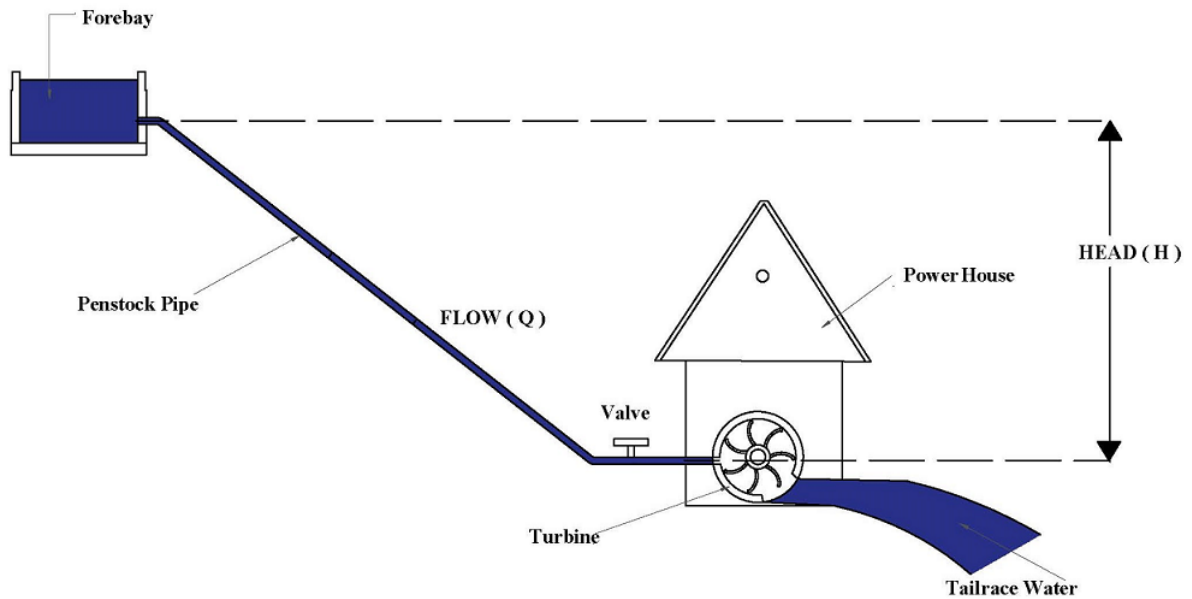


Figure 1.2: General layout - micro hydro system [14]

Micro-hydropower plants can generate electricity from 5kW to 100kW [15]. Tanzania has substantial potential for micro-hydropower development and the potential is estimated to be about 315MW, however, only around 25MW which is only about 8% of this hydro power potential that has been developed so far [16].

There are a couple of known reasons as to why the only small capacity of the hydropower potential has been developed in Tanzania. Some of the major obstacles adversely hindering exploitation of the micro-hydropower potential in Tanzania include; lack of or inadequate hydrological data (i.e. river flowrate data) due to few gauging stations for taking measurements and poor records management for the river flow data [17], higher initial cost of purchasing hydropower electro-mechanical equipment and specifically when importing from abroad due to import duties and taxes, improper and/or inadequate procedures of turbine type selection for local environment due to lack of knowledge and skills on hydropower technologies to suit the local environments, in-adequate assessment of power demand and lack of or in-adequate environmental and economic assessments of the local rivers [18].

The other important note is that a significant amount of water from small rivers in Tanzania is also utilized for other economic activities such as irrigation, domestic water supply and fishing activities which are mostly ignored in most new hydropower projects [19]. So, for developing a micro-hydropower plant many factors need to be considered not only the technology part but also the water usage in the local area. On the other hand, since most rural areas are very scattered and spread out geographically, it is not economical for grid

extension and in this case a better option is to establish the local mini-grid from the developed micro-hydro turbine system [20]. For places where there is adequate availability of water on streams and rivers, micro-hydropower is the best energy supply option compared to any other energy resources in terms of least cost of energy it produces [21]. It should also be noted that, as the need for reliable and sustainable electrical power in rural and off-grid areas increases, it is important to focus on the micro-hydropower technology development which has the advantage of reducing the technology problems while increasing the viability and as a cost-effective energy supply solutions in the rural and off-grid areas [22].

In Tanzania, there are many potential sites available for micro-hydropower development and most of them are in the rural areas of the country and have not been studied and assessed. One of the potential sites for the development of the micro-hydropower plant is in the Mbulu district in Manyara region, North-West of Tanzania. The site location is about 200 km from the Arusha region in Northern Tanzania in the remote rural and off-grid area of Mbulu. The local area has water resource from a river called Hhaynu which has potential to develop a micro-hydropower that will be able to supply electricity to the local off-grid villages.

The Hhaynu micro-hydropower potential site is used as a case study site for this research to demonstrate the local technology. So, the development and implementation of this micro-hydropower project in remote rural areas of Mbulu district using locally available renewable energy technologies will provide access to electricity from renewable energy for the poor and marginalized communities that including public services eg. Schools and health centres. The project site will also be used as a case study research site for the local technology development on the micro-hydro turbine and specifically when integrated with other renewable energy or energy storage.

Based on the site information obtained from the field visit and site assessment, the research study location is not connected to the national electrical grid and currently there is no electricity in the local villages, so people rely on other sources of energy like kerosene and firewood for cooking and lighting. Due to the lack of electricity in the project area, few economic activities are present which have reduced significantly the income generating activities for the community. The main economic activities in the area are smallholder agriculture and trade, which involve crop and livestock production. The farming activities grow food and cash crops which include maize, sorghum, potatoes, wheat, cassava, beans, oilseed crops, bananas, coffee etc.

The lack of reliable power sources in the villages made the local farmers send their post-harvest crops to the nearby towns which is costly due to the nature of transport and road networks. This in turn, increases the prices of processed crops like maize flour and rice in the local villages. In addition to that the local schools and health centres are not supplied with reliable electricity, as a result, the local quality of education has dropped significantly and also health care to children and pregnant women has been affected significantly as compared to the neighbouring nearby villages with access to electricity [23].

To address these problems, a reliable electricity source needs to be developed in the area that will supply a sustainable power to the local community and this is what this research project work will be addressing.

Based on the site information, there is a water source which has the potential to develop a small hydropower plant on which its capacity will depend on the amount of water available from the local river, but a question may arise to say, **“Is the anticipated power produced enough to supply all the hourly load demand in the area?”** Studies have shown that most of the load demand power fluctuates while the hydropower produces a constant power output at any given time. This phenomenon is resulting in un-balanced power between the power supply and the load demand which is observed in most small hydropower systems. To overcome this problem, an energy storage option needs to be developed which will consider innovative renewable energy storage like the current hydrogen energy storage.

The produced electrical power from the small hydropower plant will not only be used for the household lighting purposes and power in the local area, but also small and medium enterprises will be established which will increase the household's income through increased economic activities and add value to the local products by bringing about a change in life of the marginalized communities and public services [24]. Literature has shown that rural area with access to electricity has increased economic activities and significantly reduced poverty and mortality rate.

1.1.3 Value of the research project

The development of the micro hydropower plant in the project area will bring many benefits to the local community which includes the following:

- (a) Reduction in the use of traditional energy like firewood, charcoal, kerosene, fossil fuels and batteries which lead to cash savings for the households that are to purchase flashlight and rechargeable lights that are free from health adverse effects

- (b) Providing reliable electricity to the rural and remote areas which will improve access to radio, TV and mobile phone communication technologies in the beneficiary community areas and hence increase the living standard
- (c) Improving student's performance at the local schools by increasing night study hours and ability to make use of electronic equipment's to enhance teaching and demonstration eg. the use of computers, laptops and printers
- (d) Improving health services by using diagnostic medical equipment's like ultrasound, x-ray and medical refrigeration equipment's in the local health centre

1.1.4 Problem statement

The research study is expected to explore and develop a novel idea of integrating micro-hydropower technology with other renewable energy storage systems for the use in supplying electrical power to off-grid areas of Tanzania. The present research study is also expected to strengthen the energy policy, regulatory and institutional framework supporting the hydropower technologies development for use in rural and off-grid areas electrification projects in Tanzania [25].

In recent years Tanzania has emphasized Renewable Energy technology development which includes small hydropower technology development, by creating conducive environment like establishing the Rural Energy Agency- REA for managing rural energy funds and introducing credit facility (feed-in tariffs) for micro scale renewable energy projects. This could facilitate the local technology development of micro scale electricity production by using renewable and sustainable energy technologies like micro-hydropower [26].

But studies show that most micro-hydropower system installations are in off-grid rural and remote areas of the country and the available load demand power is relatively low due to low economic activities and low population density. This effect causes more power to be produced than it can be consumed on which an energy storage option may be a better solution. But due to the cost limitation on investment, most of the micro-hydropower plants prefer to use battery energy storage (cheaper option) for storing electrical energy that is produced. Based on the small power plants in operational, the commonly used storage batteries in micro-hydropower plants have limited storage capacity, charging and discharging efficiency and low service life, so when installed in these systems it leads to a large percentage of excess electrical energy to be dumped to the ballast as thermal loads which is wasted power during low demand hours of the day. So due to this effect, different

kinds of energy storage systems which are used today need to be studied and analysed in order to bridge the gap in the knowledge which lies on the optimization of the available excess electrical power produced from the micro-hydropower plant that will result to a minimum power loss to the dump loads and also the use of renewable energy storage system which is environmentally friendly like the use of hydrogen energy storage.

1.2 Aim and objects of the study

The aim of this research study is to design and develop a community based micro-hydro turbine system with renewable energy storage for electricity supply in off-grid rural areas of Tanzania.

The designed micro-hydropower system components for the research study has been fully optimized to the local environment that includes an energy storage option. The system will be developed with the available local expertise, machines/equipment, material and technology, thus ensure its sustainability and affordability to the local off-grid rural areas of Tanzania.

Based on the above-stated research study aim, the project objectives are outlined in the following:

- To assess and gather site information and river volumetric flow in the research study area in order to obtain the design data
- To design and develop a micro-hydro turbine system with increased energy utilization and minimum energy losses using an integrated energy storage system
- To analyse the project costs for the designed micro-hydro turbine system to determine the economic and environmental feasibility of the system

1.3 Introduction to research contribution and methodology

1.3.1 Research study rationale

The motivation for this research study is that there are no known widely publicized regional and local studies that have focused on the design and development of a micro-hydro turbine system which is integrated with renewable energy storage technologies. This has raised concern in developing a better optimised system design for the rural application. But why few studies have highlighted this concern? This is probably due to the fact that the development of micro-hydropower plants in Tanzania had faced a number of challenges and obstacles which among them include unfavourable conditions [27], while other factors include the in-adequate knowledge and technology to exploit the micro-hydropower

potential sites. Based on the hydro technology in Tanzania, there is no appropriate technology developed in the local area that has a scope of cost reduction and self-reliance [28].

Preliminary surveys and previous studies carried out in Tanzania indicated that almost all the micro-hydropower electro-mechanical turbine equipment's are imported from various countries outside Tanzania and especially from Asian and European countries. Most of the imported electro-mechanical turbine equipment's are expensive due to the additional cost on importation and the lack of local support services in terms of spare parts and maintenance. This has raised a concern to think about developing local turbine technology that is suitable to the local environment and especially in rural and off-grid areas. So in this case, there is a need for the development and optimization of micro-hydro turbine systems using locally available resources in terms of materials and technology in order to make a breakthrough in solving the scarcity of this renewable energy technology for electricity generation to the rural and off-grid communities. But does the locally developed turbine technology reduce the project costs? Theory shows that most of the costs are associated with importing the hydro turbines are due to taxes and import duties. On the other hand, and looking into another perspective, the theory also shows that integrating different renewable energy technologies or the use of energy storage will improve energy efficiency and system stability on the hydropower system. This has not been proven by small-scale and isolated renewable energy systems. So, in this case, there is a need to model the renewable energy storage system with different scenarios to see if there will be an improvement through energy optimisation. Looking into the local technology development there are very few research studies that have highlighted the locally manufactured hydro turbine components in Tanzania. Does this mean that no local technicians to do the job? From the studies, it is noted that more research needs to be conducted for the locally manufactured hydro turbine components to explore additional reasons. Few previous studies have also highlighted the area of parametric studies on the turbine components and the improvement in different design parameters for better system performance and stability of the locally designed and developed micro-hydro turbine system [29]. Those studies were based on the assessment done by a few technicians that were involved in the fabrication of turbine-related components.

So, based on the above information there is a need to develop a micro-hydro turbine system that will be applicable to local and rural off-grid areas. But will the hydro turbine design and development accommodate all the constraints based on the local rural setting? If not,

additional research needs to be conducted which will include more field tests that will give more realistic values for the locally designed turbine technology. On the other hand, the reduction in rainfall in recent years in Tanzania and the introduction of irrigation activities in farming have affected the hydropower sector in terms of water availability [30]. So, the possibility of integrating more than one renewable energy source could be a viable option which will result to energy efficient utilization of the renewable energy resources and sustainability on the technology and this is why integrating micro-hydro with energy storage technologies could be the better option. But looking into another perspective, a question may arise, i.e. will the new design consideration improve system stability in terms of energy balance as highlighted from the theory? This is due to the fluctuation of water flow in most local small rivers which in theory will lead to fluctuation in base power. To overcome this, the excess energy storage technology has been used to supply additional energy required during the peak hours. Therefore, integrating micro-hydropower with energy storage technology seems to be more energy efficient and cost-effective micro-hydropower system design for energy storage from a couple of hours to several days [31]. Several energy storage options are available with the micro-hydropower but the newly developed storage technology with hydrogen production from excess electrical energy seems to provide higher energy value and will be discussed in detail in the next Chapters.

1.3.2 Outline of the methodology

The research study has initially involved desk studies and pilot data collection from the case study site in Mbulu - Tanzania. Some of the methods that have been used include data and statistics compilation, literature review, review of power master plan, energy policy and rural electrification master plan on research study areas. Searching for study materials on the literature about renewable energy and energy demand at the research study areas. This also includes studying the latest information of current researches, potentials, technologies and government policies on the micro-hydro turbine system and especially with integration with other renewable energy sources.

In general, the following research methodologies have been used in this research study project:

(a) Extensive field study and data collection and analysis on the research and case study area which include site data measurement of the river hydrology (including historical data), water flows, elevation and topography, energy usage, energy demand and energy, supply

options, current practices, willingness to pay for electricity from the community, meetings with the villagers and village leaders together with the local council

(b) Extensive literature survey to review the previous and recent research related to the study area on small-scale hydropower technology specifically micro hydropower systems

(c) System design based on the field data and historical data obtained and analysed from the local research study area

(d) Developing a computational model and simulation results based on the system design parameters using MATLAB/Simulink and HOMER Energy modelling software.

Figure 1.3 summaries the research methodology plan with dotted lines showing research activities for year 1, year 2, year 3 and year 4 respectively. Detailed explanations for the methodologies have been explained in the coming sub-sections.

From Figure 1.3 below, the first part of the research activities was mostly focusing on extensive research literature review to gather information on previous research studies and other related information that are related to my research project in order to highlights the area to focus on and finding the research gap which will lead to the formulation of the research problem based on the current situation on the local area. In addition to the literature review, detailed data collection and analysis have also been conducted on the selected research study site in Tanzania. The selected site area is in a rural and off-grid location which is not connected to the national electrical grid and is also far from the town centres and their characteristics are composed of villages with small communal houses. Several wards and villages at the research site and location have been used for the case study because the villages have a common source of income and have no access to electricity. Site surveys for data collection as well as energy estimation have been conducted on the selected villages that the studies have been conducted. The study has also involved a field trip between June 2016 to August 2016 on which the research team travelled from Newcastle in the United Kingdom to Mbulu – Tanzania where the case study site is located. The site survey has been carried out using field observation, historical data collection and taking actual site measurements data as shown in Figure 1.3 below.

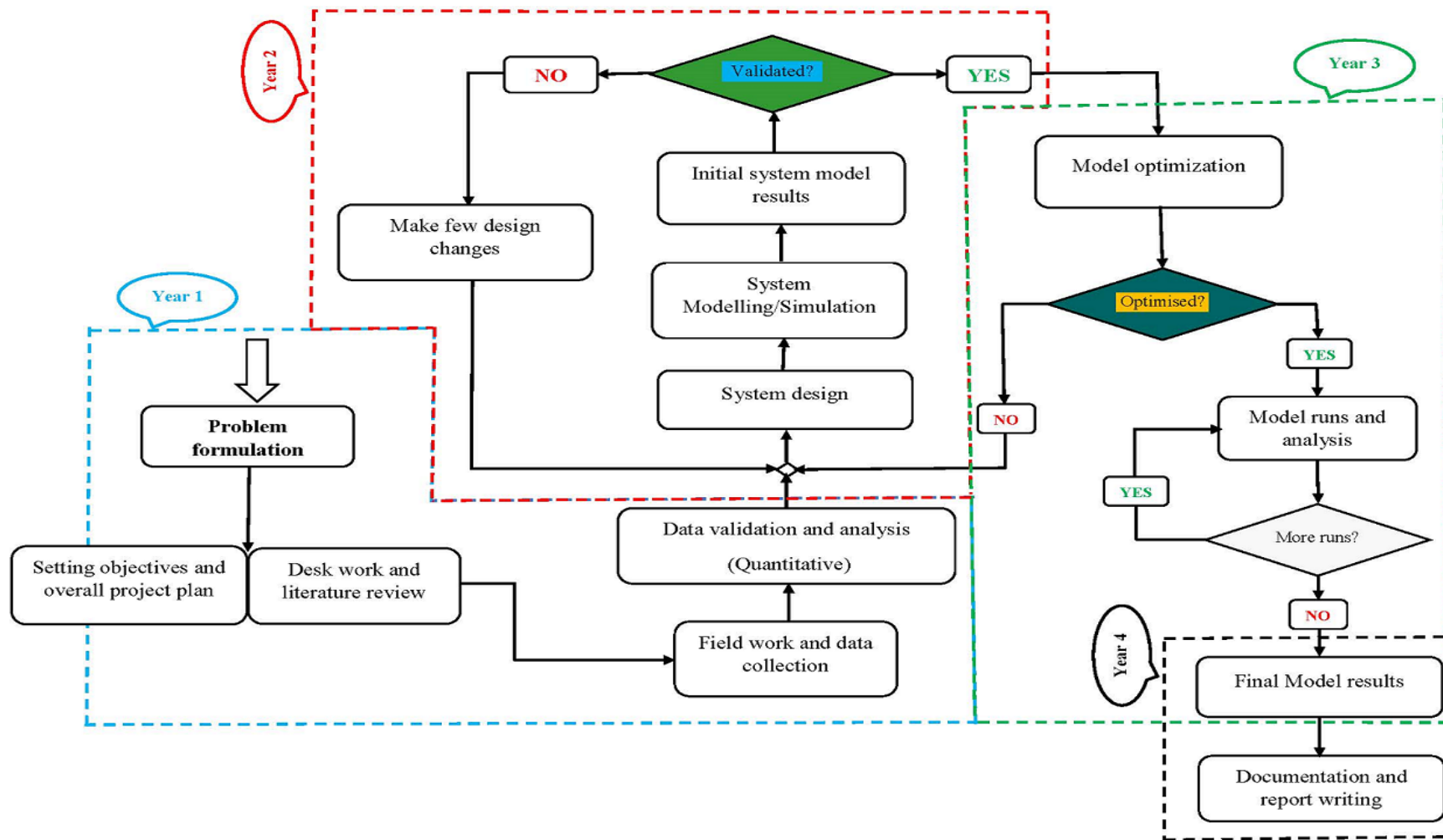


Figure 1.3: Outline of the research plan

The second part of the research activities was mainly based on the system design parameters and determined values which have been developed based on the data collected and analysed. Standard mathematical formula and scientific relations have been used and the obtained values have been used as inputs to the developed system model which are also called model parameters.

The site data have first been interpreted, analysed and then used for the system design model which have led to the development of system design options based on the model of integrated renewable energy systems that are suitable to the local environment and may be applicable to any similar potential site in Tanzania or in any other developing country.

The primary data collection was collected over a period of more than a year on which at the initial stage pilot study was conducted to highlight the viability of the collected data and make some adjustment. On the other hand, for the preliminary study, additional secondary data for the research study have been few but some information have been used from other similar research studies that have been conducted and documented in other parts of the country which include some other feasibility study reports that have been resourced for this research. There are several other similar micro-hydropower potential sites that their feasibility studies have also been conducted and their reports documented. However, most of the data in this research came from primary and secondary data that has been collected and gathered from the case study site and also data collected through meetings and first-hand observations and participating in village life to see the actual energy demand/usage has been practised. The process has also include gathering site historical information, analysing the data, system designing, modelling/simulation, validation and optimization of the developed system.

In the third part of the research activities, the developed turbine system model has been validated and optimized based on the input values from the system design parameters. Initial validated parameters have been based on the publications of previous similar research studies areas in other parts of the world. Also, several model parameters were selected, computed and compared to the values on the published research journals or using standard values. System optimisation, on the other hand, makes better use of system design parameters on which simulation results are compared with the design/selected values to fully utilize the system performance and increase its reliability.

The original idea of this research is based on the proposal to develop an actual micro-hydro turbine system with an integrated energy storage system that will be added if resources become available and project time does not exceed the specified duration. The system

installation and operation will be used to highlight the designed and modelled system performance and obtain the data that will be used to validate and optimise the designed, modelled and simulated system parameters. In order to fully validate the system parameters, the idea is to use the installed system performance information which will be analysed over a period of at least one year even after the end of the research study and the information will be used during and after the research study period to fine tune the system performance with the modelling/simulation during system design and this will lead to an improvement in the system design parameters and hence system optimization for the local environment.

1.3.3 Research questions

This research study of designing and development of the micro-hydropower project for Mbulu – Tanzania is focusing on answering the following research questions:

- (a) How the water flow velocity measurement methods for small rivers affects the accuracy volumetric flow of the river?
- (b) How can you maximise the volumetric flow to generate electricity under varying flow conditions and electricity demand?
- (c) Does the development of a micro hydro turbine system in rural and off-grid areas have the capability to supply enough electricity to the local villages?
- (d) How is it possible to integrate electricity storage into a micro-hydro turbine which is cost effective and sustainable?

1.4 Contribution and outline of the thesis

Many existing literatures and research reports have highlighted the usefulness of installed micro-hydro turbine system for supplying electricity to the rural and off-grid areas. There are different kinds of micro-hydro turbine technology but in terms of their configuration, both types are used to supply constant power to the load demand in the local community. Studies have shown that the load demand power is not constant and changes each hour of the day and this does not couple with the power supply capacity. This unbalancing power between the supply and the demand causes excess electrical power to be produced in the micro-hydro system.

To reduce this effect, most of the existing installations and research reports show that several micro-hydro turbine system designs include dump load components on which all the excess electrical power produced is diverted into these dump loads. Depending on the

available load demand power at the available time, the amount of dump load power capacity can be up to the rated power capacity of the micro-hydro turbine which is a lot of power wastage. Some of the literature also shows that few of the micro-hydro turbine system uses the excess electricity produced to be stored in battery storage systems which is the common method of energy storage used with the micro-hydropower system. But due to cost limitation, conversion efficiency and storage capacity, the battery energy storage systems do not provide enough capacity to the required load demand power and their installation does not reduce significantly or eliminate the availability of dump loads on the micro-hydropower systems.

Therefore this thesis is presenting a number of contributions to existing research in a form of detailed design and development of a micro-hydro turbine system for electricity supply that makes use of excess electrical power by optimizing power supply and demand in order to eliminate dump loads or reduce their power capacity to a minimum. Also, in this research work, computational modelling and simulation have been used to investigate the performance and operational characteristics of the designed micro-hydro turbine system in areas of the hydraulic, turbine, control, generator power and consumer load. A direct comparison to equivalent micro-hydro turbine systems has been presented, allowing an evaluation of potential advantages of the micro-hydro turbine system with zero or no dump load concept on a fundamental level.

The outline of the thesis report and the information on the contribution to the existing knowledge is presented in the following nine (9) Chapters of the research study together with several sub-sections that highlights the importance of this research work and is summarised below:

- Chapter 1, consists of an introductory and background information which is the description and an overview of the research topic in relation to the energy sector in Tanzania as well as energy resources availability. The chapter also includes the description of the problem statement, research project rationale, aim and objectives and the summary of the research methodology used. This Chapter introduces the research work by analysing the background information and sets the goals for doing the research work.
- Chapter 2 focuses on the literature review related to the research in this project. Several published journals and books have been studied and used as reference material in this

research project to highlight the available and current technology which helps to formulate research gaps in knowledge and develop research questions.

- Chapter 3 is explaining about the theory of hydropower from the early water power technologies to the current hydropower development. This include the science and formulation of power and energy equations from the falling/flowing water in a river for the hydropower technology.
- Chapter 4 presents the research activities related to fieldwork that involves energy demand assessment and analysis from the consumers which is the information for the site energy use that has been gathered from the research study villages.
- Chapter 5 is related to resource assessment for the case study site that involves water flow discharge measurements from the local river and assessment of other energy resources. The site information for energy demand and energy resources are the inputs for the system design and development and the information obtained has been used throughout the next Chapters of the thesis report.
- Based on the information obtained from the previous chapters, Chapter 6 consists of the system design and development based on the case study data and other related published information. Different system design options have been studied and analysed using different criteria and assumptions. In this Chapter also, the micro-hydro turbine system configuration has been designed to supply the base load power and is considered as the main system
- Chapter 7 presents the research activities related to modelling and system optimization of the micro-hydropower which consists of different block diagrams of hydraulic turbine model, control governor model and generator model with their tuning values on which the required equations for parameter determination have also been formulated. Different system model diagrams have been developed and evaluated based on the set values and operational condition.
- Chapter 8 is the simulation results and discussion. In this Chapter, the static and dynamic simulation results for the design turbine model has been presented and these simulation results and outcome have been discussed and analysed in detail. In the Chapter also, the system stability studies have been analysed and the results are compared with the standard known values.
- Chapter 9 is mostly focusing on the conclusion and recommendation for further work which is the summary of the main key information and findings that found in this

research project. It is also highlighting the recommendations for the future work to be done which include other system optimisation and more detailed modelling and simulation results under different dynamic conditions.

The designed micro-hydro turbine system has been evaluated in relation to the need for optimization of excess electrical power to provide efficient utilization of available power with increased energy utilization and reduce energy loss. This will allow the supply of available power to other renewable energy systems like the electrolyser system. The new design concept satisfies the requirement of a sustainable and cost effective micro-hydro turbine system configuration with no dumping power for supplying electricity to the rural and off-grid areas of Tanzania.

Chapter 2 Literature review

2.1 Introduction

Many research studies have been conducted in Africa based on different case studies for the sustainability of renewable energy technologies in off-grid rural areas. Barry et al (2011) [32] highlighted several factors to be considered in developing sustainable renewable energy technologies in Africa. Among them include the ability to do maintenance, proper site selection, government support and financial capacity. This demonstrates that the technical factors to be involved for rural off-grid electrification go beyond the selection of suitable technology as it was previously thought. This should also include the knowledge to properly manage the technology and be able to follow and interpret the local regulatory and environmental implications [33].

In comparison with the different power generation technologies for use in rural and off-grid areas, Kishore et al (2013) [34] provide useful overview when comparing different technologies like micro hydro, solar PV, biomass gasification, small wind and biodiesel. Based on his study, he pointed out that when choosing a particular technology, a multi-criteria decision aids should be used that is most appropriate with the local setting and his ideas has resulted to a positive outcome and also sustainability of most energy project in the African countries like Tanzania on which the issue of community involvement during the project development is very much considered.

Many studies on energy in recent years has been focusing on renewable energy and energy efficiency utilization [35]. This is due to the effect of climate change caused by the rise in temperature and pollution from the utilization of non-renewable energy sources. Renewable energy has a lot of advantages compared to conventional energy and fossil fuels which include reduction in environmental pollution and effects on climate change [36, 37]. This has been highlighted by many studies which pointed out the outcome of advancement in Renewable Energy Technology development made the supply of electricity to remote and rural areas more attractive [38]. In looking on the global development of renewable energy resources in recent years, European and American countries are leading in the utilization of the resource, followed by Asian countries and Australia [39]. African countries have the least renewable energy resource utilization and especially Sub-Saharan African countries where Tanzania is among them.

Several studies have shown that there is a large proportion of renewable energy resources in Africa, but only a small percentage of it has been utilized [40]. The study results shows that Africa have the largest renewable energy resources that have not been exploited and among them, hydropower potential has the largest proportion on which only 8% have been developed so far [41]. Although other renewable energy resources are also readily available in most African countries their exploitation, as well as the development, has been relatively low. Among the renewable energy resources utilization, hydropower related technology seems to exist for a quite long time, almost a century ago although the technology was very inefficiency to today's standards [42].

2.2 Hydropower

The Hydropower technology is the most reliable and cost-effective renewable energy generation technology to date [43]. The early developed hydropower technology was around 17 century and it was broadly used for activities related to milling and especially grain and lumber, but also in other areas it was used for pumping irrigation water [44]. The technology was based on a water wheel on which the power of water used to rotate the wheel and in turn use the mechanical shaft power to drive mechanical systems [42]. This development in hydropower resulted in the introduction of hydroelectric generation stations. The early development on hydropower began around 1870 in England when the first hydro-electric power plant was installed at Cragside. But the actual commercial use hydropower generation station started around 1880 in the USA, with a dynamo driven by a water turbine and at that time it was only producing 12.5 kW of power that can be equated to 250 lights [45]. This invention made several countries in the world to adopt to the technology and 120 years later in the 1990s almost 300 hydroelectric plants were developed around the world [46].

Nowadays most of the existing hydropower plants are used to generate electricity for domestic (household) and commercial use and despite its age, hydropower development has increased tremendously in the last decade contributing to more than 17% of the world electricity generation worldwide and about 90% of global renewable power [41]. Due to their nature, most hydroelectric power plant technology can respond to fluctuation on power demand more quickly than fossil fuels such as thermal electric power stations and this adds to their advantage on flexibility [47]. In terms of energy conversion, hydroelectric power plants can achieve a high system efficiency of around 85% compared to that of thermal electric power plants of less than 50% [48]. Also, when looking at technology

perspective, hydropower technology is the only renewable energy technology that can be used to store large quantities of energy (water) in a clean and environmental way in reservoirs and dams [49]. In terms of energy technology, even though hydropower development is a mature technology but still new innovations, research and development on integration with other renewable energy technologies need to be studied in order to provide better utilization of the resources.

2.3 Types of hydropower schemes

To date, several types of hydropower schemes do exist, but from literature, three large scale scheme types are mostly described.

2.3.1 Reservoir (Dam) hydro storage scheme (Impoundment)

This type is the dam based hydro scheme which is associated with the existence of a large dam of water on the upstream used to store water to provide enough flow throughout the year round [50]. The stored water is mostly used to generate enough electricity during peak load and in dry seasons. This type of schemes needs special features for the dam construction and in most cases, they are better suited to large rivers with gently graded slope [51] as shown in Figure 2.1 below. The dam-based scheme has its advantage as it has the capability to store enough water which could be utilized when needed to balance the power output [47]. Despite its advantages, this type of scheme is very costly as a large area is needed for the dam construction and maintenance of the dam [52]. Most of this type of schemes are based in developed countries and in total they account for a small percentage of the existing hydropower plants [53]. Recent research studies have been focusing on dam management and safety, rather than power optimization and integration which include the aspect for flood control and irrigation [54].

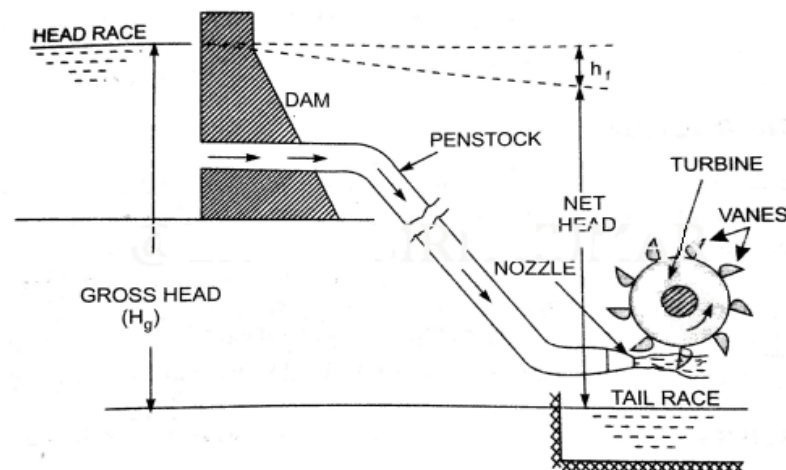


Figure 2.1: Dam hydro storage scheme [55]

2.3.2 Pumped hydro storage scheme

In a pumped storage plant configuration, water is pumped back after being utilized to the turbine and stored upstream. Usually, there are two reservoirs in this configuration, one upstream (upper reservoir) and other downstream (lower reservoir) [55, 56]. During low-load periods or when the cost of electricity generation is lower, water is pumped from the lower reservoir back to the upper reservoir and stored. This stored energy in the form of water is then used to generate additional electricity during the peak hours or when there is a high load demand. The technology has nowadays developed rapidly and to date more than 300 installations with a total capacity around 127GW in 2010 [57-59] and nearly 140GW at the end of 2011 [41]. Currently pumped storage accounts for 99% of on-grid electricity storage [60]. Early pumped storage systems were using a configuration with separate pump and turbine unit's setups [61] as shown in Figure 2.2 below.

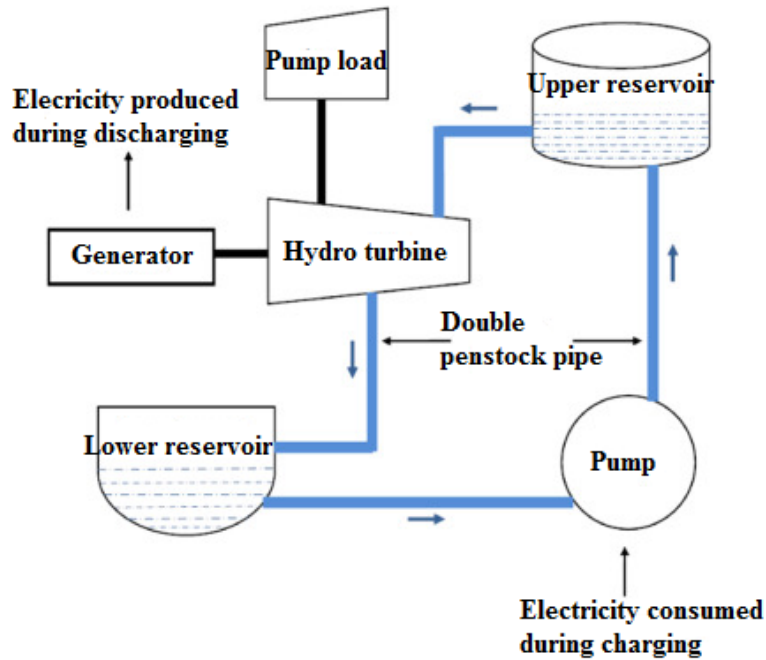


Figure 2.2: Pumped hydro storage system [59]

Most of the existing pumped-storage schemes are commercial means of large-scale grid connected energy storage which in-turn result in the improvement of the generation capacity factor [38]. Several system configurations do exist for this type of scheme with several combinations such as wind pumped hydro energy storage plants [62], Solar photovoltaic pumped hydro energy storage plants [63] and the combination of solar and wind which produces less variability than the above individual systems [64]. From recent literature, three main component setups are widely described in the pumped storage system [65-67].

- (a) **Four unit's setup:** Consists of a pump driven by an electric motor on one side and a turbine connected to a generator on the other side. When generating, the turbine side coupled with the generator produces electricity. When excess electricity is produced during low demand, some of it is used to power the motor to drive the pump. Due to its configuration and setup, the system occupies a large amount of space, so it become uneconomical, hence now days it is no longer being used.
- (b) **Three unit's setup:** In this configuration both the pump and turbine units are coupled to a single unit reversible motor-generator. Sometimes the pumping needs to be achieved at the higher head, so in this case, the optimisation is done by multi-stage pumps which increase the efficiencies of the pump and turbine. Its downside is that the system of this setup increases the overall cost, hence not economical.
- (c) **Two unit's setup:** The setup consists of a single reversible pump-turbine unit which is coupled to a single reversible motor-generator unit. The turbine on the reverse act as a pump and the generator on the reverse act as a motor [51]. In comparison to the above setups, this configuration takes a smaller space area and as a result, it also has the lower installation cost and hence it has been widely used from the early 1950s

Despite their wide use in recent years, the technical downside of pumped hydro storage is that the configuration setup does not improve the efficiency and generally these systems require a substantial amount of water volume or sometimes a variation in height [38]. Although some literature points out that the energy efficiency of many pumped hydro energy storages varies and ranges between 70% and 80% [68-71] with some claiming up to 87% [72]. On the other hand, integrating wind power and pumped hydro energy storage has been found be more economical and very competitive technology in many areas where there is the availability of wind power [62, 73, 74].

Even though most pumped hydro energy storage has been used for large scale hydro systems eg. 4,000MW energy storage capacity [75], Yin et al, [76] proposed a smaller version of a micro-hybrid energy storage system which consists of a pumped storage plant with a micro-pump turbine system and compressed air energy storage attached with two tanks. Despite its small size concept, the system had some disadvantage that the micro-pump turbine utilises excess power from the grid to pump the water to compress the air. In conclusion and according to Lee and Gushee [77], electricity storage technologies are crucial and needed for renewable energy sources and especially when pumped storage technologies are to become sources of base load power.

2.3.3 Run-of-river scheme

To reduce the investment cost associated with the large pumped hydro storage plants and attract private investors, most small scale hydro power plants installations prefer to operate as a run-of-river scheme (water diversion). Literature shows that this type of hydropower scheme is among the early hydro power facilities to be developed [37]. They are basically known as run-of-river schemes because they do not include any significant water storage eg. a dam, but they can have a small reservoir called poundage (short term storage) [78]. The schemes divert the water directly from the river and make use of it for power generation. Despite their simplicity, most of these schemes need to be feasible because they depend on the natural head and also they are vulnerable to water fluctuation as a result when rivers have reduced flow, the run-of-river schemes are unable to generate the required capacity of electric power due to a shortage of water [79]. In terms of layout, most run-of-river schemes involve a diversion weir at the water intake, either at the side of the river or at the river bed [80]. The weir acts as a barrier to direct water to the intake and other subsequent structures on the layout which is a penstock [81]. Due to its simple layout, the run-of-river hydropower scheme has the advantage in terms of cost implication compared to other schemes and have been extensively used in small and micro-hydropower development [82].

The most common types of run-of-river hydropower plants are in the small-scale hydropower category on which the installed power capacity ranges from 1 MW to 100 MW that can be equated to supplying power from 100 homes up to 10,000 homes. Some of these schemes are also connected to the national grid. Most of the independent power producers in Africa and Asia which are connected to the grid are on this category because it is one of the most attractive hydro schemes in terms of the business model (easier to fund) and also has fewer issues on social and environmental impacts [83]. Due to its wide range of application in small scale, small hydro power technologies are vital in improving access to modern energy and poverty alleviation in rural communities which in turn can improve social and economic development in rural areas [41]. So, for the hydropower technology development especially in rural and off-grid areas, new researches and studies are necessary to adapt small scale hydropower designs to accommodate local characteristics and to develop economically feasible hydro projects, which include the widely used micro scale hydropower technologies.

2.4 Micro-hydropower scheme

In small off-grid communities where water resources from small rivers are available, the micro-hydropower technology provide the suitable type of installation to supply the required village load demand power. The micro-hydropower capacity ranges between 5 kW to 100 kW system [84] and is a suitable alternative to the rural and isolated areas where there is no feasible future for grid connection [85]. These types of hydropower plants can supply power to between 5 to 100 homes which seems to be suitable for rural and isolated off-grid areas [86]. Also, they are very cost effective in terms of initial investment and maintenance cost because they can be developed economically with a simple design of turbines, generators and the civil works [87]. They are mostly setup on the run-of-river scheme and can be installed to even small rivers and small streams. Micro-hydropower can be often implemented on local isolated mini and micro grids to be able to offer a higher level of energy needs and services when compared to solar PV which seems to have higher investment cost [88].

The development, operation and maintenance of the micro-hydropower plant can be easily adapted locally with the local technology and expertise, hence make micro-hydropower very suitable technology for most rural areas of Sub-Saharan Africa countries where there is much potential [32]. Many studies have been conducted in Africa for the micro-hydropower potential and the results show that there is huge potential for the micro-hydropower but very few potentials have been developed so far [89]. A research study was done by Maher et al (2003) [88] in Kenya and revealed that micro-hydro turbines are able to supply electrical power to the households at a fraction of the cost to the end user as compared with Solar Photovoltaic or grid connected battery charging stations.

In Tanzania, micro and small hydropower potential are not well known but recent studies estimate at around 250 MW [90]. Few scholars have highlighted the reasons as to why despite huge potential, most of the micro hydro potential in developing world like in Africa have not been much exploited and developed [91]. When considering among the hydropower-based energy technologies, small hydropower (micro hydro and mini hydro) are the only classes that suit best with typical conditions of several off-grid and rural areas of developing countries especially in Africa [92]. But despite their technological advantage, there has been very little on their development and the level of installations is very low and this is due to several factors which among them include, small hydropower technologies is quite lacking in the region and other factors that are taken into account include financing

and policy issues, which in recent years has been addressed [32, 93]. Despite these challenges, still, micro-hydropower can be set up in the rural and off-grid areas with minimal investment cost from the private investor or government subsidies and also within a short period of time with the local community ability to take charge of the plant [94, 95]. In remote areas where the energy demand of the rural communities is mostly limited to several local villages, micro-hydropower schemes are the best suitable technology that can meet the energy needs because they can be adapted to the local demand and also are able to integrate with other renewable energy systems.

In recent years, research in renewable energy development in off-grid remote areas of developing countries like Tanzania has been focusing on the integration of different renewable energy technologies to effectively and efficiently utilise the available resources. This is due to the effects caused by the dynamic nature of load demand, a variation of water flow rate for micro-hydropower development which have been caused by seasonal climate changes, multipurpose water usage in streams and rivers eg. Irrigation and water supply usage [96]. Literature has shown that there are several combinations of renewable energy technologies at the micro level on which some of them includes several combinations for integrated micro-hydro turbine with solar PV, wind systems and energy storage systems [97].

2.4.1 Integrated micro-hydropower schemes

In the micro-hydropower with a solar photovoltaic system, water from the small river is used to supply the micro hydro turbine for power generation, while solar PV, on the other hand, add extra power capacity to the system. The disadvantage of this system is that the power from the Solar PV is only available during the day when there is sunshine because free energy from the sun is intermittent in nature and also PV power output cannot be used directly and in this case, the energy needs to be stored [98]. Therefore, most of the solar PV systems have an additional battery energy storage system component which in turn reduce the overall system efficiency due to energy storage and conversion efficiencies. For a small scale, energy supply system few literatures have highlighted the integration of micro-hydro turbine and solar PV with battery storage. The reasons for this could be that the cost of PV systems is very high, so the system becomes un-economical and the energy output does not provide the consumer with the level of energy services needed [99].

In areas where wind and small river resources are available, there is a configuration which combines micro-hydropower plant with the wind turbine and in this case, the energy

supplied by the wind turbine is used as additional energy required to sustain the load demand [100]. But the problem with this type of combination is that wind resource is always unreliable and unpredictable and its potential is available to few places, so in most cases cannot rely to supply peak load [101]. Another integration that is commonly used with the micro-hydro turbine system is to include battery storage on which some of the power produced is stored into the batteries system. But studies have found that most of the micro scale battery storage systems use DC current and because of conversion efficiency, there is usually a power loss during charging and discharging phases [102]. Also, battery systems have a limitation on the storage capacity, high in maintenance cost and produce pollution with health risks.

So, to overcome these problems, a micro-hydro turbine system needs to be integrating with an energy storage system that will be able to offer a higher level of energy storage even during peak hours with minimum losses and free from environmental pollution. On the other hand, when looking into technology perspective, micro-hydro turbine system has proven to replace diesel generators in off-grid rural and remote areas when implemented with an energy storage system and in line with other renewable energy technologies [103]. One of the energy storage technology that has not been exploited in all these literatures is the use of hydrogen storage, so this research study will focus much more on this new energy storage technology although other energy storage technologies have been widely used as shown on Figure 2.3 below.

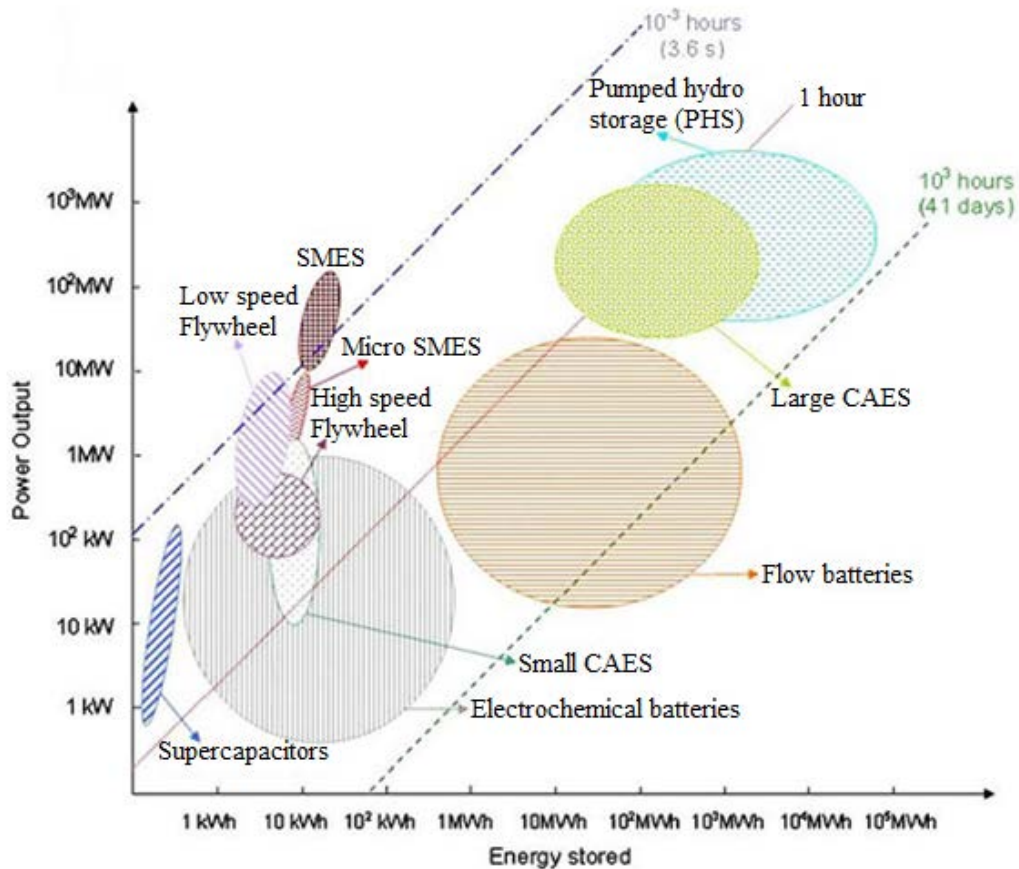


Figure 2.3: Available electrical energy storage technologies [5]

2.4.2 Classification of mini/micro-hydro turbine system

A hydro turbine system converts energy from the falling water to produce mechanical (shaft) power that is used to drive the generator to produce electrical power. There are several types of hydro turbines systems that are available on the market and according to C. Penche [104] all the hydro turbines are classified into two main categories of impulse turbines or reaction turbines.

2.4.2.1 Impulse turbines

In the impulse turbine classification, the turbine runner operates in air and driven by a single or multiple jets of water flow that make contact with the turbine runner blades (buckets) which are the rotating elements. These types of turbines use accumulated water pressure (potential energy) to create water flow velocity jets from the nozzles that hits the buckets to gain kinetic energy that makes the turbine spinning and hence gain momentum as shown in Figure 2.4 below.

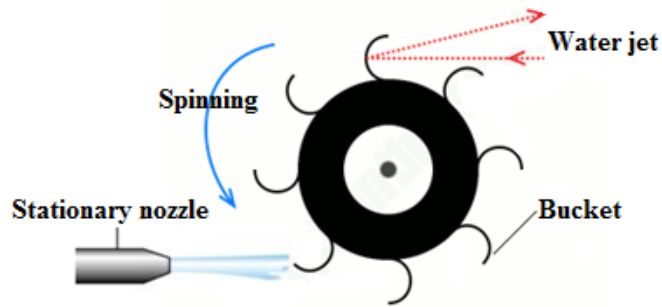


Figure 2.4: Impulse Pelton turbine [105]

In the impulse turbines, no pressure changes occur at the turbine blades (works at atmospheric pressure) and hence there is no need to seal the turbine housing. Examples of impulse turbines with their respective operated head range includes the following:

- (a) High head turbines: Pelton ($100\text{m} < H < 1300\text{m}$) and Turgo ($100\text{m} < H < 250\text{m}$)
- (b) Medium head turbines: Cross-flow, Multi-jet Pelton and Turgo ($50 < H < 100\text{m}$)
- (c) Low head turbines: Cross-flow ($3\text{m} < H < 50\text{m}$)

2.4.2.2 Reaction turbines

In the reaction turbine, the turbine runner is usually fully submerged in the water flow (to create water pressure) and enclosed in a pressure casing to create suction that make them to work above atmospheric pressure. Its turbine technology is based on the runner blades which are profiled in a such a way that pressure difference across the blades creates a lift forces that make the runner blades to rotate as shown in Figure 2.5 below.

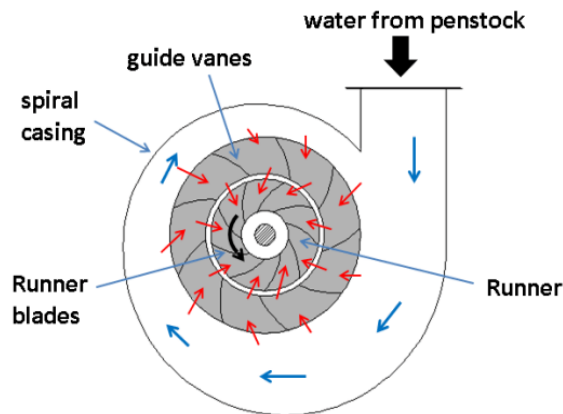


Figure 2.5: Reaction Francis turbine [105]

These turbines operate in a low and medium head application and some of the common examples based on head include the following:

- (a) High head turbines: Francis ($100 < H < 350$)
- (b) Medium head turbines: Francis and Pump-as-Turbine (PAT) ($50 < H < 100\text{m}$)
- (c) Low head turbines: Francis ($10\text{m} < H < 50\text{m}$)

: Kaplan and Propeller ($2\text{m} < H < 50$)

In comparison with the above two turbines classification, impulse turbines are generally more suitable for small hydro turbine applications (mini and micro scale) as compared with the reaction turbines because impulse turbines have a greater tolerance to small sand particles in the water (no pressure seal inside the casing) and also easier to fabricate and maintain at the local level.

2.5 Technical aspects of micro-hydropower schemes

Micro-hydropower schemes have the potential to produce electrical energy in off-grid rural areas and when this energy is utilized it gives environmentally friendly generation of electrical power from local small rivers [106]. In many parts of the rural off-grid areas where water resources are available micro-hydropower schemes have been successfully implemented to provide energy technologies to small villages [107]. Many studies have shown that in off-grid rural areas where water resources are available, micro-hydropower schemes have replaced traditional diesel generators and majority of the schemes are implemented in a hybrid system together with the solar powered technologies.

2.5.1. Role of micro-hydropower in development

In off-grid rural areas where there is an availability of a micro-hydropower plant that produce electricity to the local community many studies have shown that villages with provisional of electricity there is usually an improvement in the quality of life [108]. This is evidenced by the availability of lighting and power to the households, shops, small industries and village health centres. The introduction of lighting and power has led to an increased in study time for students at schools/home, availability of electrical/electronic equipment's like fridges, TV's and Radio in the households, installation of small industries and also availability of diagnostic equipment's in the village health centre that will improve health services and reduce mortality rate [109]. The availability of electricity in the villages have also proven to conserve forest and environment by promoting the use of electrical power at household level. Most rural village economic activities are related to the agricultural works and literature shows that the availability of electricity from the micro-hydropower have supplemented traditional livelihoods by introducing modern irrigation activities and agro-processing industries that have added value to the local produce [110]. Literature also shows that more than 50% of the perishable food crops like tomatoes and fruits that are produce in the villages are wasted due to the un-availability of agro-processing industries [111]. Most of the micro-hydropower schemes are associated with

the availability of water from small rivers with the provision of a water falls and recreation activities in the local village area. These activities have opened new employment opportunities in the areas of tourism, eco-tourism, marketing, information technology and processing non-wood forest products [112].

2.5.2 Choice of the micro-hydropower scheme

The choice of a micro-hydropower site for development depends on the site-specific characteristics and the available water flow discharge together with the site head. Most micro-hydropower systems are efficient energy sources because they use little amount of water to generate electricity and provide the possibility of developing cost-effective local energy distribution [113]. They are one of the reliable electricity sources for rural and off-grid areas of developing countries that use little water because there is no water reservoir required.

2.5.2.1 Site selection

Many literatures from feasibility studies, have shown that hilly/mountain terrain with availability water resources throughout the year and maximum gradient (high water head) value in a river section are found to be suitable locations for the development of micro hydropower plants [114]. But most of the site locations in hilly/mountain areas are not accessible easily due to their remoteness and bad terrain which brings many challenges during the construction. On the other hand, the large hydropower site selection is based on many factors which some of them include distance from the national grid and detailed and long-range hydrological data from the water resource are also vital and need to be studied [115]. But for micro-hydropower plants due to their small sizes in terms of power capacity, the need for long time river flow studies for site data is not required and this eliminates the need for a detailed feasibility studies and hence reduce the installation time and project cost [116].

2.5.2.2 Turbine-generator selection

Micro-hydropower system uses turbines that convert the energy of the falling water by rotating the shaft to produce mechanical power. In the micro-hydro turbine installations, the type and size of turbine selection that can be used on the site depends on many parameters but two of the most common parameters that must be determined first are the site head (H) and volumetric flow discharge (Q). In this case, the power output from the turbine-generator system is directly proportional to the head and flow discharge. Using

these two parameters from the site measurements, the type of turbine-generator system to be used in the micro-hydropower scheme can be obtained by using the following two methods [117].

(a) Graphical selection

In the graphical selection, turbine-generator system is selected according the computed river flow discharge and site head by using the logarithmic graphical method. In this method the hydro turbines selection has been based on the flow discharge to head characteristics values that will tend to run most efficiently to produce a power output range [118]. Due to the fact that most turbine types operate in a certainly range of flow discharge and head values, then their power capacity is also in a certainly range on which at a micro scale the maximum flow discharge considered is up to 4 m³/s and the maximum net head value of up to 100 m as shown in Figure 2.6 below.

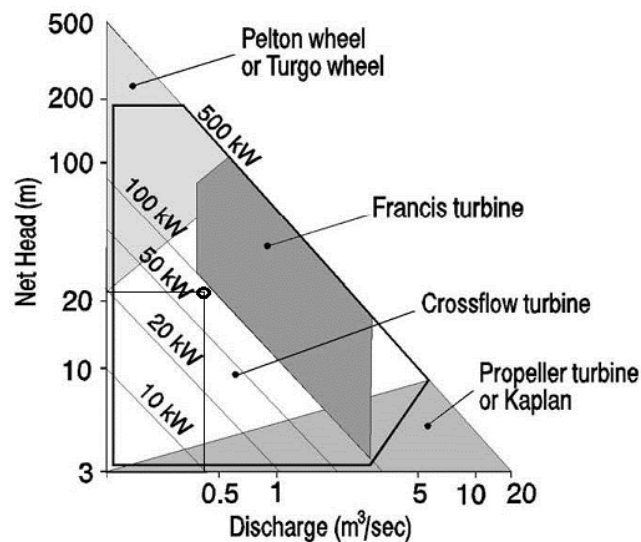


Figure 2.6: Mini/micro hydro turbine selection based on head and discharge value [119]

Based on the turbine selection chart above, it is noted that crossflow turbines have a wider range of pressure head and water flow discharge values from small to medium values, thus why they are commonly used in micro-hydropower projects in rural and off-grid areas of many developing countries like Tanzania.

(b) Analytical selection

In the analytical selection, the turbine design parameters are determined based on the head and discharge values using the following formula:

(i) Turbine power output, $P_{MHP(g)}$

$$P_{MHP(g)} = \frac{P_{MHP(t)}}{\eta} \tag{2.1}$$

where $P_{MHP(g)}$ = generator power in kW, $P_{MHP(t)}$ = turbine power in kW and η = system efficiency for the turbine system, generator system and gearbox system

(ii) Specific turbine speed, N_s

$$N_s = \frac{(N \times P_{MHP(g)})^{0.5}}{H} \left(\frac{5}{4}\right) \quad 2.2$$

where N = speed of the turbine in RPM and H = site head

Based on the calculated specific turbine speed and head value, turbines can also be classified as follows:

- Low specific speed and high head turbines like Pelton and Turgo
- Medium specific speed and medium head turbines like Francis and Cross-flow
- High specific speed and low head turbines like Kaplan and Propeller

2.5.2.3 Policy and regulations consideration

In this category the establishment of energy policy and regulations for hydropower development has highlighted different small hydropower classes below 10 MW power capacity [120]. This has provided a favourable condition for the small hydropower development in rural and off-grid areas because it has provided a standardized power purchase agreement and better energy tariffs that has attracted many private energy investors in the third world countries like Tanzania [121].

2.5.3 Basic components of a micro-hydropower

The micro-hydropower system components consist of two main sections which are civil components and electromechanical components. In civil component they include intake/diversion weir, canal, desilting tank, forebay tank, penstock pipe, power house building and tail race [122]. Most of the civil components are used to collect and transport water flow from the river to the turbine area in the powerhouse as shown in Figure 2.7 below. On the other hand, the electromechanical components include turbine system, generator and controls system and power transmission and distribution network. These components are usually used to produce, control and transmit the electrical power to the consumers.

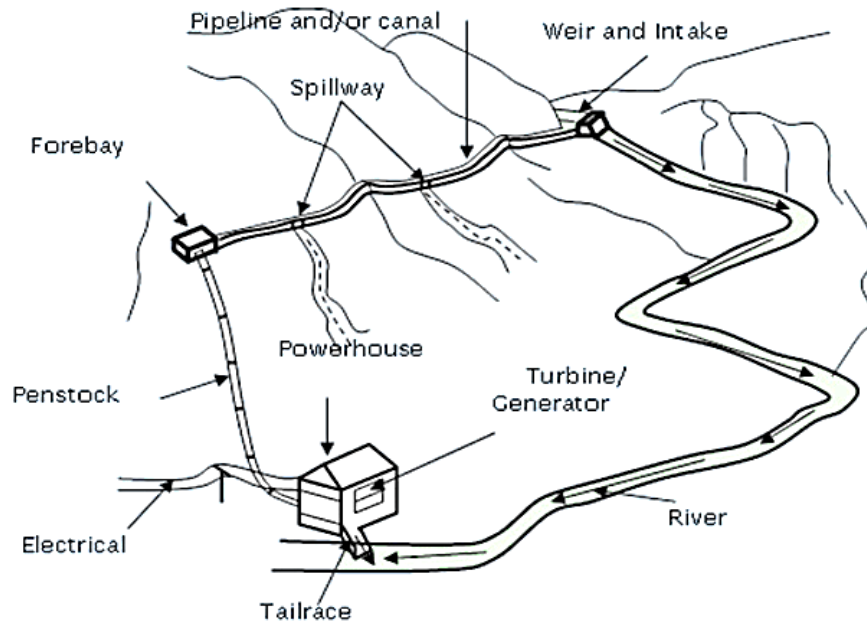


Figure 2.7: Basic components of a micro-hydropower [122]

2.5.4 Misconception on micro-hydropower technology

There are many potential sites for micro-hydropower development in developing countries like Tanzania but studies have shown that only a few of them have been developed. One of the reasons for the little development in micro-hydropower is the misconceptions in the technology on which some of the information stipulated include that micro-hydropower schemes will destroy the local ecosystem, small rivers are not economical and does not provide enough water to generate electricity and also the system usually require a water storage/reservoir that will reduce the down-stream water volume for agricultural activities [123].

2.5.5 Survey of similar micro-hydropower scheme

In recent years micro-hydropower technology has proven to be one of the major means of supplying electricity to the rural and off-grid areas of many development countries like Tanzania. Many studies have been conducted and documented for the sustainable development of existing micro-hydropower plants in several Asian and African countries. Despite a successful implementation of many micro-hydropower projects in rural and off-grid areas, many power plants had faced several problems during their operation. There are many problems that are associated with the failure of micro-hydropower plants in developing countries and some of them are related to either technical, managerial or financial aspects. Among the above factors and based on the success and failure study of micro-hydropower projects in development countries, results shows that technical aspects

(civil, mechanical and electrical) have the greatest contribution for the reliability of the hydro power plant operations. But when a failure occurs for a community micro-hydropower project at a village, studies shows that there is a discouragement of the local community to engage to other development related projects [124].

To date there are many micro-hydropower plants that are in operation in development countries like Tanzania. One of the micro-hydropower plants is that of Yongoma, Tanzania which has the capacity of 75 kW. The site was initially aimed to be connected to the grid but water resources at the site were already being exploited for irrigation activities and for sisal treatment by the local sisal estate, hence reduce significantly the amount of water required for power production [125]. Another site development in Tanzania was developed by UNIDO at Kinko, Lushoto – Tanzania which was having a capacity of 9 kW. The main use of this small amount of available electrical power was for household lighting and power. The Kinko site was operated for several years before the power plant stopped working due to the following reasons: de-silting of the storage pond, low levels of water flow during the dry season which resulted to conflicts of interest between power generation, irrigation activities and water supply projects to the local community. In recent years, the site at Kinko become unreliable and not sustainable because of technical and management problems which has not been addressed [126]. A study done by TANESCO had surveyed several small hydropower plants in Tanzania and the results of their survey lists the 19 small hydropower plants with their capacity in Tanzania as shown in Table 2.1 below.

Table 2.1: Small hydropower plant sites in Tanzania [127]

S/N	Location	Installation year	Installation capacity (kW)	Developer/Owner
1	Tosamaganga - Iringa	1951	1220	TANESCO
2	Kikuletwa - Moshi	-	1160	TANESCO
3	Kitai - Songea	1976	45	Prisons department/ Government
4	Nyagao - Lindi	1974	15.8	Catholic Mission
5	Isoko - Tukuyu	-	7.3	Mission
6	Uwemba - Njombe	1971	800	Benedict Fathers
7	Bulongwa - Njombe	-	180	Mission
8	Kaengesa Sumbawanga	- 1967	44	Catholic Mission
9	Rungwe - Tukuyu	1964	21.2	Moravian Mission
10	Nyagao - Lindi	-	38.8	Mission
11	Peramiho - Songea	1962	34.6	Benedict Fathers
12	Isoko - Tukuyu	1971	15.5	Mission
13	Ndanda - Lindi	-	14.4	Mission
14	Ngaresero - Arusha	1982	15	M. H Leach
15	Sakare - Lushoto	1948	6.3	Benedict Fathers
16	Mbarari - Mbeya	1972	700	NAFCO/Government
17	Ndolage - Bukoba	1961	55	Catholic Mission
18	Ikonda - Makete	1975	40	Catholic Mission
19	Mbalizi - Mbeya	1958	340	TANESCO

M. A. Wazed et al [128] described a micro-hydropower plant in Bangladesh with the capacity of 20 kW which was implemented to provide power for irrigation activities. The results show that it has enabled the local farmers to use electricity from the plant for daytime irrigation activities that has increased crop yields while the remaining power produced is used to power the community grain mills and supply electricity to the local battery charging station. In Nepal, there are several micro-hydropower plants that supply electricity to the rural and off-grid areas of the country and Sugam Maharjan et al studied one of the schemes called Chauri Khola IV micro-hydropower plant which has the power capacity of 45 kW. This micro-hydropower plant is supplying electricity for lighting and power to the local community and this project has attracted the small businesses as well as modernization of the village houses. But during its operation, studies has shown that Chauri Khola IV micro-hydropower plant had faced several challenges during its operation which among them include intake washed off during floods, land slide of canal, water leakage in the valve, low power output and unsafe location of power house [129]. All the above problems have affected the power plant operation by increasing minor and major repair and maintenance cost. In this case, research have shown that the reduction in repair and maintenance cost

together with reliable function of plant are the major factors for the sustainable development of micro-hydropower plants.

In other countries like China which has often quoted as the most impressive success story for small hydropower development in the world [130] which is currently operating 42,221 small hydropower plants with a total installed capacity of 28,489 MW and supplying electricity to more than 300 million people. China accounts for 39% of the worldwide small hydropower capacity [131]. On the other hand, in Thailand in the year 2002 only 59 community micro-electric systems had been built but two thirds of the existing small hydropower have been replaced by the national grid or fallen into disrepair which resulted to only 24 small hydropower plants that were in operational in 2003 [132]. Despite the huge grid extension projects in recent years in Thailand, rural household in those regions with grid access are still poor and cannot afford the grid connection costs.

2.6 Summary

When considering the power quality point of view and base load capacity, small hydro power technology has the ability to provide committed and reliable power in rural and off-grid areas [133] and according to Kear and Chapman survey [134], large and medium pumped hydro schemes seem to be costly and also suitable locations for the constructions of pumped hydro energy storage plants are now becoming rare [79]. Also, nowadays the availability of technically and economically potential and suitable sites are also rare [135]. So, in this case, the relatively small capacity hydro turbine systems, specifically at the mini or micro scale are the best alternative to provide affordable and reliable electricity especially in rural and off-grid community areas of developing countries like Tanzania. In addition to that, the integration of micro-scale hydropower system with other renewable energy systems can be very beneficial and cost-effective option for rural electrification [136], even though wind and solar power are unreliable, unpredictable and uncontrollable. The primary purpose of most micro-hydro turbine system in rural and remote off-grid areas of developing countries like Tanzania is to generate and supply electricity to the village community. But, based on literature review and by referring to the above information of using micro-hydropower system as the only source of electricity, the following question may arise from the research study, **“How is it possible to integrate electricity storage into a micro-hydro turbine which is cost effective and sustainable”?** This statement forms the basis for this study project as one of the research question that need to be answered.

Chapter 3 Theory of hydropower

3.1 Introduction

In early days before the development of hydropower, the idea of harnessing water energy was started by using the potential energy of falling water to rotate a waterwheel. The waterwheel is attached with a pulley and belt to create a rotational mechanism for different machines like grinding mills, sledge hammers, textile machines, sawmills and in some areas the rotational mechanism is used to pumping water for irrigation purposes [137]. The waterwheel technology on the other hand uses the potential or kinetic energy of the water flow to rotate the waterwheel which cause rotational motion on the pulley and belt section. It consists of a large circular rotating wheel which is made of wooden or metallic material that consists of several blades/buckets which are installed tangentially outside the wheel rim as shown in Figure 3.1 below.

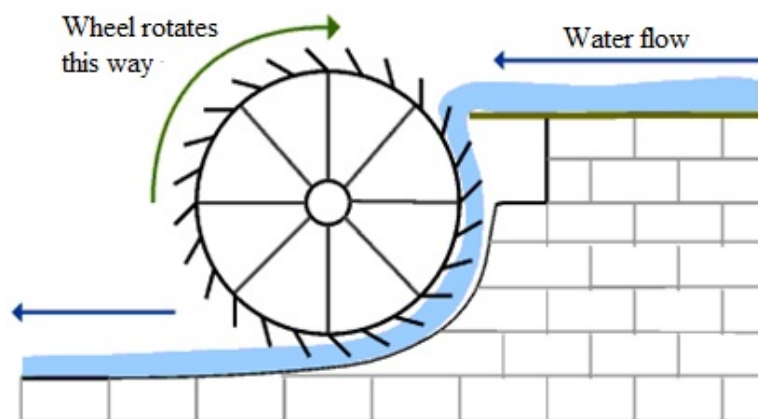


Figure 3.1: Waterwheel layout [138]

The technology of waterwheel was substituted by the development of hydropower in the early 1820's [139] due to their poor flexibility during variations of water flow discharge and this made waterwheels less efficient as compared to the current hydro turbines [140]. Due to their less application in today's water power technologies and poor system efficiency, water wheels will not be discussed further in this thesis.

3.2 Hydro-power technology

The hydro-power which is also known as water power is the type of technology at which the energy produced by the falling water is extracted by the turbine-generator system at a site to produce electrical power. In this system the turbine is the type of machine that uses the power of falling water to gain potential energy which is converted to kinetic energy under pressure to gain rotational speed of the turbine wheel. This rotational energy

produces mechanical power at the turbine output shaft which is then connected to the generator system to produce electrical power [141]. In the hydropower technology, the potential energy is created by the mass (m) of the falling water from a particular height (H) while the converted kinetic energy that creates rotational speed is also created by the mass (m) and velocity (U) of the flowing water using the following formula:

$$PE = mgH \quad 3.1$$

$$KE = \frac{1}{2}mU^2 \quad 3.2$$

where PE = potential energy, KE = kinetic energy, m = mass, g = gravity, H = head (height) and U = water flow velocity.

When considering the hydropower system, the maximum potential energy is obtained at the water entry to the penstock pipe (point 1) with the pressure p_1 and head H_1 . The water from the reservoir is conveyed to the turbine through a penstock pipe and the maximum kinetic energy of the water is obtained at the water exit (point 2) with pressure p_2 and head H_2 as shown in Figure 3.2 below.

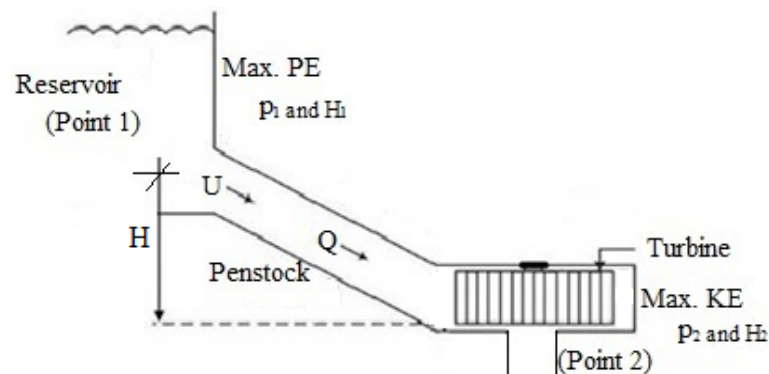


Figure 3.2: Water energy conversion to produce hydro power

By considering the water flowing from point 1 (penstock entry) with the following values, pressure p_1 , head H_1 and velocity U_1 to point 2 (penstock exit) with the following values, pressure p_2 , head H_2 and velocity U_2 . The energy equation for hydropower system is determined using the Bernoulli equation as follows:

$$p_1 + \frac{1}{2} \rho U_1^2 + \rho g H_1 = p_2 + \frac{1}{2} \rho U_2^2 + \rho g H_2 \quad 3.3$$

In hydropower system the water flow velocity, U in the penstock pipe with the same cross-section area is maintained at a constant value from the entry (point 1) to the exit (point 2) so, in this case $U_1 = U_2 = \text{constant}$ as shown in Figure 3.3 below.

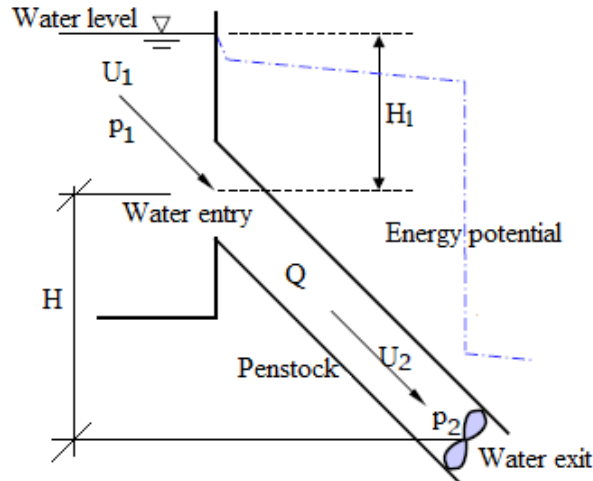


Figure 3.3: Penstock pipe layout

Simplifying and re-arranging the equation 3.3 gives the following relation:

$$\Delta p = \rho g \Delta H \quad 3.4$$

where Δp = changes in pressure ($p_1 - p_2$), ρ = density of water, g = gravity and ΔH = changes in head ($H_1 - H_2$).

But in the penstock pipe with uniform diameter, the pressure, p is given by the following equation:

$$\text{Pressure, } \Delta p = \frac{\text{Force (F)}}{\text{Area(A)}} \quad 3.5$$

where F = force in N and A = area in m^2

The pressure value is acting on the entire span of the penstock pipe so, when introducing the length factor, L on both the numerator and denominator for the above equation 3.5 gives the following pressure relation:

$$\Delta p = \frac{F \times L}{A \times L} = \frac{\text{Workdone}}{\text{Volume}} = \frac{\text{Energy (J)}}{\text{Volume (m}^3\text{)}} \quad 3.6$$

$$\Delta p = \frac{E}{v}$$

$\Delta H = H$ and v = volume (m^3)

Note: 1 Joule = 1 N.m.

Substituting the pressure value, Δp from the above equation 3.6 to the equation 3.4 gives the following energy equation:

$$E = \rho g v H \quad 3.7$$

But all hydro turbines produce power and not energy, so using the power and energy relation:

$$\text{Energy} = \text{Power} \times \text{time} \quad 3.8$$

This gives the following power equation for the hydropower systems:

$$Power = \rho g \frac{v}{t} H$$

$$P_{HP} = \rho g QH \quad 3.9$$

where P_{HP} = power output for the hydropower system in kW, Q = water flow discharge in m^3/s and H = site head in m.

The above equation 3.9 represent the theoretical output power for the hydropower system, but in obtaining actual power output for the hydropower plant, the theoretical output power from equation 3.9 needs to be multiplied by the total efficiency (η_{total}) due to losses during the power conversion in order to obtain the electrical power output from the generator system as follows:

$$P_{HP} = \rho g QH \eta_{total} \quad [kW] \quad 3.10$$

where η_{total} = system efficiency which is given as turbine efficiency (η_t) x generator efficiency (η_g)

Thus, from the above equation 3.10 it is noted that the power capacity generated by the hydropower system depends upon the density of water (ρ), gravitational force (g), water flow discharge (Q), elevation head (H) and total efficiency of the hydropower system (η_{total}). Among the above parameters for hydro power output determination, only two parameters of water flow discharge and elevation head are usually obtained from site measurement of river volumetric flow (Q) and site elevation head (H) respectively.

3.3 Parts of a hydropower system

The main parts of a hydropower system from the intake to the power house may be classified into two main groups as follows:

- (a) The hydraulic system components
- (b) The power and control system components

3.3.1 Hydraulic system components

The hydraulic system components in a hydropower system consists of all the main water handling sections from the water intake to the penstock area. The main components in this section include diversion weir and intake, canal or conduit, settling basin, forebay and penstock pipe

3.3.1.1 Weir and intake

The weir is the concrete wall structure that is used to create enough upstream water depth for a water intake. It is usually installed across the river section at the intake area and in large or small hydropower system it creates a dam or reservoir wall structure while in mini

and micro hydropower system which are mostly run-of-river system it creates a small water pondage in order to get enough water flow discharge to the canal.

On the other hand, literature have shown that there are many types of weir structures but the main types that are commonly used include concrete weir, masonry block weir, rockfill weir, gabion weir etc as shown in Figure 3.4 below.

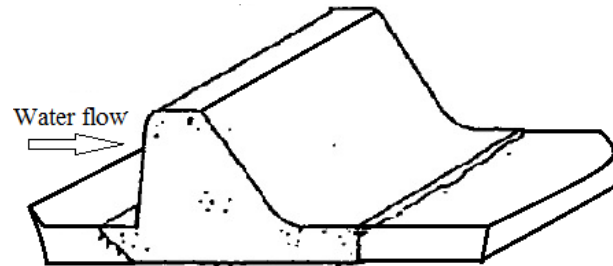


Figure 3.4: Concrete weir

To determine the size of the weir structure, the minimum water flow discharge and environmental flow needs to be determined using the following equation [142]:

$$Q_D = \frac{1}{2} C_d \times g (n_w - 0.2\Delta h_n) \Delta h_n^{1.5} \quad 3.11$$

$$Q_E = 2.5(n_w - 0.2\Delta h_n) \Delta h_n^{1.5} \quad 3.12$$

where Q_D = water flow discharge, Q_E = environmental flow, C_d = coefficient of discharge, g = gravity, n_w = weir notch width, Δh = notch head difference

When the amount of water flow volume is accumulated at the weir structure, the required water flow discharge is directed to the intake structure. There are two types of intake structures that conveyed water flow discharge to the canal from the weir which include side intake or bottom intake as shown in Figure 3.5 below.

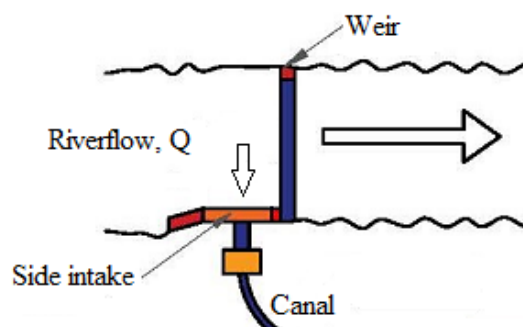


Figure 3.5: Side intake

The size of the intake in a hydropower plant is usually determined by the amount of water flow discharge that is required to be conveyed to the turbine unit. In this case the main determining parameters are the water flow velocity which is maintained at a constant value and the cross-sectional area of the intake using the following equation:

$$Q = A \times U \quad 3.13$$

where Q = flow discharge (m^3/s), A = intake cross-sectional area (m^2) and U = water flow velocity (m/s).

Since the value of flow velocity for the intake structures is kept at a constant rate, then the determining factor for the intake sizing is the area of the intake opening called orifice which is used to allow water to pass through it in order to convey water to the canal. Most of the orifice structures are constructed in a rectangular or square shape with the width (w) and height (h) as shown in Figure 3.6 below on which the corresponding cross-sectional area is given as follows:

$$A = w \times h = \frac{Q}{U} \quad 3.14$$

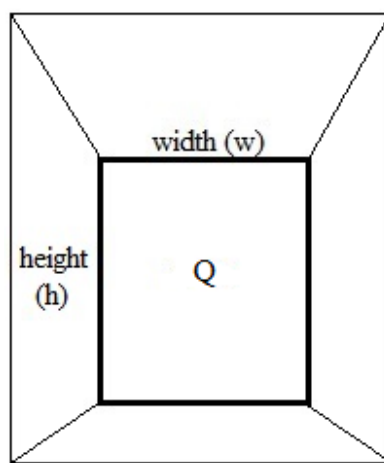


Figure 3.6: Side intake with rectangular orifice

3.3.1.2 Headrace canal/conduit

When water flow discharge is collected at the intake it must be conveyed to the turbine unit. The structure that is used to transport this flow discharge is called canal or conduit and it link the intake to the subsequent water conveying structures. The size of the canal structure is determined by the amount of water flow discharge that need to be transported. In this structure the water flow velocity is maintained at a constant value, hence using the equation 3.13 the size determining factor is the area of the canal given by equation 3.14. Most canal structures are made up of either concrete, cement mortal blocks or stone masonry materials. There are three main types of canal structures based on shapes that are commonly used in small hydropower plants. This include rectangular/square shape, round shape or trapezoidal shape as shown in Figure 3.7 below.

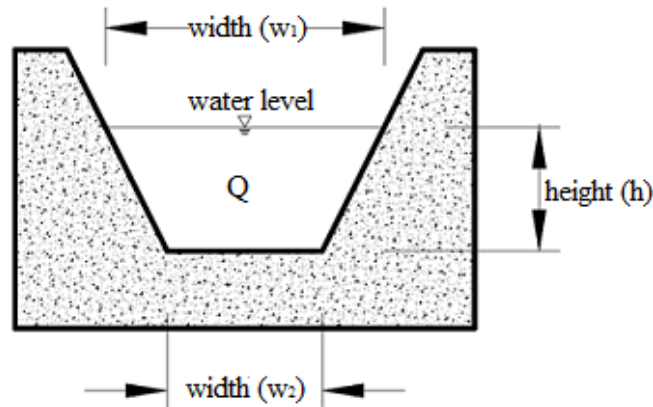


Figure 3.7: Trapezoidal shape canal

For the trapezoidal shape which is the mostly applicable type of canal structure, the cross-sectional area of the canal system is given by the following formula:

$$A = \frac{1}{2} \times (w_1 + w_2) \times h = \frac{Q}{U} \quad 3.15$$

3.3.1.3 Settling basin and forebay

(a) Settling basin

The amount of water flow discharge conveyed by the canal is transported across the settling basin to the forebay tank. Most of the water flowing from the canal are not clean and they contain some debris and sand particles which must be removed before the water enters to the forebay. The function of the settling basin is to settle and remove the sand and debris that have entered to the canal from the intake. It has a gentle slope that allow sand and debris to be trapped and removed. In addition to that, settling basin structures also contain other features such as spillway that removes excess water flow that enters the intake during floods and exceed the required flow discharge needs to be spilled away in order to minimize structure collapse. The other feature that is incorporated in the spillway structure is the flushing gate which is used to flush/remove bottom settled sand at the basin. To determine the dimensions of the spillway structure, the following formula is used [143]:

$$L_{spillway} = \frac{(Q_{flood} - Q_{design})}{C_w(H_{flood} - H_{spillway})^{1.5}} \quad 3.16$$

where $L_{spillway}$ = spillway length (m), C_w = crested weir coefficient for a round edges profile which is 1.6 [144], Q_{flood} = flood flow discharge (m^3/s), Q_{design} = design flow discharge (m^3/s), H_{flood} = flood level height (m), $H_{spillway}$ = spillway crest height (m),

$$H_{flood} - H_{spillway} = H_{overtop}$$

The longitudinal and cross-section structure of the spillway with design parameters is shown in Figure 3.8 and Figure 3.9 below [145]:

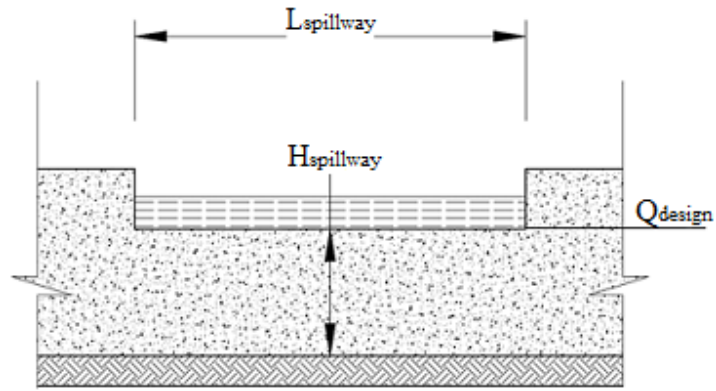


Figure 3.8: Longitudinal section of a spillway

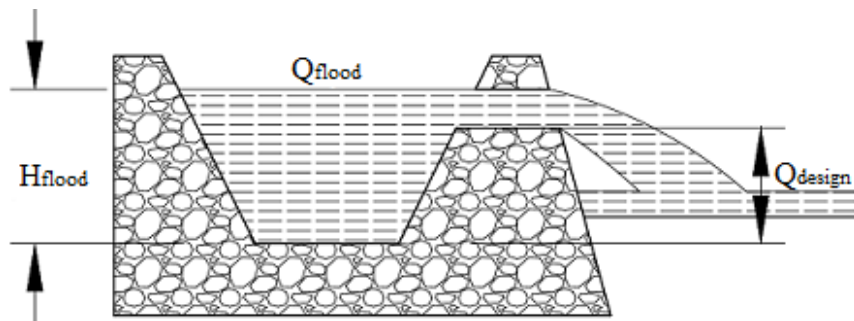


Figure 3.9: Cross-section of a spillway

(b) Fore-bay (Head tank)

The forebay is the civil structure that is used as a head tank to retain the required amount of water flow before allow it to enter the penstock pipe. It is usually located at the end of the headrace canal just after the settling basin. The structure has an air vent that is used to release trapped air by the water entering the penstock pipe. The operation head of the hydropower scheme is usually determined by the water level at the head tank. In the fore-bay structure there is also a small overflow that maintain the required volumetric water flow by spilling excess water during floods. The water flow velocity at the fore-bay is much slower than in the headrace canal which allow the sediments to get settled down. For the safe removal of the sediments the flushing gate or pipe is also required at the fore-bay structure. The penstock pipe is usually connected at the end point of the fore-bay as shown in Figure 3.10 below.

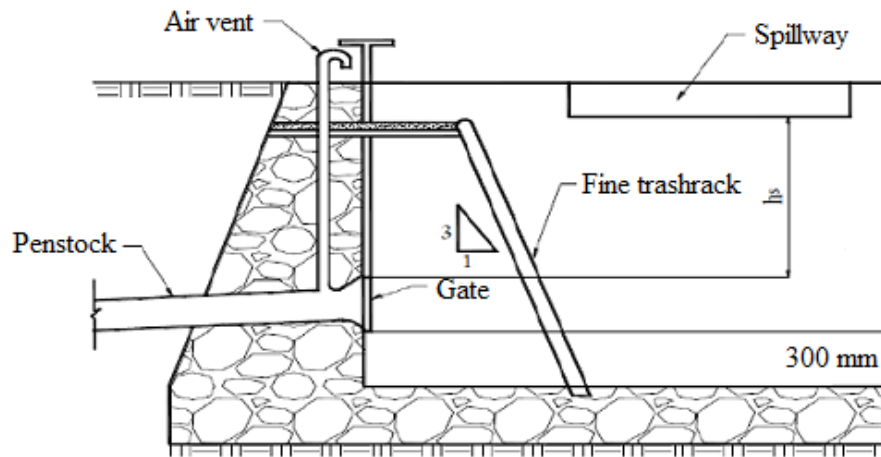


Figure 3.10: Fore-bay layout [145]

(c) Penstock pipe

The penstock is the pipe material that conveyed the required water flow discharge from the fore-bay structure to the turbine unit. It is usually made up from different materials and the commonly used materials are mild steel and HDPE pipes. At higher heads or large water volume, steel pipes are better suited due to their resistance to higher water pressure values while at lower heads or small-scale hydropower plants HDPE pipes are commonly used due their relatively low cost and easy to join and repair. Other materials for the penstock pipes include uPVC, concrete and ductile Iron as shown in the following Table 3.1.

Table 3.1: Commonly used penstock materials [146]

Material	Pressure resistance	Corrosion resistance	Weight	Easy of joining	Friction loss	Cost
Mild Steel	Excellent	Average	Average	Good	Average	Good
HDPE	Good	Excellent	Excellent	Poor	Excellent	Average
uPVC	Good	Good	Excellent	Good	Excellent	Good
Concrete	Poor	Excellent	Poor	Average	Poor	Average
Ductile Iron	Good	Good	Poor	Excellent	Good	Poor
Asbestos cement	Poor	Good	Good	Average	Average	Average

When water flow in the penstock pipe, the conversion of potential energy of water at the penstock entry into kinetic energy at the penstock exit is usually taking place as explained in section 3.2 and shown in Figure 3.11 below. The recommended water flow velocity in the penstock pipe is usually kept at a constant value between 2 – 3 m/s in order to reduce the energy loss when water velocity is much lower or higher which will make the hydropower scheme un-economical in the power production [147].

To determine the amount of water flow discharge through the penstock pipe, its diameter need to be determined using the following equation [148]:

$$d_p = \left(\frac{m_c^2 \times Q_p^2 \times L_p}{H} \right)^{1/5} \quad 3.17$$

where d = diameter of the penstock pipe (m), m_c = manning coefficient (0.012 for mild steel pipes), Q_p = water flow discharge in the penstock pipe (m^3/s) and L_p = length of the penstock pipe (m) and H = head (m) as shown in Figure 3.11 below

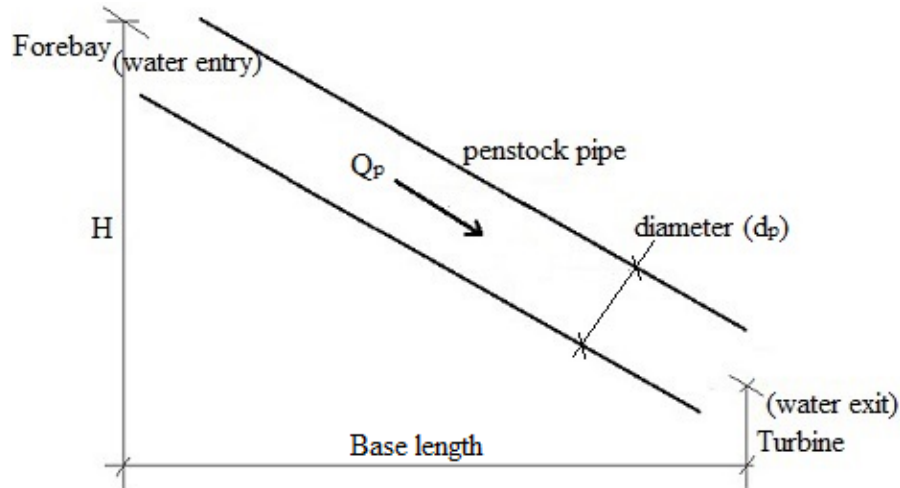


Figure 3.11: Penstock pipe layout

3.3.2 The power and control system components

The power and control system in the hydropower system consists of the turbine unit, generator unit and control system. The turbine system is the prime mover that utilizes the energy of the water flow conveyed by the penstock pipe to rotate the turbine runner and produce mechanical power at the turbine shaft. The amount of mechanical power produced by the hydro turbine depends on the main three parameters of water flow discharge (Q), head value (H) and efficiency of the turbine as explained in detail in section 3.2. On the other hand, this mechanical power from the turbine unit is used to drive the generator system to produce the electrical power. The power conversion from mechanical to electrical is determined by the conversion efficiency as shown in equation 3.10. To maintain smooth power output, the turbine and generators system need to be controlled. For the turbine system, the control action is done by the governor that regulates the amount of water flow discharge (Q) to the turbine unit. The common types of control governors that are widely used in hydropower plants are the hydraulic-mechanical governor and electro-hydraulic (PID) governor (digital governor). During the control action, the amount of power produced by the turbine unit (P_m) is directly proportional to the water flow discharge conveyed by the penstock pipe (Q) and the pressure head (H) as shown in Figure 3.12 below.

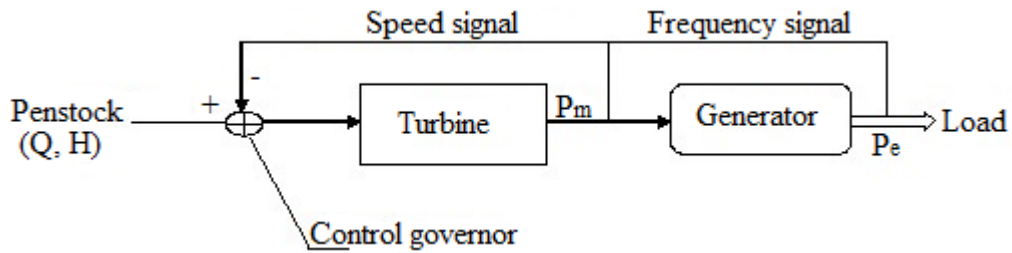


Figure 3.12: Turbine-generator power and control system layout

From the diagram above it is noted that the turbine shaft power (P_m) is directly connected to the generator unit and this causes the generator to spin and hence produce electrical power (P_e) that is supplied to consumer load. In the turbine-generator system the speed (RPM) and frequency (Hz) needs to be maintained at the rated value, so in this case the speed signal from the turbine and frequency signal from the generator is fed back to the control governor to regulate the amount of water flow discharge (Q) in order to maintain the required turbine speed and also synchronized generator frequency.

3.4 Advantages of hydropower plants

Most hydropower plants are used to generate electricity and supply it to the consumer load demand. In large hydropower plants, the produced electrical power is usually connected to the national grid and distributed to the entire nation. Hydropower plants have a lot of advantages and some of them include:

- (a) Low operating and maintenance costs: - The cost of running a hydropower plant is relatively low due to the low in labour cost because of few operators during the normal operation. Also, most parts of the hydropower plants have higher life time which have resulted to the reduction in the maintenance cost.
- (b) Energy storage: - Large hydropower plants with pumped hydro storage are used to store water energy during off-peak hours by pumping it to the upper reservoir and used to produce additional power during high peak demand hours.
- (c) No fuel cost involved: - Hydropower plants does not require any fuel to produce electrical power like most of other conversional power plants. This has resulted into low electricity cost as compared to other power plants which makes hydropower as one of the cheapest source of energy.
- (d) No air pollution: - Hydropower is the energy source with no pollution and hence when used in a big scale it saves the environment by reducing the greenhouse gas emissions and other forms of pollution.

- (e) Reliability: - Hydropower is a very reliable technology because it is a source of electricity that stay for many years in their service life. A typical hydropower plant can last for a very long time if well maintained and have high load factor.
- (f) Small size development is possible: - Hydropower plants can be scaled down to small sizes that are mostly applicable to small rivers and streams. The small sizes ranges from mini, micro or pico hydropower scale and these kinds of small-scale hydropower plants are more economical and thus can be applicable to rural and off-grid areas for village-based electrification.

3.5 Summary

The hydropower system uses the energy of the water flow to rotates the turbine wheel to produce mechanical power at the turbine shaft which is attached to the generator system to produce the electrical power. From the river flow, the water is collected at the intake canal after being accumulated at the dam/reservoir by the intake weir structure. The water is then transported by the canal/conduit structure from the intake through the settling basin to the head tank (forebay). At the end of the forebay structure the penstock pipe that conveyed water flow discharge to the turbine unit is connected. At the penstock entry, the maximum potential energy (PE_{max}) is obtained due to the presence of maximum water pressure column (H_f) in the forebay. This potential energy is then converted to maximum kinetic energy (KE_{max}) at the turbine nozzle/jets due to the presence of maximum water flow velocity (U_{max}). This causes the turbine wheel to spin and produce mechanical power (P_m) that drives the generator system to generate electrical power (P_e) that is supplied to the load demand (consumers) or connected to the national grid.

Chapter 4 Demand analysis

4.1 Introduction

In the village community of the research study village there is no availability of electricity or grid connection, so most people in the area rely on other means of energy sources for lighting and power which include kerosene lamps as well as firewood and charcoal. In some areas, few households have managed to use solar rechargeable lanterns and also batteries specifically for lighting. Small businesses and industries are also available in the area, but due to un-availability of electricity in the area, most of these businesses use diesel generators to provide power. During the site visits in the area, there was a lot of challenges associated with the types of energy sources that the local villages are using. In the households, firewood, charcoal and kerosene cause indoor air pollution which resulting in health risks especially children and environmental pollution and degradation as trees are cut down for firewood and charcoal. Also, the use of solar equipment and batteries for lighting in the households become expensive for most of the families because of low income for most of the people in the area. In small industries, diesel generators when running they produce smoke with pollutants and affect the environment. Also, the unit cost of diesel is now high as compare to the unit cost of electricity which make most of the small businesses not economical and hence operate only a few hours in a day. So, in order to analyse the situation in the area, the assessment of the consumer load demand power for the households, small businesses and small industries have been determined based on the current average monthly electricity usage estimation in the village community.

4.2 Methodology

In this research, the demand analysis was done to determine the actual power and energy values in the case study area that forms the basis for the required power and energy supply in the village community. The following Figure 4.1 shows the methodology layout for power and energy demand determination that has been used to determine the actual power and energy demand values.

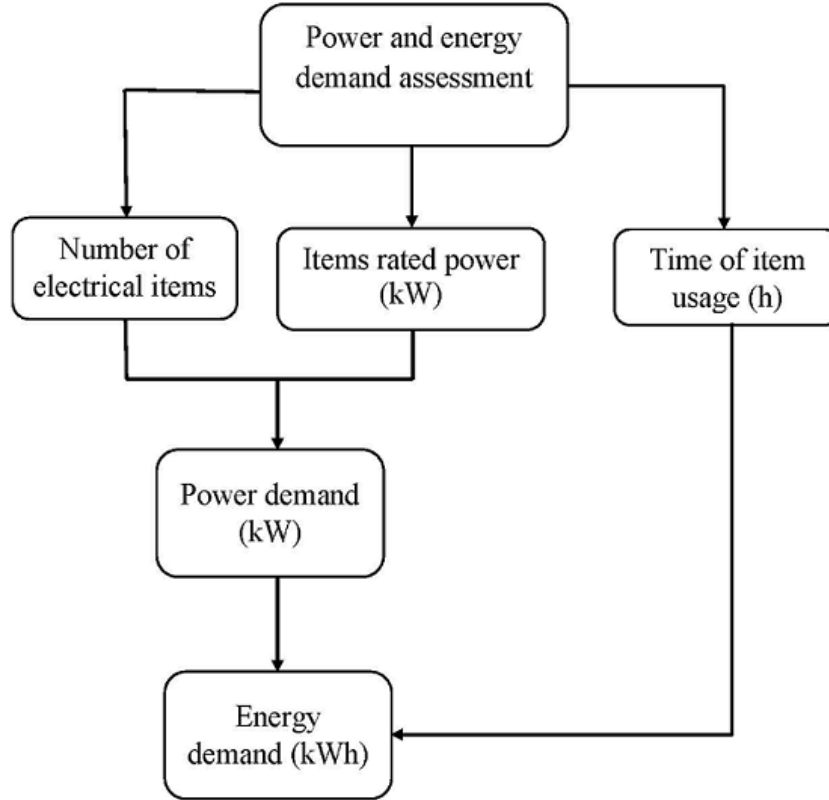


Figure 4.1: Power and energy demand determination

4.2.1 Energy demand determination methods

The Energy demand values has been calculated based the end user energy values using the actual energy demand values that were previously supplied by the diesel generators, battery storage, kerosene, and solar technologies in the village community. In this case the amount of power required at a particular time in a day is multiplied by the time of usage and number of electrical items. If a certainly amount of power is needed on a particular hour of the day, then its value is called the hourly energy demand. The hourly energy demand is determined using the following equation [149]:

$$E_{D(hourly)} = \sum_1^n (P_{D(hourly)} \times t) \quad (4.1)$$

where: $P_{D(hourly)}$ = hourly power demand value (kW), t = time of usage (hour) and n = number of electrical items

Then by using the above equation with average hourly energy demand, the daily average energy demand can be determined using the following equation:

$$E_{D(hourly \text{ avg})} = \frac{\Sigma E_{D(hourly)}}{24} \quad (4.2)$$

where: $E_{D(hourly \text{ avg})}$ = hourly average energy demand (kWh), $\Sigma E_{D(hourly)}$ = total hourly energy demand

$$\text{Alternatively, } E_{D(\text{hourly avg})} = \frac{1}{2}(P_{D(\text{hour1})} + P_{D(\text{hour2})}) (t_2 - t_1) \quad (4.3)$$

where: $P_{D(\text{hour1})}$ = demand power at time t_1 and t_1 = Time at the first hour

$P_{D(\text{hour2})}$ = Power at time t_2 and t_2 = Time at the next hour

At any particular time, when there is a prolonged period of energy usage of more than a month, the monthly average energy demand is determined by the following equation:

$$E_{D(\text{monthly avg})} = E_{D(\text{daily avg})} \times \text{days/month} \quad (4.4)$$

where: $E_{D(\text{monthly avg})}$ = monthly average energy demand (kWh/m) and $E_{D(\text{daily avg})}$ = daily average energy demand ($P_{D(\text{hourly})} \times 24\text{hours}$)

4.3 Power and energy demand determination

4.3.1 Household power and energy demand determination

The power and energy demand for each household in the village area have been estimated using the actual electrical equipment's and fixtures that the local houses own. Due to the unavailability of electricity in the study village, some of the houses uses small gasoline powered generators to provide electricity for lighting and power and others use solar powered technologies like the solar lantern. In this research study, the power and energy demand analysis have been taken into consideration electrical items the houses will have after the introduction of electricity. Thus, the current energy demand for the case study village have been considered for current 234 houses based on the field visit and feasibility study conducted in June/July 2016 that also shows that the population in the village area is between 1,000 to 1,500 people. The assumptions made in the study is that the power and energy supply used in the houses are mainly for lighting and power. So, no commercial facilities or small-scale industries that are attached to the household's electricity supply.

Based on the power rating of the electrical equipment's that are available in the houses in the research study village, the daily average energy demand for one household is computed to be 3.3 kWh/day. In the study, energy demand in the household have been categorizing into two areas, electricity demand for lighting, which is basically the energy demand required for lighting purposes and the second category is the energy demand for power which include all other electrical items in the houses. The maximum power demand value in each household that need to be supplied by the power sources have been calculated to be around 550 Watt as shown in detail in the Table 4.1 and Table 4.2 below.

Table 4.1: Domestic electricity allocated for a single household – Lighting
(actual values)

A: Electricity for Lighting						
S/N	Location	Number of bulb(s)	Wattage (W)	Time of usage	Time (hours/day)	Energy (Wh/day)
1	Kitchen	1	11	05:00 – 07:30	3	33
		1	11	18:00 – 22:00	4.5	49.5
2	Dining room	1	11	19:00 – 23:00	4.5	49.5
		2	7		4.5	63
3	Sitting room	2	11	18:00 – 23:00	5.5	121
		2	7		5.5	77
4	Room 1	1	11	18:00 – 23:30	6	66
		1	7		6	42
5	Room 2	1	11	18:00 – 23:30	6	66
6	Room 3	1	11	18:00 – 23:30	6	66
7	Toilet	1	7	18:00 – 00:00	6.5	45.5
8	Bathroom	1	7	18:00 – 21:00	3.5	24.5
9	Corridor	1	7	18:00 – 00:00	6.5	45.5
10	Security lights	4	9	18:00 – 06:00	12.5	450
11	Chicken house	2	40	18:00 – 22:30	5	400
Sum of bulbs Power (A)		260 Watt				1,598.5

Table 4.2: Domestic electricity allocated for a single household – Power (actual values)

B: Electricity for Power						
S/N	Location	Electrical Items	Wattage (W)	Time of usage	Time (hours/day)	Energy (Wh/day)
1	Kitchen	Small Microwave	55	06:30 – 07:30	1.5	82.5
			55	12:30 – 13:30	1.5	82.5
			55	19:00 – 20:00	1.5	82.5
		Small Refrigerator	80	14:00 – 17:30	4	320
		Small Juice Blender	40	12:30 – 13:30	1.5	60
2	Sitting room	Small TV	80	15:30 – 23:00	8	640
		Decoder	10	14:30 – 23:00	9	90
		Phone charging	10	14:30 – 23:00	9	90
			10	07:00 – 08:30	2	20
		Radio	15	06:00 – 23:00	17.5	262.5
Items Power demand (B)			290 Watt	Items Energy demand (B)		1,730
TOTAL POWER DEMAND (A + B)			550 Watt	TOTAL ENERGY DEMAND (A + B)		3,328.5

Due to the economic development and availability of electricity in few rural village areas of Tanzania in recent years, the above mentioned electrical items are standard in majority of semi-urban houses on areas with electricity supply and have been identified based on the current energy uses in the houses supplied by means of electrical generators and solar/battery storage facilities.

The standard house type in consideration for this research study consist of a maximum of 3 bedrooms, 1 kitchen, 1 sitting room, 1 dining room, 1 toilet and 1 bathroom. Although some houses may have less than 3 bedrooms which is the common house type in the village settings at the moment. This is because the village houses that have been used in this research study have been considered to cater for future economic development in the village area. The power demand estimation for lighting has been calculated based on utilizing energy saving light bulbs, which consumes less energy than that the standard light bulbs or halogen bulbs. During the feasibility study in the area, it has been found out that in few houses lighting demand is provided with solar light technologies from solar power which is expensive and few people can afford to buy those types of solar equipment's or sending the batteries for charging. This situation forced many families to rely on kerosene as a fuel for lighting in lamps and pays around 1 USD for a litre of kerosene which will last for less than a week and if used for cooking it may last for 2 days.

The hourly average power and energy demand value on each household and the entire study area have been determined based on the actual power consumption in the local village houses which has been computed on hourly basis for the 24 hours duration. Using the computed hourly average power demand on each household and in the study area, the energy demand has been calculated based on a numerical method using the trapezoidal system for the village community based on the actual power demand values as shown in Table 4.3 below.

Table 4.3: Power and energy demand values for each household (actual consumption)

Time of the day [Hour]	Actual power demand [W]	Hourly average power demand [W]	Energy demand on each hour [Wh]	Cumulative hourly energy demand [Wh]
00:00	50	43	43*	43.0
00:30	36			
01:00	36	36	36	79.0**
01:30	36			
02:00	36	36	36	115.0
02:30	36			
03:00	36	36	36	151.0
03:30	36			
04:00	36	36	36	187.0
04:30	36			
05:00	47	47	47	234.0
05:30	47			
06:00	62	71.5	71.5	305.5
06:30	81			
07:00	91	91	91	396.5
07:30	91			
08:00	25	25	25	421.5
08:30	25			
09:00	15	15	15	436.5
09:30	15			

Table 4.3 (continued)

Time of the day [Hour]	Actual power demand [W]	Hourly average power demand [W]	Energy demand on each hour [Wh]	Cumulative hourly energy demand [Wh]
10:00	15	15	15	451.5
10:30	15			
11:00	15	15	15	466.5
11:30	15			
12:00	15	60	60	526.5
12:30	105			
13:00	105	105	105	631.5
13:30	105			
14:00	95	105	105	736.5
14:30	115			
15:00	115	155	155	891.5
15:30	195			
16:00	195	195	195	1,086.5
16:30	195			
17:00	195	195	195	1,281.5
17:30	195			
18:00	339	339	339	1,620.5
18:30	339			
19:00	419	419	419	2,039.5
19:30	419			
20:00	419	391.5	391.5	2,431.0
20:30	364			
21:00	364	360.5	360.5	2,791.5
21:30	357			
22:00	357	351.5	351.5	3,143.0
22:30	346			
23:00	266	178	178	3,321.0
23:30	90			
Total daily power demand (24 hours)		3,321		
Average daily power demand		138.38		

Note*: Hourly energy demand = $\frac{1}{2}(50+36) (1) = 43$ Wh

** : Hourly cumulative energy demand = 43 Wh + 36 Wh = 79 Wh

The energy demand in the research study village has been estimated from the end user using the available rural energy supply practises which include the current diesel generators, batteries, kerosene and solar lanterns etc. Several households have been among the beneficiary for the project and in this study, the daily average power capacity for each household power demand has been set to 138.69 Watt mainly for lighting and power (due to huge end user demand in the area and based on rural electrification energy master plan). Based on the above computed 30 minutes and hourly average power demand values for a typical household, the energy demand values has been plotted to analyse the daily power demand curve of the household and its general characteristic for a typical rural village community in the research study area. From the results of the energy demand values, the overall daily energy demand value of 3.3 kWh/day has been considered as total daily energy demand for the village household which is around 1,204.5 kWh/year (365 days). This value resembles a typical value for the third world country household energy consumption like Tanzania as compared to energy consumption of around 3,100 kWh/year in the UK for a medium household [150].

Similarly the maximum power demand for the household have been estimated based on the total usage power demand and according to the feasibility studies in the study area, the maximum usage power demand value in the household is around 419 Watt while the power allocated is around 550 Watt as shown in Figure 4.2 below which is also aligned with the household rural energy supply from Rural Energy Agency - Tanzania on its rural energy master plan.

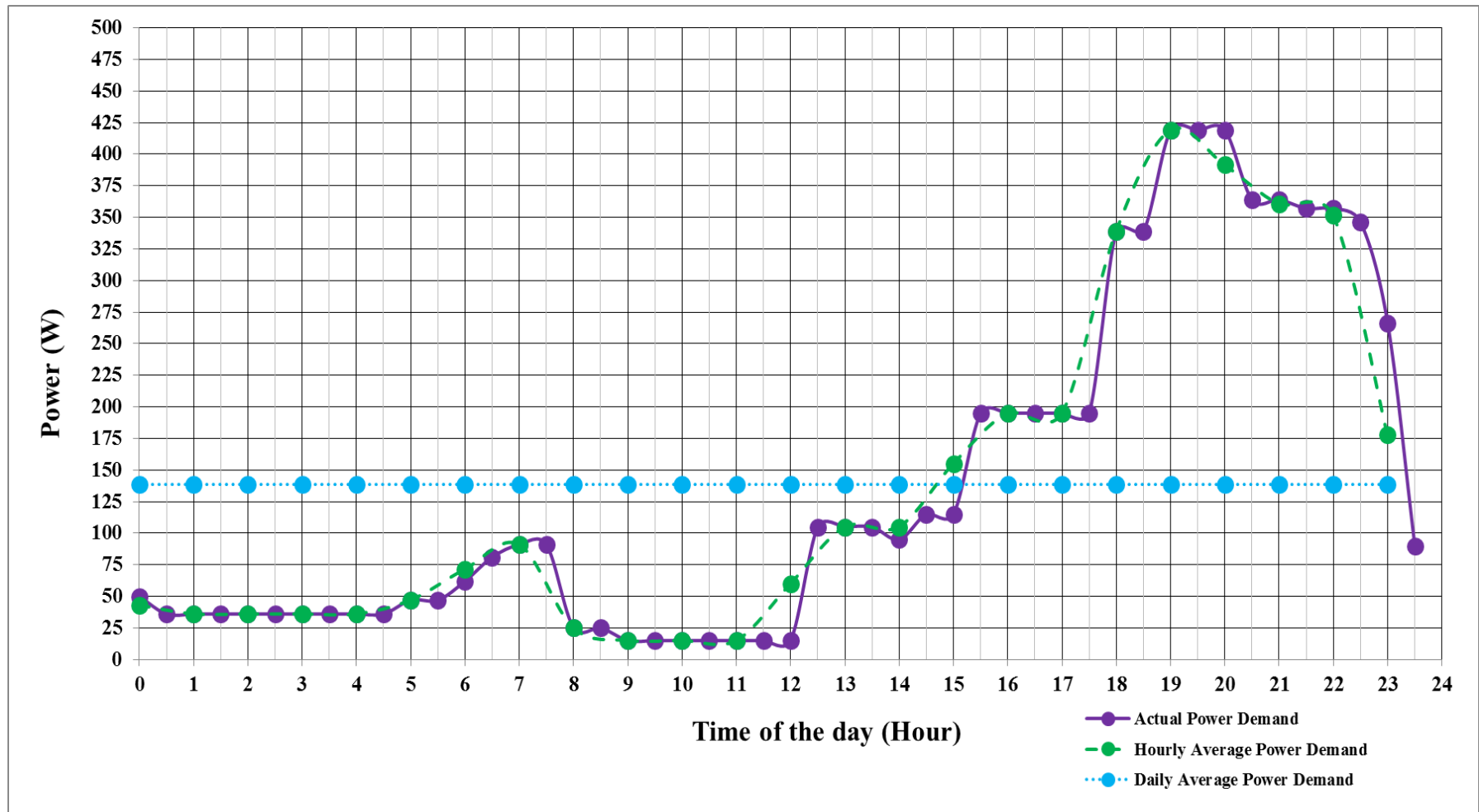


Figure 4.2: Actual power demand curve for a single household

In the research study village, the current population is around 1,250 people with the current total households of around 234. Based on the daily total energy demand per household which is 3.3 kWh/day and looking on daily power demand values on Figure 4.2 above, the minimum daily Power demand per household is a little bit low at 15 Watt between 9 am to 11 am because most of the electrical equipment's have been switched off due to the fact that majority of the occupancy in the house have gone to the farm, while kids have gone to school and others to their businesses. Similarly, the maximum power demand for a day is around 419 Watt which is found to be around 7 pm to 8 pm due to the fact that most of the people are back inside the house and also many electrical equipment's are switched on. On the other hand, the daily average power demand in each household is estimated to be 138.38 Watt based on the actual maximum and minimum power demand in the households. The power and energy values determination have been based on the fact that the main economic activity in the area is agriculture with other economy potential from small-scale farming of food and cash crops and also small-scale industries/business for timber and milling businesses.

Also, the household power demand curve highlights the time of the day when more power is needed (peak hours) and this is shown during the following times: breakfast time (6 am – 8 am), lunch time (12 noon – 14 hour) and also at night during dinner time (19 hour – 21 hour). The peak loads have been computed based on the number of electrical items that are switched on simultaneously at that particular time. The power for each household use may differ slightly from house to house or place to place but the hourly characteristic pattern for the daily power demand is likely to be the same with three distinctive high-power demand peaks. Urban areas may have higher power demand peaks above average than in rural area and also large family in the same house could increase the energy usage in same cases as well.

4.3.2 Total energy demand in the village community

4.3.2.1. Daily estimates

Since the economic activity in the area is improving, several industries, small businesses, shops, offices and schools have started and in this research study, a number of business end users have been included in the area during the determination of the total energy demand. The energy demand determination in this case, has been categorised into two areas, the current demand and future demand. The current energy demand has been obtained based on the field work and conducted feasibility study in the research site area while the

provision for the future energy demand estimation has been based on the percentage of population growth and economic activities in the area.

In this case, not only household energy demand are considered for the power/energy demand values, but there are other facilities that have also been included in the determination of power/ energy demand in the area. These include small industries like flour and timber mills, shops, small businesses, offices, schools, religious facilities etc. The daily energy demand determination is based on operating hours/day for each facility, a number of facilities available, their rating capacities in kW and operating days per month that is based on the number of weekdays and weekends. In this case, the current energy demand has been calculated based on the available items or facilities that require the supply of electrical power or that have been previously supplied by the diesel generators or solar technologies. Some of the available items include the current number of households in the case study area, small businesses, shops, offices, schools, health centres, social community centre etc. From the demand analysis and based on the total energy demand result values, the average energy demand per day is 1,114.38 kWh/day as shown in Table 4.4 below.

Table 4.4: Power and energy demand data for the community (actual values)

S/N	Time of the day [hour]	30 Minute's power demand [kW]	Hourly average power demand [kW]	Energy demand on each hour [kWh]	Cumulative hourly energy demand [kWh]
1	00:00	11.70	10.06	10.06*	10.06
2	00:30	8.42			
3	01:00	8.42	8.42	8.42	18.48**
4	01:30	8.42			
5	02:00	8.42	8.42	8.42	26.9
6	02:30	8.42			
7	03:00	8.42	8.42	8.42	35.32
8	03:30	8.42			
9	04:00	8.42	8.42	8.42	43.74
10	04:30	8.42			
11	05:00	11.00	11.00	11	54.74
12	05:30	11.00			

Table 4.4 (Continued)

S/N	Time of the day [hour]	30 Minute's power demand [kW]	Hourly average power demand [kW]	Energy demand on each hour [kWh]	Cumulative hourly energy demand [kWh]
13	06:00	14.51	16.73	16.73	71.47
14	06:30	18.95			
15	07:00	28.79	28.79	28.79	100.26
16	07:30	28.79			
17	08:00	33.85	33.85	33.85	134.11
18	08:30	33.85			
19	09:00	31.51	31.51	31.51	165.62
20	09:30	31.51			
21	10:00	45.51	45.51	45.51	211.13
22	10:30	45.51			
23	11:00	45.51	45.51	45.51	256.64
24	11:30	45.51			
25	12:00	47.09	56.83	56.83	313.47
26	12:30	66.57			
27	13:00	66.57	66.57	66.57	380.04
28	13:30	66.57			
29	14:00	62.73	65.07	65.07	445.11
30	14:30	67.41			
31	15:00	62.91	64.77	64.77	509.88
32	15:30	66.63			
33	16:00	66.63	60.38	60.38	570.26
34	16:30	54.13			
35	17:00	54.13	54.13	54.13	624.39
36	17:30	54.13			
37	18:00	87.83	87.33	87.33	711.72
38	18:30	86.83			

Table 4.4 (Continued)

S/N	Time of the day [hour]	30 Minute's power demand [kW]	Hourly average power demand [kW]	Energy demand on each hour [kWh]	Cumulative hourly energy demand [kWh]
39	19:00	105.55	101.80	101.8	813.52
40	19:30	98.05			
41	20:00	98.05	91.61	91.61	905.13
42	20:30	85.18			
43	21:00	85.18	84.36	84.36	989.49
44	21:30	83.54			
45	22:00	83.54	82.25	82.25	1071.74
46	22:30	80.96			
47	23:00	62.24	42.64	42.64	1,114.38
48	23:30	23.04			
Sum daily demand (24 hours)			1,114.38	1,114.38	-
Average daily power demand			46.43		

Note*: Hourly energy demand = $\frac{1}{2}(P_1 + P_2) (\Delta t) = \frac{1}{2} (11.70 + 8.42) (1) = 10.06$ kWh

** : Cumulative hourly energy demand = 10.06 kWh + 8.42 kWh = 18.48 kWh

The power and energy demand on each consumer power category have also been computed on each hour of the day and from the results, it is noted that maximum power demand is found at around 19:00 hours which is 101.8 kW. On the other hand, the minimum power demand value occurs during the mid-night hours between 1:00 AM to 4:00 AM. This is because most of the electrical load in the area are not operating. Due to this effect of low power demand value, most of the power supply from the power source may not be used and hence may accumulate as excess power to the energy system at the low energy demand hours on each day. In terms of daily energy demand for each category, the domestic use will consume 778.88 kWh/day while the productive use only takes 257.80 kWh/day and social infrastructure demand accounts for only 77.80 kWh/day. The combination of all the total energy demand values accounts for about 1,114.38 kWh/day as shown in Table 4.5 below.

Table 4.5: Hourly Power demand and daily energy demand values for the case study area

Time of the Day [Hour]	1	2	3	4	5	6	7	8	9	10	11	12	13	14	15	16	17	18	19	20	21	22	23	24	Daily Total Energy [kWh]
Domestic use [kW]	8.42	8.42	8.42	8.42	11	16.73	21.29	5.85	3.51	3.51	3.51	14.57	24.57	24.57	36.27	45.75	45.75	79.25	98.05	91.61	84.36	82.25	42.64	10.06	778.78
Productive use [kW]	0	0	0	0	0	0	7.5	17.5	17.5	31.5	31.5	31.59	31.5	31.5	24.5	13	8.38	8.08	3.75	0	0	0	0	0	257.80
Social Infrastructure [kW]	0	0	0	0	0	0	0	10.5	10.5	10.5	10.5	10.67	10.5	9	4	1.63	0	0	0	0	0	0	0	0	77.80
Hourly Total Power [kW]	8.42	8.42	8.42	8.42	11.00	16.73	28.79	33.85	31.51	45.51	45.51	56.83	66.57	65.07	64.77	60.38	54.13	87.33	101.80	91.61	84.36	82.25	42.64	10.06	1,114.38

The computed hourly power demand values from Table 4.5 above with different energy demand category can be presented using a bar chart to represent the daily load demand curve of village community. The plotted graph shows distinctive features for a typical load demand curve with low power demand (off-peak hours) during the mid-night hours, increased demand during the morning hours (breakfast time) and mid-day hours (lunch-time). The results also show peak power demand values during the evening hours at around 19:00 hours to 20:00 hours, which reflects the typical high-power demand values in most houses in a particular time of the day. The daily total energy computation has also considered the general energy usage between weekdays and weekends on which weekends households consume more energy compared to weekdays as shown on Figure 4.3 below for the computed hourly power demand values for the research study village community.

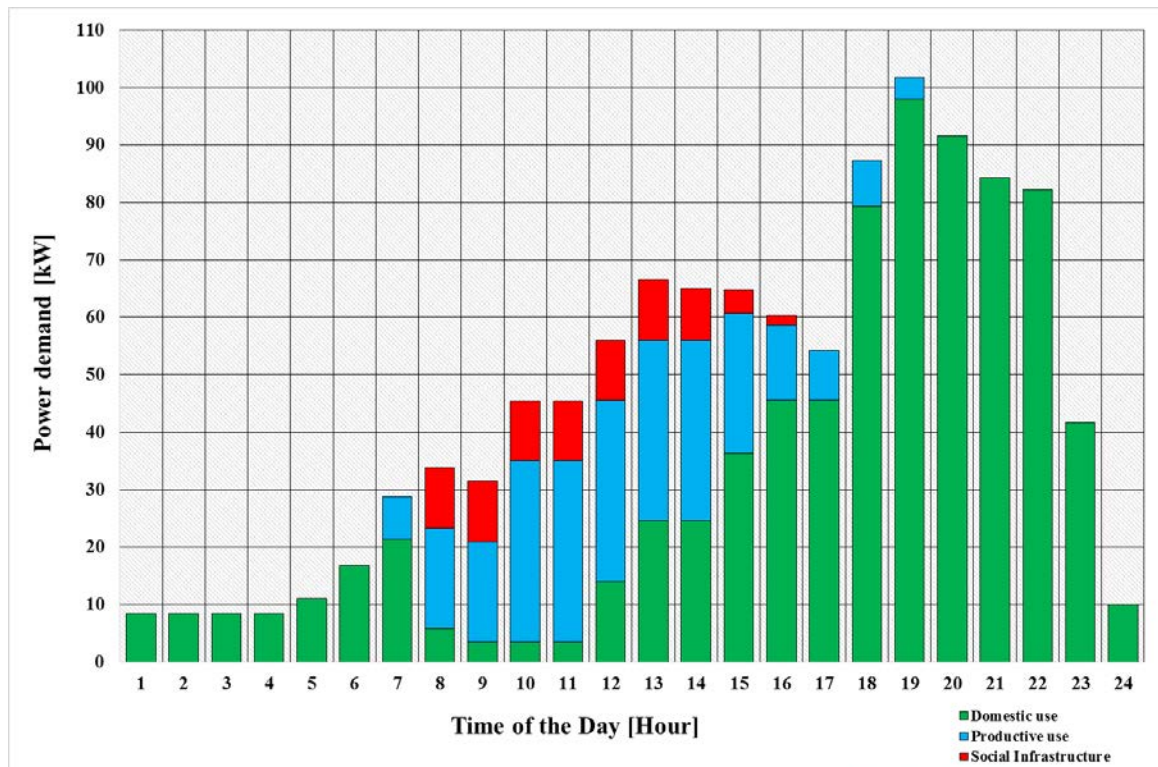


Figure 4.3: Power demand curve for the village study community

4.3.2.2 Monthly energy demand determination

During the feasibility study and field visit in the research village household, it was observed that during the daytime on weekdays (Mondays to Fridays), most of the family members are not staying in their houses. Parents go to farming or small businesses and children go to schools. This result to the reduction in energy consumption in the households during the daytime hours on weekdays. However, during the weekends, almost all the family members stay in the houses and this lead to more time of usage for the electrical items eg. more hours

on watching TV. In the daily energy determination, the power rating for each electrical item is multiplied by the duration (time) of usage. However, in determining monthly energy demand, both weekdays and weekends need to be considered separately as the energy consumption is not the same (low on weekdays and higher on weekends). Based on the household daily energy consumption results during the fieldwork, it was observed that there is an increase of 50% in the daily energy consumption during the weekends (Saturdays and Sundays) and this energy increase has been considered in the determination of the monthly average energy consumption.

By taking into consideration the hourly power demand, the total daily energy demand for the research study village has been determined to be 999.72 kWh/day and the monthly average energy demand have been calculated based on the following assumptions:

- (a) Daily average energy usage is not constant
- (b) For domestic use, weekends usage is 1.5 times more than the weekdays usage
- (c) The average number of days per month to be 30 days

These assumptions are based on the fact that energy usage varies between times of the day and days of the month. In calculating the monthly energy demand values, the energy determination have been based on total daily values and for the first month of January, the daily energy demand for the village community is 999.72 kWh/day.

This energy has been calculated based on the domestic energy use for the month of January by taking the average of 30 days (20 weekdays and 10 weekends) which gives the daily energy demand for domestic use (households) as 778.88 kWh/day.

So, $E_{D(\text{monthly domestic})} = E_{D(\text{daily domestic})} \times 20 \text{ weekdays} + E_{D(\text{daily domestic})} \times 1.5 \times 10 \text{ weekends}$
 where: $E_{D(\text{monthly domestic})}$ = monthly domestic energy demand and $E_{D(\text{daily domestic})}$ = daily domestic energy demand

This gives the monthly domestic use energy demand for January to be 27,243.2 kWh/month while the Total energy demand for domestic energy use, productive use and social infrastructure is calculated to be 35,907.7 kWh/month.

For the other months of February to December, the calculations method is the same and their computed values are obtained as shown in details in Table 4.6 below.

Table 4.6: Current monthly energy demand in the research study village community

S/N	Type of business	Qty	Average Power [kW]	Operating time of the day	Operating hours per day	Daily Energy demand [kWh]	Operating days per month	Monthly Energy demand [kWh]
A: Domestic use								
A.1	Households – Lighting & Power	234	0.13869	00:00 AM – 23:59 PM	24	778.88	30	27,243.2
Sub-Total A						778.88		27,243.2
B: Productive use								
B.1	Flour Mills	2	3.5	10:00 AM – 15:00 PM	5.5	38.5	25	962.50
B.2	Timber Mills	2	3.5	10:00 AM – 15:00 PM	5.5	38.5	25	962.50
B.3	Men Saloons	3	1.5	8:00 AM – 16:00 PM	8.5	38.25	25	956.25
B.4	Women Saloons	3	1.5	8:00 AM – 16:00 PM	8.5	38.25	25	956.25
B.5	Shops	5	1.5	7:00 AM – 19:00 PM	12.5	93.75	30	2,812.50
B.6	Mobile/battery charging	1	1	8:00 AM – 18:00 PM	10.5	10.5	30	315
Sub-Total B						257.75		6,965.0
C: Social infrastructure								
C.1	Social Centre	1	1.5	8:00 AM – 16:00 PM	8.5	12.75	25	318.75
C.2	Village Office	1	1	8:00 AM – 15:00 PM	7.5	7.5	25	187.50
C.3	Church	1	1.5	8:00 AM – 13:30 PM	6	9	12	108
C.4	Health Centre	1	2	8:00 AM – 16:00 PM	8.5	17	25	425
C.5	Schools	3	1.5	8:00 AM – 14:30 PM	7	31.5	20	630
Sub-Total C						77.75		1,669.25
TOTAL ENERGY DEMAND (A+B+C)						1,114.38		35,877.45

4.4 Summary

When analysing the research study village power demand values, the results shows that it is characterized by two (2) major distinct power demand pattern. The first part is the hours with the maximum power demand values on which the peak value reached up to 101.8 kW is at around 19:00 hours. This is when most of the family members are at home and therefore use several electrical equipment's especially in the kitchen for cooking, watching TV and electrical lights are switched on at this time of the day. Most of these electrical equipment's consume a considerable amount of electricity at this particular time of the day and hence when combining total load demand in the village area it results to a raised peak demand for electricity consumption. On the other hand, the second part shows the minimum power demand values (low demand hours) on which the lowest power demand value dropped to about 8.42 kW during the mid-night hours. Based on the analysed data, the daily average power demand value in the village community is 46.43 kW. The general trend shows that the power demand values are not constant and are characterised by a high power fluctuation which result to a big power range of 93.38 kW between the high peak and low peak power demand values and this effect need to be taken into consideration during the resource assessment of power supply options. The total daily energy demand for the village community in the research area is estimated to be 1,114.38 kW/h.

Chapter 5 Resources assessment for the case study site

5.1 Introduction

The Hhaynu micro-hydropower site is located in rural Mbulu district which is at the following latitudes and longitudes, -3.9631 South and 35.6219 East. The distance to the site location from Mbulu town centre is around 26 km using the roads that is in very bad condition. Several villages are located near the micro-hydropower site but because of the limitation in the project funding due to the remoteness of the site location which have increased the cost of power transmission. The closest village to the site location that have directly benefit with the local project development is called Kwermusl village. It is the nearby village to the site location and most of the local schools, health centre and businesses which are the main beneficiaries of the project are also located in this village. Despite the selection of Kwermusl village community as the main village area for the research study, the distance which will include the power transmission from the site location to the load centre in the village area is also a bit long which is about 5.87 km. Also, based on the nature of the site terrain and feasibility study report of the village power demand, the selected transmission distance to the village location is the most feasible in terms of accessibility and value for money as shown in Figure 5.1 below.

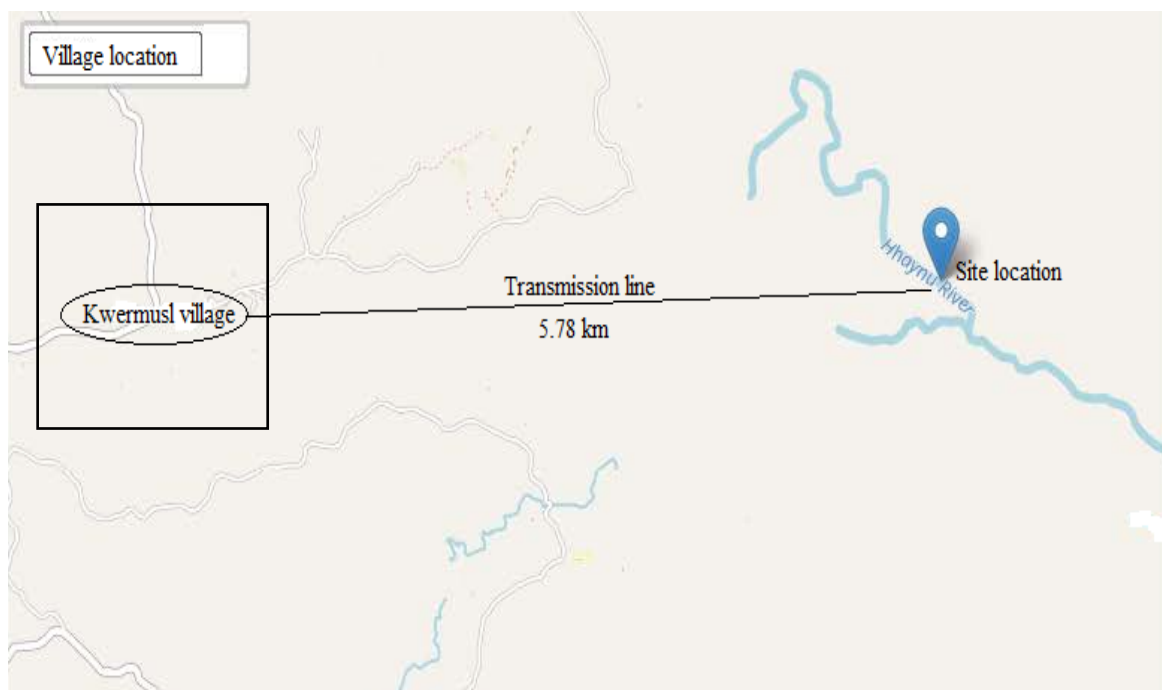


Figure 5.1: Village location in relation to the distance from the site area

The information and data for this research study have been gathered from the case study area which is in Mbulu district in Tanzania. This field work was conducted between June

to August 2016 on which the research team travelled to Mbulu district in Tanzania to do the site feasibility study. The data and information that have been collected include river volumetric flow, village population, site location and markings, meetings and planning for the project execution.

In the local area there a river called Hhaynu which has a gentle slope across the river-valley and a small fall along the river just near the site area. The site is located near the forest area which is the catchment where the river water sources come from and surrounded by agricultural land. The hills and river valleys in the site area contributed to the formation of the natural head for the water power to generate electricity. Due to its location in high altitude above 1,740m above sea level, the river banks consists of different types of rocks both on the surface and beneath the soil ground which made it difficult in the construction especially the civil works as shown on Figure 5.2 below.



Figure 5.2: Landscape of Hhaynu micro-hydro power site location

5.2 Methodology

The methods used in the resource assessment is basically based on the field work activities which include, data measurement and power/energy determination. The initial assessment was done to determine the power and energy demand in the area which form the basis for the resource assessment and data measurements. The obtained site information has been used as input parameters on the design and development of an energy system that will supply power to the consumer load demand. The following Figure 5.3 shows the methodology layout used for the field work and data measurement which include power and energy determination.

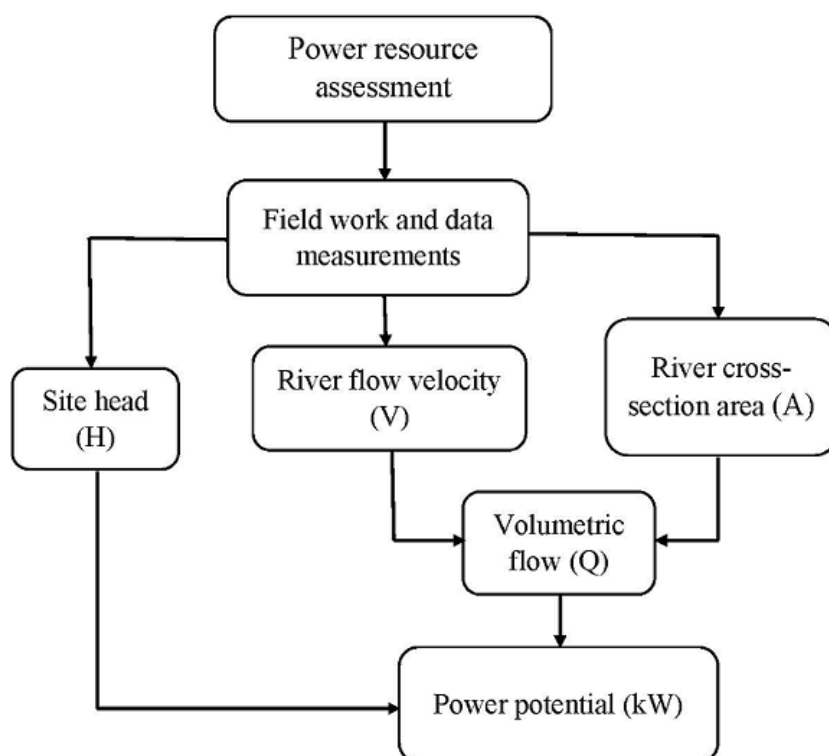


Figure 5.3: Resource assessment methods

5.3 Field work and data measurements

Based on the field work assessment for the energy resources in the research study area, the results show that there is an availability of Hhaynu river in the area which has the potential to develop a micro-hydro turbine system in the area. In order to determine the power and energy capacity that could be produced by the availability of water from the river, then the site data values need to be determined which include river flow velocity (U), river cross-section area (A) and site head (H). In the assessment methods, the first process is the

measurement of site head and then measurement of mean water flow velocity together with the determination of the cross-sectional area of the river.

The mean river flow velocity is the average water flow velocity that needs to be determined using the two commonly used flow velocity measurement methods, floating method and current meter method [151]. Both methods will be presented and analysed in detail in the following sub-sections.

5.4 Site head measurement

The difference in elevation from the intake to the power house area is called site head on which its value needs to be determined in order to calculate the site power potential. Different locations along the river in the site location were assessed to see the possibility of a power house location. According to the feasibility study and also actual field work site measurements, three (3) locations were identified for the possibility of power house location as shown in Figure 5.4 below.

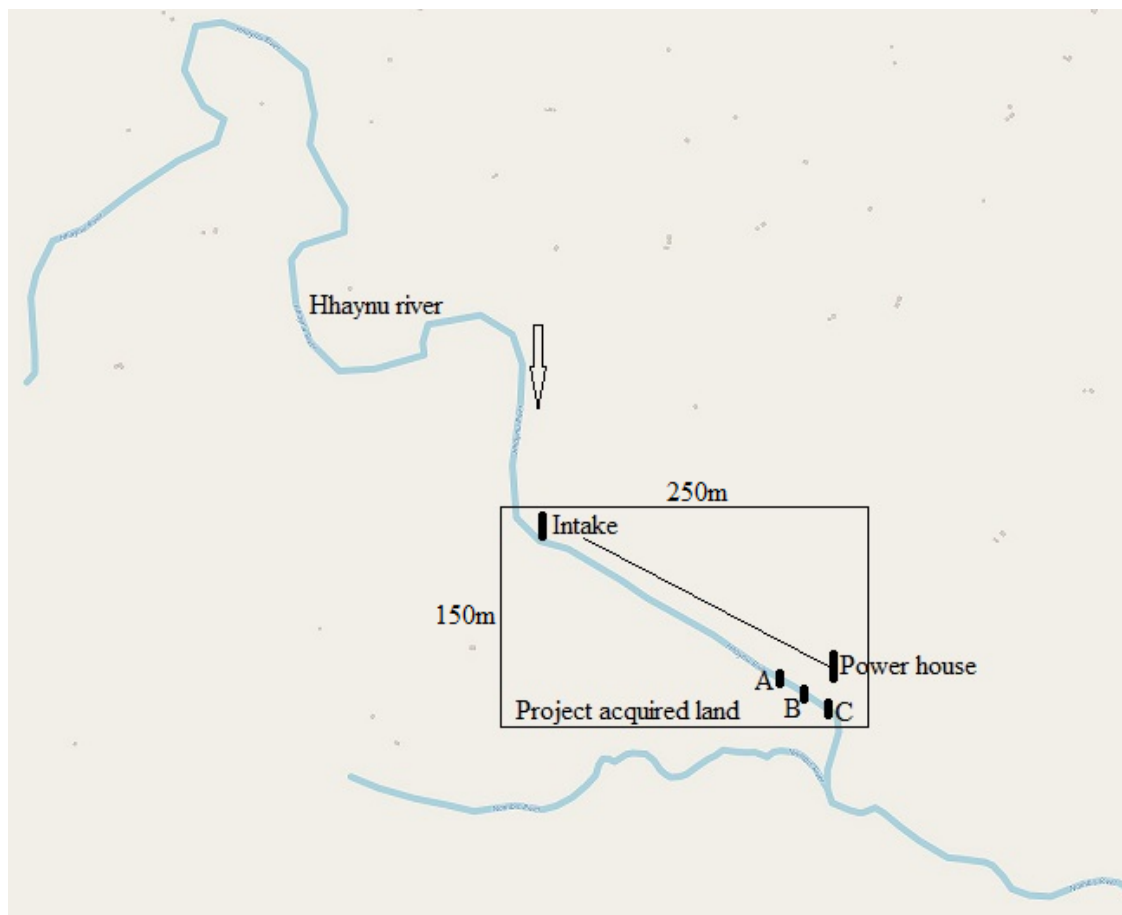


Figure 5.4: River flow layout and site location

The three (3) head measurement locations on the site were located based on the site topography, maximum head value and also possibility of power house construction. Based

on the site measurement, the head location at point A have the value of 18m while the head location at point B have the value of 22m and the head location at point C have the value of 25m. The determining factor for the site head has been based on the maximum head value, nature of topography which include accessibility and also possibility of power house construction with least cost as shown in Table 5.1 below.

Table 5.1: Evaluation of site head locations

Measured			
location	A	B	C
Head value	18m	22m	25m
Topography	Rocky	Steep slope	Gentle slope
Power house construction	Need rock blasting	Possibility of land slides	Good location
Remark	Minimum head	Medium head	Maximum head

The selected maximum site head value of 25m and its location along the river have been evaluated further to determine the length of penstock pipe that carries water from the forebay to the power house. From the site measurement results, the total linear length of the penstock pipe is around 162m as shown in Figure 5.5 below.

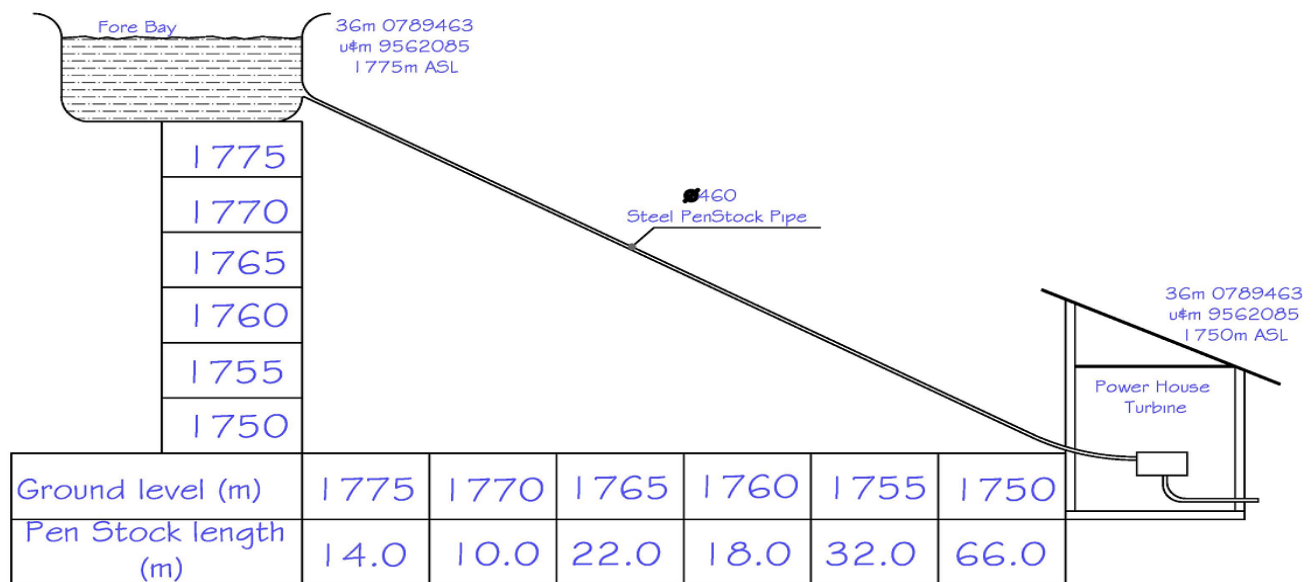


Figure 5.5: Penstock profile with site elevation

5.5 Water resource measurement methods

5.5.1 Floating object flow discharge measurement method

The floating method is a simple method to estimate the flow discharge of a river by estimate the flow velocity and cross section area. The flow velocity is estimated by measuring the time taken for a float to travel a pre-define distance downstream along the river. On the river profile, the water flow velocity is usually not that same across the river, it is usually slower at the river sides and river bottom and flow faster close to the river surface. Figure 5.6 below shows the water flow velocity profile across the river section.

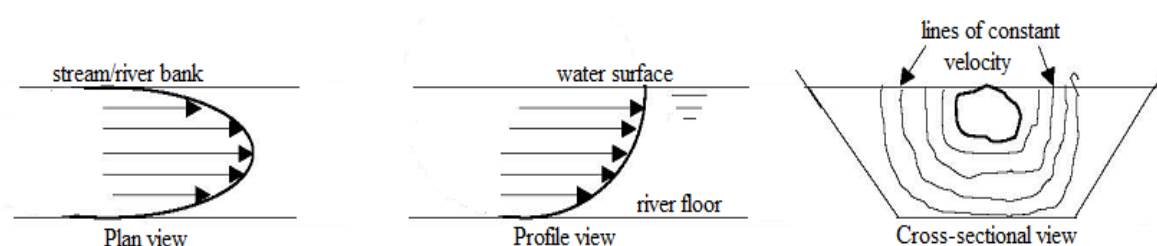


Figure 5.6: Water flow velocity profile across the river [152]

In this case, the floating object is positioned on the surface of the water, on a predefined distance and use a stopwatch to record the time for the floating object to move on predefined distance. This type of volumetric flow measurement method is mainly suitable for small and straight rivers flow area with low and medium flow velocity on fairly even and the regular regime which are the characteristics of Hhaynu river and is given by:

$$U = \frac{S}{t} \quad (5.1)$$

where S = distance travelled and t = time taken

To determine the average water flow velocity (U_m), the calculated flow velocity value have to be multiplied by a correction factor that take care of the river roughness coefficient and the factor ranges between 0.45 to 0.85 depending on the river flow depth and bank roughness (In this study 0.65 is taken as is a well-accepted value for small rivers like Hhaynu).

So, the corrected mean flow volume is calculated as follows:

$$U_m = 0.65 \times U_{surface} \quad (5.2)$$

where: $U_{surface}$ = surface flow velocity

5.5.2 Current meter method

The current meter is an instrument used to measure the flow velocity of flowing water in canals and rivers. It has a rotating small propeller which is turned by the flowing water on

the river. The current meter measurement method determines the water flow velocity across the river depth (top to bottom) and along the river width. The instrument uses a propeller that is connected to a rotating counter which records the number of rotations the propeller rotates when immersed in river water flow as shown on Figure 5.7 and the measurement values obtained after measurements using the current meter are recorded at each point measuring point.

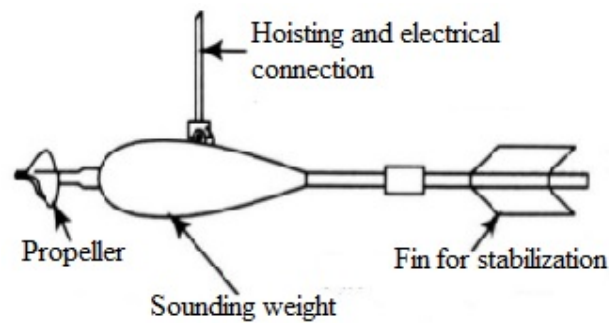


Figure 5.7: A propeller type current meter [153]

During the fieldwork and site measurements with a current meter, the cross-section of the Hhaynu river was measured to be 6 metre and was divided into 20 strips of equal width of 30cm. In current meter water flow velocity measurement method, the mean water flow velocity for each segment is determined from the average of the velocities measured at 20%, 60% and 80% of the depth on each section.

In calculating the water flow rate, the measured mean flow velocities at each strip are multiplied with an area of that strip which gives the flowrate for the particular strip. The total flowrate is now the sum of the individual strips as calculated below using one-point, two-point and three-point current meter measurement methods.

5.5.2.1 One-point measurement

In the one-point measurement, the mean velocity for each segment is estimated from the average of the velocities measured at 60% of the river depth level.

$$U_{mean} = U_{0.6} \quad (5.3)$$

This is usually applicable in shallow water where the water depth is limited and cannot accommodate the two or three point measurement methods.

5.5.2.2 Two-point measurement

In order to make accurate flow velocity estimation, the average water flows velocity determined by taking two readings in each sub-section measured at 20% depth level and 80% depth level.

$$U_{mean} = 0.5(U_{0.2} + U_{0.8}) \quad (5.4)$$

5.5.2.3 Three-point measurement

The three-point current meter flow velocity measurement method involves measuring the velocities at 0.2h, 0.6h and 0.8h of the depth of each strip as shown on Figure 5.8 below and the mean water velocity is calculated using the following formula:

$$U_{mean} = 0.25(U_{0.2} + 2U_{0.6} + U_{0.8}) \quad (5.5)$$

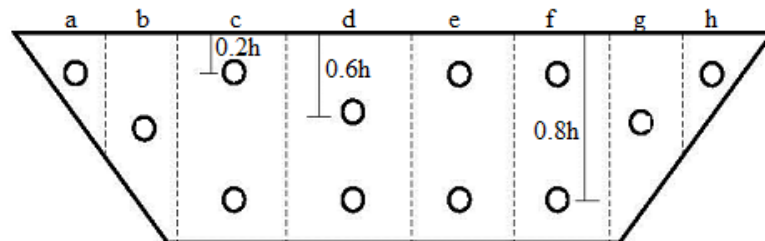


Figure 5.8: Flow velocity measurements depths [154]

○ = point of velocity measurement and h = measured depth

5.6 River cross-section area measurement

Cross-sectional shapes of rivers vary with the location and terrain along the river section which affects the water flow velocity and discharge. The deepest part of the river section occurs where the stream velocity is the highest, an example in steep slopes, gorges, canyons and mountain areas. Both river width and river depth may increase downstream because water discharge is sometimes increased downstream due to the river tributaries that join the main river. As river water flow discharge increases the cross-sectional shape of the river will also change to accommodate the increased amount of water volume and this result to the increased size of the river in terms of depth and width as shown in Figure 5.9 below.

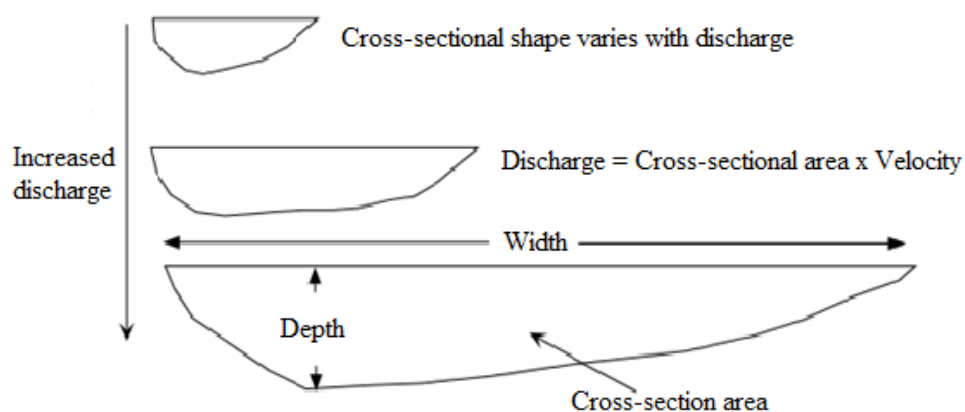


Figure 5.9: River cross-sectional area shape showing length and width

As the depth of the river is non-uniform across the river width, the correct method in cross-section area calculation is to divide the river width into sub-sections of equal size of at least 30cm and determine the depth of each sub-section. The river cross-sectional area

for each sub-section is calculated multiplying section width with the section height for each strip and the total area is estimated by summing up the individual strip areas as shown in Figure 5.10 and Figure 5.11 below.

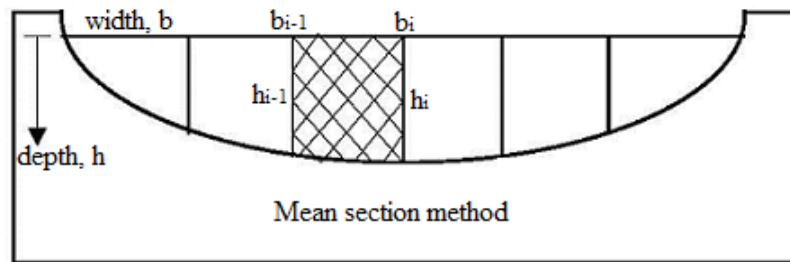


Figure 5.10: Model river sub-sections along the river cross-section area [154]

Based on the river sub-sections of the above Figure 5.10, the average river cross-sectional area A is given by the following equation:

$$A = \left(\frac{h_{i-1} + h_i}{2}\right)(b_i - b_{i-1}) \quad 5.6$$

where h = river depth and b = width (distance of measuring point (i) from a river bank datum), $i = 1^{\text{st}}$ to n^{th} measured points



Figure 5.11: Hhaynu river cross-section area measurement

In this case, the estimated average river flow discharge Q on is given by the following equation:

$$Q = \left(\frac{U_{i-1} + U_i}{2}\right)\left(\frac{h_{i-1} + h_i}{2}\right)(b_i - b_{i-1}) \quad (5.7)$$

where U = water flow velocity

The accurate area calculation on each divided strip is estimated by diving each strip into rectangular and triangle shapes depending on each stream on the river profile the individual areas for each river strip.



Figure 5.12: Hhaynu river depth measurement

In the Hhaynu river cross-section area measurement, 21 strips were divided along the length of the river and each about 0.3m wide which gives the river width of about 6.3m at that particular area measurement location. On the other hand, the maximum depth of the river at the measurement location is 0.9m on the edges of the river width while the minimum river depth is around 0.65m at the mid-section of the river depth. The calculated values for the river cross section area based on sub-sections in Figure 5.13 and calculated as shown in Figure 5.13.

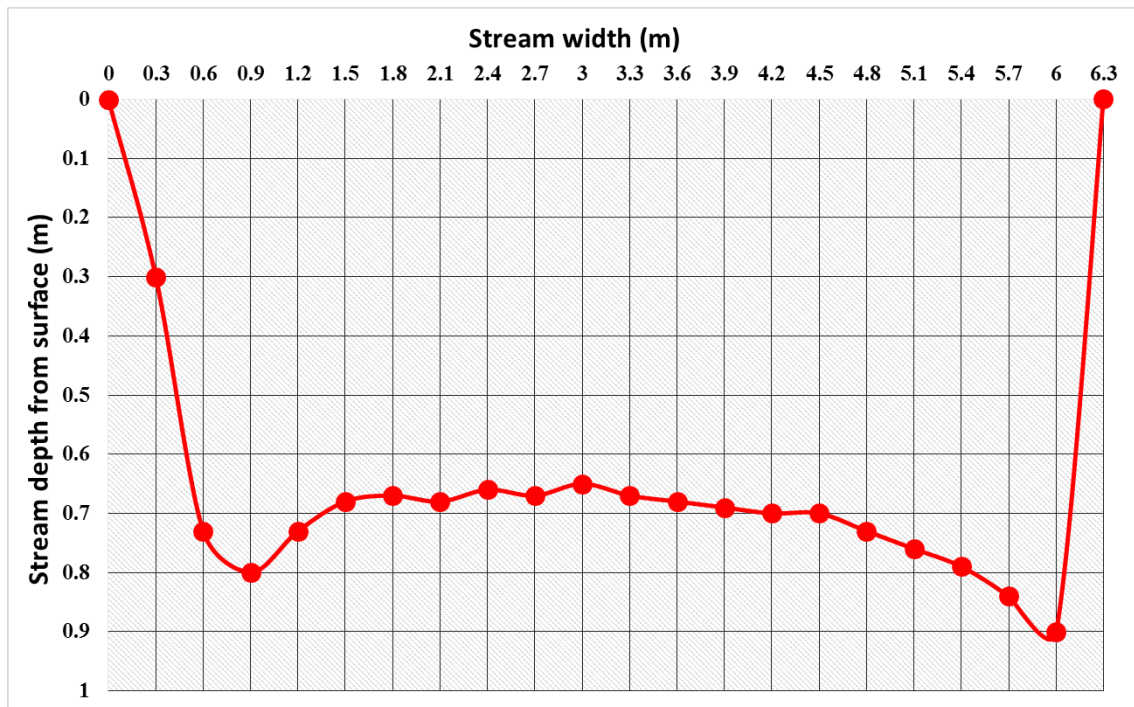


Figure 5.13: Hhaynu river depth profile and width sub-sections at the measurement location

The results from the measurement of the river cross-section area using strips or sections show that the river at the measured point is having a cross-sectional area of 4.09 m² and this value will be used to calculate the river flow discharge as shown below.



Figure 5.14: Hhaynu river flow velocity and area calculations

So, in order to determine the volumetric flow value (Q) of the river, the obtained mean water flow velocity (U) is multiplied by the cross-sectional area (A) as shown in the following equation:

$$Q = A \times U_{mean} \quad (5.8)$$

where: Q = river flow discharge (m^3/s), A = river cross-sectional area (m^2) and U_{mean} = average river velocity (m/s)

5.8 Flow velocity and discharge measurement results

In order to determine the power supply capacity that can be produced from the available local river water resource, the amount of water flow discharge Q , need to be determined on which the power supply capacity will then be established. In determining the water flow discharge value Q , the water flow velocity U and the river cross sectional area A , have to be determined first. In this research, two types of river flow velocity measurement methods have been used, floating method and the use of current meter flow velocity measurement me. Both measurement methods have been applied and compared and the measurement results for each measurement method is shown in the following sub-sections.

5.8.1 Floating method flow velocity measurement results

During the site measurements in determining river flow velocity using the floating method, at least 10 readings were taken for a floating object to move on the surface of a river for a distance of about 3 meters and their values are recorded. The drawback of this measurement method is that the river cross-sectional area may be difficult to determine, especially when the river banks at the measurement location is not uniform. The analysed data from the floating method shows that the average river flow discharge value of $0.92 \text{ m}^3/\text{s}$ is obtained which is very close to the site measured value of June 2016 which is around $0.90 \text{ m}^3/\text{s}$.

It has been noted that the accuracy of this method is influenced by the human error and the number of readings taken and also the river cross section area calculation method that has been used. One of the ways to reduce this measurement error is to compute the average of at least 5 measurement readings and also put a reasonable distance for the floating object to travel from the starting area to the finishing point of at least five meters.

The calculated river flow velocity and discharge measurement in this method has been validated using a pre-define water flow structure with a known volume (width, length and height) using known unit scale sizes from zero as the start point to one metre as the end

point. In this case, the floating object is used as an object to determine the time taken for it to travel from the starting point zero meters to the end point at a distance of at least 1 m as shown on Figure 5.15 below.

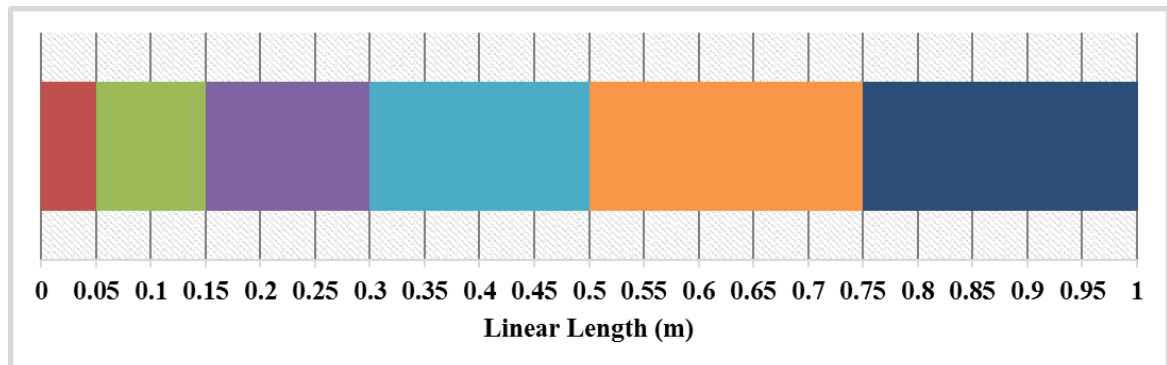


Figure 5.15: A linear scale for the travelling distance of the floating object

The dimensions of the water flowing structure is a small rectangular shaped channel of 0.4m high, 0.6m wide and 1m long with the pre-determined water flow volume of 69.4 litres/second as shown on Figure 5.16 below.

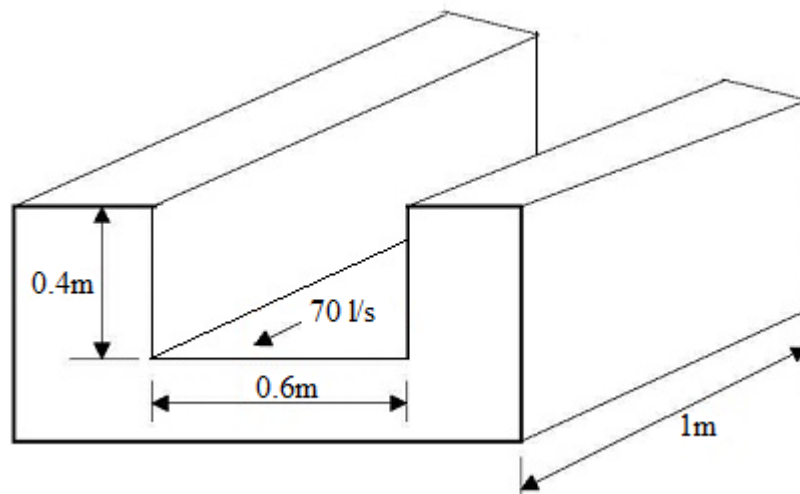


Figure 5.16: Pre-defined flow channel dimensions

To calculate the channel volumetric flow the following formula is used:

$$Q = U \times A \quad (5.9)$$

Re-arranging;

$$U = \frac{Q}{A} = 0.28 \text{ m/s}$$

This is the water flow velocity through the given channel,

where area $A = 0.24 \text{ m}^2$ and assume flow discharge $Q = 0.07 \text{ m}^3/\text{s}$

So, for the case of time taken for the water to travel pre-defined distance of 1m;

$$\text{Time } t = \frac{L}{U} = 3.57 \text{ seconds}$$

where length $L = 1 \text{ m}$ and velocity $U = 0.28 \text{ m/s}$

5.8.2 Current meter flow velocity measurement results

In the current meter river flow measurements method at least twenty (20) readings were taken for the flow velocity values at 20% river depth level, 60% river depth level and 80% river depth level. In the current meter river flow velocity measurement method, the specification of the measuring instrument used, i.e. Geopacks Advanced Stream Flow Meter with Model - ZMFP126-S and serial number PGL-3610-B which have water flow velocity measuring range between 0.05 m/s to 8.0 m/s and with the accuracy of around $\pm 7\%$.

Before site measurements, the current meter was calibrated using the pre-defined Trapezoidal section structure with known water flow velocity and discharge values using equation defined from Figure 5.17 below.

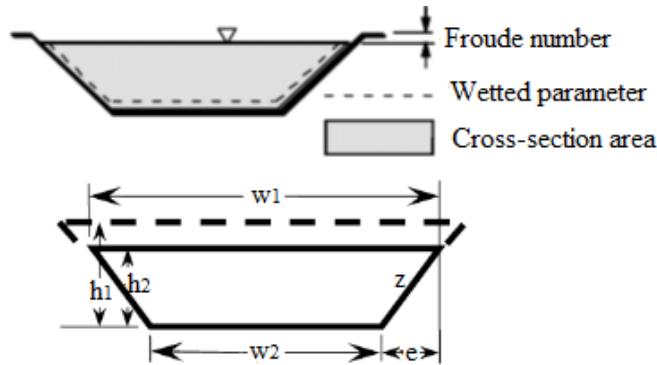


Figure 5.17: Pre-defined structure for flow velocity measurement

In this case the cross-sectional area, $A = \frac{1}{2}(w_1 + w_2) \times h_2$

Note: $z = h_2\sqrt{(1 + e^2)}$ and $w_1 = w_2 + 2e$

The used trapezoidal channel dimensions are as follows: $w_1 = 0.9\text{m}$, $h_2 = 0.4\text{m}$, $w_2 = 0.4\text{m}$, $e = 0.25\text{m}$ and $z = 0.412\text{m}$

So, from the above values, the average flow velocity (m/s) is given by;

$$U = \frac{Q}{A} \quad (5.10)$$

U = flow velocity, Q = flow discharge ($0.07 \text{ m}^3/\text{s}$) and A = cross-sectional area (0.26 m^2)

This gives the average water flow velocity value for the above designed channel size to be 0.269 m/s .

5.8.3 Flow discharge determination

From the measurement and calculations results in Table 5.2 below, it is shown that three-point water flow velocity measurement method with more divisions across the river width gives more accurate results for the river discharge value as compared to one-point flow

measurement, two-point flow measurement and the floating method. In the above accurate method, the obtained discharge value for Hhaynu river from the site measurements is 0.90 m³/s which will be used in this research study.

From the results on Table 5.2 below it is noted that one-point discharge measurement method produces +10% less accurate results than the three-point discharge measurement method and the two point discharge measurement method produce -6.7% less accurate results than the three point discharge measurement method. In this case, the error margin for the one point and the two points velocity/discharge measurement method compare the more accurate three-point measurement method is within $\pm 10\%$ margin. This is also valid to the simple river flow velocity measurement method by using a floating object which in this research study it produces only +2% less accurate flow velocity results than the three points current meter measurement method as shown in Table 5.2 below.

Alternatively, the site flow discharge, Q_{site} can be calculated if the catchment area of the local river is known together with the rainfall available data either in daily or monthly average. In this case the catchment area is the area on which the rain run-off flows into the river regime. For run-off of the river hydro power scheme, the site flow discharge (Q_{site}) is given by the following equation [155].

$$Q_{site} = S_f \left[\frac{A_{site}}{A_{Catchment}} \right] Q_{catchment} \quad (5.11)$$

where from site data, Q_{site} = river flow average discharge at the site location (0.9 m³/s), $Q_{catchment}$ = catchment flow discharge from the run-off (23.5 m³/s), A_{site} = site area (37,500 m²), $A_{catchment}$ = catchment area (112,500 m²) and S_f = scaling factor (0.115)

Table 5.2: Hhaynu river flow velocity and flow discharge measured values

Section/strip	Flow velocity (m/s)			Mean velocity: 1 point measuring method	Mean Velocity: 2 points measuring method	Mean Velocity: 3 points measuring method	Section/strip Area (m ²)	Flowrate: 1 Point measuring method [0.6h] (m ³ /s)	Flowrate: 2 points measuring method [0.2h]	Flowrate: 3 points measuring method [0.2h, 0.6h and 0.8h] (m ³ /s)
	0.2h	0.8h	0.6h	$U_{mean}=U_{0.6}$	$U_{mean}=0.5(U_{0.2}+U_{0.8})$	$U_{mean}=0.25(U_{0.2}+2U_{0.6}+U_{0.8})$				
1	-	-	0.14	0.14	-	-	0.05	0.01	-	-
2	0.11	0.14	0.22	0.22	0.13	0.17	0.15	0.03	0.02	0.03
3	0.2	0.14	0.16	0.16	0.17	0.17	0.23	0.04	0.04	0.04
4	0.24	0.19	0.46	0.46	0.22	0.34	0.23	0.11	0.05	0.08
5	0.21	0.23	0.27	0.27	0.22	0.25	0.21	0.06	0.05	0.05
6	0.25	0.21	0.22	0.22	0.23	0.23	0.2	0.04	0.05	0.05
7	0.23	0.25	0.18	0.18	0.24	0.21	0.2	0.04	0.05	0.04
8	0.23	0.33	0.24	0.24	0.28	0.26	0.2	0.05	0.06	0.05
9	0.14	0.23	0.23	0.23	0.19	0.21	0.2	0.05	0.04	0.04
10	0.22	0.32	0.3	0.3	0.27	0.29	0.2	0.06	0.05	0.06
11	0.27	0.22	0.28	0.28	0.25	0.26	0.2	0.06	0.05	0.05
12	0.31	0.23	0.26	0.26	0.27	0.27	0.2	0.05	0.05	0.05
13	0.21	0.27	0.26	0.26	0.24	0.25	0.21	0.05	0.05	0.05
14	0.24	0.28	0.29	0.29	0.26	0.28	0.21	0.06	0.05	0.06
15	0.25	0.23	0.29	0.29	0.24	0.27	0.22	0.06	0.05	0.06
16	0.18	0.27	0.16	0.16	0.23	0.19	0.23	0.04	0.05	0.04
17	0.18	0.16	0.22	0.22	0.17	0.20	0.23	0.05	0.04	0.04
18	0.18	0.18	0.23	0.23	0.18	0.21	0.24	0.06	0.04	0.05
19	0.2	0.17	0.25	0.25	0.19	0.22	0.26	0.07	0.05	0.06
20	-	-	0.09	0.09	-	-	0.22	0.02	-	-
TOTAL								0.99	0.84	0.90

5.8.4 Validation of flow discharge measurement values

To validate the measured values of river flow discharge, a hydrological study for the Hhaynu river have been conducted. This is based on both measured and historical data for the river flow in a certainly period. In this case, the site measured and determined river flow discharge values is compared with the historical flow discharge values using flow duration curves.

The monthly average volumetric flow for Hhaynu river has been measured and analysed for a period of more than a year. Also, the historical river flow regime from the previous river flow discharge data values which are the recorded volume of river flow for the past several years have also been analysed. The historical river flow data were obtained from the local river basin authority and they represent the actual volumetric river flow for the period from 1985 to 2007 [156]. The obtained historical river flow values have been computed and analysed to obtain the monthly average and compared with the site measured volumetric river flow values as shown in Table 5.3 below.

Table 5.3: Historical and site measured monthly discharge values [156]

Month	Measured average river flow (Sept.2015-Aug.2016) [m³/s]	Historical average river flow (1985-2007) [m³/s]	The difference in flow (Site measured – Historical) [m³/s]
January	0.84	0.89	-0.05
February	0.83	0.82	0.01
March	1.22	1.14	0.08
April	2.30	2.66	-0.36
May	1.59	1.63	-0.04
June	0.90	0.96	-0.06
July	0.74	0.76	-0.02
August	0.66	0.68	-0.02
September	0.62	0.64	-0.02
October	0.60	0.60	0
November	1.05	0.98	0.07
December	1.01	0.92	0.09
Average	1.030	1.057	-

Note: The negative numbers on the flowrate difference column values are the ones below a minimum value and positive values are the ones above a minimum value. Minimum discharge value is obtained in the month of October on which the river flow discharge value is at 0.60 m³/s.

The historical data have been used to validate the site measured data and the general trend shows that both data show similar patterns with high discharge in March, April and May due to a lot of rains in the area and low discharge in September and October due to relatively dry weather in the area. The historical data has a bit high discharge values in many months due to the fact that there was a lot of volumetric water flow to the river in the area because of less environmental degradation eg. Deforestation and farming activities near the river banks and in recent years irrigation activities have increased which resulted in the reduction of the river volume significantly. Now days these activities are practised in the local villages in most rural areas and affect significantly the river flow pattern due to their effects on rainfall and run-off.

From the theoretical design point of view, the high-water volume during the rain months could be stored in a reservoir and used during the dry months to produce additional energy required from the demand. But in many micro scale schemes this idea may not be feasible options due to the fact that it requires additional facilities for the reservoir which in turn will increase the project cost duet to the acquisition of land and compensations and also the landscape need to be favourable to support the additional reservoir structure which is not for the case for Hhaynu hydropower project.

The maximum difference in value between the site measured river flow values and historical river flow values ranges between $0.36 \text{ m}^3/\text{s}$ below the minimum value (i.e. negative) to $0.09 \text{ m}^3/\text{s}$ above the minimum value (i.e. positive). In this research study, the amount of flow discharge value that is utilized for the turbine system design is around $0.45 \text{ m}^3/\text{s}$ which is the discharge value available for both measured data and historical data when considering environmental flow. So, in this case, the minimum residual flow around $0.15 \text{ m}^3/\text{s}$ (150 l/s) which is mostly available during the dry month of October based on the fact that there is no depleted reach on the river flow throughout the year as shown on Figure 5.18 below.

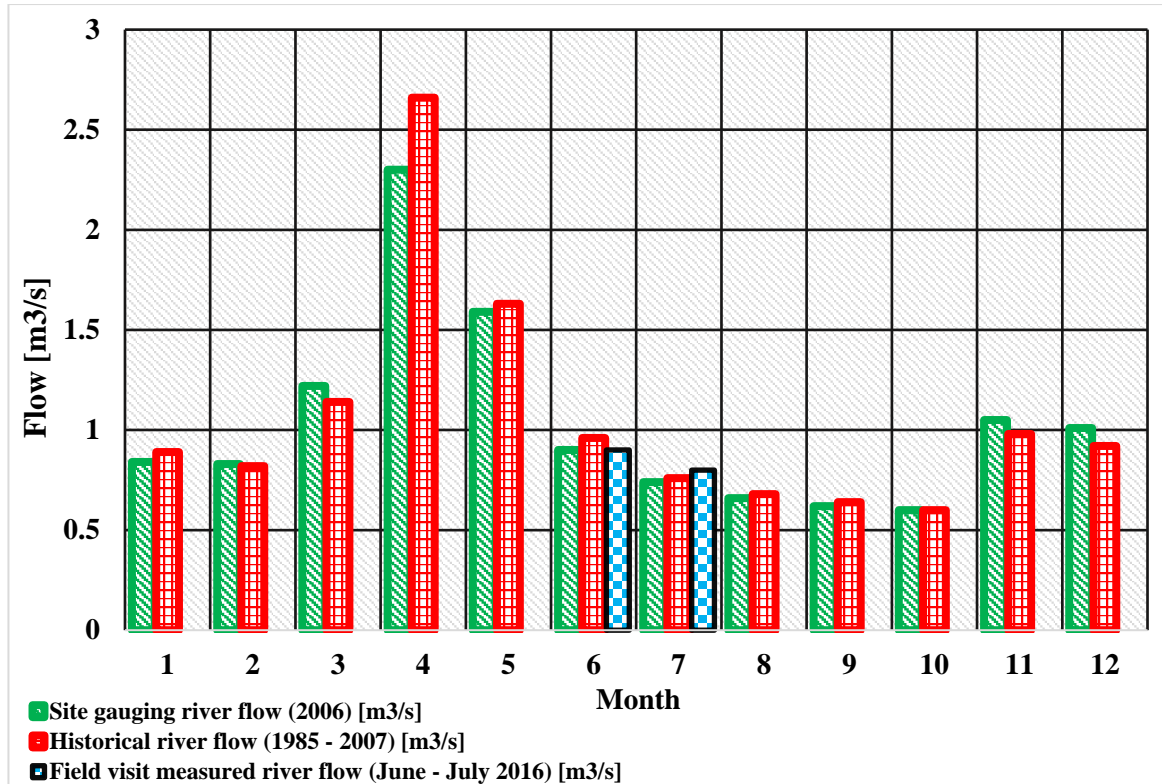


Figure 5.18: Hhaynu river water flow capacity - measured and historical flowrate

The minimum water flows discharge amount that may be available for power generation throughout the year for both the site measured data and historical data when not having an intake with a pondage (weir) for small water storage is around $0.6\text{m}^3/\text{s}$. In consideration of the residual flow, the value of $0.45\text{m}^3/\text{s}$ will be used as the turbine design base flow discharge for the Hhaynu river. The annual Hhaynu river hydrograph with the daily river flow and residual flow is shown in Figure 5.19 below.

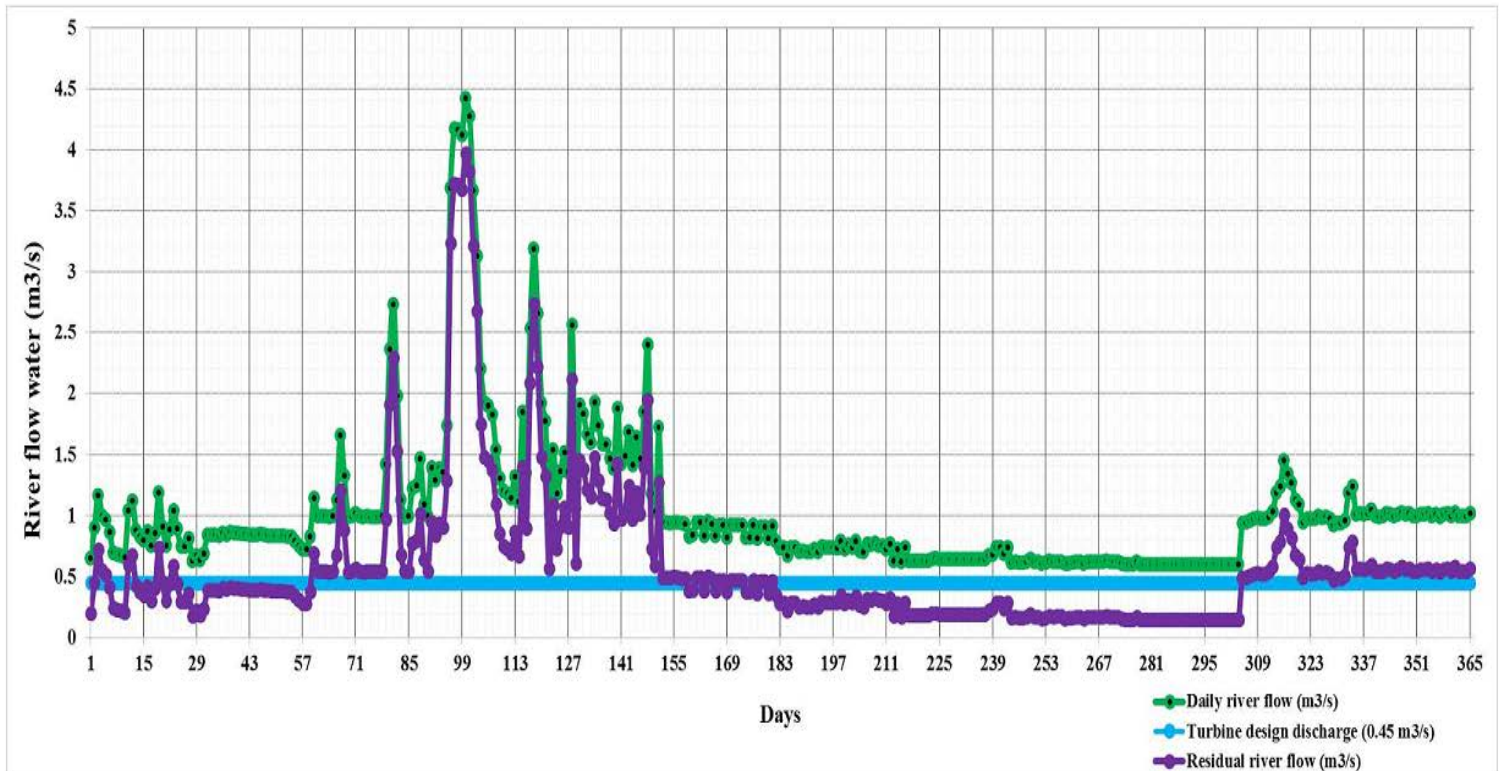


Figure 5.19: Annual Hhaynu river hydrograph

5.8.5 Importance and limitations of flow discharge measurement methods

In order to estimate and calculate the amount of water flow volume in a particular river, several parameters need to be measured. The flow volume on rivers depends on the two main parameters that need to be determined on site which are the water flow velocity and the river cross-section area at the point of measurement. The cross-section area measurements are obtained by the river width and the river depth at a particular river section. Since most rivers are not uniform in terms of their depth and width, this method of cross-section area measurements needs to be sub-divided into sections in order to reduce the error during the measurement because of un-even nature of river profile. Due to the varying depths in most of the river profile, the used method of river flow velocity measurement is limited to areas with wider and uniform depth and its values obtained from the measurements and calculation are the average values.

On the other hand, in the flow velocity measurement methods, different techniques are used but the common and more accurate method is the three-point measurement method on which water flow velocity is measured at three different water depths. This is because water flows at different speed across the river depth on which the water has medium speed at the top-section, high speed at the mid-section and low speed at the bottom-section. So, due to this phenomenon, the water flow velocity on rivers need to be taken at different heights

along the river depth and also repeating the measurements, in order to reduce the error in measurement. Although this measurement method seems to be more accurate than the other velocity measurement methods the downside is that it needs the use of velocity measurement instruments which have to be calibrated before use. In addition to that, the river flow at the point of velocity measurements needs to be quasi steady with average flow speed which is not common on small rivers like Hhaynu on hill side locations at the measurement point which is close to the catchment area.

5.8.6 Water flow discharge duration curve determination

During the fieldwork and data analysis, a total of 8,280 stage river flow data have been analysed that were recorded from January 1985 to December 2007 and these are the latest data available from Hhaynu river basin. The site data collection was done during the site Field visit which was conducted on June to July of 2016 on which the water volumetric flow height gauge was at 50.25cm which corresponds to a flow discharge of 0.90 m³/s. The site measurements were done during the dry season of the year on which the measured volumetric flow value seems to be close to the mean flow rate Q_{mean} of 0.95 m³/s which have been computed from the historical river flow data. The measured volumetric flow value is also within the typically river water flow range i.e. between Q_{30%} and Q_{40%} on the FDC for small rivers and based on the computed river flow values the Q_{mean} for Hhaynu river is around Q_{39.3%} which is typically volumetric flow for small rivers as shown in Table 5.4 and Table 5.5 below.

Table 5.4: Percentage of exceedance with river flowrate

% exceeded	Time Flow rate [m³/s]
8	2.3
17	1.59
25	1.22
33	1.02
42	0.92
50	0.86
58	0.79
67	0.74
75	0.69
83	0.65
92	0.62
100	0.60

Table 5.5: Standardised % of exceedance with river flowrate

% Time exceeded	Flow rate [m³/s]
Q ₁₀	2.14
Q ₂₀	1.45
Q ₃₀	1.10
Q ₄₀	0.94
Q ₅₀	0.86
Q ₆₀	0.78
Q ₇₀	0.72
Q ₇₅	0.69
Q ₈₀	0.67
Q ₉₀	0.63
Q ₉₅	0.61
Q ₁₀₀	0.60
Q_{mean} = Q_{39.3%}	0.95

From the analysis (as shown on Table 5.4 or Table 5.5 above) the results show that a river flow of approximately 0.60 m³/s have a 100% of being exceedence, while that of approximate 2.14 m³/s have a 10% of being exceedence. Also from the calculations, it is shown that a flow of approximately 0.86 m³/s has a 50% chance of being exceedence while a flow of 0.63 m³/s has a 90% of exceedence. From these values and also due to the nature of the run-of-river schemes, the turbine design discharge value to be considered for this research study must be exceeded 95% of the year (Q_{95%}) and in an additional to that consideration have to be on the environmental flow as the residual water flow value that have to be taken as the flow characteristics value for minimum river flow [157]. The Q_{95%} from FDC is the amount of river flow discharge that will be available for hydropower electricity generation throughout the year round because there is no provision for water storage in this research design only a small pondage (weir) will be installed. During the field work and site measurement in June/July 2016, the river flowrate reveals a discharge of 0.90m³/s which is around 44.7 percent of being exceeded as shown in Figure 5.20 below.

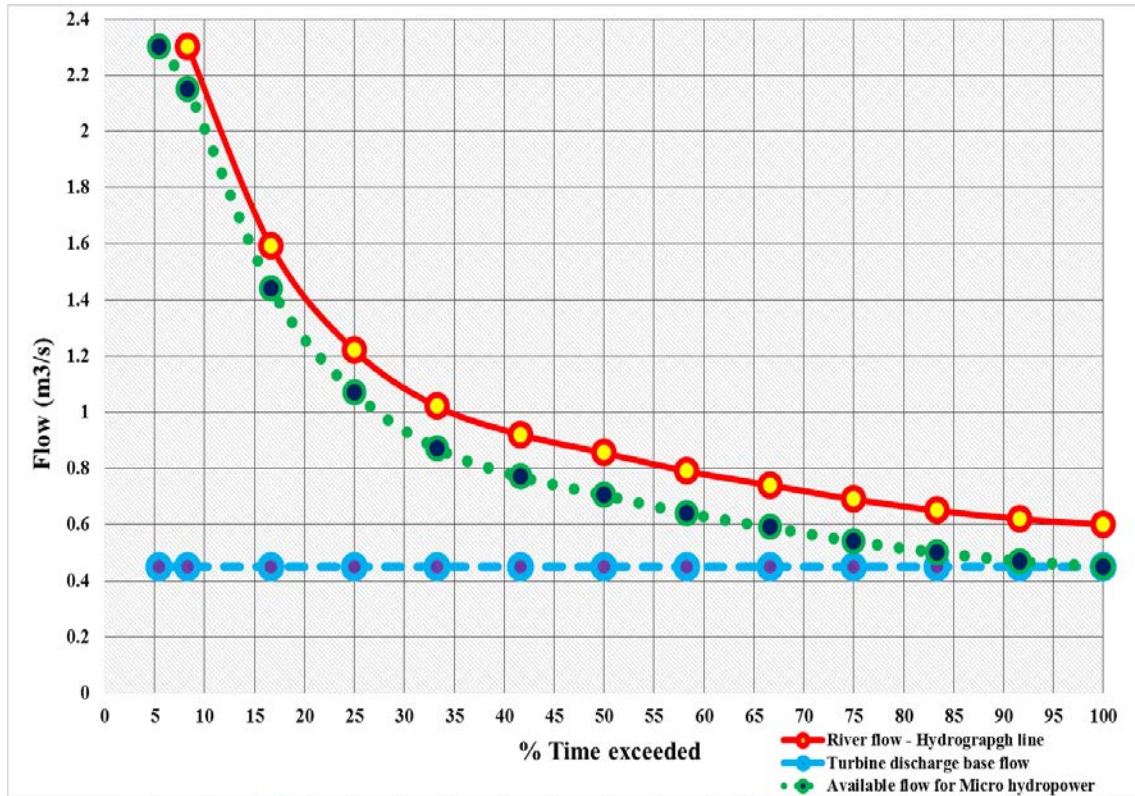


Figure 5.20: Hhaynu river flow duration curve

From Figure 5.20 above, the results show that the lowest flow at 10% of the time is 2.14% while the medium flow at 50% is 0.86% and high flow at 95% of the time is 0.61 m³/s. In addition to that, the flow at 100% of the time is found to be 0.60m³/s which is the minimum available river volumetric flow throughout the year. In determining the design discharge and energy estimation for the micro-hydro turbine system with river flow data of more than 10 years like that of Hhaynu river, its FDC has to be drawn from the river flow value of more than 90% time of exceedance.

5.8.7 The accuracy of flow discharge measurement methods

The validation of the hydrological data was done by triangulation method on which measured data (one-year measured data) was compared with the historical data (more than 10 years) and the results show the similarity on their seasonal trends and monthly average values.

Discharge measurements using the velocity-area method without the use of a weir provide a good estimate for stream flow and discharge. However, this method assumes several things, including a constant cross-sectional area (which is not always the case, as streams are erosive, dynamic systems), a strong relationship between stage height and discharge, and little human error in measuring velocity, stage height, and cross-sectional area.

The measured volumetric flow for Hhaynu river that has been used in this research study is 0.90 m³/s which is based on the three-point measuring method for the flow velocities. In addition to that, both measurement methods resulted in almost similar values, i.e. discharge of 0.92m³/s for the floating method and discharge of 0.90m³/s for the three points volumetric flow measurement method respectively. The accuracy of these computed values has been compared by the >20 years historical flow rate data (1985 to 2007) on which the results show the average volumetric flow of 0.96m³/s for the month of June. This accounts for 4.35% difference with the floating water flow measurement method and 6.67% difference with the current meter water flow measurement method. The measured values are within the range of the accuracy of the instrument that has been used to do the measurement which is around ±7%.

The results of the volumetric river flow measurement methods show that both the floating method flow measurement and the use of the current meter produces results that are very close to the actual river flow value and this answers one of the research questions, i.e. How the water flow velocity measurement methods for small rivers affect the accuracy of volumetric flow of the river.

5.9 Water flow discharge determination for hydropower potential

From the river, volumetric flow curve based using the historical data and also taken into consideration the environmental flow of 0.15 m³/s as the minimum value, the water discharge duration curve with the turbine design flow has been derived and shown in Table 5.6 and Table 5.7 below with the respective discharge flow duration curve on Figure 5.21.

Table 5.6: Available flow discharge for micro-hydro turbine

Percentage of exceedence (%)	Available flow for hydro [m ³ /s]
5	2.3
8	2.15
17	1.44
25	1.07
33	0.87
42	0.77
50	0.71
58	0.64
67	0.59
75	0.54
83	0.50
92	0.47
100	0.45

Table 5.7: Standardised design flow discharge for the micro-hydro turbine

Standardised % time exceedence	Flow rate [m ³ /s]
Q ₁₀	1.99
Q ₂₀	1.30
Q ₃₀	0.95
Q ₄₀	0.79
Q ₅₀	0.66
Q ₆₀	0.63
Q ₇₀	0.57
Q ₇₅	0.54
Q ₈₀	0.52
Q ₉₀	0.48
Q ₉₅	0.46
Q₁₀₀	0.45
Q_{mean} (Q_{41%})	0.78

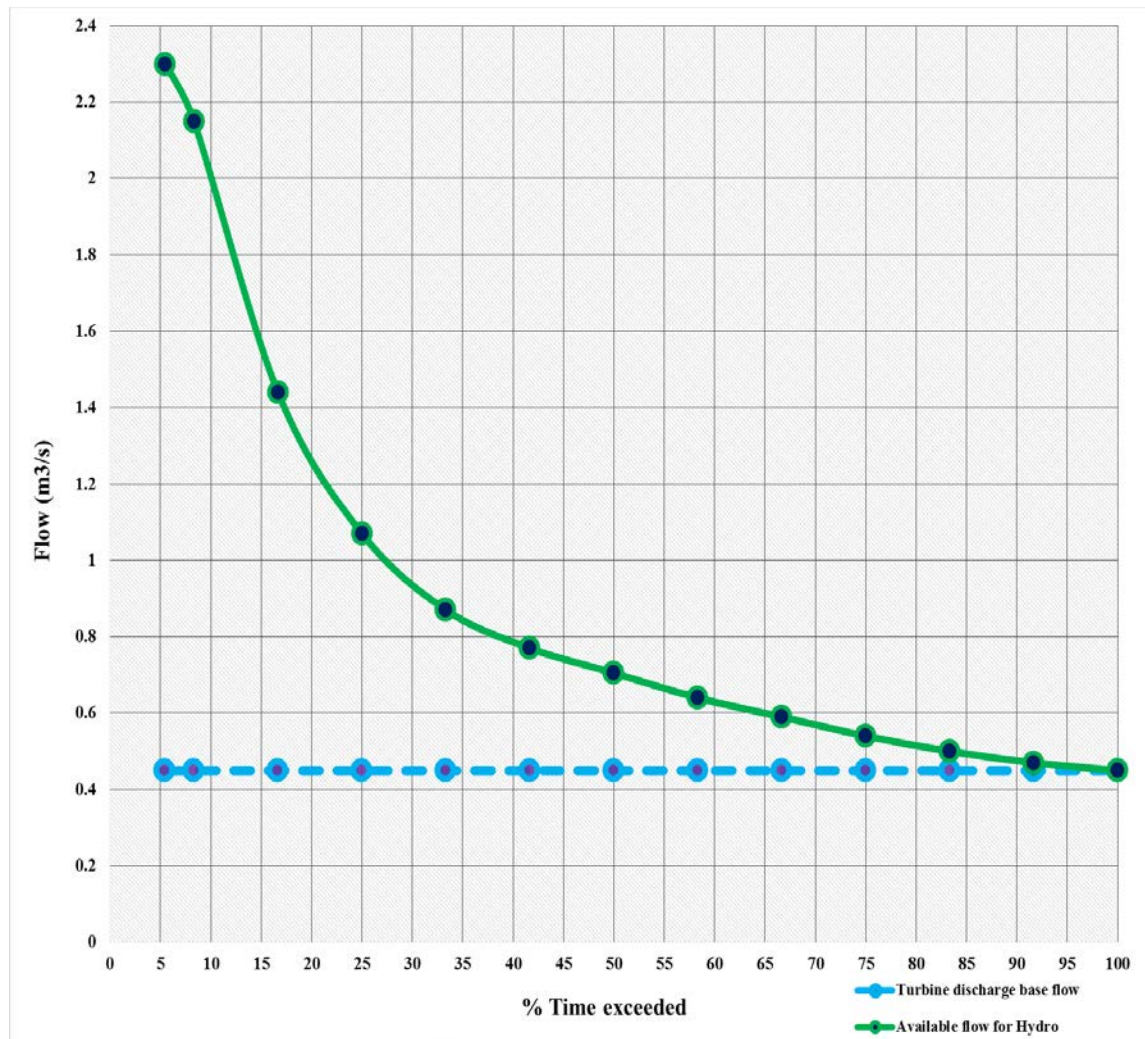


Figure 5.21: Micro-hydro turbine design discharge flow duration curve

From the above Figure 5.21 above, the available river flow for hydropower development at $Q_{95\%}$ is found to be $0.46 \text{ m}^3/\text{s}$ and that of the Q_{mean} is equivalent to flow at $Q_{41\%}$ which is $0.78 \text{ m}^3/\text{s}$. From literature and relative to FDC charts, mean flow for typical small rivers should be in a range between Q_{30} and Q_{40} . The Q_{mean} value is slightly above Q_{40} value due to the fact that the research study river flow has a slightly higher base water flow which satisfies the following condition that $Q_{95}/Q_{mean} > 0.4$. Therefore, the value taken for the design discharge base flow is $0.45 \text{ m}^3/\text{s}$ at $Q_{100\%}$ and this indicates a high base flow value for the size of a micro-hydropower system like that of Hhaynu river.

5.9.1 River flow discharge optimization

In micro-hydro power plants, optimal water flow discharge is determined based on the available river flow discharge and this affects the power output from the power plant. Using the results from the flow duration curve with $0.78 \text{ m}^3/\text{s}$ as mean flow (Q_{mean}) and $0.45 \text{ m}^3/\text{s}$ as a design flow (Q_D) which is equivalent to 56.92% of the available water flow (i.e $0.577 * Q_{mean}$). In most mini and micro-hydropower schemes without storage the optimal design flow discharge capacity (Q_D) is normally between Q_{mean} to $0.5 Q_{mean}$ (40% to 60% of the available water flow) as shown in Table 5.8 below.

Table 5.8: Typical optimal water flow values for mini and micro hydropower schemes

Design flow $Q_D =$ $0.45 \text{ m}^3/\text{s}$	Available water flow capacity	% of available water flow	Remarks
$1.3Q_{mean}$	$1.014 \text{ m}^3/\text{s}$	33%	
Q_{mean}	$0.78 \text{ m}^3/\text{s}$	40%	The optimal operating range for the micro- hydro turbine
$0.75Q_{mean}$	$0.585 \text{ m}^3/\text{s}$	50%	
$0.577Q_{mean}$	$0.45 \text{ m}^3/\text{s}$	56.92%	
$0.5Q_{mean}$	$0.39 \text{ m}^3/\text{s}$	60%	
$0.33Q_{mean}$	$0.257 \text{ m}^3/\text{s}$	70%	

The percentage of available water flow between Q_{mean} to $0.5Q_{mean}$ is a typical value used for small hydropower schemes designs that seem to give a satisfactory return on the project investment [158]. The design value selected for this research is within the specified capacity factor range at 56.92% ($0.577Q_{mean}$) which is o the recommended capacity factor range, although in practical terms, most small hydro turbines can operate over a certain range of design water flows to even 10% to 30% below their rated capacity water flow values.

In the design flow for the micro-hydropower plant and based on the flow relationship of Q_{95}/Q_{mean} which mathematically is equal to $\frac{0.46}{0.78}$ that gives the value of 0.5897 and since the calculated value is above 0.2 it indicates that the designed micro-hydropower scheme has

a high base flow. Based on Low Abstraction Sensitivity Band (ASB1) for water body in England and due to high base flow for the water discharge, the Hands off flow (*HOF*) for the designed micro-hydropower scheme is taken above Q_{97} which is equivalent to $0.453 \text{ m}^3/\text{s}$ and maximum abstraction of $1.3 \times Q_{\text{mean}}$ which is equal to $1.014 \text{ m}^3/\text{s}$ for $Q_{\text{mean}} = 0.78 \text{ m}^3/\text{s}$. These values are used in the design of the civil structures for the intake to accommodate the available water flow as shown in Table 5.9 below.

Table 5.9: Design flow values for hydropower schemes [159]

River type	High sensitivity ASB3		Medium sensitivity ASB2		Low sensitivity ASB1	
	Low/med base flow	High base flow	Low/med base flow	High base flow	Low/med. base flow	High base flow
Q_{95}/Q_{mean} value	Below 0.2	0.2 and above	Below 0.2	0.2 and above	Below 0.2	0.2 and above
HOF	Q_{95}	Q_{97}	Q_{95}	Q_{97}	Q_{95}	Q_{97}
Maximum abstraction	$1.3 \times Q_{\text{mean}}$	Q_{mean}	$1.3 \times Q_{\text{mean}}$		$1.3 \times Q_{\text{mean}}$	
% take above HOF	35%		40%		45%	

5.10 Power and energy potential assessment

The data related to the energy resource for the hydro power plant has been gathered from the amount of water available from the local river flow. In order to estimate the available energy for the hydro turbine, the amount of water flow discharge from the river have been measured and determined.

Based on the availability of a micro-hydropower plant, which will operate 24 hours a day giving a constant power supply capacity, but due to the nature of the load demand, the results shows that there are two power demand characteristics, high load demand phase (peak hours) and low load demand phase (off-peak hours). Due to this effect, the micro hydropower plant will have to operate at a certainly capacity in order to meet all the load demand. The plant capacity factor depends on many factors but the most considerable measure is the amount of hydro energy generated per year which is produced from the available flow discharge have been analysed in the following sub-sections.

5.10.1 Micro-hydro power potential

The first consideration is for isolated/off grid scheme, where the energy assessments consideration prior to the power potential study is necessary so that the installed power capacity is enough to meet the local energy demand and also a consideration for growth in power demand for the next 5 to 10 years. The design discharge for this case should have

more reliability due to its nature as an isolated scheme, so for this situation, the discharge installed capacity value has been taken to correspond to $Q_{100\%}$ with residual flow consideration on the hydrograph and flow duration curve which is $0.45 \text{ m}^3/\text{s}$ and is the minimum water available on the river throughout the year after considering the environmental flow. In determining the electrical power output, the efficiency of the turbine-generator system has to be known and from the British Hydropower Association, a guide to UK Mini-Hydro Development V3.0, the overall system efficiency for micro hydro system ranges from 60% to 80% which include all system structures from intake to power house [160]. In reference to the micro hydropower potential, the mechanical power/turbine power which is transferred to the generator shaft behaves a non-linear function of the discharge Q and pressure head H and is expressed by the following relation;

$$P_{MHP(t)} = f(QH) \text{ which gives the following equation:}$$

$$P_{MHP(t)} = gQH\eta_{turbine} \text{ (kW)} \quad (5.12)$$

where $P_{MHP(t)}$ = micro hydro turbine power (mechanical power), g = acceleration due to gravity (9.81 m/s^2), Q = discharge at the site (m^3/s), H = effective pressure head (m), $\eta_{turbine}$ = turbine efficiency and $\eta_{generator}$ = generator power

Note: Mechanical power $P_{MHP(t)}$, is related to the generator power $P_{MHP(g)}$ by the following;

$$P_{MHP(g)} = P_{MHP(t)} \times \eta_{generator} \quad (5.13)$$

So, based on the above equations and the site data values, the results of the determined power and energy potential values for each month on a year is shown in Table 5.10 below.

Table 5.10: Hydro power and hydro energy potential

S/N	Month	Design flow discharge [m^3/s]	Hydro Power potential [kW]	Hydro Energy potential [kWh]
1	January	0.45	75.5 ^a	56,172 ^d
2	February	0.45	75.5	50,736
3	March	0.45	75.5	56,172
4	April	0.45	75.5	54,360
5	May	0.45	75.5	56,172
6	June	0.45	75.5	54,360
7	July	0.45	75.5	56,172
8	August	0.45	75.5	56,172
9	September	0.45	75.5	54,360
10	October	0.45	75.5	56,172
11	November	0.45	75.5	54,360
12	December	0.45	75.5	56,172
	Average	0.45	75.5	55,115

d = a x b x c b = 24 hours/day c = 31 days/month

The hourly power demand from Table 5.10 above has been graphically represented for the 24 hours duration in a typical day to characterise its general pattern, trend and also highlight some common features for the power usage in a day. Due to low in energy demand on some hours of the day, some of the produced energy from the micro hydro power will not be consumed. This is evident by the daily average energy surplus which is equivalent to 690.19 kWh/day. This amount of excess daily energy produced is high around 38.09% of the average energy demand per day and could be used for other useful energy demand applications in the local area as shown in Figure 5.22 below.

5.10.2 Power potential and water flow discharge optimization

It should be noted that the electrical power potential from a micro hydro turbine-generator system depends on the amount of water discharge entering the turbine unit through a penstock pipe. Thus, changes in water discharge into the turbine, intentionally through the change in gate valve opening position will result in changes in the power output from the turbine-generator unit which in turn will affect the system efficiency. The effects of water discharge and power potential in relation to system efficiency have been studied in order to see the system stability for the power supply when supplying the required load demand. The result shows that power values of 40 kW and 75 kW could be used as power supply capacity during the low demand and high demand phases respectively. This results also confirm that both power supply values are feasible because the power output that is produced is above 50% rated system efficiency which is the minimum recommended operating efficiency for the micro hydro turbine technologies as shown on Table 5.11 below.

Table 5.11: Optimisation of power potential with the availability of water flow discharge

Water flow discharge [m ³ /s]	% Design flow discharge	Mechanical	Electrical	% of Total power	Remarks
		power potential [kW]	power potential [kW]		
0.45	100	79	75.05	100	Max. power
0.40	88.89	70.63	67.10	89.41	
0.35	77.78	61.80	58.71	78.23	
0.30	66.67	52.97	50.33	67.06	
0.27	60.00	47.68	45.29	60.35	
0.24	53.33	42.38	40.26	53.64	Min. power
0.22	49.69	39.48	37.50	49.98	

Note: Mechanical efficiency (Hydraulic and Turbine = 72%) and Electrical efficiency (Generator = 95%)

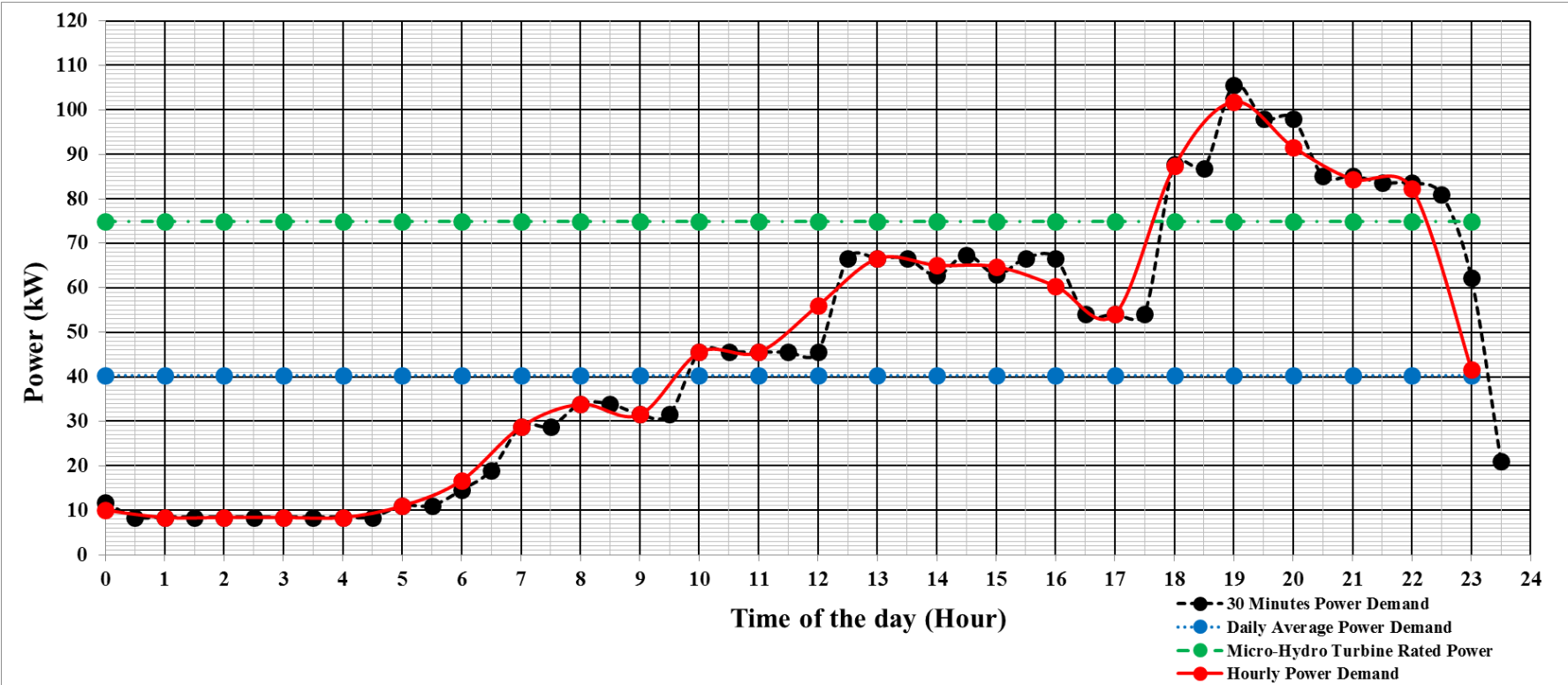


Figure 5.22: Daily power supply and demand for the local community (Study area)

From the result of the above Figure 5.22 the 40 kW (average 40.26 kW) generator power potential has also been simulated based on the available minimum load demand during the night and morning hours when the load demand is too low. When the turbine is running at this power output range, the system efficiency is reduced by 53.3% of the rated values while the water flow discharge will also be reduced to 0.24 m³/s. These values are the minimum recommended values for the system design to operate under stable condition. On the other hand, during an increased load demand, the power supply needs to be increased and in this case, the maximum generator power output of around 75.05 kW is produced which is the rated power value for the turbine unit. From Figure 5.23 below, the rated water flow discharge for the micro-hydro system is 0.45m³/s and the system efficiency of 68.4% (72% for the turbine x 95% for the generator). But during low demand hours, the rated turbine-generator power value is reduced to 40.26 kW. In this case, 46.67% of the rated water flow discharge is bypass back to the river and not utilised during the low demand phase. This will increase the environmental flow in the river but also the available bypass water is ideal for the pumped water storage system and other application like irrigation or hydrogen production as shown in Figure 5.23 below.

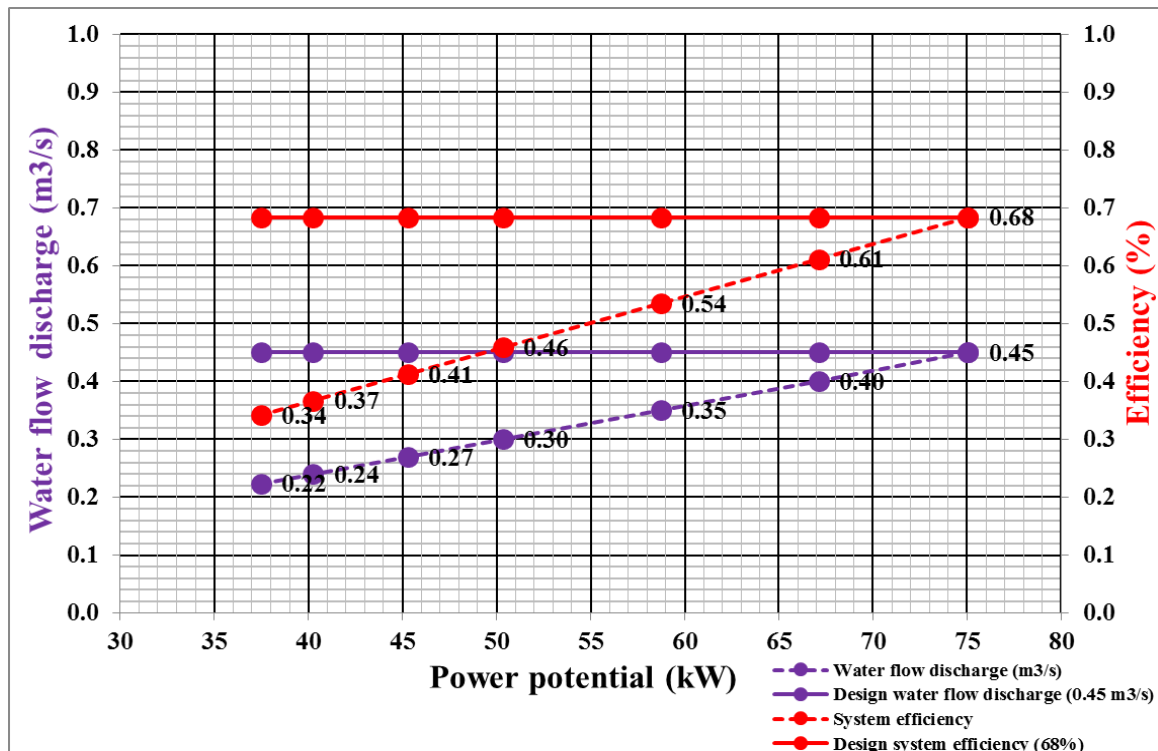


Figure 5.23: Power potential in relation to water flow discharge and system efficiency

5.11 Summary

Based on the available water flow from the river and in relation to the hydropower system design, the water flow discharge to be used by the micro-hydro turbine is based on the amount of water available throughout the year i.e. at Q_{100} which is $0.6\text{m}^3/\text{s}$ and when considering the environmental flow of $0.15\text{m}^3/\text{s}$, it gives the value of $0.45\text{m}^3/\text{s}$ as the turbine design discharge. Using river flow data from the hydrological study and flow duration curve, the amount of water flow discharge that is supplied to the micro-hydro turbine is $0.45\text{ m}^3/\text{s}$ based on the minimum available water flow from the river as there is no provision for water storage. On the other hand, field work activity has also included measurement of other site parameter which include the site head i.e. elevation between the forebay and the power house which was measured to be 25m. Now, using these two sites measured values of water flow discharge, Q and head, H , the average power and energy potential from the micro-hydro turbine has been estimated to be 75.5 kW with the daily energy potential of 1,812 kWh/day.

Chapter 6 System design

6.1 Introduction

The general layout of a micro hydropower system configuration consists of mainly three main areas that include the intake system which mainly comprises of civil components, while the other part is the turbine system which mainly consists of mechanical components and the last part is the generator and load system which is mainly electrical system components.

The intake system consists of civil structures that are used to divert water discharge from the river flow to the canal known as a run-of-river system. Main components of the intake system include weir, intake, canal, settling basin and forebay. The required amount of water discharge is diverted from the river flow and allowed to flow through the canal to the settling basin and then down to the forebay which is attached to the penstock pipe.

A turbine system, on the other hand, consists of the following structures, penstock pipe, gate valve, turbine and its components. The penstock pipe direct water from the forebay to the turbine, while the gate valve is used to control the amount of water flow to the turbine unit.

The generator and load system is connected after the turbine system and consists of the generator unit and also load power system from the consumers as shown in Figure 6.1 below.

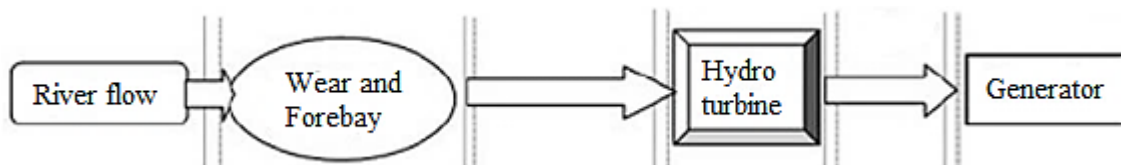


Figure 6.1: Schematic layout diagram of the hydro turbine-generator system

For the micro-hydro turbine system with small output power and not connected to the grid (off-grid), the generator power is usually supplied to the main load but during low demand, the excess power is diverted to the shunt loads using the generator controller as shown on Figure 6.2 below

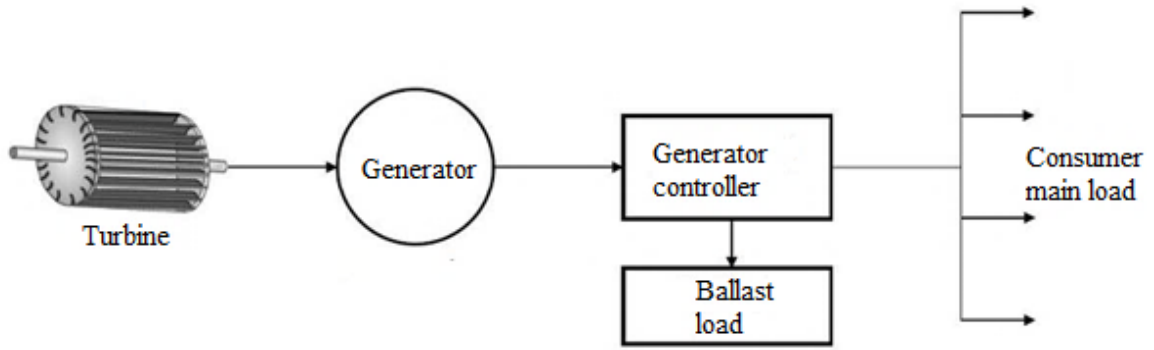


Figure 6.2: Layout diagram of the hydro turbine-generator and load system

6.2 Design methodology

The design of a micro-hydro turbine system with an integrated energy storage system using the developed layout is undertaken by using a number of design equations and relations as shown in detail in the following sub-sections.

6.2.1 Micro-hydropower system

The micro-hydro turbine system uses the power of moving water to drive a turbine that rotates the generator system which produces electrical energy. This electrical power output is used to supply power to the consumer load demand.

6.2.1.1 Power and energy supply

In order to obtain the power supply, the mechanical (turbine) power need to be obtained first using the Equation 5.11 in Chapter 5.

The obtained mechanical power is used to drive the generator system and the output electrical power supply value is given by the Equation 5.12 in Chapter 5.

During the system operation, the designed micro-hydro turbine system does not provide 100% of the required power supply capacity, so in order to determine the actual turbine capacity factor the following equation is used:

$$C_f (MHP) = \frac{P_{avg}}{P_{max}} \quad (6.1)$$

where $C_f (MHP)$ = macro hydropower capacity factor, P_{avg} = average power output and P_{max} = maximum power capacity

6.2.1.2 Consumer load demand

The load energy demand is the amount of energy that the consumers use when supplied by the available electrical power at a given time from the micro-hydro turbine system and is given by Equation 4.1 in Chapter 4.

6.2.1.3 Excess power and power deficit

When the power supply from the micro-hydro generator system is higher than the available consumer load demand power then the excess power is produced which is given by:

$$P_{MHP(excess)} = P_{MHP(g)} - P_D(l) \quad (6.2)$$

For the excess power to be produced the above equation must produce a positive value ($P_{MHP(g)} > P_D(l$) and when the above condition produce a negative value ($P_{MHP(g)} < P_D(l$) then the obtained value is the power deficit.

6.2.1.4 Dump load

Dump loads are obtained when the total excess power obtained from the micro-hydro turbine is not utilised and hence it is shunted to the ballast units to protect the generator system. The amount of dump load depends on the amount of excess power available and is given by the following equation:

$$E_{MHP(dump)} = \sum[(P_{MHP(excess)} - P_{stored}) \times t] \quad (6.3)$$

where P_{stored} = stored power

When there is no provision for power storage in a micro-hydro turbine system, then all the excess power produces is sent to the dump loads as shown in the equation below:

$$E_{MHP(dump)} = \sum(P_{MHP(excess)} \times t) \quad (6.4)$$

6.2.2 Energy storage

In order to reduce power loss due to the dumping of excess electrical power, the possibility of energy storage needs to be considered. Several energy storage combinations are available with the micro-hydro turbine system but in this research study four (2) energy storage systems have been studied, i.e. battery storage and hydrogen storage

6.2.2.1 Battery storage

The battery system is another option that has been integrated with micro-hydro system for energy storage. The battery system uses excess electrical energy to store power that will be used to supply peak demand and load deficit. In order to store excess power in a form of energy to the batteries, the minimum size of the battery storage need to be determined first and also the total energy deficit value needs to be calculated based on the hourly average values from 18:00 hours to 22:00 hours as follows:

$$E_{D(deficit)} = \sum(P_{D(deficit)} \times t) \quad (6.5)$$

where $E_{D(deficit)}$ = energy demand deficit, $P_{D(deficit)}$ = power demand deficit and t = time during power deficit

The total energy deficit can be used in the calculation of the battery storage capacity using the following equation:

$$B_{storage(c)} = \frac{E_{D(deficit)} \times t}{\eta_{inv} \times DoD \times V_{battery}} \quad (6.6)$$

where $B_{storage(c)}$ = battery storage capacity in Ah, t = time in days of autonomy, η_{inv} = inverter efficiency, DoD = depth of discharge and $V_{battery}$ = nominal battery voltage.

For the battery storage analysis, the following parameters have been used:

- (i) Inverter efficiency of 85% (conversion efficiency from AC to DC)
- (ii) Overall round-trip battery efficiency of 60%
- (iii) Days of autonomy to be one [Note that the batteries will supply power to the load deficit which is round 5 hours each day]
- (iv) Battery nominal voltage to be 24V

In the system design, the selected batteries for use are the lead acid type with a single per unit battery storage capacity of 400 Ah, so the minimum amount of batteries required to supply the power deficit per day is given by:

$$N_{battery(min)} = \frac{B_{storage(c)}}{B_{storage(c/u)}} = \frac{B_{storage(c)}}{400} \quad (6.7)$$

where $N_{b(min)}$ = number of battery units, $B_{storage(c)}$ = total battery storage capacity in Ah and $B_{storage(c/u)}$ = per unit battery storage capacity in Ah

But because the lead acid batteries have special characteristics called state of charge, on which they must be charged to 100% and discharged to a minimum of around 40%, so in this case the useful storage capacity of the battery that needs to supply energy to the power deficit is 60% and this is called depth of discharge value (DoD).

In this case, the maximum battery storage capacity required to supply the required energy deficit is calculated using the following equation:

$$B_{storage(c)[max]} = \frac{B_{storage(c)}}{DoD} \quad (6.8)$$

Then the maximum number of storage batteries to be used in the storage system is calculated by using the following equation:

$$N_{b(max)} = \frac{B_{storage(c)(max)}}{B_{storage(c/u)}} \quad (6.9)$$

The power supply from the micro-hydro turbine is in AC current while the battery uses DC power, so there is a need for AC-DC conversion using inverter-charger. In calculating charging or discharging current, the system phase voltage need to be considered and since the turbine-generator system is in three phases and the inverter-charger is in a single phase,

then charging or discharging current need to be converted to a single phase using the following equation:

$$I_{(AC)} = \frac{P_{MHP(g)}}{(\sqrt{3} \times P_F \times V_o)} \quad (6.10)$$

where $P_{MHP(g)}$ = power value (+ve is charging and –ve is discharging), P_F = power factor of resistive impedance load (1.0) and V_o = phase output voltage (240V).

But the battery storage system uses DC current during charging, then the calculated AC current value needs to be converted to DC current using the following equation:

$$I_{(DC)} = \frac{I_{(AC)}}{P_F} \quad (6.11)$$

where P_F = power factor (usually 0.8 for Inductive loads). Power factor of an AC power system is the ratio of the real power consumed by the electrical load to the apparent power flowing in the electrical circuit. Example of P_F values for some designed inductive electrical loads ranges between 0.5 to 0.98. In the generator system, the P_F value is used because electrical generator sets are rated in kVA at 0.8 power factor lagging, so in conversion from kVA to kW rating the P_F value of 0.8 is used eg. 100kVA generator rating produces 80kW of electrical power

When calculating the charging current for the lead acid batteries, consideration should be made for determining the maximum charging current rate which is usually $\frac{1}{8h}$ of the battery Ampere-hour (Ah) capacity and is expressed as:

$$C_{rate(max)} = \frac{B_{storage(c)}}{8h} = 50A \quad (6.12)$$

where $C_{rate(max)}$ = maximum charging rate (A), $B_{storage(c)}$ = battery storage capacity (400Ah)

But in actual operation, lead acid needs to be charged at a lower value (longer time) than the maximum charging rate which is given by the following equation:

$$C_{rate(max)} = \frac{B_{storage(c)}}{16h} = 25A \quad (6.13)$$

In inverter/converter design, there should be a safety factor consideration, which is usually 25% – 30% more than the maximum power deficit value.

$$P_{inv/conv} = P_{D(deficit)[max]} \times 1.3 \quad (6.14)$$

where $P_{inv/conv}$ = converter/inverter power size and $P_{D(deficit)[max]}$ = maximum demand power deficit

6.3 System design optimization using HOMER

HOMER is the short form of “Hybrid Optimization Model for Electrical Renewable”. It is a micro power and energy optimization model that evaluates renewable energy system designs for either grid-connected or off-grid connected power systems for different application. The HOMER modelling software also uses optimization and sensitivity analysis algorithms which make it easier to evaluate many possible integrated system components such as solar PV, wind turbine, hydropower, biomass, Co-generation, diesel generator, battery storage, fuel cell, hydrogen storage etc [161].

In this research study, two system designs options have been optimized using HOMER optimization model:

- (a) Micro-hydropower integrated with battery energy storage system
- (b) Micro-hydropower integrated with electrolyser and hydrogen engine-generator system

In the above system designs, HOMER software was able to analyze and optimize different scenarios based on various factors that gives the best option with high energy efficiency and minimum cost [161, 162]. Also when analyzing the energy system model, HOMER is capable to displaying the simulation results with values and graphs that can be easily compared and evaluated based on the technical and economic benefits of the energy project [163].

The modelling and simulation process used in this research study have been given the basis to ensure the produced power supply from the energy sources have met all the load demand given. The system components for the present study include, a micro hydro turbine system together with the battery system, electrolyser system and hydrogen engine-generator system have been evaluated to determine their feasibility and capacity. The final energy system design simulation values have also been determined in order to evaluate the system operational characteristics that are related to energy production, electrical loads, excess electricity, renewable energy fraction, cost and also if there is any capacity shortage or unmet electric load on the system.

In this research study, the system modelling has been done based on the system design layout on which different sections have been modelled separately as block diagram which will be explained in more detail in the next sub-sections.

In literature the use of HOMER optimization model for renewable energy system has been reported and highlights the following advantages [164]:

- (a) HOMER simulates and display the performance of a real energy system

- (b) HOMER shows very detailed results for analysis and evaluation
- (c) HOMER determine the best energy system combination based on a number of available energy technology options

6.4 System design configuration

In the design configuration, the micro-hydro turbine will be the main system to supply the required electrical power to the daily consumer load demand power. From the power and energy resource assessment in Chapter 5, it has been concluded that the micro-hydro turbine system could supply a constant power capacity of about 75.5 kW while the load demand power values are changing at the different time of the day. The effect of load demand power changes produces two demand power phases, low demand power and high demand power. The results also show that during the high demand power phase, the available power supply from the micro-hydro does not provide enough power to meet the peak demand and this cause a power deficit. On the other hand, during the low demand power phase more power is produced than it can be consumed and this effect causes excess power on the system. In many micro-hydro turbine systems, this excess power is wasted as the dump loads (ballast) using water or air heaters. This condition of dumping excess electrical energy does provide a solution to solving the daily energy deficit during peak hours of the day. In order to mitigate this problem of daily energy deficit using the current system design, consideration has been taken to utilize the available excess electrical energy by means of storage. There are several electrical energy storage options that could be used with a micro-hydro turbine system but in this research study, two main options have been studied and analysed. The design configuration for the energy storage system consist of the following system combination:

- (a) Micro-hydro turbine system with battery storage
- (b) Micro-hydro turbine system with hydrogen storage

In the above system design configuration options, the daily load demand power deficit is supplied from the energy storage system by using excess electrical energy to charge the battery for the battery storage and to produce hydrogen for the electrolyser system as shown in block diagram in the Figure 6.3 below.

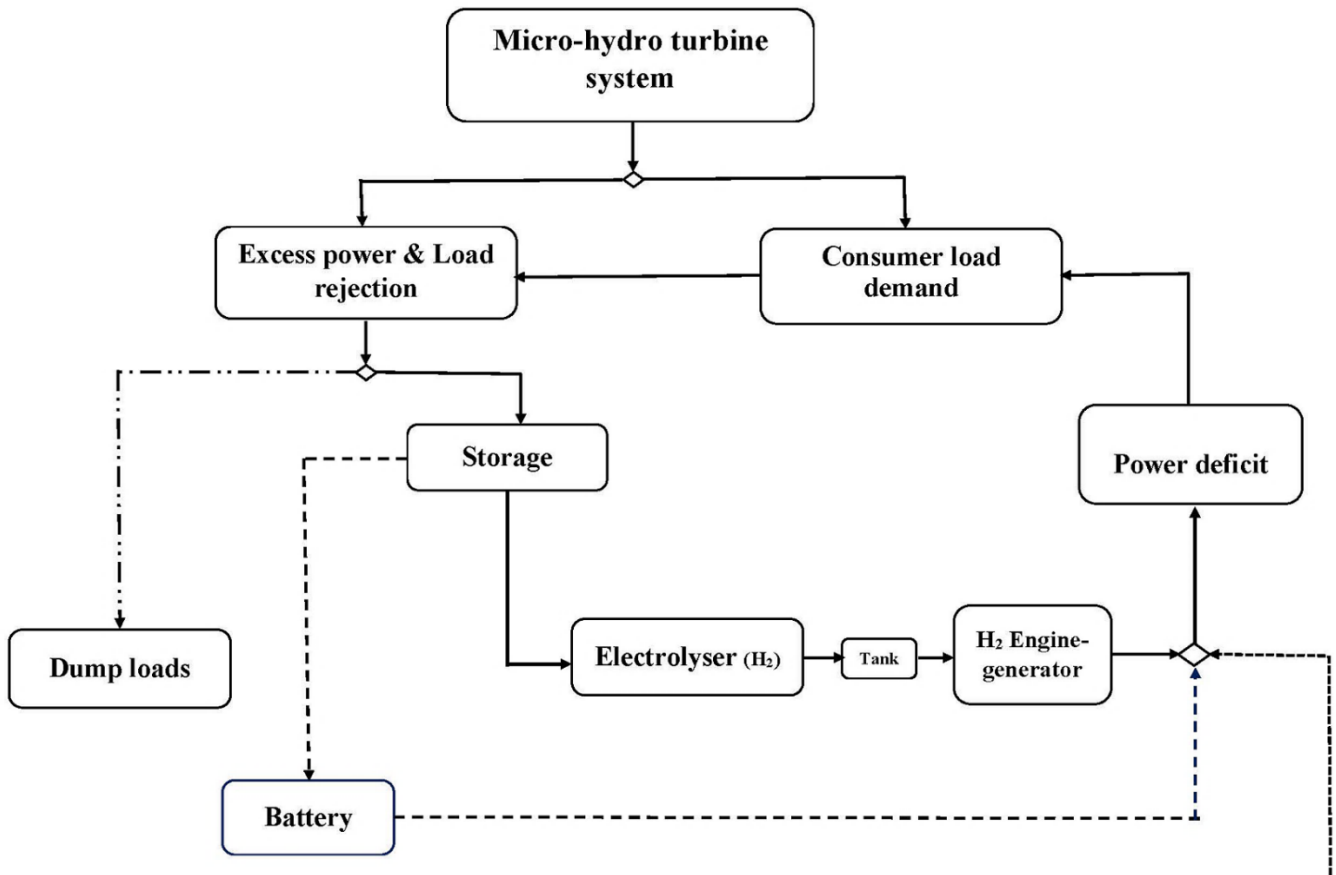


Figure 6.3: Systems design configuration

The design configuration for the micro-hydro turbine system has been focusing on supplying power to the consumer load demand. But results from the existing system design shows that the micro-hydropower system without energy storage is not able to supply enough power to the peak hours of the day, hence causes power deficit. This effect in power shortage and the option of supplying additional power to the load demand during peak hours has been analysed and evaluated in detail with the results from HOMER optimization model for renewable energy in the sub-sections below by integrating the micro-hydro turbine in the following energy technology system combinations:

- (a) Micro-hydro turbine system without energy storage
- (b) Micro-hydro turbine system with battery storage
- (c) Micro-hydro turbine system with hydrogen storage

6.5.1 Micro-hydro turbine system without energy storage

The system configuration for the micro-hydro-turbine system without any form of storage consists of water intake, piping system, controls, turbine and generator system. In this design, the water flow discharge from the river will be used to power the turbine and supply the required energy demand for the community. From the feasibility study data, the amount

of water flow discharge taken from the river to the turbine through the penstock pipe is 0.45 m³/s. This water flow amount through a turbine together with the site head elevation level of 25m will result in the generator power produced from a turbine amounting to 75.5 kW. Most micro hydro turbine system like Hhaynu operate as a run-of-river system which takes water directly from the river only the amount required to produce electricity and with no water storage or reservoir facility.

The daily power produced from the turbine system is supplied to the consumers in the local area and the study shows that the available load demand is not constant while the power supply is at a constant value. This fluctuation in the power demand, causes effect to the available power supply on which during low demand hours more power is produced than it can be consumed by the available load demand power hence excess power is accumulated while during the high demand and peak hours less power supply is available which result to power deficit on the system. The characteristics of this system configuration is that there is no energy storage option which means that the available power produced at a particular time is only supplied to the available power demand at that particular time of the day. This phenomenon of micro-hydro turbine systems to produce more power than the available load demand will result in the instability of the generator system by increasing its speed and frequency. In order to reduce this effect, most micro-hydro turbine systems are installed with the ballast loads component which is used to consume all the excess power and load rejection as shown in Figure 6.4 below.

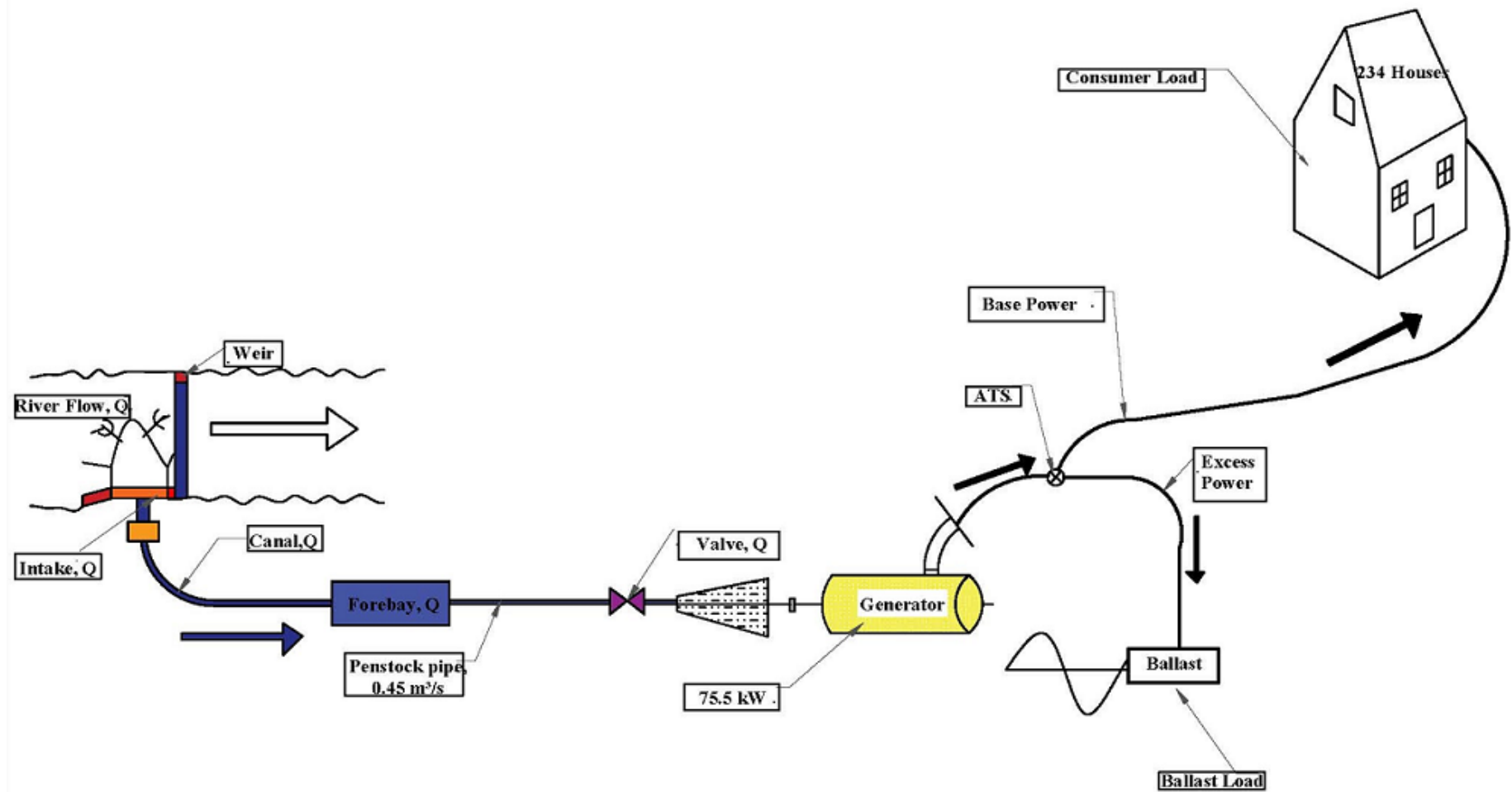


Figure 6.4: Hydro-turbine system configuration without storage

In the above system design layout and when considering the daily energy demand (low and high) with the energy supply in the area without the energy storage option, it is obviously that the micro-hydro turbine system without integrating it with the energy storage will not be able to supply the required energy deficit needed during the peak hours of the day.

So, in this case, a viable energy storage option needs to be considered and one of the possible scenarios to integrate micro-hydro turbine system with an innovative renewable energy storage system like the use of hydrogen storage or battery energy storage that will supply the required energy deficit during the peak hours of the day. The selected energy storage options have been discussed in detail in the next sub-sections.

For this option of the micro-hydro turbine only, the system can be represented as a single power supply source with the main and only power output comes from the hydropower system. The optimized system design values from the model results show that the peak power demand is around 101.8kW which is specifically at 19:00hours each day and the total energy demand per day is 1,114.38kWh/d which must be supplied by the hydropower system.

Due to the absence of storage component on this system design, the power produced from the micro hydro turbine has high renewable energy penetration and this effect causes stability problem on the system. The stability issue, in this case, is related to the generator over speed due to excess power produced which makes this system design layout not a very suitable option.

On the other hand, the optimization results obtained in this design highlights this effect and suggest the solutions to eliminate this problem. In consideration of the consumer load, the power demand consists of two phases, high demand phase or peak demand hours and low demand phase or off-peak hours. In this system design it is noted that, during the peak demand hours, all the power produced from the micro hydro turbine system is supplied to the main load demand which resulted to no excess power available that have to be sent to the ballast load.

On the other hand, during the low demand phase or off-peak hours, part of the power produced from the hydro turbine is used by the main load while the excess available power is sent to the ballast loads in order to stabilize the system. For this study, the minimum demand power value from the consumer load is around 8.42kW (after mid-night) when the turbine is producing 40kW (53.33% of rated capacity) power supply, thus in this case around 31.58kW is sent to the ballast load using Electronic Load Controller (*ELC*) and Automatic Transfer Switch (*ATS*). The energy production and consumption from the

hydropower is based on the results from the optimization of the system design. In this case, the average power produced from the optimized micro hydro turbine system is 70.12 kW while the nominal capacity is 75.5 kW.

On the other hand, excess electricity produced seems to be high at 39.6 % of the total hydropower production which is equivalent to 666.8 kWh/d and this is because of high hydro penetration. The optimization results also show that the occurrences of excess power at different power capacity values. The results also show that most of the excess power produced is between 4% to 21 % of the time. The 4% of the time occurrences of excess electricity is the lowest and have the values at 5 kW, 10 kW, 15 kW, 17.5 kW, 30 kW, 37.5 kW, 40 kW, 42.5 kW, 55 kW and 60 kW. In addition to that, the other medium frequency of occurrence is at 8.5% of the time which have the following excess electricity values 7.5 kW and 25 kW while the highest frequency of occurrences for the excess power values occurs at 21% of the time which have the value of 2.5 kW and 62.5 kW.

The minimum excess electricity value produced in this system design is 2.5 kW which occurs during the high demand hours that is mostly in the afternoon and evening hours. This is the time when most of the power supply is required to supply to the peak demand hours hence less or no excess power is produced. On the other hand, during the low demand and off-peak hours excess electricity is produced and in this system design the maximum excess electricity value of 62.5 kW is produced during the night hours. The usefulness of knowing excess electricity values at a different time of the day is to be able to properly design the shunt load rating capacity. Thus, in this system design option the selected ballast load values should have a minimum of 2.5 kW and a maximum of 62.5 kW rating capacity in order to consume all the excess power that the system will produce a different time of the day as shown on Figure 6.5 below.

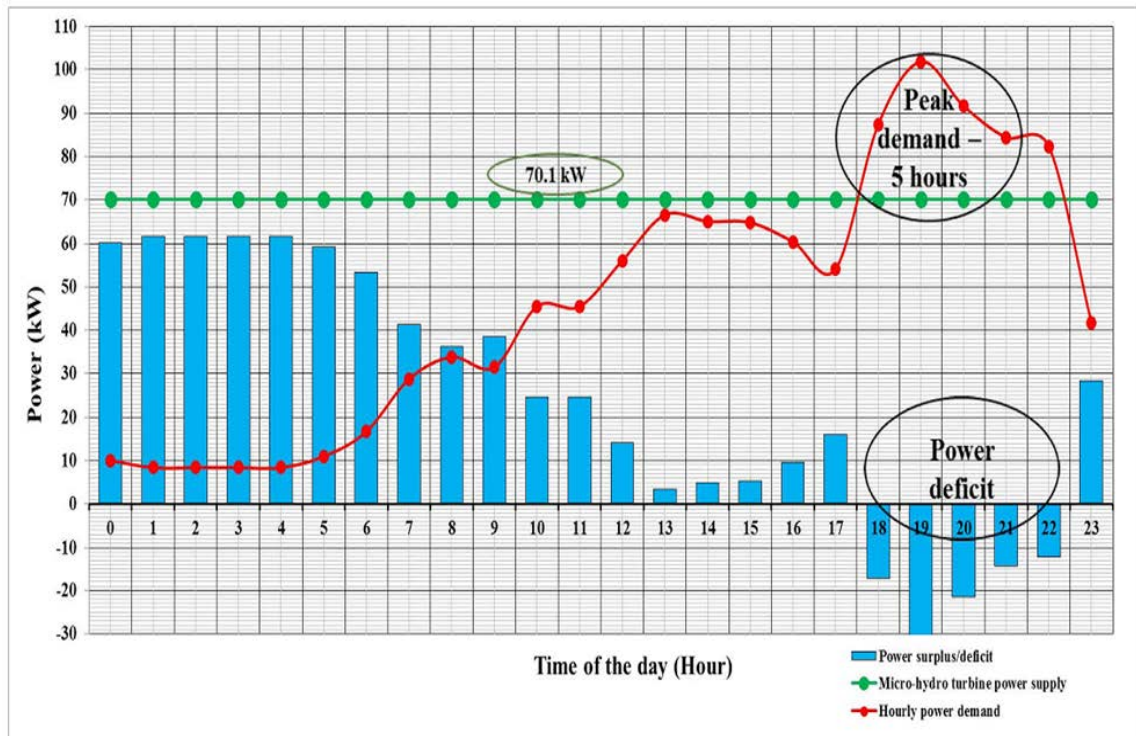


Figure 6.5: Micro-hydropower supply to the load demand without energy storage

From the operational point of view, it has been noted that micro-hydro turbine systems power output operate close to the load demand power values due to the nature of their operation in off-grid conditions. The power generated is mostly used to supply the actual load demand during peak hours and off-peak hours. Most of the micro-hydro turbine system has no options for power storage due to cost constrains and this in turn result to excess electrical energy production during the low power demand and off-peak hours, which is usually wasted (dumped) as thermal loads to the ballast (water or air heaters). During the peak hours or abrupt increase in power demand, the power supply without energy storage cannot cope with the dynamic change in power demand and in this case, it resulted in the power deficit (load shedding) which is very common in isolated small scale hydro turbine systems without any form of electrical energy storage.

So, in order to minimize the energy loss in the system in terms of power supply and load demand optimization, the excess electrical energy which is produced during low demand is effectively utilized in a form of energy storage and supplied to other renewable energy components. The stored electrical energy is also used during the peak hours or load demand increase to supply the additional electricity demand needed during the deficit hours of the day. So to make better utilization of these available renewable energy resources with the continuous electricity supply to rural and off-grid areas, a novel energy storage option must be developed which will store the available electricity and then use the stored energy during

the high demand and peak hours. Its system configuration should be based on micro-hydro for the base load capacity and other available renewable energy sources or energy storage for the peak loads. This development concept is the main focus of this research study. The idea is on the possibility of integrating micro-hydro with other renewable energy technologies and energy storage system configuration on which different energy storage options are available.

There are several types of power storage technologies in use now days on which most of them are categorized based on the storage duration and storage capacity.

In the first system design layout, there is a need to introduce an energy storage component which will be used to store excess electricity that can be used to supply stored energy required during the peak hours of the day. The selection of energy storage technology in this research study have been based on the following factors:

- (i) The cost to be minimal
- (ii) Locally available technology
- (iii) Compatible with micro hydro turbine system (< 100 kW)
- (iv) Storage time to be in hours.

Thus, based on the above factors and also according to the required maximum energy storage capacity which has to be supplying power during the peak hours, the first energy storage technology to be considered in the system design is the battery storage. From the design calculations, the required storage capacity that should be supplied from the battery energy storage during the peak hours is 72.35 kWh with the maximum power of 26.80 kW at 19:00 hours. Using these two design values the appropriate battery storage technology to be used based on the calculated values are the electrochemical batteries because of their wider range of applications at micro-scale.

6.5.2 Micro-hydro-turbine system with battery storage

The second option for a micro-hydro turbine with energy storage is the use of battery storage. During low energy demand hours, there is usually excess power produced which could be used to supply energy deficit during the peak hours. One of the useful ways to store this excess power is the use of battery storage which will be charged during the low demand hours.

From the power supply and demand analysis, it has been found that in a 24 hours power supply cycle, there are 5 hours of power deficit which is found between 18:00 hours to 22:00 hours and the maximum deficit is at around 19:00 hours, which is the peak demand

hour of the day. Based on the design calculations and also simulation results, it is conclusive that in order to supply the required load demand from the battery storage during the peak hours of the day, the available energy storage capacity from battery system must be at least 72.35 kWh. On the other hand, it should be noted that the excess power for battery storage comes from the micro-hydro turbine system and is in *AC* power while the battery system uses *DC* power. So in this case, the operations of the battery storage system must follow the following phases:

- (i) Conversion phase: A conversion from *AC* to *DC*
- (ii) Charging phase: During low demand hours, excess power produced from the power supply is used to charge the batteries
- (iii) Storage phase: The charging power (electrical energy) is stored in the batteries in a form of chemical energy
- (iv) Discharging phase: During the peak hours and power deficit, the stored energy (*DC*) is converted back to *AC* and supply the required additional power needed

6.5.2.1 Batteries storage capacity

There are several types of battery technologies that can be used to store energy but in this research, the deep cycle lead acid battery has been selected as storage batteries because they can be discharged to low energy levels and quickly re-charge with many charging and discharging cycles for years. Also, these batteries are available locally during the maintenance or replacement hence reduce the maintenance cost.

The battery storage capacity is determined based on the amount of energy required to supply the power deficit during the peak hour's demand. Based on the power supply and demand analysis, the minimum energy storage required to be stored during the day to supply power deficit during the peak hours should be kept above 72.35 kWh for each day. The specific type of battery selected for the energy storage is the Yuasa *EN400* Industrial *VRLA* battery because this type of battery technology can be commercially available in small capacity sizes to suite for the storage system design and also the battery system can be simulated with HOMER to highlights its storage capacity vs cost.

From the battery design calculation results, the minimum battery storage capacity value is 6,000 Ah and if the use of battery capacity is limited to 400 Ah per single battery then the minimum amount of battery required to supply the peak demand per day is 15 pieces. But because the lead acid batteries have low storage capacity, on which they must be charged to 100% and discharged to a minimum of around 40% on which the useful storage capacity

of the battery that needs to supply the energy deficit is 60%. Based on this condition then the maximum battery storage capacity required to supply the power deficit hours of the day is 10,000 Ah which gives the maximum number of battery storage to be 25 pieces.

It should be noted that, when considering the state of charge for the battery capacity, 100% maximum state of charge is equivalent to 10,000Ah (25 batteries x 400Ah), while at a minimum state of charge at 40% is equivalent to 4,000Ah (25 batteries x 160Ah each). Therefore, in order to supply the power deficit from the battery storage bank, the amount of energy required to be stored on the battery bank each day is 72.35 kWh which is equivalent to 25 pieces battery bank of 400 Ah and 24V capacity each connected in parallel.

6.4.2.2 Inverter-charger current values

Since the battery only uses the *DC* power and the load demand power is in *AC*, then there is a need to design an inverter-charger which will be used to convert *AC* power to *DC* during battery charging and also *DC* power to *AC* during discharging. The estimated value of the inverter is based on the total power values of the load demand and also need to have the same nominal system voltage. For the islanding system like the one for the present study, the inverter rating capacity should be 25% to 30% more capacity than the maximum power required by the system load demand.

So, it is noted that daily there are 5 hours of power deficit from the primary source and in this case, the additional power supply needs to be supplied from the battery storage by consuming the respective current on each particular hour as shown on Table 6.1 below.

Table 6.1: Daily hours of Power deficit

Time of the day [hour]	Power deficit [kW]	Required DC discharging current [A]	Remarks
18:00	11.68 ^a	38.33 ^b	
19:00	26.83	88.04	Max value
20:00	16.64	54.60	
21:00	9.16	30.06	
22:00	6.69	21.95	

$$AC = \frac{a}{\sqrt{3 \times P_F \times V_o}} \text{ with } P_F = 1 \quad DC = b = \frac{AC}{P_F} \text{ with } P_F = 0.8$$

6.5.2.3 System layout

In this layout, an additional system to the micro-hydro turbine system which is the battery energy storage component has been added in order to store excess electrical energy produced by the main power supply. The system works in such a way that the micro-hydro

turbine system is the main power source supplied to the load demand and during the power production some of the excess energy produced is not wasted but sent to the battery system for storage. Due to the nature of the battery system, the excess power produced from the main source needs to be converted to *DC* power by the use of a converter. A converter can be used to convert *AC* to *DC* during charging and also *DC* to *AC* during discharging. In controlling power to the different components, the power management unit called Automatic Transfer Switch (*ATS*) is used which allows power output to be directed to different consumer loads. In this system design, the battery system will only take around 7% of the energy produced while consumer load takes 66% of the energy produced. The rest of the available power produced which is around 27% of the energy produces will be available as excess power and because of no usage it is sent to the dump loads as shown in schematic diagram in the Figure 6.7 below.

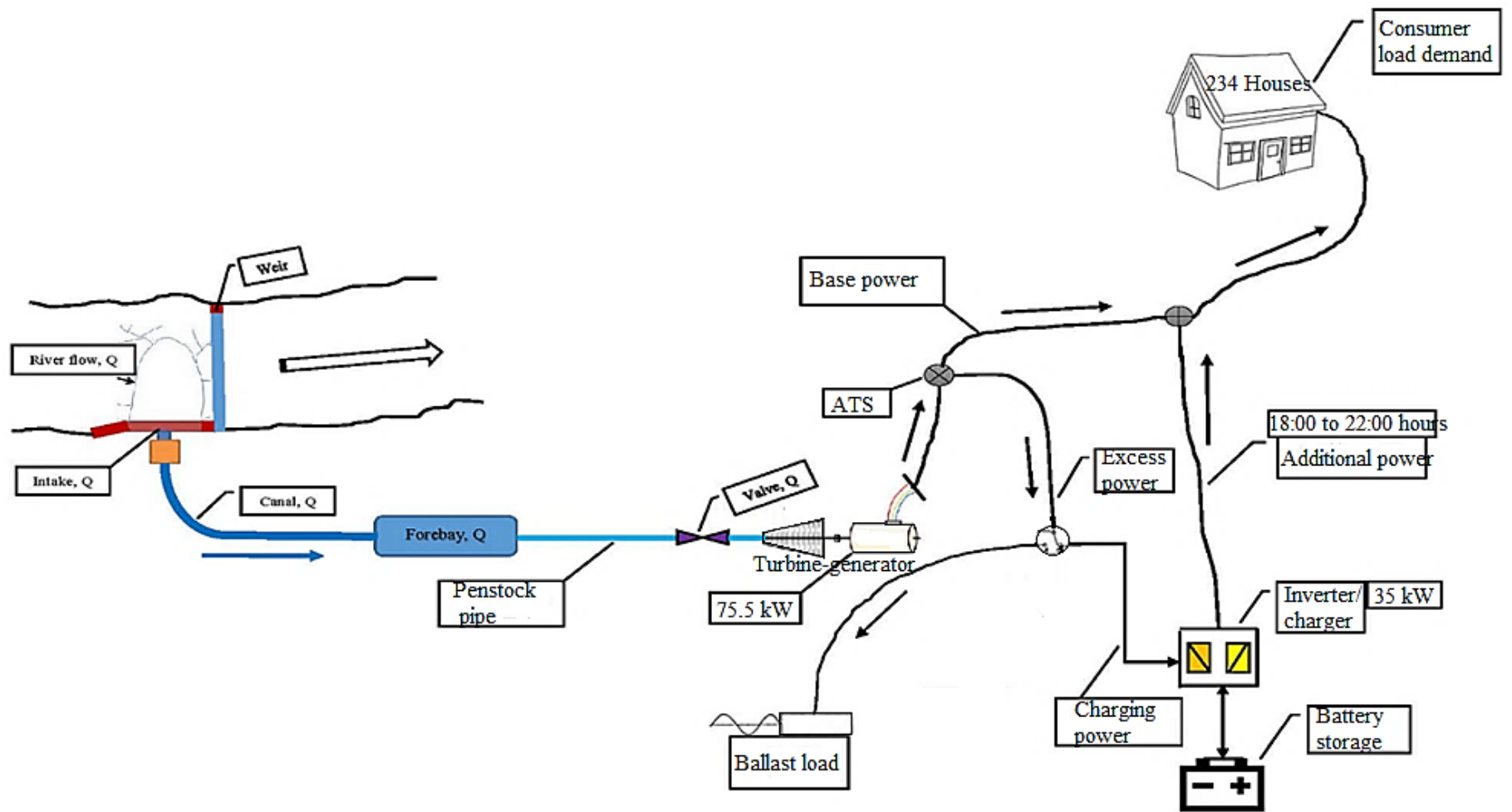


Figure 6.7: Micro-hydro turbine with battery energy storage

The battery energy storage option, in this case, has been selected due to its quick power responses, so it is best suitable during the power demand spikes and quick response power supply hours eg. during peak hours of the day. The limitation of the battery energy storage option is its low in energy storage capacity and also frequency replacement cost, thus it should only be used to supply intermittent load demand during the peak hours of the day. In calculating the battery storage capacity, the following configuration on Figure 6.8 has been used.

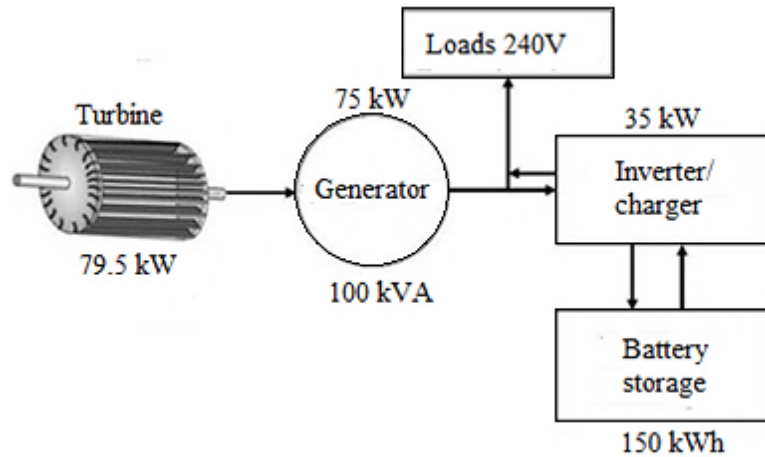


Figure 6.8: System configuration for the hydro turbine with battery storage

6.5.2.4 Available AC charging current and SoC

The summary results of the available AC charging current and battery state of charge for each hour of the day that has been shown in Table 6.2 below.

Table 6.2: Power surplus with available AC charging current and battery charge

Time of the day (hour)	Power surplus/ deficit (kW)	Available AC charging current (A)	Start-up charging current (A)	Start-up battery charge (Ah)	Start-up SoC (%)	24h charging current (A)	24h battery charge (Ah)	24h SoC (%)
00:00	65.44	157.45 ^a	25	25	6	10	249	62
01:00	67.08	161.39	25	50	13	10	259	65
02:00	67.08	161.39	25	75	19	10	269	67
03:00	67.08	161.39	25	100	25	10	279	70
04:00	67.08	161.39	25	125	31	10	289	72
05:00	64.5	155.19	25	150	38	10	299	75
06:00	58.77	141.40	25	175	44	10	309	77
07:00	46.71	112.38	25	200	50	10	319	80
08:00	41.65	100.21	25	225	56	10	329	82
09:00	8.49	20.43	25	250	63	10	339	85
10:00	29.49	70.94	25	275	69	10	349	87
11:00	29.49	70.94	25	300	75	10	359	90
12:00	18.96	45.61	25	325	81	10	369	92
13:00	8.43	20.28	25	350	88	10	379	95
14:00	9.93	23.89	20	370	93	5	384	96
15:00	10.23	24.61	10	380	95	5	389	97
16:00	14.62	35.17	10	390	98	5	394	98
17:00	20.87	50.21	10	400	100	5	399	100
18:00	-12.33	-30.66	-30.66	369	92	-30.66	368	92
19:00	-26.8	-70.43	-70.43	299	75	-70.43	298	74
20:00	-16.61	-43.68	-43.68	255	64	-43.68	254	63
21:00	-9.36	-24.05	-24.05	231	58	-24.05	230	57
22:00	-7.25	-17.56	-17.56	214	53	-17.56	212	53
23:00	33.35	80.23	25	239	60	10	222	56

$$a = I_{(AC)} = \frac{P_{MHP(g)[surplus]}}{(\sqrt{3} \times P_F \times V_o)}$$

By referring to the available AC charging current from above Table 6.2 that could be used to charge the batteries for energy storage, it is noted that when using lead acid battery technology there is a need to consider the maximum charging rate which is usually about $\frac{1}{8}$ of the battery Ampere-hour (Ah) capacity which is expressed as $\frac{C}{8}$. So, in this case, when using the selected lead acid battery of 400Ah capacity, the maximum charging current value that should be applied to the batteries is 50A. But in actual operation, lead acid batteries need to operate at a lower value than the maximum charging capacity and from Table 6.2 above, the maximum charging capacity considered for the selected batteries is around 25A which is 50% of the maximum charging current value.

Due to the nature of the lead acid batteries used, it is not recommended to use higher current when charging or discharging the lead acid batteries. From the above results, it is recommended to take the maximum available AC charging current of 25A and the minimum charging current of 5A. In this case, it should be noted that not all the available AC current is sent to the converter and used to charge the batteries, only a percentage of it based on the following conditions:

- (i) Recommended lead acid battery charging and discharging current range
- (ii) Nature of batteries connections as in parallel connection
- (iii) The charging of lead acid batteries depends on the SoC

6.5.2.5 System architecture

The system design parameters for this layout have been analysed using Homer Energy software on which the design data have been optimized to obtain the best system values. In this case, there are both AC and DC busbars that are interconnected by a converter. The AC power source from the micro-hydro turbine system supply power to the load demand and converter system that convert AC power to DC power for charging the batteries. The ballast loads in this system design makes use of the excess energy produced from the hydro turbine system during the low demand hours and serves as safety system (power sink) during abrupt excess power production or power rejection in order to stabilise the generator system as shown on Figure 6.9 below.

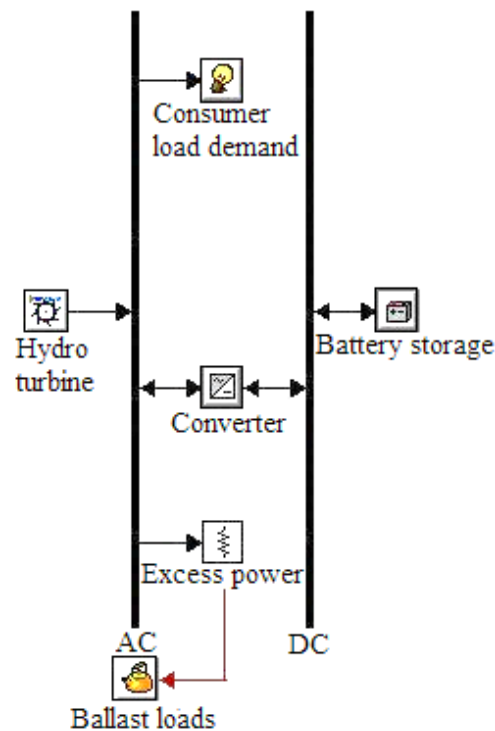


Figure 6.9: Hydro turbine with a battery storage system

The energy production from the hydro turbine system design is similar to the previous design layout with an annual energy production capacity of 614,284 kWh/year. The produced energy need to supply power to the AC primary load amounting to 406,269 kWh/year (66%) for the consumer load demand, 43,000 kWh/year (7%) for the battery storage from the converter and 165,710 kWh/year (27%) as excess energy to the ballast loads as shown in Table 6.3 below.

Table 6.3: Micro-hydro turbine with a battery storage system

Item	kWh/year	%	Remarks
Micro-hydro turbine	614,284	100	Production
AC primary load	406,245	66	Consumption
Excess energy (ballast loads)	165,710	27	Consumption
Battery energy storage	43,000	7	Consumption

6.5.2.6 Battery system

The sizing of the battery capacity depends on the energy storage required for a particular time or application. In this design, the battery energy storage will only be used to supply the additional required energy during the peak hours which is 5 hours each day. The required number of batteries from the design and simulation results is 25 pieces that should be connected in parallel with 24V bus voltage as shown in Table 6.4 below.

Table 6.4: Battery parameters and energy storage capacity (simulation results)

Item	Value	Units	Remarks
Number of batteries	25	pcs	System parameters
Bus voltage	24	V	
Nominal capacity	240	kWh	60 %
Usable nominal capacity	144	kWh	efficiency
Lifetime throughput	3,750	kWh	
Energy in	79,67	kWh/year	60%
Energy out	47,794	kWh/year	efficiency
Storage depletion	128	kWh/year	
Losses	31,756	kWh/year	
Annual throughput	61,703	kWh/year	Average

From the design optimization results in Table 6.4 above, it is shown that the useful energy capacity for the battery system is only 60% of the nominal capacity value. This is one of the characteristics of the lead acid batteries on which they can be charged to 100% SoC and discharged to a minimum of 40% SoC. When relating to the energy in and energy out for the battery system, the results show that the charging and discharging efficiencies in the system is also at 60%. Due to this effect, there are energy losses to the battery system that

occur which accounts for 39.86% and also storage depletion which accounts for 0.16% of the energy in (charging).

6.5.3 Micro-hydro turbine system with hydrogen storage

In this integration, the system design consists of a micro hydro-turbine system which will be used to supply the base load and because of surplus power to most of the time, additional systems are added. This include an electrolyser system together with hydrogen ICE engine-generator. Electricity surplus during low demand is used to power this additional system, especially during the night hours. Electrolyser is used to produce hydrogen gas by the electrolysis of water. During the peak hours of the day the micro-hydro turbine is not able to supply the required electricity demand and in this case, peak electricity demand is supplied by the ICE engine-generator system which is fuelled by the hydrogen gas. In this system design layout, no electricity storage is provided, instead the excess power produced is supplied to an electrolyser system. In order to stabilize the system, ballast loads are installed to consume the power due to abrupt changes in consumer load and load rejection. The electricity supply from the micro hydro turbine to the consumers, electrolyser and ballast loads are controlled and managed by automatic transfer switch (ATS). The produced hydrogen from the electrolyser is stored in a tank and is used to power the engine-generator system that supply additional electricity needed during the peak hours. On the other hand, the excess hydrogen produced by the system will be sold to the local fertilizer and oil industries to be used in the production of fertilizers and oil refinery processes respectively. The advantage of this system layout as compared to the previous systems is that there is no energy storage with the batteries or pumped storage which have some drawbacks and also additional electricity supply during the peak hours is done by the hydrogen supplied ICE engine-generator which seems to be a viable option because no excess electricity is lost to the ballast loads in this design layout as shown in Figure 6.10 below.

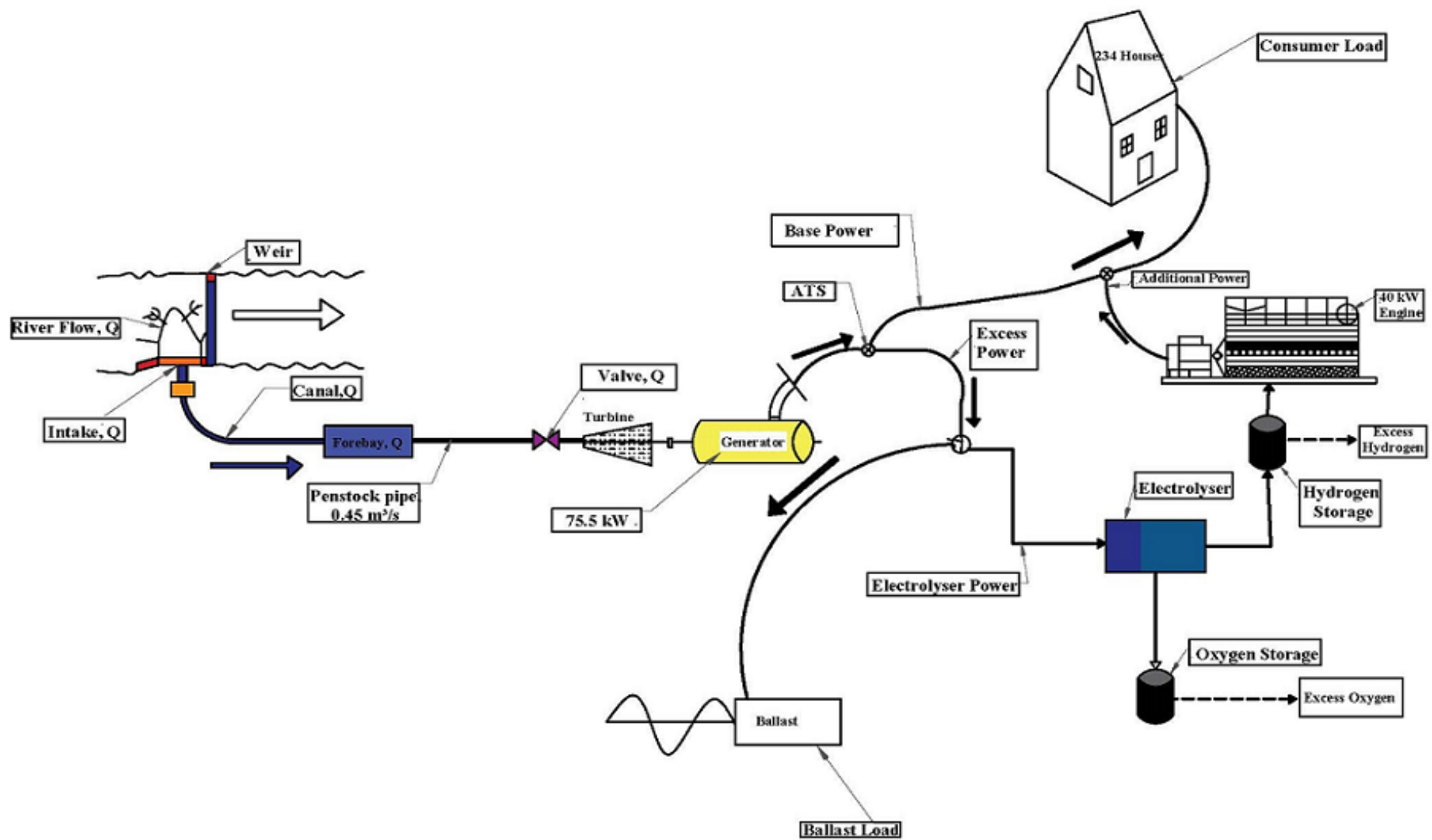


Figure 6.10: Micro-hydro turbine with an electrolyser and hydrogen engine

6.5.3.1 System architecture

The system architecture have also been developed and optimised by Homer Energy System Software and based on the energy supply and demand results, the system will consist of 75.5kW micro hydro turbine as a primary power supply, 40kW engine-generator system as a secondary power supply, 70 kW electrolyser system, 1,114.38 kWh/day consumer load demand and dump load (ballast). The electrolyser system is operated during the low demand hours of the day and supplied by the the excess electricity from the micro-hydro turbine. The produced hydrogen gas in the system design will be stored in a hydrogen tank and with the maximum storage tank capacity of 30 kg as shown in Figure 6.11 below.

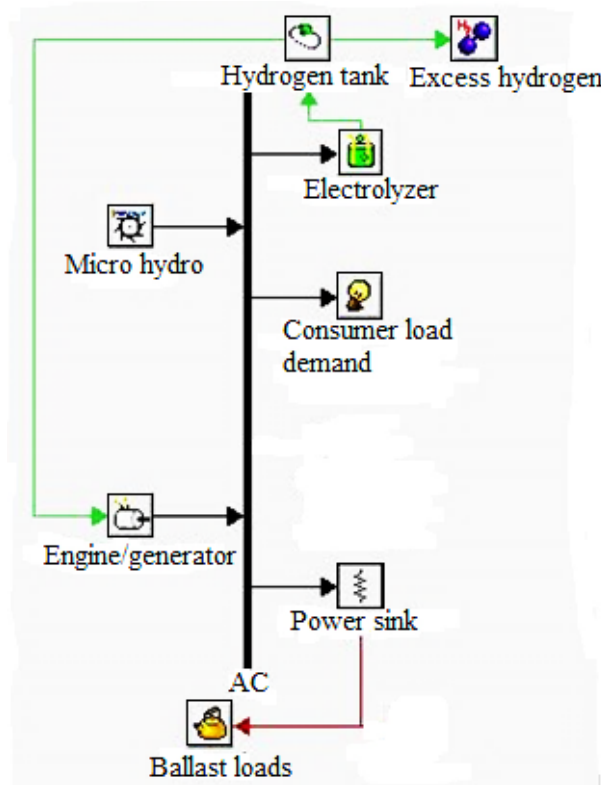


Figure 6.11: Micro-hydro turbine with an electrolyser and hydrogen engine-generator

In this system design, an additional source of electricity production is from the hydrogen ICE engine-generator system with the 40kW rated capacity which will be operating during the peak hours and power deficit hours of the day. In comparison between the two electricity production sources, the hydro turbine will have the major contribution of around 95% of the power supply while the engine-generator can only supply around 5% of the required load which is mainly during the peak load demand hours of the day.

Energy consumption is also divided into two main categories, which are AC primary load that accounts for about 63% of the total load demand and an electrolyser load for the hydrogen production that accounts for about 37% of the total load demand. These two

consumer loads are the main energy consumption for the system on which there is no excess electricity that is produced and sent to the ballast loads as shown in Table 6.5 below.

Table 6.5: Annual energy production and consumption

Item	kWh/year	%	Remarks
Hydro turbine	614,284	95	Energy production
Engine/Generator	35,374	5	
A/C primary load	406,269	63	Energy consumption
Electrolyser load	243,385	37	

6.5.3.2 Electrolyser

An electrolyser is an apparatus in which electrolysis is carried out by splitting water molecule into hydrogen and oxygen gas by using excess electrical energy. It utilises the process technology called Proton Exchange Membrane (PEM) which is the decomposition of a water molecule into oxygen and hydrogen gas atoms. This is done by passing an electric current through the water. The purity of hydrogen produced depend on the source of electric input and when comes from the renewable energy source, the hydrogen gas that is produced has no carbon footprint [165]. The size of the electrolyser system depends on the amount of hydrogen gas produced which is also directly proportional to the amount of electric current being passed through the water.

The majority of electrolysis process in the PEM uses excess electricity from the electricity source (in this case a micro-hydropower system) to breakdown the water molecules to hydrogen ions, oxygen gas and electrons as illustrated in Figure 6.12 below.

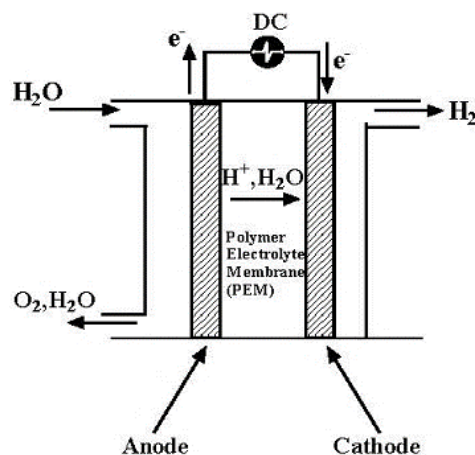


Figure 6.12: Working of PEM electrolysis [165]

In the process of slitting water molecules, electricity is supplied to the electrodes to initiate the electrochemical reactions while water is fed to the anode to lose electrons and decompose into hydrogen gas and oxygen gas.

Mathematically:



The combination of produced oxygen gas together with the water that have not been reacted are collected at the anode side as shown in the following equation.



On the hand, the produced hydrogen ions together with the un-reacted water molecules diffuse through the proton exchange membrane to the cathode side whereby they receive electrons to reduce to hydrogen gas as shown in the following equation.



In electrolysis modelling, the required equation for total electrical voltage for PEM electrolysis process is given by the following equation:

$$U_T = U_{equil} + U_{ohmic} + U_{actv,a} + U_{actv,c} \quad (6.18)$$

where U_T = total voltage, U_{equil} = equilibrium voltage, U_{ohmic} = ohmic overpotential across the PEM, $U_{actv,a}$ = activation overpotential at the anode and $U_{actv,c}$ = activation overpotential at the cathode. In the above equation the concentration of overpotentials is neglected due to the insignificant of gas transport limitations in thin electrodes for PEM electrolysis under normal operation conditions [166]. The equilibrium voltage for PEM type electrolysis is expressed empirically using the following equation [167].

$$U_{equil} = 1.23 - 0.9 \times 10^{-3}(T - 298) + 2.3 \frac{RT}{4F} \log (P_{H_2}^2 P_{O_2}) \quad (6.19)$$

where R = universal gas constant ($8.3 \text{ J mol}^{-1} \text{ K}^{-1}$), F = faraday constant ($9.65 \times 10^4 \text{ C mol}^{-1}$), T = absolute temperature, P_{H_2} = partial atmospheric pressure of hydrogen and P_{O_2} = partial atmospheric pressure of oxygen.

During electrolysis, the ohmic over potential across PEM is caused by the resistant of the membrane to the hydrogen ions transported across it. In modelling, the local ionic conductivity of the PEM is related to the amount of water available, the thickness of the membrane and also the membrane temperature. This can be determined empirically using the following equation [168].

$$\sigma[\lambda(x)] = [0.514\lambda(x) - 0.326] \exp [1268(\frac{1}{303} - \frac{1}{T})] \quad (6.20)$$

where x = location interface in the membrane measured from the cathode side, $\lambda(x)$ = water content at x and is expressed using the following equation:

$$\lambda(x) = \frac{\lambda_a - \lambda_c}{L} \quad (6.21)$$

where L = PEM thickness, λ_a = anode membrane water content, λ_c = cathode membrane water content.

By integrating the above equation, the overall ohmic resistance can be determined as follows:

$$R_{PEM} = \int_0^L \frac{dx}{\sigma[\lambda(x)]} \quad (6.22)$$

But using the ohm's law, the ohmic overpotential can be expressed using the following equation:

$$U_{ohmic} = \phi R_{PEM} \quad (6.23)$$

where ϕ = current density

In the electrolysis process the activation overpotential at the electrodes is the measure of the activity of the anode and cathode and is expressed by using Butler Volmer equation as follows:

$$U_{actv,i} = \frac{RT}{F} \sinh^{-1} \left[\frac{\phi}{2\phi_{o,i}} \right] \text{ and when expanding gives the following equation;}$$

$$U_{actv,i} = \frac{RT}{F} \ln \left[\left(\frac{\phi}{2\phi_{o,i}} + \sqrt{\left(\frac{\phi}{2\phi_{o,i}} \right)^2 + 1} \right) \right] \quad (6.24)$$

where $\phi = \phi_{o,i} \left[\exp\left(\frac{\alpha z F \eta_{actv,i}}{RT}\right) - \exp\left(\frac{(1-\alpha) z F \eta_{actv,i}}{RT}\right) \right]$

and $\phi_{o,i}$ is the exchange current density for PEM electrolysis for hydrogen production and is given by the following equation [169]

$$\phi_{o,i} = \phi_i^{ref} \exp \left(-\frac{U_{actv,i}}{RT} \right) \quad (6.25)$$

i = subscript representing anode and cathode sides respectively, $\phi_{o,i}$ = exchange current density, α = symmetrical factor (0.5 for water), z = number of electrons involved (2 for water) [170], ϕ_i^{ref} = pre-exponential factor, $U_{actv,i}$ = activation energy for anode and cathode. In PEM electrolysis modelling the input parameters with their values are shown in Table 6.6 below.

Table 6.6: Modelling parameter values for PEM electrolyser

Parameter	Units	Values	Reference
P_{H_2}	Atm	1.0	[171, 172]
P_{O_2}	Atm	1.0	[171, 172]
$U_{actv,a}$	kJ/mol	76	[169]
$U_{actv,c}$	kJ/mol	18	[169]
λ_a	-	14	[168]
λ_c	-	10	[168]

The electrolyser rated power capacity have been selected in order to meet the load demand with the available energy supply and the system design layout have been optimised with the values shown in Table 6.7 below.

Table 6.7: Power capacity for the electrolyser (simulation results)

Quantity	Value	Units	Remarks
Rated capacity	70.0 ^a	kW	
Mean input	33.53 ^b	kW	
Minimum input	9.16	kW	
Maximum input	58.0 ^c	kW	82.86% ^y
Total input energy	243,385	kWh/y	
Capacity factor	47.9 ^x	%	
Hours of operation	5,840	hours/year	

$$x = \frac{b}{a} \qquad y = \frac{c}{a}$$

The capacity factor for the electrolyser has been determined based on the rated capacity and the mean power input and based on the calculation results, the value of the capacity factor is 47.9% which is within the recommended system capacity factor range, i.e. between 44.8% to 69.35% [165]. On the other hand, the summary of hydrogen production from the electrolyser system and also hydrogen consumption by the engine-generator system is shown in Table 6.8 below.

Table 6.8: Hydrogen gas production and consumption (simulation results)

Production			
Quantity	Value	Units	Remarks
Average hydrogen output	0.423	kg/h	
Minimum hydrogen output	0.054	kg/h	
Maximum hydrogen output	0.938	kg/h	10.66 Nm ³ /h
Total hydrogen production	3,702	kg/year	
Specific consumption	65.74	kWh/kg	
Consumption			
Engine/generator	2,074	kg/year	56.02%
Excess hydrogen gas	1,628	kg/year	43.98%

6.5.3.3 Daily average hydrogen production

Based on the mean hydrogen output from Table 6.8 above, the daily average hydrogen production can be estimated as follows:

Daily average hydrogen production (kg/day) is given by the mean hydrogen output (kg/h) times 24 hours/day which gives the value of 10.15 kg/day.

6.5.3.4 Selected commercial electrolyser

The commercial electrolyser is available with different power rating capacity and hydrogen production. Based on the design optimization results, the 10.66 Nm³/h pure hydrogen electrolyser from National Renewable Energy Laboratory – the USA and Pure Energy Centre – the UK with the following specifications have been selected as shown in Table 6.9 below.

Table 6.9: Commercial selected Electrolysis unit [165, 173]

Manufacturer	Technology	System Energy Requirement (kWh/kg)	H ₂ Production Rate (kg/year)	Power Req for Max. H ₂ Production Rate (kW)	H ₂ Product Pressure (psig)
Proton	Proton Exchange Membrane - PEM	62.3 – 70.1	400 – 7,900	3 - 63	~200*

Note*: 200 psig = 14.8 Bar

Based on the average power consumption for the electrolyser system which is 33.53 kW that will produce an average hydrogen gas capacity of 0.423 kg/hour, then the average value of energy to mass ratio of the electrolyser system is 65.74 kWh/kg. This means that every kg of hydrogen produced requires 65.74 kWh of energy from the hydro system which confirms the selection of the Electrolyser system as shown in Table 6.9 above.

In the electrolyser system, the water to hydrogen conversion efficiency range from 80% to 95% and hydrogen purity range from 99.8% to 99.9998%. On the other hand, the system energy efficiency can be defined as the higher heating value (HHV) of hydrogen with every kilogram of hydrogen produced divided by the energy consumed by the electrolysis system which includes electrolyser, rectifier and auxiliaries.

From the design calculation results of the electrolyser system, the system energy efficiency value is around 60% and based on the selected Proton's proton exchange membrane (PEM) electrolyser, the system energy efficiency process ranges from 56% to 73% which is within the calculated efficiency value [165]. Based on the above values, the capacity factor ranges of the electrolyser system have been estimated to be 44.8% as a minimum value and 69.35% as the maximum value which coincides with the capacity factor range for the selected electrolyser system as shown in Table 6.10 below.

Table 6.10: Electrolyser detailed technical specification [173]

Quantity	Value
Maximum Hydrogen Production	10.66 Nm ³ /h
Maximum Oxygen Production	5.33 Nm ³ /h
Maximum electricity consumption	58 kW @ 400V AC 50Hz
Production variation range	20% to 100% of max. capacity
Water consumption at full power	9 litres/hour
Hydrogen purity before purifier	99.3% to 99.8%
Capacity factor	44.8% to 69.35%
Outlet gas pressure	up to 12 bar
Temperature range	5 to 35 °C
Cooling system	Air or liquid
Dimensions (L x D x H)	950 mm x 2000 mm x 200 mm
Weight	1600 kg

Note: The standard unit for hydrogen production is Nm³/h which refers to normal meter cubed per hour and it is used to measure hydrogen flow rate.

In this case, the units have been derived from the normal operating conditions of 0°C temperature and 1 atmosphere pressure (101.325 kPa) which is equivalent to 1 bar.

Advantages of the selected hydrogen electrolyser:

- The technology has a low cost due to the absence of noble metals like gold, silver and platinum

- When using renewables with excess or intermittent power, the electrolyser can be connected directly to produce hydrogen
- Technology is also user friendly and has no dangerous caustic electrolyte
- It can directly compress the hydrogen gas, so no need for a compressor
- The equipment is very safe, reliable efficient as well
- As shown on the system layout, the electrolyser can be easily integrated with engine-generator

6.5.3.5 Hydrogen gas storage

The produced pressurized hydrogen gas is stored in the storage tank and in this system design, the rated capacity of the hydrogen tank is 30 kg. Based on the available excess electricity the produced hydrogen storage tanks will have the following characteristics from the design optimization results as shown in Table 6.11 below.

Table 6.11: Hydrogen storage tank capacity

Quantity	Value	Units	Remarks
Maximum tank storage	30.0	kg	Rated capacity
Energy storage capacity	1,000	kWh	1 MWh
Tank autonomy	21.6	hours	
Minimum tank storage	15.0	kg	50% rated capacity

In this case, the minimum tank level that the system can operate is 15 kg (50% rated capacity) which is often available at the beginning of the cycle while the maximum tank level for hydrogen gas storage is 27 kg (90% rated capacity) at the end of the cycle year. Based on this result, the tank level can operate at a range of 12 kg (40%) capacity throughout the year.

The hydrogen tank level capacity between 15 kg to 27 kg operated at different cycles in a year and the frequency of occurrences at this capacity range is between 0.5% and 15.4%. Lowest and highest hydrogen tank capacity levels occur at around 0.5% of the time and 1% of the time respectively. The most frequency tank level capacity occurs at around 15.4% of the time with the capacity of 23 kg (76.67% rated capacity). For safety reasons, the tank level is only filled from 50% rated capacity to 90% rated.

6.5.3.6 Hydrogen internal combustion engine-generator (H₂ - ICE)

There are two types of hydrogen engines, a hydrogen fuel cell engine which uses electrolyte/electrodes and a hydrogen internal combustion engine which uses the combustion process. Both engines use hydrogen gas to generate power at different rates and energy intensity. The fuel cell technology is a more expensive method of power/electricity generation because it uses expensive catalysts and is more sensitive to impurities. Due to this effect of the hydrogen fuel cell technology as compared to the hydrogen internal combustion engine, in this research study, more focus will be on the hydrogen internal combustion engines due to the financial limitation.

In recent years, hydrogen gas production from excess electricity produced from renewable energy sources like hydropower plants has increased tremendously. This is because, current technology development has shown that hydrogen gas can be used as a fuel source to power internal combustion engines (hydrogen internal combustion engines) for transport (cars) or the production of electricity (generators) with zero pollution. In a recent book by Frano Barbir et al, Part Two: Hydrogen combustion and metal hydride batteries, Section 7: Hydrogen-fuelled Internal Combustion Engines there is an explanation about the Neat Hydrogen Engine which point out that hydrogen engine is capable of operating from ultra-lean mode to stoichiometric conditions without any problem of backfire [174]. In terms of hydrogen engine technology development, there is also a number of companies that run internal combustion engines with the hydrogen engine solutions and one of them is Pure Energy Centre in the UK. They offer practical solutions for conversion of petrol internal combustion engines to run on hydrogen fuel for stationary and industrial applications that gives no CO₂ and very low NO_x emissions [173]. Also, in the former lab of Sir Joseph Swan Centre for Energy Research - Newcastle University, a previous PhD student has modified a diesel engine to run on hydrogen fuel and the engine has been tested [175, 176]. The common hydrogen powered engines have been developed by converting Internal Combustion Engine – ICE (petrol engines) to run on hydrogen and they are similar to any standard ICE engine. The only difference is that the hydrogen engines run on hydrogen as fuel and emits very low NO_x emissions and zero CO₂ when compared to other engines, hence they are very environmentally friendly engines. The hydrogen engine (H₂-ICE) in this research study will be coupled with a generator system which provides additional electricity during the peak hours of the day. The produced hydrogen gas from the electrolyser will be fed to the engine as fuel and run for 5 hours each day at different power

capacities. From the system design optimization results, the rated capacity of the engine-generator is 40 kW. The engine capacity selected is available commercially with the use of different fuel gases as shown in Table 6.12 below.

Table 6.12: Hydrogen engine-generator system capacity (simulation results)

Quantity	Value	Units	Remarks
Hours of operation	1,825	hours/year	5 hours/day
Number of starts	365	starts/year	
Operational life	8.22	years	
Electricity production	35,374 ^a	kWh/year	Production
Mean electrical output	19.4	kW	
Minimum electrical output	12.2	kW	
Maximum electrical output	31.7	kW	
Hydrogen consumption	2,074	kg/year	Gas consumption
Specific fuel consumption	0.059	kg/kWh	
Fuel energy input	69,120 ^b	kWh/year	
Energy efficiency	51.2 ^c	%	

Note: Density of Hydrogen (H₂) gas = 0.090 kg/m³ @ 0°C/32°F, 1 bar and $c = \frac{a}{b}$

From the above Table 6.12, the energy efficiency is calculated based on the ratio between the electricity production (kWh/year) to fuel energy input (kWh/year) and the specific fuel consumption is the ratio between hydrogen consumption (kg/year) to electricity production (kWh/year). Based on the above simulation results which shows that energy efficiency value is above 50% and this conclude that the system design specifications are on the recommended range for the chosen engine-generator size. The engine specific fuel consumption is determined in terms of how much quantity of gas consumed (kg) in order

to produce a unit amount of energy (kWh) and from the design calculations, the specific fuel consumption is 0.059 kg/kWh.

The interpretation of this value is that, for every 0.059 kg of fuel hydrogen gas consumed by the engine unit can produce 1 kWh of electrical energy on which this can be interpreted as 1 kg of fuel hydrogen gas can produce 16.95 kWh of energy (which is 50.9% of the LHV)

6.5.3.7 Engine-generator type selection

Based on the calculated design parameters and optimized design values, the gas engine selected is PRAMAC, GGW50G with 5.4L and 50kVA, Industrial Spark-Ignited Generator Set. It has the following specifications: Power ratings, three-phase 400 VAC @0.8pf, with standby values: 50 kVA/40 kW with 72 Amps and Prime values: 45 kVA/36 kW and 65 Amps. The engine fuel consumption depends on the percent of the load as shown in Table 6.13 below.

Table 6.13: Fuel consumption rates

Percent Load	Standby [m³/h]	Prime [m³/h]
25%	7.6	6.8
50%	13.1	11.8
75%	17.7	15.9
100%	21.8	19.6

Most gas engines-generator systems that produce electricity uses different types of gas fuels with different energy capacities. In recent years hydrogen gas has been used as fuel in many applications and from the energy content point of view, hydrogen gas shows advantages as compared to other fuels used in engine-generators. The Table 6.14 is the comparison of hydrogen gas fuel with other gases and liquids fuels used in today's engines-generator systems.

Table 6.14: Gas and liquid fuel comparison [177]

Fuel	Density	Higher Heating Value		Lower Heating Value	
	@ 0°C/32°F, 1 bar	(HHV) (Gross Calorific Value -GCV)		(LHV) (Net Calorific Value - NCV)	
Gaseous fuel	kg/m³	kWh/kg	MJ/kg	kWh/kg	MJ/kg
Acetylene	1.097	13.9	49.9	-	-
Hydrogen	0.090	39.4	141.7	33.3	120.0
Methane	0.716	15.4	55.5	13.9	50.0
Natural gas	0.777	14.5	52.2	13.1	47.1

Fuel	Density	Higher Heating Value		Lower Heating Value	
	@ 0°C/32°F, 1 bar	(HHV)		(LHV)	
Liquid fuel	kg/l	kWh/kg	MJ/kg	kWh/kg	MJ/kg
Diesel fuel	0.846	12.67	45.7	11.83	42.6
Petrol	0.737	12.89	46.4	12.06	43.4
Kerosene	0.821	11.94	43.0	11.94	43.0
LPG	0.537	13.69	49.3	12.64	45.5
Ethanol	0.789	8.25	29.7	7.42	26.7

From Table 6.14 above, it is noted that hydrogen gas fuel has the highest energy value as compared to other fuels although it has the lowest density. Due to this property hydrogen gas can be used as a fuel to power engine-generator system in order to produce electricity without emissions, thus why it has been selected as a fuel for this research project. The system design optimization results show that the hydrogen energy (heating) content as input to the engine is 16.95 kWh/kg which can also be obtained from the product of the lower heating value for hydrogen fuel (33 kWh/kg) and engine-generator energy efficiency (51.2%).

The selection of an engine-generator system that will use hydrogen gas has been considered based on the following hydrogen fuel advantages:

- It stores energy more efficiently than the batteries system
- It can provide more energy storage capacity
- It has a high energy density
- It does not rely on any fossil fuel and when used its waste product is water vapour and hence no emission products to the environment.

6.5.4 Micro-hydro turbine design calculations

The type of micro-hydro turbine system to be used in this research project has been selected based on the data obtained from the site area. The two main parameters that are required in

order to determine the type of turbine to be used are the available river flow rate (Q) and site head (H). On the other hand, in the literature, there are two general types of a water turbine, Reaction turbine and Impulse turbines on which each type have specific site characteristic in order to be selected for a particular application. In terms of their characteristics reaction turbines require a substantial amount of water flow discharge while impulse turbines are much more dependable on medium and high head site locations.

Based on the feasibility study report and flow measurements, Hhaynu river flow discharge is $0.9 \text{ m}^3/\text{s}$ and from the hydrological study only $0.45 \text{ m}^3/\text{s}$ is feasible from the river flow to be used as flow discharge to the turbine to allow for environmental flow during the dry season. In addition to that, the maximum gross head obtained after taking the site measurements is 25m and this is the distance from the forebay area to the power house location. Using these two values obtained from the site measurements, then the type of turbine used in this research study project has been selected to be Crossflow turbine type which will be used in this research study. In recent years there has been a quite number of turbine technology development and based on many studies in mini and micro scale application, crossflow turbines are well adapted in rural/local environment (because they can be manufactured locally), robust, low in maintenance (no need of an expert) and also have a wider range of application based on the available head and flow discharge from low to medium values [29]. This is why they are mostly applicable to micro-hydropower systems in rural areas of developing countries like that of Hhaynu micro-hydropower plant in Mbulu, Tanzania.

6.5.4.1 Micro-hydro turbine mechanical system design

More detailed turbine design calculation values are shown in the appendix and below is the summary of the main turbine mechanical parameters

(a) Turbine speed

Cross flow turbines use pulley and belt as the transmission drive from the turbine to the generator unit which means that the turbine speed is usually lower than the generator speed.

In calculating the generator speed the following formula is used:

$$N = 513.25 \times \frac{(H_g)^{0.745}}{\sqrt{P_{MHP(t)}}} \quad (6.25)$$

Where; N = Turbine speed in RPM, H_g = Gross head (m) and $P_{MHP(t)}$ = micro-hydro turbine Power (kW)

(b) Turbine shaft diameter

The turbine shaft diameter is calculated using the Power – Torque equation as follows;

$$P_{MHP(t)} = T_q \cdot \omega. \quad (6.26)$$

Where; $P_{MHP(t)}$ = micro-hydro turbine power, T_q = Torque, ω = rotational speed in radians and N = rotational speed in RPM

Also, the Torque can be calculated using the following shear stress equation as follows;

$$T_q = \frac{\pi D^3 \tau_s}{16} \quad (6.27)$$

where D = shaft diameter and τ_s = shear stress

The calculated turbine values for the hydro system are shown in Table 6.15 below.

Table 6.15: Main turbine design values

Parameter	Value	Unit	Remarks
Turbine speed	635	RPM	Selected value
Speed ratio	1:2.36		
Turbine torque	1.5	kNm	
Turbine shaft diameter	60	mm	Selected value

6.5.4.2 Micro-hydro turbine penstock pipe design

The penstock is the steel pipe that conveys water with pressure from the forebay to the turbine unit in the power house. The water in the forebay is stored in a form of potential energy and when delivered to the turbine through penstock pipe they produce kinetic energy which rotates the water turbine.

The penstock steel pipe wall thickness depends on the pipe materials, diameter and operating pressure and is calculated as follows:

(a) Penstock diameter and thickness

$$D_p = 2.65 \times (m_c^2 \times Q^2 \times L_p / H_g)^{0.204} \quad (6.28)$$

where m_c = manning coefficient for the mild steel penstock pipe = 0.012

$$Q = \text{design flow discharge} = 0.45 \text{m}^3/\text{s}$$

$$L_p = \text{length of the penstock} = 162 \text{m}$$

From literature, the minimum penstock pipe wall thickness is given by the following equation;

$$t_p = \frac{D_p + 508}{400} + 1.2 \text{mm} \quad (6.29)$$

t_p = minimum penstock thickness (mm)

(b) Water flow velocity in the penstock

The water flow discharge to the turbine passes through the penstock pipe and is given by the following equation:

$$Q = AU_{water} \tag{6.30}$$

where Q = water flow discharge, A = penstock pipe area and U_{water} = water flow velocity

Making U_{water} the subject from the above equation gives;

$$U_{water} = \frac{Q}{A} = \frac{4 \times Q}{\pi D^2} \tag{6.31}$$

(c) Area of the Penstock pipe

Area of the penstock pipe is given by the following equation;

$$A = \frac{\pi \times (D_p)^2}{4} \tag{6.32}$$

(d) Penstock head loss

Head loss in the penstock can be calculated using the following equation;

$$Head\ loss = \left[\frac{10 \times m_c^2 \times Q^2}{D_p^5} \right] \times L_p \tag{6.33}$$

Where; m_c = Manning coefficient value, Q = Design flow discharge, D_p = Diameter of the penstock and L_p = Length of the penstock

(e) Percentage of head loss

The recommended economical head loss for most small hydropower schemes should be below 10%

$$\% \text{ Head loss} = \frac{\Delta H}{H_g} \tag{6.34}$$

The calculated penstock values for the hydro system are shown in Table 6.16 below.

Table 6.16: Penstock pipe design values

Parameter	Value	Unit	Remarks
Penstock diameter	460	mm	18” Selected design value
Water velocity in the penstock	2.7	m/s	1m/s – 2.8m/s water flow velocity range
Area of the penstock pipe	0.166	m ²	
Penstock head loss	2.29	m	
Percentage of head loss	9.16	%	Value is below 10%

6.5.4.3 Micro-hydro turbine pulley and belt design

In order to calculate the pulley and belt parameters, the following standard values have been selected based on the turbine design calculations;

Turbine parameters:

- (i) Turbine speed = 635 RPM
- (ii) Turbine mechanical power = 79.5 kW
- (iii) Turbine operation time 24 hours

Generator parameters:

- (i) Generator speed = 1500 RPM
- (ii) Generator electrical power = 75.5 kW
- (iii) Synchronous, 3 phase, 90KVA with power factor 0.8
- (iv) Generator pulley diameter = 150mm (OK because > 140)
- (v) Generator operation time 24 hours

(a) Turbine pulley diameter using speed ratio

In calculating the turbine-generator speed ratio the turbine and generator speed and diameter ratios need to be considered.

$$\text{Turbine speed ratio} = \frac{N_1}{N_2} = \frac{D_2}{D_1} \quad (6.35)$$

N_1 = turbine speed (635 RPM), N_2 = generator speed (1500 RPM), D_1 = diameter of turbine (large) pulley (355mm) and D_2 = diameter of small (generator) pulley (150mm)

(b) Sizing of the belt length

The belt length is determined using the following relation

$$\text{Belt length} = 2C + \frac{\pi(D_1+D_2)}{2} + \frac{(D_1-D_2)^2}{4C} \quad (6.36)$$

(c) Turbine pulley belt speed (velocity)

The turbine velocity is given with the following equation

$$\text{Velocity} = \frac{D}{2} \times \omega \quad (6.37)$$

where; ω is the rotational turbine speed given as $\frac{2\pi N}{60}$

(d) Belt centre distance

Centre distance C is calculated as follow;

$$C = D_2 + D_1 \quad (6.38)$$

$$C = 505\text{mm}$$

But the exactly centre distance can be calculated using the following formula;

$$C = A + \sqrt{A^2 - B} \quad (6.39)$$

But; $A = \frac{L}{4} - \frac{\pi}{8}(D_2 + D_1)$ and $B = \frac{(D_2 - D_1)^2}{8}$

(e) Power per belt

Interpolating from the given Table on page 63 [14]

- Rated power per belt = $(20.75 + 23.56)/2 = 22.155$ kW
- Additional power = $(1.50 + 1.75)/2 = 1.625$ kW

Therefore, the basic power per belt = 22.155 kW + 1.625 kW = 23.78 kW

(f) Correction power per belt

From Table on page 58 the combined correction factor is 0.85 [14]

Therefore, correction power per belt = 23.78 kW x 0.85

(g) Number of belt

Number belt for the belt design is given as follow;

$$\text{Number of belts} = \frac{P_T}{P_{c/b}} \tag{6.40}$$

where P_T = total power and $P_{c/b}$ = correction power per belt

(h) Net driving force

The net driving force from the turbine pulley is given from the following equation;

$$F_d = F_f - F_b \tag{6.41}$$

The calculated turbine pulley and belt components for the hydro system are shown in Table 6.17 below:

Table 6.17: Pulley and belt drive design values

Parameter	Value	Unit	Remarks
Turbine pulley diameter	355	mm	Selected design value
Generator pulley diameter	150	mm	
Length of the belt	1825	mm	SPB1825
Belt velocity	11.7	m/s	Value is below 40
Belt centre distance	505.69	mm	
Number of belts	4	pcs	
Net driving force	8.42	kN	

6.5.4.4 Micro-hydro turbine electrical system design

The electrical components consist of the generator system and transmission system. These components are related to the electrical power produced and transmission.

(a) Generator system

The generator system will be operated with the following rated capacity values;

Frequency, $f = 50\text{Hz}$

Generator power, $P_{MHP(g)} = 75.5\text{kW}$

Efficiency, $\eta_{generator} = 95\%$

Rotational speed, $N = 1500\text{ RPM}$

Number of poles, $n_p = 4$

Power factor, $P_F = 0.8$

The generator power can be calculated based on the available turbine power and efficiency value. The turbine efficiency value depends on the type of turbine used and for the selected cross flow turbine technology, the efficient value is 72% as shown in Figure 6.13 below.

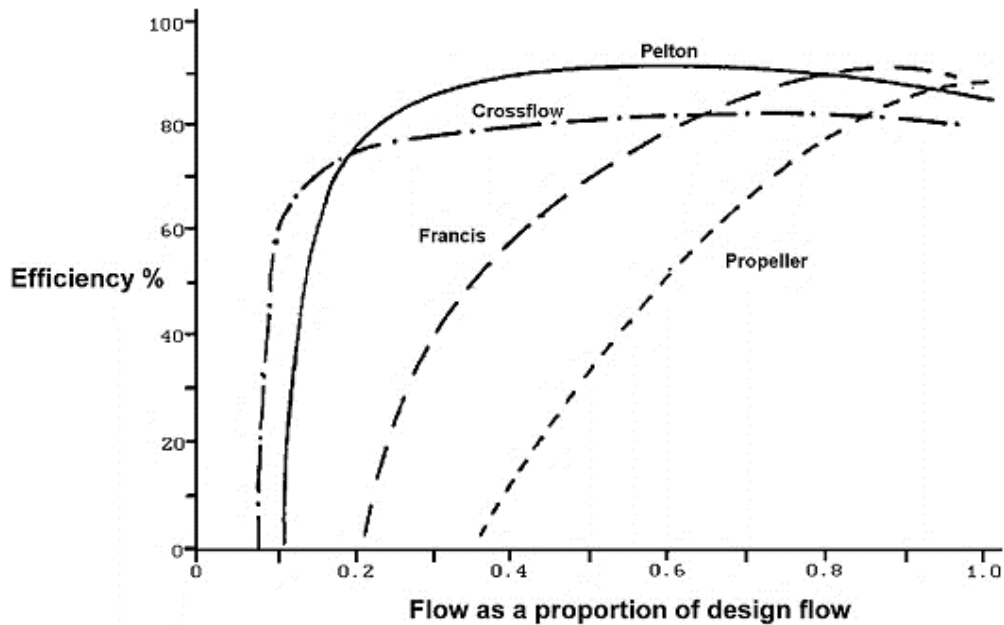


Figure 6.13: Efficiency range with design flow discharge for different turbines [8]

The generator power output will be supplied to the main load through the local grid connections in the area. The generator design capacity value has been influenced by the turbine output power and the synchronous speed, ω_s of the generator is related to the speed N and is given as:

$$\omega_s = \frac{2\pi N}{60} \quad (6.42)$$

At the rated condition $N = 1500\text{ RPM}$

This can also be calculated using the following equation;

$$\omega_s = \frac{4\pi f}{n_p} \quad (6.43)$$

In operation, the speed of the generator changes with the load demand changes and this affects the actual speed of the generator. This speed is the difference between the actual generator speed and synchronous speed and is the one that determines the instantaneous generator speed under different loading condition as shown in Table 6.18 below.

Table 6.18: Generator power and speed at different rated capacity

Supply power (kW)	Generator speed (RPM)	Generator speed (rad/s)	Remarks
75	1500	157	Rated capacity
40	1520	159.09	Minimum load demand
101.8	1494	156.37	Maximum load demand

Therefore, the difference in speed (RPM) from the above three scenarios can be calculated as follows;

$$\Delta N = \frac{60}{2\pi} \Delta\omega \quad (6.44)$$

6.7 Summary

In the chapter, the system design model has been developed and analysed together with the energy storage technology options as follows:

- (i) Micro-hydro turbine without storage
- (ii) Micro-hydro turbine with battery storage
- (iii) Micro-hydro turbine with an electrolyser system and hydrogen engine

From the results of the system design and also analysis of the above energy storage options, the use of electrolyser system and hydrogen engine-generator system which is currently available on the market have significantly reduced the loss of excess electricity to the ballast loads (waste electricity) and this resulted to the increase in the energy storage capacity as compared to the battery energy storage system.

So in conclusion and based on the positive results of energy utilization by using hydrogen gas that is produced by an electrolyser system as a fuel that is currently undergoing more research and development, it is obvious that the system design model of micro-hydro turbine with an electrolyser system and hydrogen engine promises better prospects in terms of innovations, better energy utilization, more research and development and hence it has been selected and analysed further in the next Chapters.

Chapter 7 Modelling

7.1 Introduction

The system design from the previous Chapter on which the micro-hydro turbine parameters have been obtained is used as input in modelling and simulation in order to analyse and evaluate the system stability and highlight its performance characteristics. In modelling, the input parameters from the system design values are fed to the computing software program which has been developed to resemble the system being modelled and simulated in order to produce the system behaviour and evaluate its performance and operational characteristics. There are many software's that are used in modelling and simulation for engineering related research but in this research study, two types of modelling/simulation software's have been used, i.e. MATLAB/Simulink and Homer Energy. The reason for using these two software is that they can represent a typical design layout of the micro-hydro turbine system in operation and also in terms of research, these softwares have been extensively used in many study works related to modelling and simulation of Renewable energy systems and hence there is an extensively published journal articles/reports that are useful to validate my research work.

7.2 Hydro Turbine System Modelling

Micro-hydropower plant modelling can be done by taking into consideration the physical arrangement of its hydraulic turbine system. The general arrangement of the micro hydro turbine system consists of a weir, intake, canal, forebay, penstock and turbine/generator system. The weir is used to divert the water from a river and direct it to the intake and canal. At the end of the canal, there is a forebay which is a temporary water storage tank and is usually connected to an elevated head penstock (pipe) that carry water flow discharge with high pressure and velocity to the water turbine unit which is connected to the generator that rotated and produces electricity as shown on Figure 7.1 below.

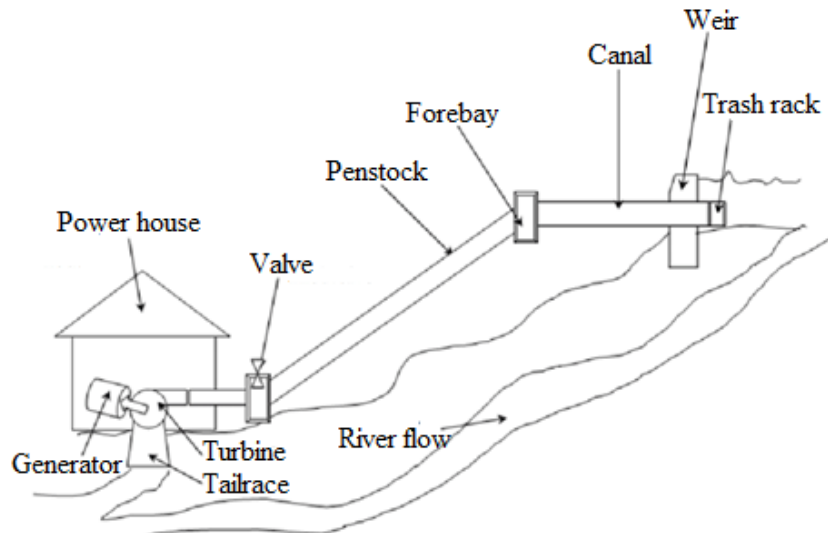


Figure 7.1: Schematic diagram of a micro-hydropower plant [178]

In micro-hydro-turbine modelling, the tangential characteristics of the micro-hydropower plant are determined by the penstock dynamics, turbine dynamics, turbine control dynamics, generator dynamics and load dynamics as shown in Figure 7.2.

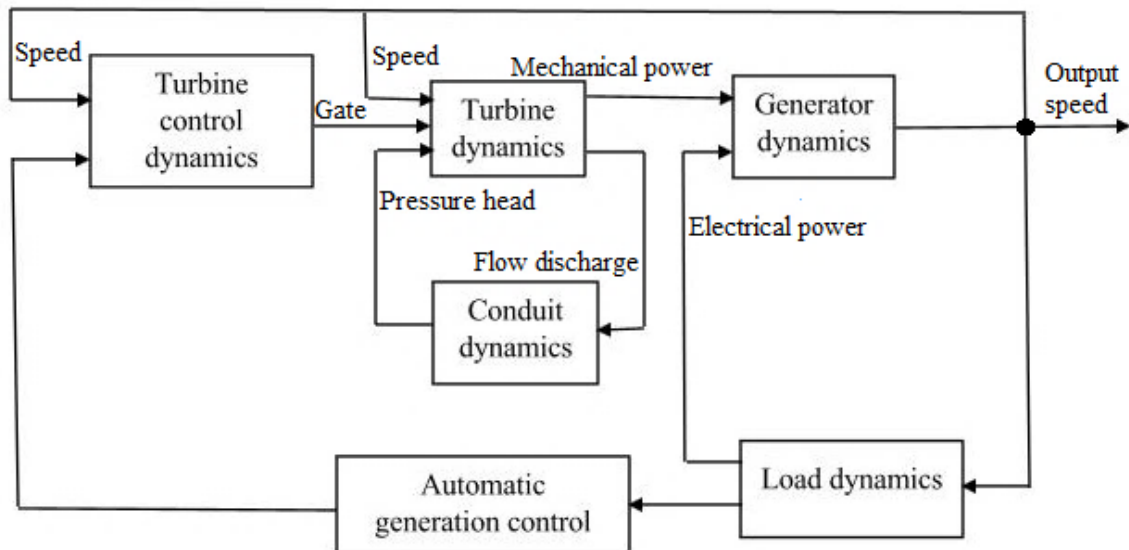


Figure 7.2: Hydropower plants functional block modelling diagrams

The turbine conduit dynamics is related to the dynamics of the water flow in the penstock which is determined by the water flow rate value Q , pressure head H , flow velocity U and the length of the penstock L . In this relationship, the turbine and penstock dynamics are determined by the four basic relations between the turbine power P_m , velocity of the water in the penstock U and the acceleration of water column H as shown in Figure 7.3 below.

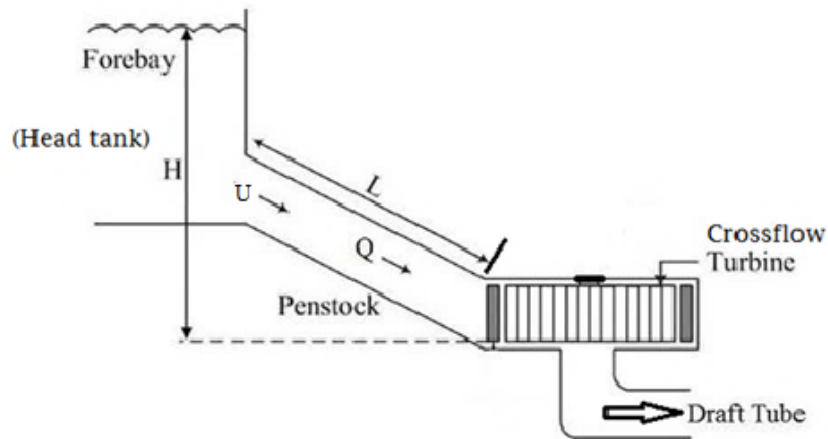


Figure 7.3: Components layout of a hydro turbine system [179]

On the other hand, the turbine/generator dynamics are determined by the power/torque and the rotational speed of the prime mover which has to be maintained and controlled by turbine control dynamics through gate position from the servo motor.

With linear blocks, the micro hydropower plant model can be presented as shown in Figure 7.4 below as a closed system with a feedback loop. The plant dynamics consists of gate positioner, hydraulic system and turbine/generator system. On the other hand, load disturbances are related to the unpredicted load that may be introduced into the system and may affect the system performance and stability by reducing/increasing the generator rotational speed and hence the frequency.

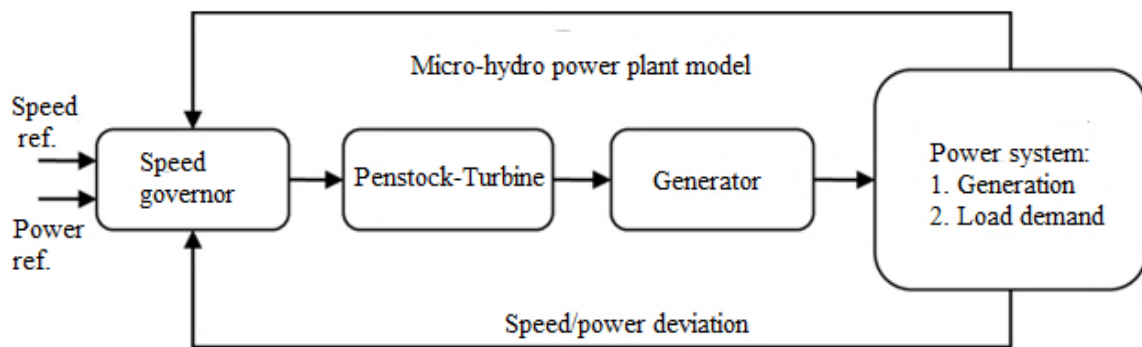


Figure 7.4: Micro-hydro power plant block diagram

7.2.1 Hydraulic Turbine dynamics

Electricity generated from micro hydropower plants is an important renewable energy source in many rural areas of the developing countries which provide significant flexibility during its operation phase (off-grid operation). When most of the micro hydro turbine is in operation, their dynamic operating behaviour is mostly determined by the transient characteristics of the water flow in the penstock, although from the literature it is noted that the turbine energy conversion process has been involved non-dynamic characteristics

[180]. In broad categories, micro-hydro power plants system models can be classified into two major segments based on the complexity of their transfer functions/equations involved in the modelling process i.e. the linear models which sometimes called non-elastic model and non-linear models which sometimes called elastic model.

In the modelling of a micro-hydro turbine system, the use of transfer functions/equations with linear and non-linear behaviour have to be used. The transfer functions are mathematical equations which are essential tools for the simulation of micro hydro turbine systems which will be explained in details in the following sub-sections.

7.2.2 Hydraulic Turbine transfer function

Most linear hydropower models are calculated around an operating point and they are extracted from basic equations of turbine and penstock hydraulic characteristics. The model equations are based on the transfer function which relates to the turbine mechanical output power to the gate opening signal. Considering the studies based on system stability, the formulation of the representation of the hydraulic turbine is based on the following assumptions:

- (a) The penstock pipe is in-elastic and water is incompressible
- (b) The hydraulic resistance in the system is negligible
- (c) The water flow velocity in the pipe varies directly with the gate opening and with the root square of the net head
- (d) The hydraulic turbine output power is proportional to the product of the head and volume of flow

7.2.3 Penstock Pipe and Turbine system

In a micro hydro turbine system, the penstock is the pipe which carries water discharge from the head tank (forebay) to the turbine unit. The velocity of the water in the penstock will be determined by the pressure head/elevation between the intake and the powerhouse. The appropriate water velocity and pressure head inside the penstock will determine the turbine speed and hence the generator speed but due to the fluctuation of water volume in the penstock pipe, the speed of the turbine/generator varies as well which affect generator rotation speed and frequency. In a normal application, the speed and frequency of the micro-hydro generator system must be maintained at a constant nominal value of 1500 RPM and frequency of 50 Hz but when connected to a local grid there is usually a tolerance of $\pm 5\%$. So, in order to maintain this constant generator speed and frequency value, most

micro-hydro turbine system regulates the rate of water discharge to the turbine which in turn change the turbine-generator speed by the use of speed governing system.

During the turbine operation when water discharge flow through a penstock pipe, the micro-hydro turbine system responses consists of two scenarios:

- (a) The transient response: which is the initial state of the turbine-generator speed response caused by the initial pressure change due to the introduction of water flow to the turbine system. In this case, the system is unstable due to changes in turbine power and speed.
- (b) The steady state response: when the turbine-generator system stabilizes and gives the steady-state values of speed and mechanical power

7.2.3.1 Penstock Pipe

A: Discharge $Q(s)$ and Pressure head $H(s)$

Considering the water flow in the penstock pipe from the inlet as point 1 (water entrance) and the outlet as point 2 (water exit) in Figure 7.5 below, the volumetric flow rate in the penstock Q is given by;

$$Q = A_1U_1 = A_2U_2 \quad (7.1)$$

where Q = water discharge (m^3/s), A = penstock cross-sectional area (m^2) and U = water flow velocity in the penstock (m/s), H or H_s = Water height (m) (In steady state operating condition, $H = H_s$ while during transient's condition $H \neq H_s$)

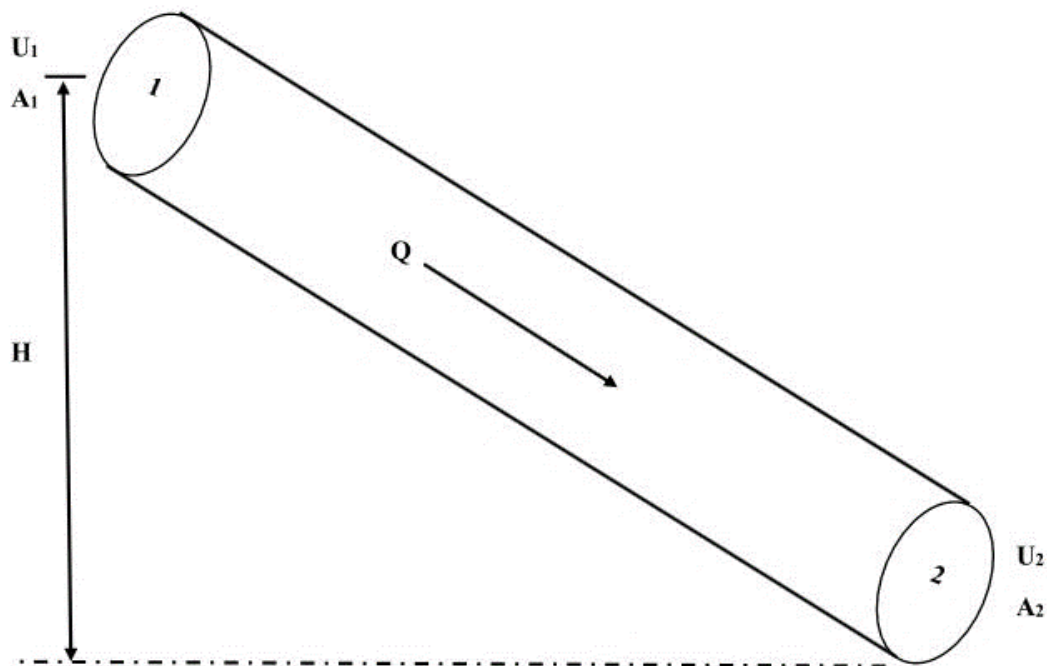


Figure 7.5: Water flow discharge through a penstock pipe

Water flowing in the penstock from the intake at point 1 and exit at point 2 and when considering the volume flow rate in the penstock, the amount of water flow at point 1 and point 2 will remain the same [181] and thus the water flow discharge Q can be written as:

$$Q = AU \quad (7.2)$$

From the above equation, the value of Q can be interpreted as the rate of change volume discharge Δv (m^3) with a change in time Δt (s) and depends on the water flow velocity U and penstock cross section area A .

So applying Δv to the above equation, the change in volume flow of the water is given by:

$$\frac{\Delta v}{\Delta t} = AU \quad (7.3)$$

Where: Δv = change in volume flow and Δt = change in time

Re-arranging the above equation gives, $\Delta v = AU\Delta t$ and when differentiating with respect to time it gives, $dv = AU(t)dt$

Simplifying the above equation based on the water flow velocity in the penstock as a function of time, the change in volume flow Δv becomes:

$$\Delta v = AU(t)\Delta t \quad (7.4)$$

On the other hand, the water flow in the penstock from the inlet and the exit can be related to the Bernoulli's theorem that:

$$\frac{U_1^2}{2g} + \frac{p_1}{\rho g} + H_1 = \frac{U_2^2}{2g} + \frac{p_2}{\rho g} + H_2 \quad (7.5)$$

Since both the penstock inlet and exit are exposed to the atmospheric pressure, then $p_1 = p_2$ and also the velocity at the penstock inlet U_1 is usually very small compared to the velocity at the penstock exit U_2 due to large volume of water from the forebay to the penstock inlet, so in this case, U_1 is set to be zero ($U_1 = 0$)

Thus, the above equation can be simplified and becomes;

$$\frac{-U_2^2}{2g} + 0 + (H_1 - H_2) = 0 \quad (7.6)$$

Let H represent the difference between H_1 and H_2 then the water flow exit velocity U_2 in the penstock can be expressed as:

$$U_2 = \sqrt{2gH} \quad (7.7)$$

This is the exit velocity of the water in the penstock which is the function of pressure head H and gravity. This is valid for most micro-hydro turbine systems as the velocity of the water flow in the penstock depend on the pressure head H .

Consider the water volume flow between the inlet and exit of the penstock, the total change in volume of water entering the penstock (Δv_{in}) during the change in time Δt should be

equal to the change in volume of water exit from the penstock (Δv_{exit}). The above relation is based on the law of conservation of energy.

The equation $\Delta v = AU(t)\Delta t$ can be expanded to determine the volume of water entering and exit the penstock as follows:

$$\Delta v_{exit} = A_2 U_2(t) \Delta t \quad (7.8)$$

But $A_2 = \frac{\pi D_2^2}{4}$ where D_2 = diameter of the penstock pipe at the exit point

$$\text{Then; } \Delta v_{exit} = \frac{\pi D_2^2}{4} \times \sqrt{2gH} \times \Delta t \quad (7.9)$$

When considering the $\Delta H(t)$ as the amount of water pressure head in the penstock at the incremental time Δt , then the rate of change water volume flow at the inlet Δv_{inlet} is given by;

$$\Delta v_{inlet} = -A_1 \times \Delta H(t) = -\left(\frac{\pi D_1^2}{4}\right) \times \Delta H(t) \quad (7.10)$$

The rate of volume at the penstock inlet should be equal to the rate of volume at the penstock exit, i.e. $\Delta v_{inlet} = \Delta v_{exit}$ which gives the following relation:

$$-\left(\frac{\pi D_1^2}{4}\right) \times \Delta H(t) = \frac{\pi D_2^2}{4} \times \sqrt{2gH} \times \Delta t \quad (7.11)$$

This can be re-written as:

$$\frac{\Delta H(t)}{\Delta t} = -(H(t))^{1/2} \times \left(\frac{D_2}{D_1}\right)^2 \times \sqrt{2g} \quad (7.12)$$

Considering the continuous flow of water through the penstock which will give the rate of change in time, $\Delta t = 0$

So, the above equation can be written as;

$$\frac{dH(t)}{dt} = -\left(\frac{D_2}{D_1}\right)^2 \times \sqrt{2gH(t)} \quad (7.13)$$

$$\frac{dH(t)}{dt} + \left(\frac{D_2}{D_1}\right)^2 \times \sqrt{2gH(t)} = 0 \quad (7.14)$$

The above equation can be considered for the ideal condition with no head loss in the penstock and it represents a first order differential equation of the rate of change of pressure head with time.

When considering the head losses on the system, the rate of water flow discharge per unit time on the penstock must be equal to the volumetric flow rate on the penstock, which gives:

$$\frac{dQ(t)}{dt} = \frac{dH(t)}{dt} + \left(\frac{D_2}{D_1}\right)^2 \times \sqrt{2gH(t)} \quad (7.15)$$

But, $\sqrt{2gH(t)} = U(t)$

Which gives;

$$\frac{dQ(t)}{dt} = \frac{dH(t)}{dt} + \left(\frac{D_2}{D_1}\right)^2 \times U(t) \quad (7.16)$$

The above water flow velocity with time $U(t)$ is the velocity at the inlet of the penstock;

$$U(t) = U_1(t)$$

In this case when considering the two water flow locations on the penstock inlet and exit and since water is continuously flowing on the system, so the inlet and exit water flow velocities may be represented as follows:

$A_1 U_1(t) = A_2 U_2(t)$ Substituting the value of U_1 gives;

$$U_1(t) = \frac{A_2}{A_1} U_2(t) = \left(\frac{D_2}{D_1}\right)^2 \times U_2(t) \quad (7.17)$$

Which can also be written as;

$$\frac{U_1(t)}{U_2(t)} = \left(\frac{D_2}{D_1}\right)^2 \quad (7.18)$$

Substituting the above $\frac{U_1(t)}{U_2(t)}$ values to the equation $\frac{dQ(t)}{dt} = \frac{dH(t)}{dt} + \left(\frac{D_2}{D_1}\right)^2 \times U(t)$ will give the following;

$$\frac{dQ(t)}{dt} = \frac{dH(t)}{dt} + \left(\frac{U_1^2(t)}{U_2(t)}\right) \quad (7.19)$$

The velocity $U_1(t)$ represents the water flow velocity at the penstock inlet and the velocity $U_2(t)$ is the flow velocity at the penstock exit. Since the speed of the water flows in the penstock pipe will be determined by the approach velocity from the intake which is given by:

$$U_1(t) = U_1 = \sqrt{2gH(t)} \quad (7.20)$$

Substituting the $U_1 = \sqrt{2gH(t)}$ value to the equation $\frac{dQ(t)}{dt} = \frac{dH(t)}{dt} + \left(\frac{U_1^2(t)}{U_2(t)}\right)$ gives the following;

$$\frac{dQ(t)}{dt} = \frac{dH(t)}{dt} + \frac{1}{U_2(t)} 2gH(t) \quad (7.21)$$

To maintain the constant speed of the turbine at a given time, the water flow velocity $U_2(t)$ at the exit of the penstock must be constant (U_2).

Thus, the above equation can be written as;

$$\frac{dQ(t)}{dt} = \frac{dH(t)}{dt} + \frac{1}{U_2} 2gH(t) \quad (7.22)$$

Taking Laplace transform of the above equation, assuming initial condition to be zero gives the transfer function as follows:

$$sQ(s) = sH(s) + \frac{1}{U_2} 2gH(s) \quad (7.23)$$

Also, from the design formula, water flow discharge at the exit Q_2 is given by the following relation;

$$Q_2 = A_2 U_2 = \frac{\pi D_2^2}{4} U_2 \quad (7.24)$$

In this case, considering the turbine design parameter values of $Q_2 = 0.45 \text{ m}^3/\text{s}$ and $D_2 = 460 \text{ mm}$

Putting these values to the above equation gives the following results for the water flow velocity in the penstock pipe:

$$U_2 = \frac{4Q}{\pi D_2^2} = 2.7 \text{ m/s}$$

Then, substituting the values of U_2 and using $g = 9.81 \text{ m/s}^2$ on the equation

$sQ(s) = sH(s) + \frac{1}{U_2} 2gH(s)$ gives the following relation;

$$sQ(s) = sH(s) + \frac{2 \cdot 9.81}{2.7} H(s) \quad (7.25)$$

$$sQ(s) = sH(s) + 7.27H(s)$$

$$sQ(s) = H(s)[s+7.27] \quad (7.26)$$

Re-arranging the above equation gives the following relation;

$$\frac{H(s)}{Q(s)} = \frac{s}{s+7.27} \quad (7.27)$$

This is the transfer function of the pressure head $H(s)$ to flow discharge $Q(s)$ in the penstock pipe which is represented in the following Figure 7.6 block diagram.

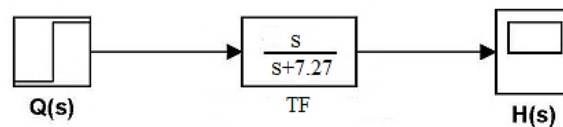


Figure 7.6: Step signal input $Q(s)$ to the signal response $H(s)$

On the other hand, when considering the water flow velocity U inside the penstock pipe and in relation to gate opening G and pressure head H , the following equation applies with per unit values [182].

$$\bar{U} = \bar{G} \sqrt{\bar{H}} \quad (7.28)$$

For the non-linear model, the water flow velocity in the penstock can be very difficult to determine, but when substituting the value of velocity U with discharge Q value as $\bar{Q} = A\bar{U}$. In this case, the following condition applies for gate valve section: $0 \leq G \leq A$ and in per unit values this can be written as $0 \leq G \leq 1$ [183]

$$\bar{Q} = A \bar{G} \sqrt{\bar{H}} \quad (7.29)$$

$$\sqrt{\bar{H}} = \frac{\bar{Q}}{A \bar{G}}$$

where: $\bar{G} = A_t \bar{g}$ and A is the penstock area where water flows and given by $A = \frac{\pi D^2}{4} = 0.166 \text{ m}^2$

$D =$ diameter of the penstock $= 460\text{mm}$

Eliminating the normalized values gives;

$$H = Q^2 / (AG)^2 = \frac{Q^2}{G^2 A^2} = \left(\frac{Q^2}{G^2}\right) \frac{1}{A^2}$$

Thus;

$$H = \left(\frac{Q^2}{G^2}\right) \frac{1}{A^2} \tag{7.30}$$

The above equation can be represented in the following block diagram with the input gate valve position G and flow discharge Q and output pressure head H as shown in Figure 7.7 below.

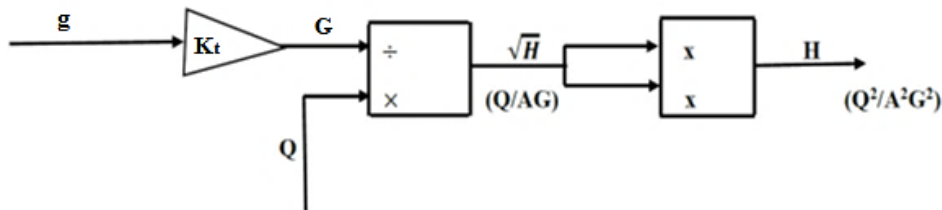


Figure 7.7: Formulation of hydraulic head H equation based on Q and G during modelling

B: Discharge $Q(s)$ and Mechanical Power $P(s)$

The Power output per second ($P(t)$) from the hydropower plant depends on the water discharge, weight per second, pressure head and system efficiency. This relation is given by the following equation.

$$P(t) = mQ\eta H(t) \tag{7.31}$$

where $P(t) =$ power per second, $m =$ mass of water flow per second, $Q =$ discharge and $H =$ pressure head and η is the hydraulic efficient.

From the above formula the value of flow discharge Q and pressure head H are usually maintained at a constant value at the turbine entry so, in this case the weight of water flowing per second can be expressed in terms of water density ρ and water volume v as follows:

$$P(t) = \rho v Q \eta H(t) \tag{7.32}$$

From the above equation the volume v per second is referred to as flow discharge, so the above equation can be re-written as:

$$P(t) = \rho Q^2 \eta H(t) (W) \tag{7.32}$$

or in terms of kW capacity

$$P(t) = Q^2 \eta H(t) \text{ (kW)}$$

Re-arranging the above equation and taking the Laplace transform we get;

$$H(s) = \frac{P(s)}{\eta Q^2} \quad (7.34)$$

Substituting the value of $H(s)$ to the above equation from the transfer function of Equation 5.28 we get;

$$\frac{P(s)}{Q(s)} = \frac{(\eta Q^2)s}{s+7.27} \quad (7.35)$$

Applying the following system design parameters, flow discharge $Q = 0.45 \text{ m}^3/\text{s}$ and hydraulic turbine efficiency = 72% to the above equation gives the following Laplace equation;

$$\frac{P(s)}{Q(s)} = 0.146 \frac{s}{s+7.27} \quad (7.36)$$

The following Figure 7.8 is the transfer function block diagram of turbine power $P(s)$ to flow discharge $Q(s)$ as shown in details below.

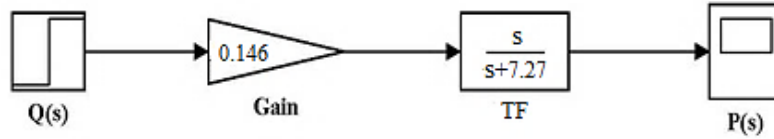


Figure 7.8: Block diagram of $Q(s)$ signal input to $P(s)$ signal output

It is noted that in this case there is a gain value of 0.146 on the transfer function for the flow discharge, $Q(s)$ to the power output $P(s)$ compared to a previous transfer function for $Q(s)$ and $H(s)$.

When relating the input signals for pressure head $H(s)$ and flow discharge $Q(s)$, the power output signal can be derived with the following relation based on mechanical power, head and flow in the turbine as follows:

For the transfer function that relates turbine velocity to the turbine head is given as [184];

$$TF(s) = \frac{\Delta \bar{U}}{\Delta \bar{H}} \quad (7.37)$$

But for a non-linear turbine model for this design where the pressure wave in the penstock and water compressibility is not considered, then the above equation becomes:

$$TF(s) = -\frac{1}{T_w s} \quad (7.38)$$

where T_w = Water starting time (1.79 seconds)

From the equation 5.38, substituting the \bar{U} with \bar{Q}/A_p we get the following;

$$TF(s) = \frac{\Delta\bar{Q}/A_p}{\Delta\bar{H}} = - \frac{1}{T_{ws}} \quad (7.39)$$

where A_p = Area of the penstock pipe

Simplifying the above equation, we get:

$$\Delta\bar{Q} \Delta\bar{H} = - \frac{A_p}{T_{ws}} \quad (7.40)$$

In relation to modelling, the value of A_p is taken as a gain (constant), so in this case, the mechanical power P_m developed in a micro-hydro turbine depends on the net pressure head ΔH and water flow discharge ΔQ .

Then the equation 7.41 below relates the turbine mechanical power P_m in with the net head ΔH and net flow discharge ΔQ as follows:

$$\bar{P}_m = \Delta\bar{Q} \Delta\bar{H} \quad (7.41)$$

But theoretically, power from the micro-hydro turbine due to water flow discharge is given by equation 5.12 in Chapter 5. So, in this case, the parameters ρg are the power gains for the system model and are represented as a constant value.

When considering per unit values of the mechanical power output, the nominal operating point of the hydro turbine need to be considered.

Thus, at the nominal operating point;

$$P_N = \rho g H (Q_N - Q_v) \text{ and also } Q_N = A G \sqrt{H_s} \quad (7.42)$$

here P_N = Nominal power of turbine, H_s = Water height, Q_N = Nominal water flow, Q_v = Volumetric flow losses.

When normalizing the above turbine power equation, we get:

$$P_m (p.u.) = \frac{H}{H_s} \frac{Q - Q_v}{Q_N - Q_v} = \frac{H}{H_s} \frac{Q_N}{Q_N - Q_v} \frac{Q - Q_v}{N} \quad (7.43)$$

Simplifying the above equation, we get:

$$P_m (p.u.) = K_P H_{pu} (Q_{pu} - Q_{v pu}) \quad (7.44)$$

In this case, the value K_p = power gain given by ρg in nominal values and $K_p = \frac{1}{1 - Q_{v(p.u.)}}$ in p.u. values.

The above Equation 7.44 with p.u. values can be simulated based on the set parameters as shown on the block diagram of Figure 7.9 below.

When turbine efficiency is considered during modelling then the output turbine power obtained is the mechanical power given by the following equation:

$$P_m = \rho g H \Delta Q \eta_t \quad (7.45)$$

The above equation 7.45 is the general equation used to calculate the potential power output from a hydro turbine system with known site parameters of head H and water flow discharge Q . The required amount of water flow is allowed to pass through the gate valve and discharged to the turbine and cause the turbine to rotate which produce hydraulic power. In the conversion process, the output hydraulic power value must be multiplied by a power gain which is ρg factor from the formula and also turbine efficiency η_t in order to obtain mechanical power as shown in Figure 7.9 below.

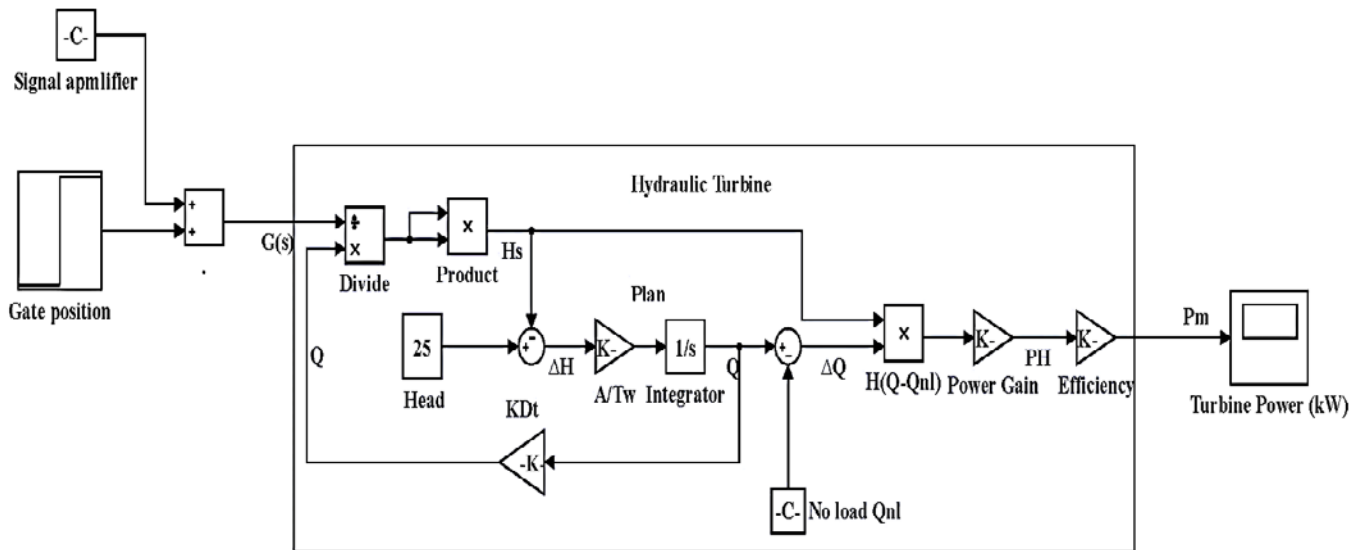


Figure 7.9: Penstock hydraulic model with power gain and efficient factor

5.2.3.2 Turbine Modelling

In micro-hydro turbine modelling with a small variation around an operating point, consideration should be made on steady-state operating conditions and also on their linearized condition which can be related by the Taylor series linear equation as follows for the change in flow discharge and mechanical power respectively [185]:

$$\Delta Q = a_{11}\Delta H + a_{12}\Delta G + a_{13}\Delta\omega \quad (7.46)$$

$$\Delta P_m = a_{21}\Delta H + a_{22}\Delta G + a_{23}\Delta\omega \quad (7.47)$$

Where the constants:

a_{11} and a_{21} = partial derivative of discharge and mechanical power with per unit deviation in head

a_{12} and a_{22} = partial derivative of discharge and mechanical power with per unit deviation in gate position

a_{13} and a_{23} = partial derivative of discharge and mechanical power with per unit deviation turbine speed.

The above two equations are related to the small change of water flow discharge, ΔQ and change in mechanical power, ΔP_m with respect to change in water head ΔH , change in gate position ΔG and change in turbine speed $\Delta \omega$. Applying partial derivative to the above equations in relation to the penstock water flow dynamics, the transfer functions of the micro hydro turbine can be developed as follows:

Equation 7.46: $\Delta Q = a_{11}\Delta H + a_{12}\Delta G + a_{13}\Delta \omega$ with partial derivative gives as follows:

$$a_{11} = \frac{\partial Q}{\partial H} \text{ and } a_{12} = \frac{\partial Q}{\partial G} \text{ and } a_{13} = \frac{\partial Q}{\partial \omega}$$

Equation 7.47: $\Delta P_m = a_{21}\Delta H + a_{22}\Delta G + a_{23}\Delta \omega$

$$a_{21} = \frac{\partial P_m}{\partial H} \text{ and } a_{22} = \frac{\partial P_m}{\partial G} \text{ and } a_{23} = \frac{\partial P_m}{\partial \omega}$$

In this case, the penstock-turbine Laplace transform transfer function related to the change of mechanical power ΔP_m , to the change in gate position, ΔG is given by [185]:

$$\frac{\Delta P_m(s)}{\Delta G(s)} = \frac{a_{23} - (a_{13} \times a_{21} - a_{11} \times a_{23})sT_w}{1 + a_{11}sT_w} \quad (7.48)$$

When considering the hydraulic turbine change in mechanical power ΔP_m to the change in gate valve position ΔG , the developed transfer function in the block diagram is given in Figure 7.10 below.

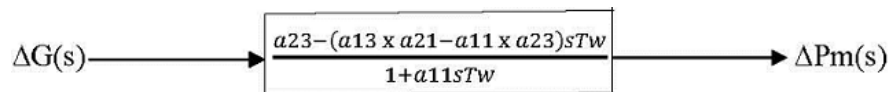


Figure 7.10: Block diagram transfer function of the linearized turbine model

To develop the system, transfer function we have to consider for an Ideal hydraulic turbine (lossless turbine) at rated speed and head with the initial values of partial derivatives as follows [183]:

$$a_{11} = 0.5, a_{12} = 0, a_{13} = 1$$

and

$$a_{21} = 1.5, a_{22} = -1, a_{23} = 1$$

Substituting the above partial derivative values for the ideal turbine we obtain the following short form linearized first-order transfer function:

$$\frac{\Delta P_m(s)}{\Delta G(s)} = \frac{1 - sT_w}{1 + 0.5sT_w} \quad (7.49)$$

The above Equation 7.49 has been represented in a block diagram as the deviation in gate position and mechanical power as shown in Figure 7.11 below.

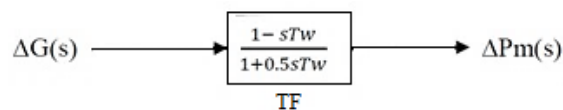


Figure 7.11: Stead state turbine-penstock transfer function block diagram

From the above Equation 7.49, it noted that the main characteristic of the transfer function is that behaves as a non-minimum phase system on the Laplace transform s-plane.

The term T_w is related to the micro-hydro turbine water starting time which depends on the speed of water flow in the penstock. It can be defined as the time required to accelerate water flow in the penstock pipe from the minimum speed at the water entering the penstock to a maximum speed of the water exit from the penstock.

Mathematically;

$$T_w = \frac{L \times Q}{H \times A_p \times g} = 1.79 \text{ seconds} \quad (7.50)$$

where L = length of the penstock (162 m), Q = design discharge (0.45 m³/s), H = design head (25 m), A_p = area of the penstock pipe (0.166 m²) and g = acceleration due to gravity (9.81 m²/s).

The value of T_w is an important parameter used in micro-hydropower modelling and this value usually varies because it depends on the speed (U) of the water flow in the penstock. Typical values of T_w for micro-hydropower systems range between 0.5 seconds to 4.0 seconds [183].

In this case, using the T_w value of 1.79 seconds for the turbine design and by referring to the equation 7.50 and Figure 7.11, the steady-state turbine-penstock transfer function for the change in gate valve position ΔG in relation to the change in mechanical power ΔP_m can be represented in the following block diagram. Also, in this case, an integrator and feedback control loop has been introduced on the model together with the signal filter as shown in Figure 7.12 below.

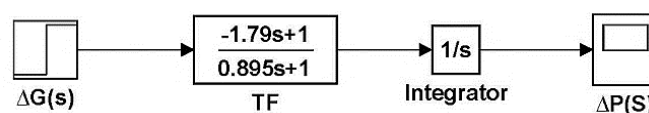


Figure 7.12: Block diagram for steady state turbine-penstock of a linearized micro hydro turbine model

On the other hand, the micro-hydropower systems with short and medium penstock length like that of Hhaynu river in Mbulu, the design consideration has been based on a non-linear system model, where the transfer function does not consider the travelling pressure wave and water compressibility, thus gives the simplified transfer function as follows [184]:

$$\frac{\Delta U(s)}{\Delta H(s)} = \frac{1}{sT_w} \quad (7.51)$$

Substituting the T_w value on the above equation gives: $\frac{\Delta U(s)}{\Delta H(s)} = \frac{1}{1.79s}$

In hydraulic modelling, the relationship between power output signal $P(s)$ to the water flow input signal $Q(s)$ is obtained by substituting the values to the above equation 7.51 with $H(s)$ values from equation 7.34 on which we obtain the following relation:

$$\frac{\Delta U(s)\eta Q^2}{P(s)} = \frac{1}{sT_w} \quad (7.52)$$

$$\frac{\Delta U(s)}{\Delta P(s)} = \frac{1}{\eta Q^2 \times sT_w} = \frac{1}{0.26s}$$

$$\frac{\Delta U(s)}{\Delta P(s)} = \frac{1}{0.26s} \quad (7.53)$$

where $Q = 0.45 \text{ m}^3/\text{s}$, $\eta = 0.72$ and $sT_w = 1.79$ seconds.

This is the transfer function between the water flow velocity in the penstock to the power output from the turbine.

5.3 Generator and Load Power System

The modelling of the turbine-generator system is set in such a way that, the output speed of rotation (frequency) of the generator needs to be maintained at a constant value. But, due to the nature of consumer load demand that the power is always fluctuating and not constant, so in order to model the hydro turbine - generator system, assumption is made in such a way that the produced mechanical (turbine) power is equated to the negative of electrical (generator) power in order to maintain a constant speed of rotation on which load demand power and generation power must balance. The difference between the mechanical torque M_T and electrical torque E_T is called the acceleration torque A_T which determines the rotational direction of the generator shaft.

Mathematically the above system condition can be represented in the following relation;

$$M_T - E_T = A_T \geq 0 \quad (7.54)$$

The above relation is called the swing equation with M_T and E_T values must be positive for a micro-hydro turbine generator. In block diagram representation of the generator modelling, the following transfer function represents the generator model;

$$\text{Generator model} = \frac{1}{2Js + K_D} \quad (7.55)$$

where J = Inertia time constant, K_D = Dumping coefficient of the generator, $\Delta\omega_r$ = change in rated speed and ω_{nl} which is no load speed

The following Figure 7.13 represents the block diagram of swing equations with transfer functions for the turbine-generator system with mechanical and electrical power inputs.

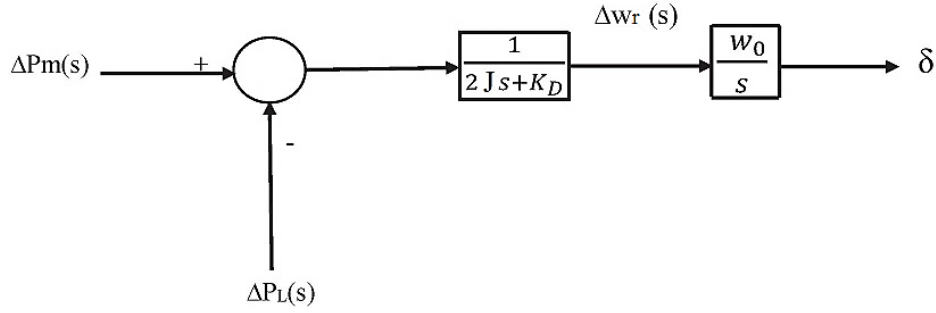


Figure 7.13: Block diagram representing a generator model

By referring to the design parameters for the micro hydro turbine system, the following values have been selected in the modelling: inertia constant $J = 4$ seconds, generator speed at no load $\omega_{nl} = 1500$ RPM, load demand power $P_L = 75$ kW (74% of the peak load) and generator number of poles is 4.

The more detailed model blocks for the generator is shown in Figure 7.14 below on which it includes the mechanical power, P_m and electrical power, P_e as inputs to the system. In the modelling blocks, the load power P_L and also generator damping coefficient K_D are the inputs to the electrical power, P_e .

Mathematically:

$$P_e = P_L + P_L K_D \Delta\omega_r \quad (7.56)$$

The generator swing equation can be expressed as two first-order differential equations as follows;

$$P_m - P_e = 2Js\Delta\omega_r \quad (7.57)$$

$$\frac{d\Delta\omega_r}{dt} = \frac{1}{2Js}(P_m - P_e) \quad (7.58)$$

But;

$$P_e = P_L + P_L K_D \Delta\omega_r$$

Note: ΔP_L = Non-frequency sensitive load change and $P_L K_D \Delta\omega_r$ = Frequency sensitive load change

$$\frac{d\Delta\omega_r}{dt} = \frac{1}{2Js}(P_m - (P_L + (P_L K_D \Delta\omega_r))) \quad (7.59)$$

Then;

$$P_m - P_L = 2Js\Delta\omega_r + P_L K_D \Delta\omega_r \quad (7.60)$$

$$\Delta\omega_r = \frac{P_m - P_L}{2Js + P_L K_D} \quad (7.61)$$

and

$$\frac{d\delta}{dt} = \omega_o \Delta\omega_r \quad (7.62)$$

Since the initial output value of the model is in electrical radians per second, (Change of rotor angle over change in time, $\frac{\Delta\delta}{dt}$) so, to convert this output value to the rotational speed in *RPM*, ($\omega_o = 2\pi f$ which is equivalent to $\omega_o = \frac{2\pi N}{60}$) the model must include a gain for $N = 60/2\pi\omega_o$.

The following Figure 7.14 represents the block diagram model of the generator swing equation with transfer function and first-order differential equations.

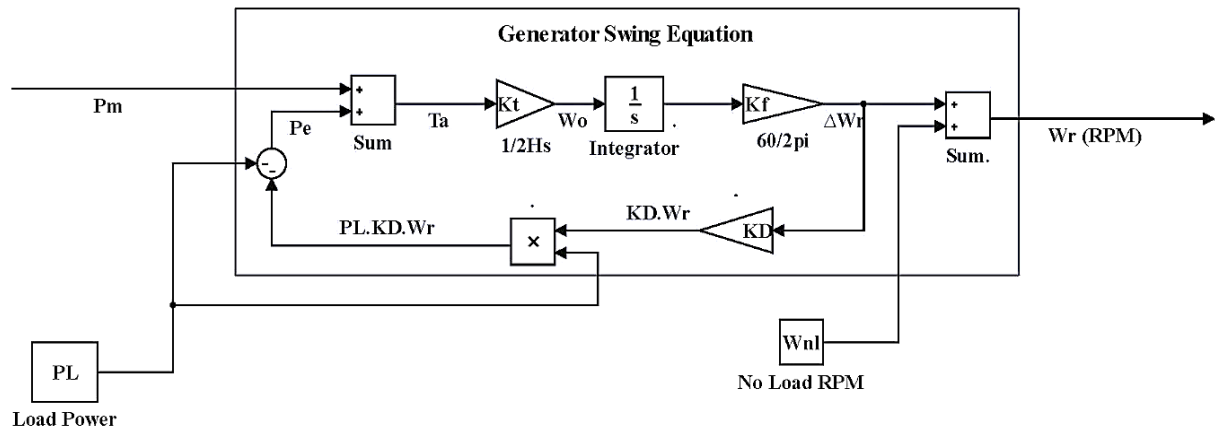


Figure 7.14: Generator swing equation block diagram

When considering per unit values for the input mechanical power, P_m and to supply 0.8 (80%) of the load which has to be supplied by the first turbine, then the generator model with input design values have been simulated based on the diagram in Figure 7.14 above. In this case, the inertial time constant J from the system design is equal to 4 seconds and also the generator damping coefficient, K_D is equal to 0.045 for *PI* controller. The feedback loop with terms $K_D \cdot \omega_r$ represent the inertia of the generator winding system and their combination with load power, P_L they form an electrical power, P_e which is given as $P_e = P_L + (P_L K_D \Delta\omega_r)$. In the micro-hydro turbine system, the generator speed, ω_o is mostly influenced by the load power, P_L which also affect the generator damping coefficient, K_D . The above consideration was mainly based on the per unit value of the system design at different loading conditions. Now when considering the modelling from the rated capacity values then the generator maximum power capacity is set to be 75.5 kW and the average load demand of 46.36 kW. The generator rotational speed ω_r in RPM is mostly influenced by the power demand P_L in kW on which increased power demand will reduce the generator speed which will affect the stability of the system. This rotational speed of the generator can also be converted to frequency using the number of poles of the generator. In this research study, the selected generator system will have 4 pole orientation due to they are

locally available and easy to maintain. See Figure 7.15 below for the RPM to frequency conversion.

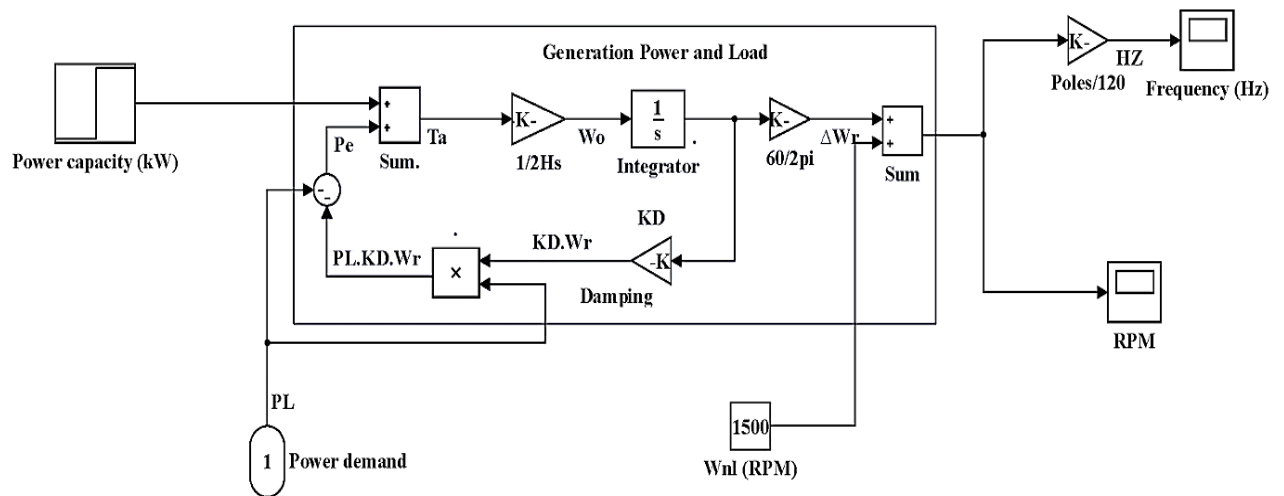


Figure 7.15: Generator speed (RPM) to frequency (Hz) block diagram

5.4 Controls and Governor System

In order to control the power output from the small hydropower plants, hydraulic turbines are mostly controlled by a governor system which is a key item for any small scale hydro turbine systems and usually consists of both control and actuating mechanism for water flow regulation, speed and power control, as well as system start/stop mechanism [186]. The general function of a governing system in small hydro turbine systems is usually to control the fluctuating power output and rotational speed/frequency. In the controlling mechanism, the speed/frequency of the prime mover will be controlled by a speed governor which is directly responsive to the rotation speed and position of the turbine-generator system. Some of the common small-scale hydropower plant equipment's used for the speed control mechanism are servomotor, lever and linkages between governor and gates/valves. In a hydro turbine control mechanism, the speed governor has a function of actuating the governor-controlled gates that regulate the water flow input to the turbine through the speed control mechanism by the servo motor. The proper designing of the governor system will play an important role in the reduction of the system error on the developed turbine model.

5.4.1 Optimization for hydro control governors

In the optimization of the turbine control governors system, two procedures need to be considered as follows:

- (i) Either use the rule of thumb and set the initial parameter values from the approximation ranges. In this case, use the minimum values or average values at the initial stage and optimize the selected values

- (ii) Or use the set of formulas, to obtain the main parameters for modelling and simulation and then optimize them

On the other hand, it should be noted that, in a hydraulic turbine and control system modelling and optimisation, the following basic sequence and procedure need to be followed:

- (a) First is to model the complete hydraulic turbine system with the associated control governor systems
- (b) Second is to obtain a dynamic response of the hydro-turbine system
- (c) The third is to use different techniques as described above in (i) and (ii) to set the initial parameters for the hydro-turbine governor.

In the hydro turbine control system, two types of control governors are commonly used for speed/frequency control mechanism which is hydraulic-mechanical governor and electro-hydraulic *PID* governor. In this research, the above two control systems have been analysed and compared with the other type of control governor system called Pseudo-Derivative Feedback (*PDF*) which is not widely used in small scale hydropower plants control systems. See Figure 7.16 below for the layout of micro-hydro turbine control system.

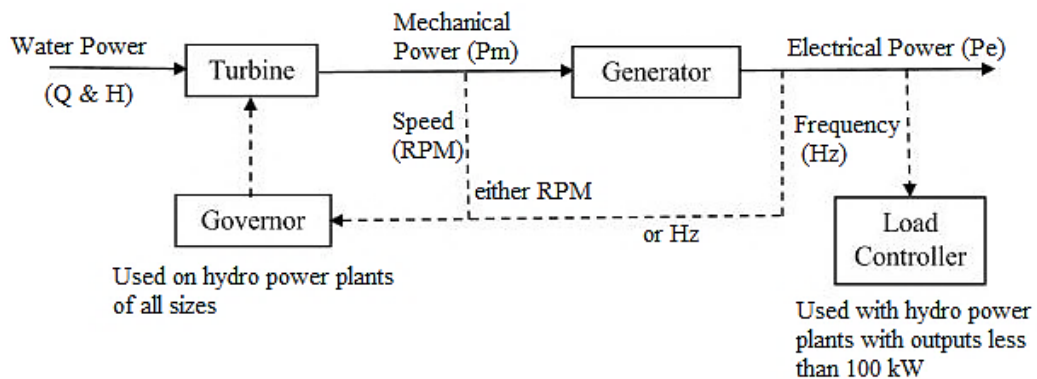


Figure 7.16: Block diagram representing the turbine, generator and control system layout

5.4.2 Hydraulic Turbine control governor

Governors are used to control the speed/frequency of rotating of the turbine-generator system, so when designing hydraulic governor, initial consideration is used with the simple governor setup that has no special features. The setting of the governor parameters will be based on requirements for system stability operations and the control function will involve a feedback speed error (ω_r) to a set speed reference (ω_{ref}). Considering the general control system set up, the governor system can be represented by a transfer function of $\frac{1}{R}$ and can be combined with the turbine linear transfer function in the block diagram of the following Figure 7.17 representation

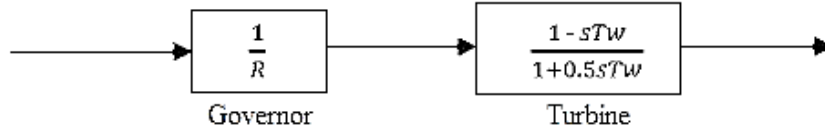


Figure 7.17: General block diagram for the turbine and governor system

From Figure 7.16 above and when we consider controlling the whole system which will include a turbine-generator system, the transfer functions can be represented by a governor transfer function, turbine transfer function and generator transfer function. In this case, the system will include the inertia of the turbine-generator system and a feedback system which is the speed deviation. The system block diagram is represented by the Figure 7.18 as shown below.

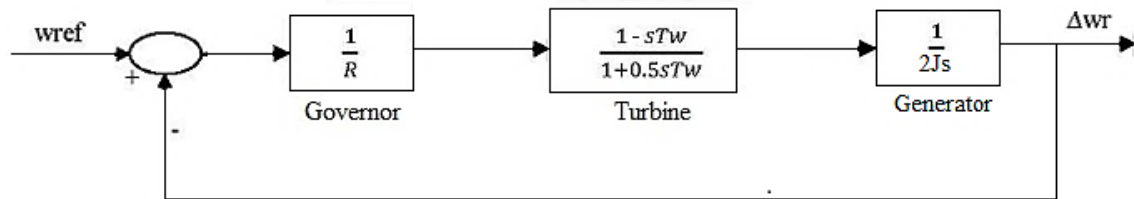


Figure 7.18: Block diagram of the turbine-generator system transfer function

In order to initially analyse the system stability of the above closed loop turbine-generator system with the control governor, we have to set initial parameters for the generator inertial (J) and water starting time (T_w).

Initial design conditions:

From the design calculation parameter $J = 4$ and $T_w = 1.79$ seconds

Then, from the block diagram of Figure 7.18 above, the forward loop transfer function of the system can be written as:

$$1 + \frac{1}{R} \left(\frac{1-sT_w}{1+0.5sT_w} \right) \frac{1}{2Js} \tag{7.63}$$

This is the characteristic equation of the system and for feedback system condition the above equation (transfer function) have to satisfy the following general condition:

$$1 + GJ = 0 \tag{7.64}$$

where G is the plant transfer function and J is the feedback transfer function.

Thus, from the above equation 7.64 we get:

$$1 + \frac{1}{R} \left(\frac{1-sT_w}{1+0.5sT_w} \right) \frac{1}{2Js} = 0 \tag{7.65}$$

Substituting the initial values for $J = 4$ and $T_w = 1.79$ we get;

$$1 + \frac{1}{R} \left(\frac{1-1.79s}{1+0.895s} \right) \left(\frac{1}{8s} \right) = 0 \tag{7.66}$$

$$8Rs + 7.16Rs^2 + 1 - 1.79s = 0$$

$$7.16Rs^2 + (8R - 1.79)s + 1 = 0 \tag{7.67}$$

The above equation 7.67 is the 2nd order characteristic equation (differential equation) for the designed micro hydropower plant which will be used to determine the value of governor condition R for system stability conditions.

The equation can be represented on the s-plane and in order for the speed governing system equation to be stable, the values of R coefficients have to fulfil the following two conditions:

- (i) $7.16R > 0$ which gives $R > 0$ which is the 1st requirement
- (ii) $8R - 1.79 > 0$ which gives $R > 0.224$ which is the 2nd requirement

(These are the two values of R for which the speed governing system theoretically is stable)

The calculated values of R gives the indication of system stability and when considering good system stability, the R -value that must be chosen should be above 22.4% ($R > 0.224$). This is the droop characteristic of the speed governor and the steady state droop must be set at 22.4% which means the governor speed deviation of 22.4% will cause 100% change in gate position which corresponds to a gain of 4.5. The value of R obtained is higher than the standard value for the speed drop taken for most of the governing systems which are usually around 4% (0.04) that corresponds to a gain of 25. So, using this standard value will affect the system stability and this is mostly observed in most governors with simple steady-state characteristics in small hydro turbine systems.

For stability studies, there is a need to consider other system condition and one of this condition is the damping effect. From the characteristic equation and when considering critically damping response the requirements will have the following relations:

$$8R - 1.79)^2 - 4(7.16R) = 0 \quad (7.68)$$

$$(8R - 1.79)(8R - 1.79) - 28.64R = 0$$

$$64R^2 - 14.32R - 14.32R + 3.2 - 28.64R = 0$$

$$64R^2 - 57.28R + 3.2 = 0 \quad (7.69)$$

Solving the above equation gives the following value for R which gives the droop characteristic value of the micro hydro turbine-generator system.

Thus;

$$R_1 = 0.8351 \text{ (83.51\%)} \text{ and } R_2 = 0.0599 \text{ (5.99\%)} \text{ (Possible governor droop value)}$$

(These are the two values of R for which the speed control system action is critically damped).

When comparing the above value to the initial value of $R > 0.224$ the results shows that R_1 have critically damped response (damp response = 1) i.e. the R -value is much greater than

the recommended value and also the value of R_2 is way below the recommended value $R > 0$ and this will give a damp response value of -1.

From the above R values, it has been noted that correct R values will determine the stability of the hydro turbine-generator system. In order to overcome the stability problems, small hydraulic turbines control governing systems need to have a special control characteristic features and these features are based on the speed control mechanism and are mostly embedded and set in the turbine governor control system as shown in Figure 7.19 below where K_s is the secondary control gain and the R_p value is the primary control (governor droop) on which its gain value σ is given by $\frac{1}{R_p}$. In this case, the input signal is speed reference ω_{ref} which is a set speed value and is compared with the actual generator shaft speed ω_t in order to obtain speed deviation (error) that need to be correct by the primary and secondary controllers. On the other hand, the servo motor has a maximum and minimum opening position which is given by z^{max} and z^{min} respectively as shown on Figure 7.19 below.

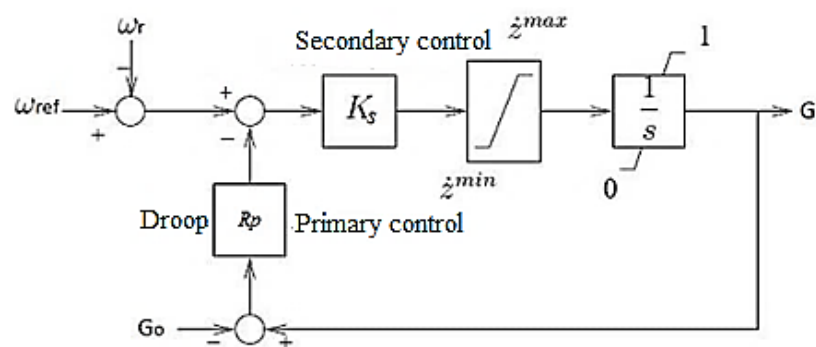


Figure 7:19: Hydraulic turbine control model block diagram

In hydro turbine control mechanisms, there are three common turbine control governor systems that are widely used to control the hydraulic turbine in micro hydropower for system stability and the governors include:

- (a) Hydraulic-Mechanical control governor
- (b) Electro-Hydraulic (*PID*) control governor (digital governors)
- (c) Pseudo-Derivative Feedback control

In isolated system like the one for this study, the control action for the governors is basically used to control the turbine-generator speed (frequency) using the following system of components: actuators which converts the control signals to a power signal, sensors (feedback signal) that provides actual output value of the plant power and reference (set-point) that represent the desired input value.

On the other hand, the following are the primary functions of the governing system in hydropower plants:

- (i) Governors maintain the generator frequency by changing the turbine output power to load changes
- (ii) Governors perform normal system shutdown or emergency shut down due to turbine over speed for system protection

5.4.3 Hydraulic – Mechanical governor

In hydraulic-mechanical governor system there is usually mechanical components and hydraulic components on which the governing functions are realised and usually, these systems are combined. The main control components in the system are the pilot valve and servo motor which control the speed of the gate valve opening. Two feedback system is considered in this governor, a permanent droop feedback loop and a transient/temporary droop feedback loop which can also be termed as a by-passed loop. The transient/temporary droop is the response for speed control in order to limit the overshoot of the gate valve opening during the transient conditions eg. during system start/stop or load changes/disturbances. In the system configuration, a dashpot which is a large temporary droop compensation is used to provide stable operation condition of the governor during the above conditions [187].

The transient/temporary droop feedback loop is represented by a transfer function equation as follows:

$$T_D(s) = R_T \frac{sT_R}{1+sT_R} \quad (7.70)$$

where R_T = Temporary droop, T_R = Reset time

In this case, the temporary droop which must be large is required for stable control performance which in most cases will give long re-settling time as required for a stable condition. This control characteristic is a response on hydro turbines and is due to the condition of water inertia in the penstock which will require most of the governors to have large droop for fast speed changes and small droop for steady state condition as shown in Figure 7.20 below.

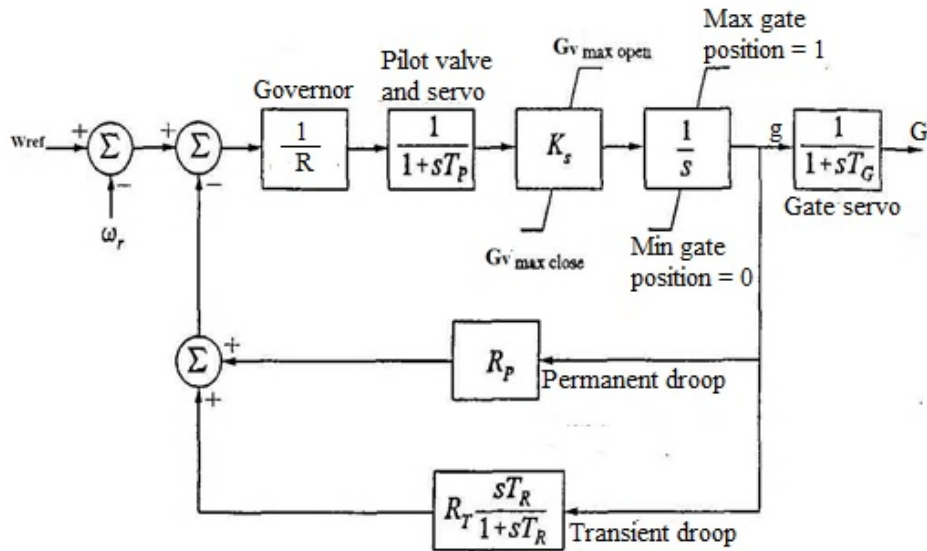


Figure 7.20: Block diagram of a typical mechanical governor

The typical values of the determining parameters are given below:

T_p = Pilot valve and servo-motor time constant (Initial value = 0.05 seconds)

K_s = Servo gain - Max and Min gain value (Initial value = 5 seconds)

$$K_s = \frac{1}{T_G} = \frac{1}{0.2} = 5 \text{ [Gain of the governor]}$$

T_G = Main gate servo time (Initial value = 0.2 seconds)

R_p = Permanent droop gain (Initial value = 0.224 seconds) [Refer to $R > 0.224$]

R_T = Temporary droop gain (Initial value = 0.56 seconds)

By definition, droop is the changes in generator frequency setting from the nominal value due to load changes. In this case, the droop values are characterised by decreases when loading increases and increases when the load is decreased and in most cases, it is expressed as a percentage of the original frequency set point (50 Hz) which is evaluated from the no load to full load operating conditions.

In most cases, the speed droop value is calculated based on the generator frequency at no load condition when the consumer load demand is disconnected to generator frequency at full load and when all the consumer load demand is connected. From the results of the present study, the generator frequency at no load is increased to 52.72Hz and the no-load setup has been made in such a way that only a limited power of 0.45 kW which is generator power that is produced and used to supply auxiliary power to the controls, indicators lights and powerhouse lighting.

The above parameter values have been obtained from the modelling and simulation results at which it gives the stable operating conditions for the micro-hydropower system design.

From the design point of view, the temporary/transient droop depends on the inertial time constant of the turbine-generator system (J) and the water starting time constant T_w . The value of the turbine-generator inertial time constant J has also been obtained from the modelling and simulation results as $J = 4$ seconds

So, mathematically reset time is given by:

$$R_T = \frac{2.5 \times T_w}{2 \times J} \quad (7.71)$$

$$R_T = 0.56 \text{ seconds}$$

where $J = 4$, $T_w = 1.79$ seconds, $T_R =$ Reset time (Initial value = 8.95 seconds)

The value of T_R depends on the water starting time T_w as follows:

$$T_R = 5 \times T_w = 5 \times 1.79 \text{ seconds} = 8.95 \text{ seconds}$$

Note: In all cases, micro hydro-turbine governor parameters should be set under normal conditions based on the following two standard techniques:

- (a) Tandem simulation
- (b) Frequency response or analysis

The general block diagram with a transfer function for a hydro turbine system using the above parameters for the mechanical governor is represented in Figure 7.21 below.

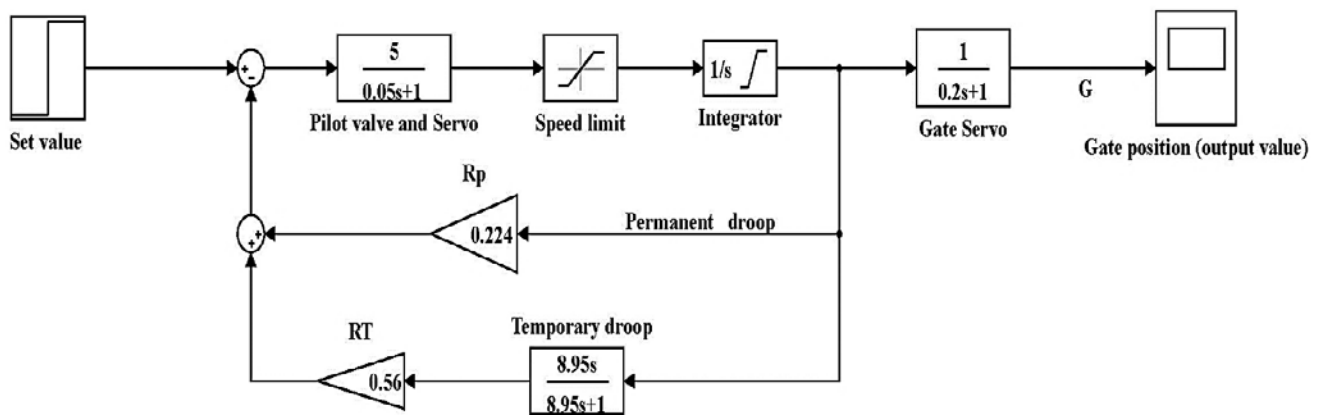


Figure 7.21: Hydraulic mechanical governor model

7.4.4 Electro-hydraulic (*PID*) governor

The *PID* controllers have set point values as inputs signals to the controller system and these values are compared with the process variables (feedback from the sensors) to produce controller output which sets the position of the gate valve. In this case, when the system is in operation a *PID* controller system compares the process variable to the setpoint values and calculates the two signal differences which are a signal error. The produced signal error value is then amplified by the *PID* controller gains in order to reduce the error effect for the gate position. *PID* controllers are based on three control gain parameters;

Proportional, Integral and Derivative control mechanism. In this case, the controller output is made up of the sum of the proportional, integral and derivative controlling actions. These three control features treat the errors at different stages on which the Proportional is responsible for present system errors, the Integral deals with the past system errors and the Derivative is responsible for the predicted (future) errors.

Mathematically *PID* controller output can be represented with the following equation:

$$PID \text{ controller output (CO)} = K_p \cdot e(t) + \frac{1}{K_i} \int e(t) dt + K_d \frac{de(t)}{dt} \quad (7.72)$$

where K_p = proportional gain, K_i = integral gain, K_d = derivative gain, $e(t)$ = error value

In a separate formula the gain values are given as follows:

$$\text{Proportional action, } u(t) = K_p \cdot e(t) \quad (7.73)$$

$$\text{Integral action, } u(t) = K_i \int_0^{\infty} e(t) dt \quad (7.74)$$

$$\text{Derivative action, } u(t) = K_d \frac{de(t)}{dt} \quad (7.75)$$

See the diagram in Figure 7.22 below for more details.

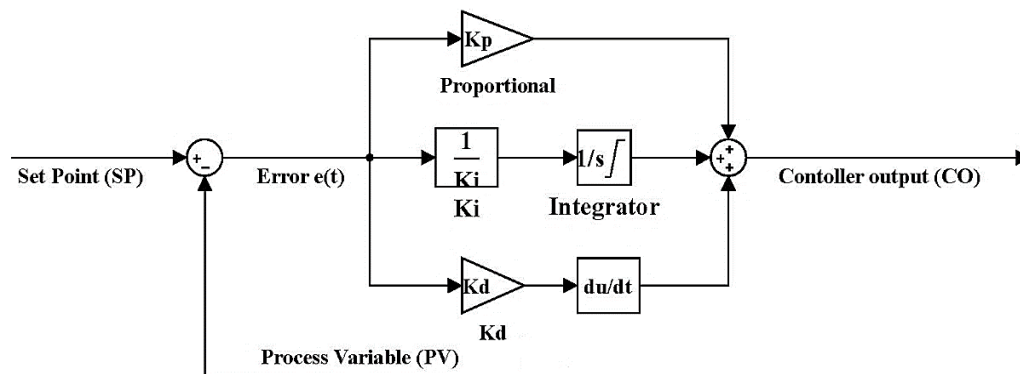


Figure 7.22: PID controller parameters

Due to their nature in dealing with all-time system errors, the hydraulic-turbine system that uses *PID* controllers have faster speed response during both transient stage and also during steady-state stages in the operation of a micro-hydro turbine system. The reasons for this is that the *PID* controllers are better in providing both transient gain increase and also gain reduction in a micro-hydro turbine system during dynamic operating conditions.

In the *PID* operation mechanism, the input values are referred to as set point and these particular values are those that we want the system to operate. During the process, there are usually disturbances which produce an error signal in the system, as a result, the output values will not be equal to the input/set-point values. In theory, the output values must be equal to the input/set-point values and in this case, the error signal value will be equal to zero because the disturbances have been minimum. In real life system operations, the disturbances do exist and causes errors on the system which in most cases can be

determined by taking the input set values minus the actual measured or operating condition values. This signal values may change the operating condition of the system and need to be corrected by a *PID* controller so that during system operations and despite system disturbances, the input set values should be equal or very close to the output values. The general arrangement of a *PID* controller is represented in the following block diagram of Figure 7.23 below.

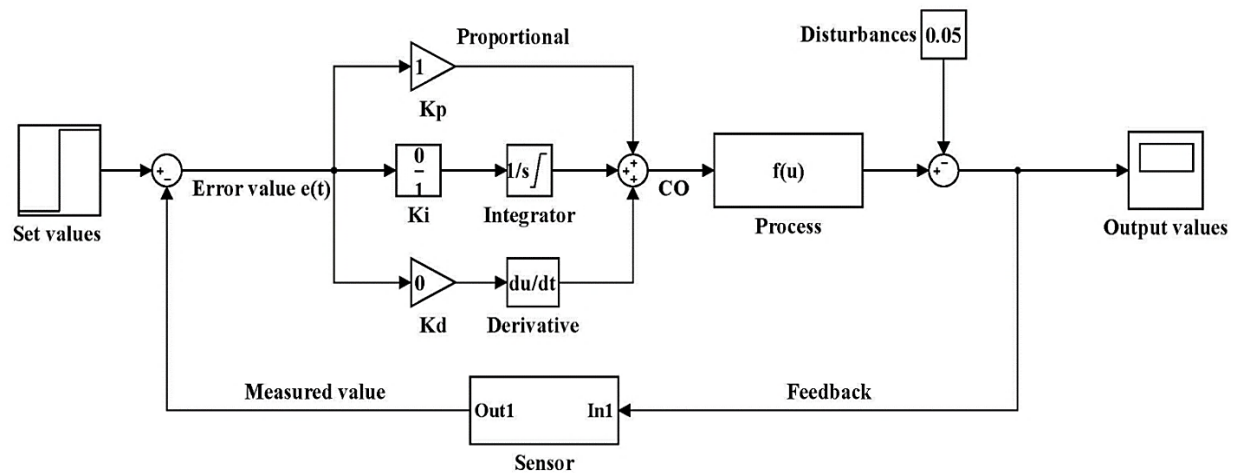


Figure 7.23: A typical *PID* control governor block diagram

The more detailed representation of the *PID* control governor block diagram includes a pilot valve and servo motor systems with transfer function block diagrams and a permanent droop feedback system. The initial *PID* values for the above block diagram in Figure 7.23 must be set to $P = 1$, $I = 0$ and $D = 0$ to simulate the initial system dynamic response. Then the *PID* values need to be tuned in order to obtain the optimised *PID* values for system performance and reduce the overall system error. Figure 7.24 below show the tuned *PID* control values and based on the simulation results for the step input signal systems with transfer functions on the block diagrams the tuned initial *PID* values for the controller are $K_p = 2.1$, $K_i = 0$ and $K_d = 0.08$. Due to the zero value on the integral action then this type of controller with only proportional and derivative action is called a *PD* controller. The tuned values when applied to the *PID* control governor system with step input values will result into a stable steady state system condition with quick system response as shown in Figure 7.24 below for the tuned *PID* controller.

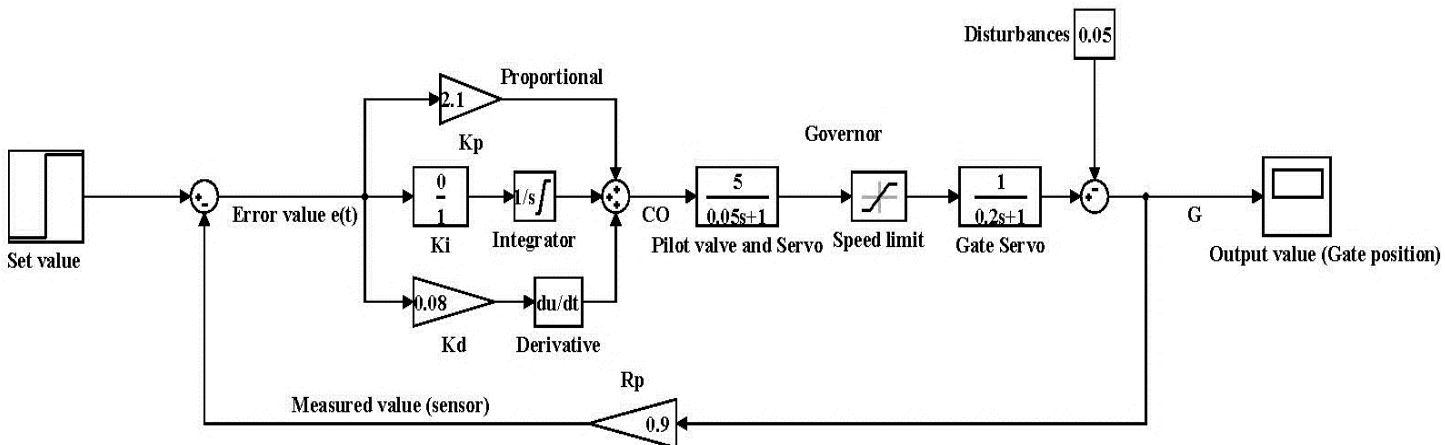


Figure 7.24: Tuned PID control governor block diagram

Also, in this case, the following parameters have been set for the pilot valve and servo. Pilot valve and servo-motor time constant, T_P of 0.05 seconds, servo gain, K_G of 5 seconds and also main gate servo time, T_G of 0.2 seconds. Also, for simulation purposes, the model also considered disturbances 0.05 which reflects the loading conditions of the system in real life applications. The feedback line with permanent droop, R_p of 0.9 (gain of 1.11) represent the measured value on the system that is compared with the set input value in order to obtain the error value that is then fed to a *PID* controller for signal corrections before being fed to the pilot valve and servo-motor in order to control the gate servo.

The above initial modelling values have been used to study the characteristics performance of the *PID* control governor based on per unit values. But in the actual operation of a *PID* controller in a micro-hydro turbine system, the controlling parameter is the electrical generator speed. In this case, the input value (set point) is the rated speed of the generator (1500 RPM) which is compared by the generator shaft speed (measured value) on which the difference is the error value. The produced error may be in three main ranges, a positive value which means the generator shaft speed is below the set point (under speed), zero value which means the setpoint speed is equal to the generator shaft speed (synchronised) and lastly negative value which means that the generator shaft speed is bigger than the set point speed (over speed). Both under speed and over the speed of the generator system will cause stability problems on the micro-hydro turbine system and will need to be corrected by a *PID* controller. In all loading conditions, the electrical generator needs to operate close to the synchronised speed on which for my case it is 1500 RPM.

The working principle of a *PID* controller is that the error signal produced from the speed difference is corrected using the tuned values of proportional, integral and derivative gains

in order to produce a control output signal that is connected to a gate servo that controls the position of the gate position. The gate servo is a motorised system inside the gate valve that controls the amount of water flow through the penstock pipe to the turbine.

Based on my research study for the designed micro-hydro turbine system, the rated values of the turbine-generator system that have been used to optimise the *PID* controller are as follows: Rated power capacity of 75.5 kW, rated generator speed of 1500 RPM, generator frequency of 50 Hz, water flow rate capacity of 0.45 m³/s and the site head of 25m.

7.4.5 Pseudo-Derivative Feedback (*PDF*) control governor

The *PDF* control system in hydropower plants was first developed by Phelan [188] and it uses integral (K_i) and pseudo-derivative feedback (K_{pd}) gain coefficients. In theory the *PDF* control system claim to provide good response time compared to some other control systems, although it is not widely used. When used, *PDF* control output will provide zero steady-state error with no overshoot under loading condition or step changes on the input signal. The *PDF* control system is set in such a way that the integral gain (K_i) is responsible for the error signal overshoot while the pseudo-derivative gain (K_{pd}) is responsible for correcting the steady-state error and system noise.

Mathematically, the *PDF* control system can be developed from the block diagram as shown in Figure 7.25 below.

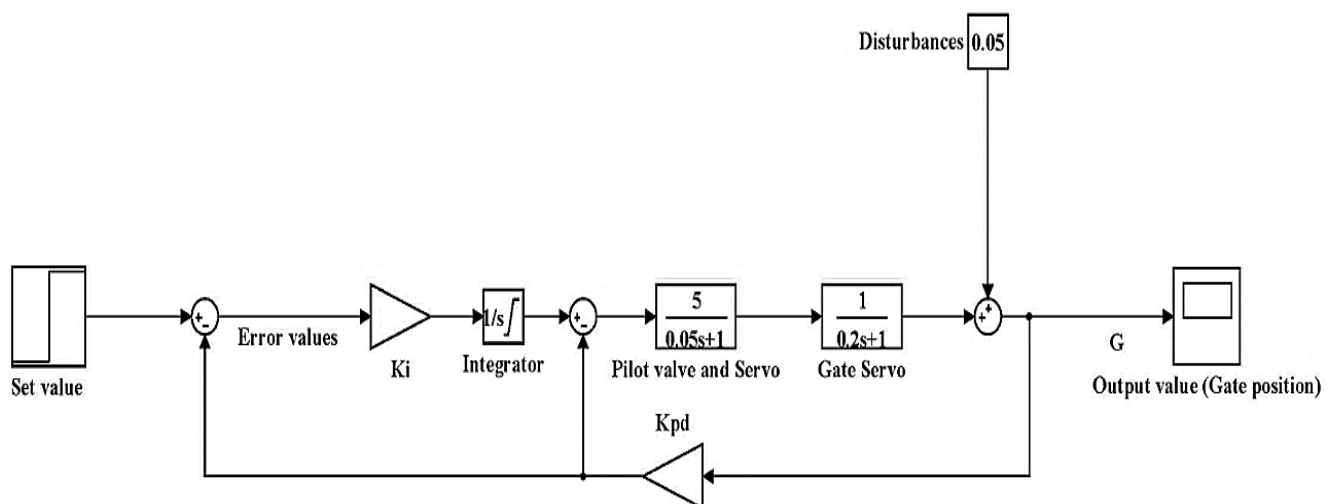


Figure 7.25: A model block diagram of a Pseudo-Derivative Feedback (*PDF*) control

In the above diagram, the initial value has set with step input i.e. set value with K_i gain of 1 while the K_{pd} gain of 0 and considering the disturbances of 5% on the system control.

When considering the step signal input as speed reference ($\omega_{ref} - \omega_r$) to gate position (G) as an output signal, the closed loop transfer function of the above system Figure 7.25 can be represented as follows:

$$\frac{\omega_{ref}-\omega_r}{G} = \left(\frac{K_i}{s^2 + (1+K_{pd})T_p \cdot s + K_i} \right) * \left(\frac{1}{T_G \cdot s + 1} \right) \quad (7.76)$$

where the parameters:

T_p = Pilot valve and servo-motor time constant (Initial value = 0.05 seconds)

T_G = Main gate servo time (Initial value = 0.2 seconds)

K_s = Servo gain - max and min gain value (Initial value = 5 seconds)

Using modelling parameters with initial optimization, the *PDF* system control with set value can be simulated and tuned with closed loop transfer functions that representing the pilot valve and servo motor as shown in Figure 7.26 below with tuned values.

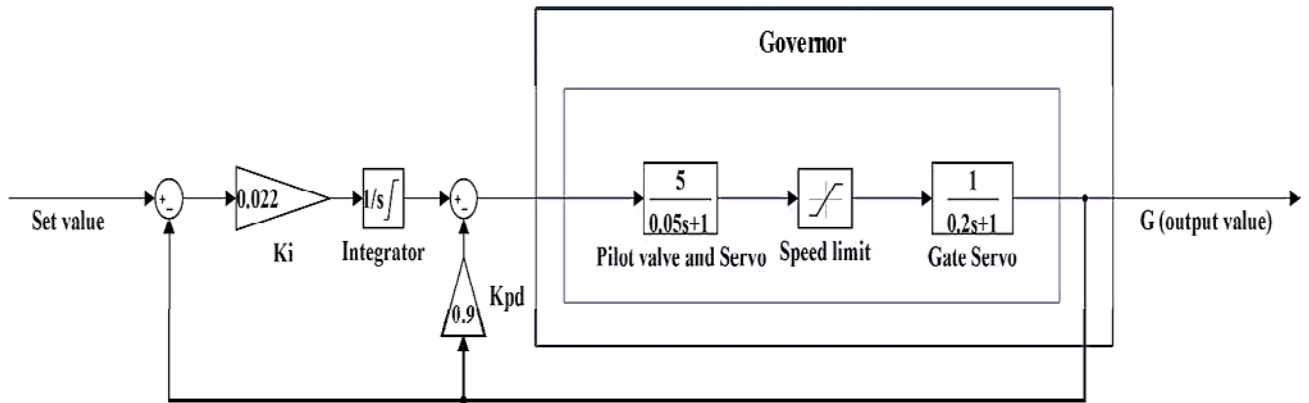


Figure 7.26: Tuned PDF control governor block diagram

5.4.6 Load control governor

In most micro hydro turbine system with small water flow discharge, the type of control governor used is called shunt load governor which uses an electronic load controller system (*ELC*). The working principle of an electronic load controller is that it matches the input values (turbine power) with the output values at the terminals (generator power). In this case, the turbine power is kept at a constant value which makes also the generator power to be at a constant value. Now, due to the fluctuations on the load demand power and in order to stabilise the system, an additional dump load is connected at the generator terminals. The function of a dump load is to divert excess power produced in order to balance the generator power output and the instantaneous consumer load in order to keep the generator speed and frequency constant as shown in Figure 7.27 below.

Thus;

$$P_D = P_L K_D \Delta\omega_r \quad (7.78)$$

On the other hand, when considering consumer load and generator frequency control, the following diagram in Figure 7.29 shows a schematic diagram representing a turbine model with hydro turbine control block diagram, governor control block diagram, droop and power system block diagram. In this case, the generator power and frequency dynamics $G_p(s)$ are influenced by the changes in consumer load demand power $\Delta P_D(s)$ and the produced turbine power $G_T(s)$. On the other hand, for the turbine power to function well as desired then the control dynamics $G_c(s)$ must be operated at the required values. The control action of the turbine system is operated based on the set values for power $\Delta P_{ref}(s)$ and the required system gain values of $\frac{K_i}{s}$ and $\frac{1}{R}$. The load frequency control action is used to control the generator speed due to changes in consumer demand power that will affect the generator frequency. In most hydro turbine generator system operates at a constant speed/frequency of 1500 RPM with 50 Hz which have to be maintained all the time despite changes in consumer load demand. See the following Figure 7.29 for more details.

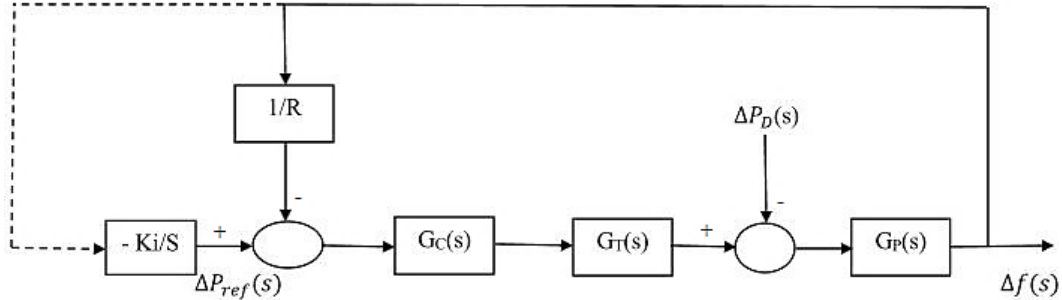


Figure 7.29: Schematic Block diagram of Load Frequency Control

From the above block diagram in Figure 7.29, the change in frequency $\Delta f(s)$ can be represented by the following Laplace transform equation:

$$\Delta f(s) = \frac{G_p(s)}{1 + G_p(s) \times G_c(s) \times G_T(s) \times (\frac{1}{R})} [-\Delta P_D(s)] \quad (7.79)$$

In this case, R is the speed regulation of the governor (Hz/kW) for a micro hydro system.

From the above equation, the Laplace transform for individual blocks can be defined as follows:

$$\text{Power system dynamics} = G_P(s) = \frac{k_p}{1+sT_P} \quad (7.80)$$

$$\text{Turbine system dynamics} = G_T(s) = \frac{k_T}{1+sT_T} \quad (7.81)$$

$$\text{Governor system dynamics} = G_C(s) = \frac{k_G}{1+sT_G} \quad (7.82)$$

T_p = Power system time constant and K_p = Power system gain

T_T = Turbine time constant and K_T = Turbine gain

T_G = Governor time constant and K_G = Governor gain

So, the Laplace transform change in frequency can be re-written as;

$$\Delta f(s) = \frac{\frac{k_P}{1+sT_P}}{1 + \left(\frac{k_P}{1+sT_P}\right) \times \left(\frac{k_G}{1+sT_G}\right) \times \left(\frac{k_T}{1+sT_T}\right) \times \left(\frac{1}{R}\right)} [-\Delta P_D(s)] \quad (7.83)$$

$$\Delta f(s) = \frac{\frac{k_P}{1+sT_P}}{1 + \frac{\left(\frac{k_P \times k_G k_T}{R}\right)}{(1+sT_P) \times (1+sT_G) \times (1+sT_T)}} [-\Delta P_D(s)]$$

$$\Delta f(s) = \frac{\frac{k_P}{1+sT_P}}{\frac{(1+sT_P) \times (1+sT_G) \times (1+sT_T) + \left(\frac{k_P \times k_G k_T}{R}\right)}{(1+sT_P) \times (1+sT_G) \times (1+sT_T)}} [-\Delta P_D(s)]$$

Simplifying the above equation by cancelling the term $(1 + sT_P)$ on both numerator and denominator gives the following simplified equation;

$$\Delta f(s) = \frac{k_P}{\frac{(1+sT_P) \times (1+sT_G) \times (1+sT_T) + \left(\frac{k_P \times k_G k_T}{R}\right)}{(1+sT_G) \times (1+sT_T)}} [-\Delta P_D(s)] \quad (7.84)$$

Which gives the following equation for the Laplace Transform of change in frequency;

$$\Delta f(s) = \frac{k_P(1+sT_G) \times (1+sT_T)}{(1+sT_P) \times (1+sT_G) \times (1+sT_T) + \left(\frac{k_P \times k_G k_T}{R}\right)} [-\Delta P_D(s)] \quad (7.85)$$

Thus, the above equation gives the changes in frequency in relation to load changes for a micro-hydro turbine system.

7.5 Hydro-Turbine and Generator System

Based on the different system model block diagrams, the final micro hydro turbine system model can be established by combining the different sub-section models. The modelled sub-sections include:

- (i) Turbine hydraulic system model
- (ii) Turbine generator system model
- (iii) Turbine control system model

In the hydraulic system model, the following parameters were used as modelling parameters, water flow discharge Q and pressure head H which have been obtained from the site location. The input parameter of this model is the water flow discharge through the penstock pipe to the turbine on which when modelled produce turbine power (Mechanical Power) as output. The mechanical power produced is related to the amount of water flow discharge to the turbine. Using the design parameters as modelling values for Q and H , the

output turbine (mechanical) power obtained during modelling is 79.5 kW with the hydraulic efficiency of 72%.

On the other hand, the generator system model input value is obtained from the turbine conversion using turbine efficiency. In this case, consumer load power and generator system dynamics form part of the generator system model. The model parameters obtained in the generator system modelling are the generator speed/frequency and the swing equation. As the power to the generator changes due to consumer load changes it affects the speed/frequency of the generator, so in this case, there is a need to stabilise the generators performance using modelling parameters. The nominal generator output speed value during modelling should be at 1500 RPM and a frequency of 50 Hz with the output power of 75.5 kW with the generator efficiency of 95%.

For a turbine to operate properly there is a need to use control governor and based on the system design for this research the type of controller used is the combination of the electro-hydraulic governor (*PID* controller) and Shunt load governor (*ELC*). Due to the nature *PID* control governors in terms of quick stability response time, they are widely used in hydro turbine system control, so for the designed micro-hydro turbine project, the electro-hydraulic governor will be used and in this case operate in a semi-automatic mode to control the water flow to the turbine in order to control water flow discharge to produce two power phases to the turbine system. First control phase is during the low power demand where the water flow is reduced to 0.24 m³/s (53% of the rated capacity). Then when the consumer load power demand is increased, the flow controller increases the water flow to the turbine to the rated value of 0.45m³/s. For this case, the controller needs to control between two power phases of 40 kW as minimum and 75.5 kW as maximum based on the daily consumer load demand profile in the project study area. On the other hand, the shunt load governor (*ELC*) will be used to control and optimize the excess power produced from the generator system in order to supply the required power to other load demand facilities like an electrolyser system.

In order to operate properly and stabilise the system, the selected *PID* control governor parameters need to be tuned for the K_p , K_i and K_d values. Based on the system stability studies the tuned governor gain values are $K_p = 0.025$, $K_i = 1.588$ and $K_d = 0$ with the speed limit on 0.50 on the governor servo. Due to the zero-gain value for the K_d parameter then this type of tuned control system is called *PI* control governor as shown in Figure 7.30 below.

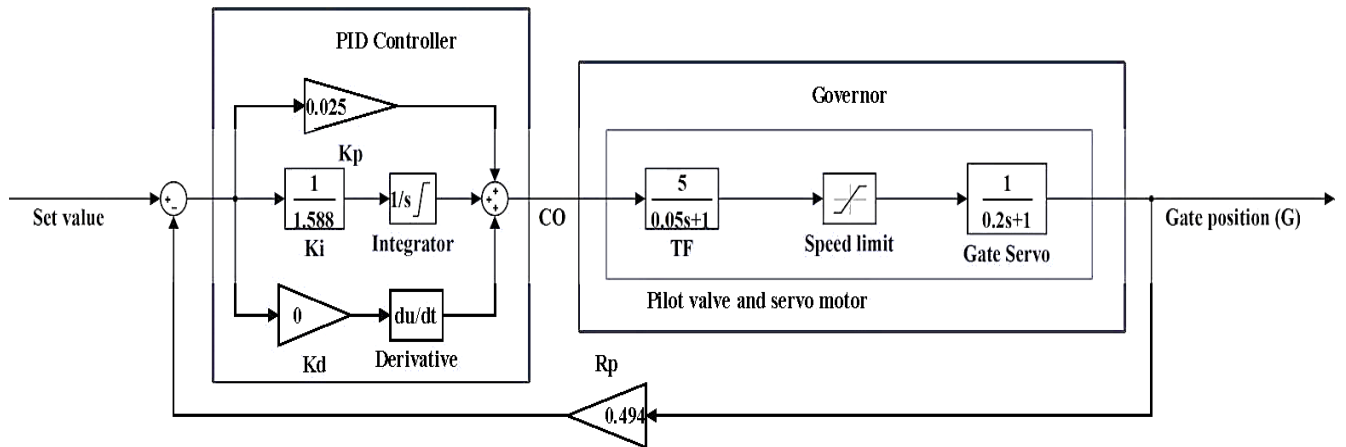


Figure 7.30: Tuned PID control governor model (PI controller)

The final hydro turbine model diagram for the system design is the combination of the sub-models of the hydraulic turbine model, generator and load model and turbine control model. For the system modelling, there are two input set values of generator speed (1500 RPM) which have to be maintained at a constant value by comparing it with the instantaneous generator shaft speed and obtain speed error. For the other input set value is the power set point on which two power values are set which is 40 kW and 75.5 kW set power. Both generator power output and generator speed need to be maintained by the control action in order to supply stable power to the consumer load demand.

The model parameters used in the hydro turbine design as shown in Figure 7.31(A & B) below have been optimised for the best system performance and also stability in order to supply the required electrical power to the case study area.

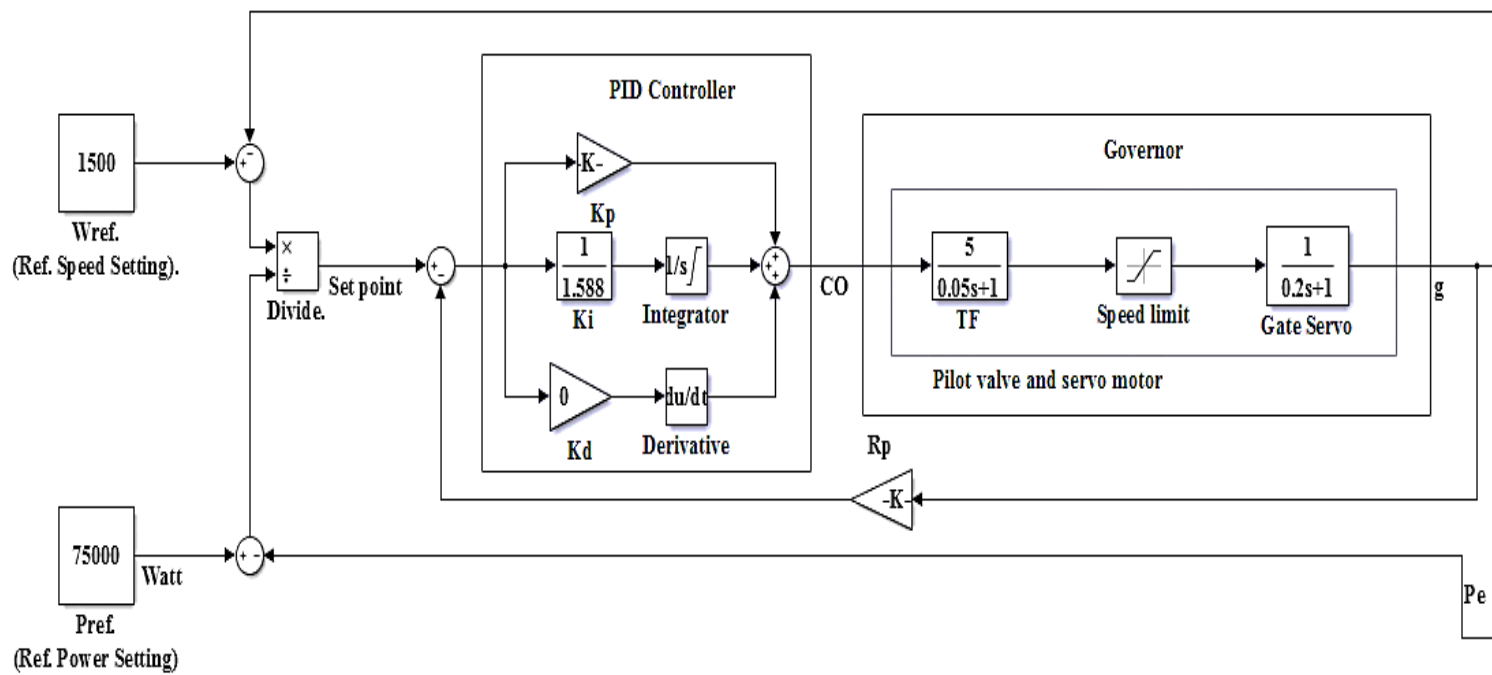


Figure 7.31A: Final model diagram (Input and controls)

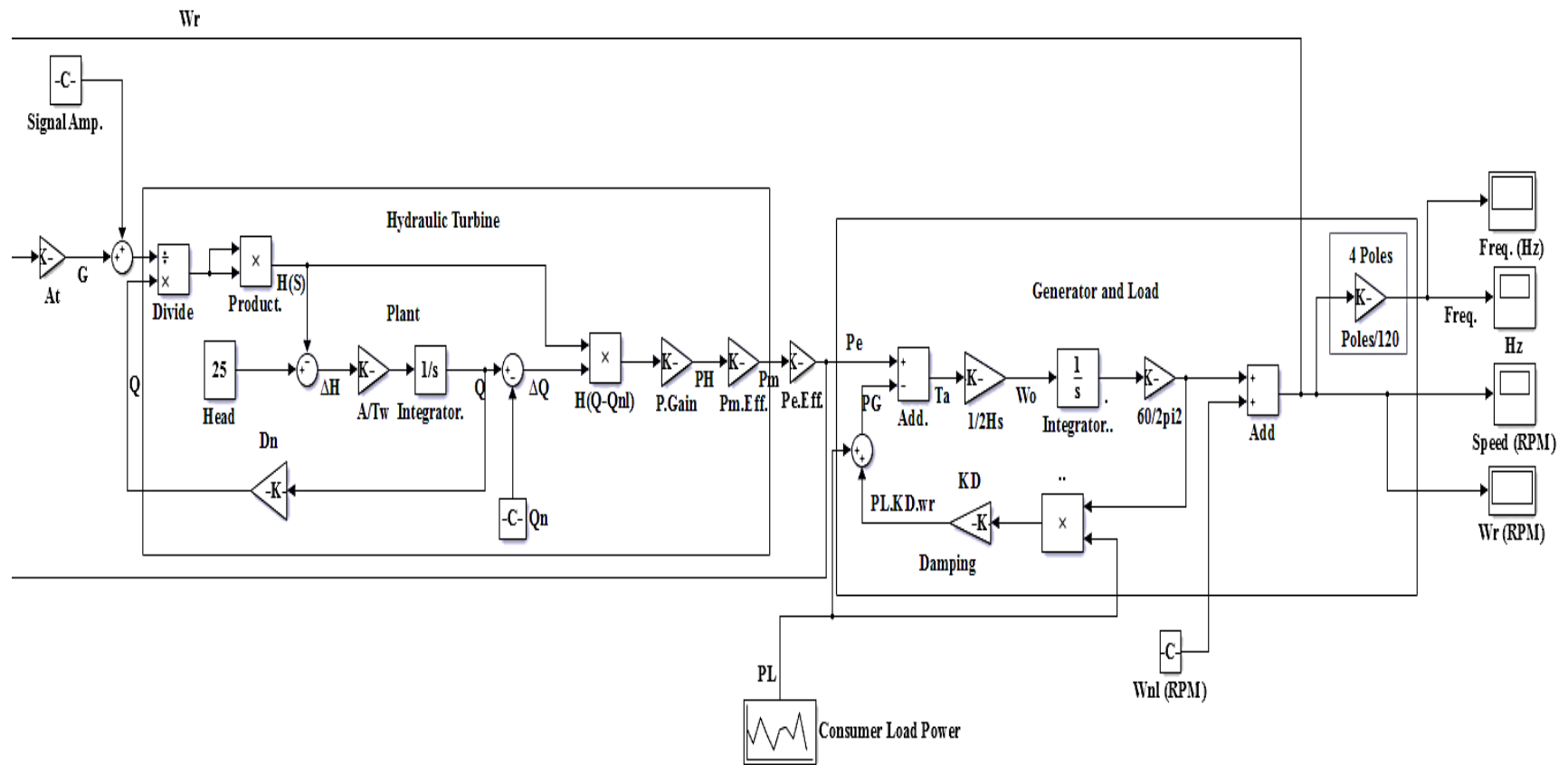


Figure 7.31B: Final model diagram (Turbine and generator)

7.6 Model validation

In the hydro-turbine model design and simulation, a set of parameters have been used to optimise the system performance and system stability. These system parameters are grouped into four main areas of operation which include control parameters, hydraulic system parameters, turbine system parameters and generator system parameters. The control parameters are basically used to control the inputs parameters to the hydraulic system which includes governor controller gains like *PID*. The different types of controller options have been used in the modelling and their simulation results have been compared and evaluated based on their performance and stability results. On the other hand, the hydraulic system includes all the parameters related to the water flow in the penstock to the turbine which includes a gate valve and servo motor. In order to model the system operation conditions when water flow discharge from the penstock pipe reaches the turbine system and power starts to be produced on which the turbine, generator and load system dynamics have been considered together with set input parameters so as to simulate the operational system conditions.

In order to properly model and simulate the hydro turbine performance, a set of above system parameters have been calculated and selected based on literature review and current turbine operating parameters. The validation of these model values has been based on the input parameters of the present study system model against other known hydropower station that are in operation. The first power plant that has been considered is the Dinorwig Hydropower Plant in Wales which has six turbine units of approximately 300 MW each and with similar simulation parameters with the present study in the penstock and turbine design model [189]. The other power plant used to validate the model/simulation parameters is the Shahid Abbaspour Hydropower Plant in Iran which has the following parameters, 250m head, discharge of $72\text{m}^3/\text{s}$ and 8 turbine units of 250MW capacity each [190]. In both hydropower plants despite the huge differences in power capacity with the present study but most of the hydraulic, turbine and generator parameters used are comparable with this design model of the present study. This is because in modelling/simulation of hydro turbine systems the input/output parameters used are usually converted and interpreted as signal values which will have similar interpretation in any hydropower plant capacity and a good example is in the control system on which gains values are obtained but also in terms of performance, the system stability time (seconds) is one of the considerable parameters. Most of the used parameters in modelling have been

optimised by focused on maintaining the required amount of water flow discharge through the penstock pipe to the turbine and the generator system in order to stabilise the system frequency and controlling load dynamics. The following in Table 7.1 shows and compare as a means of validating the hydro turbine modelling parameters and their values that have been used in the present study using the hydropower plants in operation.

Table 7.1: Validated parameters used in the modelling

Area	Name	Symbol	Mbulu Micro- hydropower	Dinorwig Hydro- power Plant [189]	Shahid Abbaspour Hydro-power Plant [190]	Value [191]
Controls	Proportional gain	K_p	0.025			2
	Integrator gain	K_i	1.588			0.4
	Droop (Permanent)	σ	0.49			0.04
Penstock	Diameter	D	0.46 m		4 m	
	Length	L	162 m		514 m	
	Pressure wave velocity	a	1440 m/s		1440 m/s	
	Pilot servomotor time	T_p	0.05 s	0.05 s		0
	Main Servo time	T_G	0.2 s	0.2 s		
	Servo gain	K_s	5.0 s	5.0 s		4 s
	Permanent droop	R_p	0.04	0.04		
	Temporary droop	R_T	0.4	0.5		
	Reset time	T_R	5.0 s	5.0 s		
	Turbine	Water starting time in the Penstock	T_w	1.79 s	0.3066 s	1.202 s
Rated mechanical shaft power		$P_{r(m)}$	79.5 kW		256 MW	285 MW
Rated discharge		Q_r	0.450 m ³ /s		72 m ³ /s	
Rated head		H_r	25 m		250 m	
Rated efficiency		η_m	0.72	-	-	-

Table 7.1 (continued)

Area	Name	Symbol	Mbulu Micro- hydropower	Dinorwig Hydro- power Plant [189]	Shahid Abbaspour Hydro- power Plant [190]	Value [191]
Turbine	Gate position at rated condition	g_{rl}	0.95	-	0.96	-
	Gate position at No load	g_{nl}	0.05	-	0.06	-
	Turbine gain	K_{tg}	1.11	1.12	1.11	-
	Wave propagation time in the Penstock	T_{ep}	0.0918 s	0.184 s	0.357 s	0.5 s
	Turbine damping coefficient	K_{td}	0.001105	0.5	0.5	-
	Head friction loss in the Penstock	h_{fl}	0.0001393 $\text{m}/(\text{m}^3/\text{s})^2$	0.0001124 $\text{m}/(\text{m}^3/\text{s})^2$	-	-
	Generator	Rated power	P_{gr}	75.5 kW	288 MW	250 MW
Rated efficiency		η_g	0.95	-	-	-
Machine starting time		T_m	1.9 s	7.99 s	-	1.9 s
Generator damping coefficient		K_D	0.045 at rated capacity, 2.030 at no load and 12.6 at the dynamic load condition	8.38	-	150
Inertia time constant		J	4 s	3.995 J nm^2/MVA	4.5 s	-
	Rated speed	ω_o	1500 RPM	3000 RPM	500 RPM	-

7.7 Model optimization

The power produces from the micro-hydro turbine is supplied to the consumer load demand that takes 63% of the available power and electrolyser system that takes 37% of the power. This power distribution is based on the fact that the available power supply is first supplied to the consumer load demand which is around 1,114.38 kWh/d with 101.8 kW peak power during the high demand hours of the day. But due to the nature of the peak power which is higher than the available power supply from the micro-hydro turbine (75.5 kW), an additional power supply system is installed using engine-generator system (40 kW) which is powered by the hydrogen gas as fuel that has been produced by the electrolyser system. In this case an electrolyser system is supplied by the excess electricity while the peak load demand power hours of the day are supplied by the hydrogen engine-generator system as shown in Figure 7.32 and Figure 7.33 below and this answers one of the research study questions.

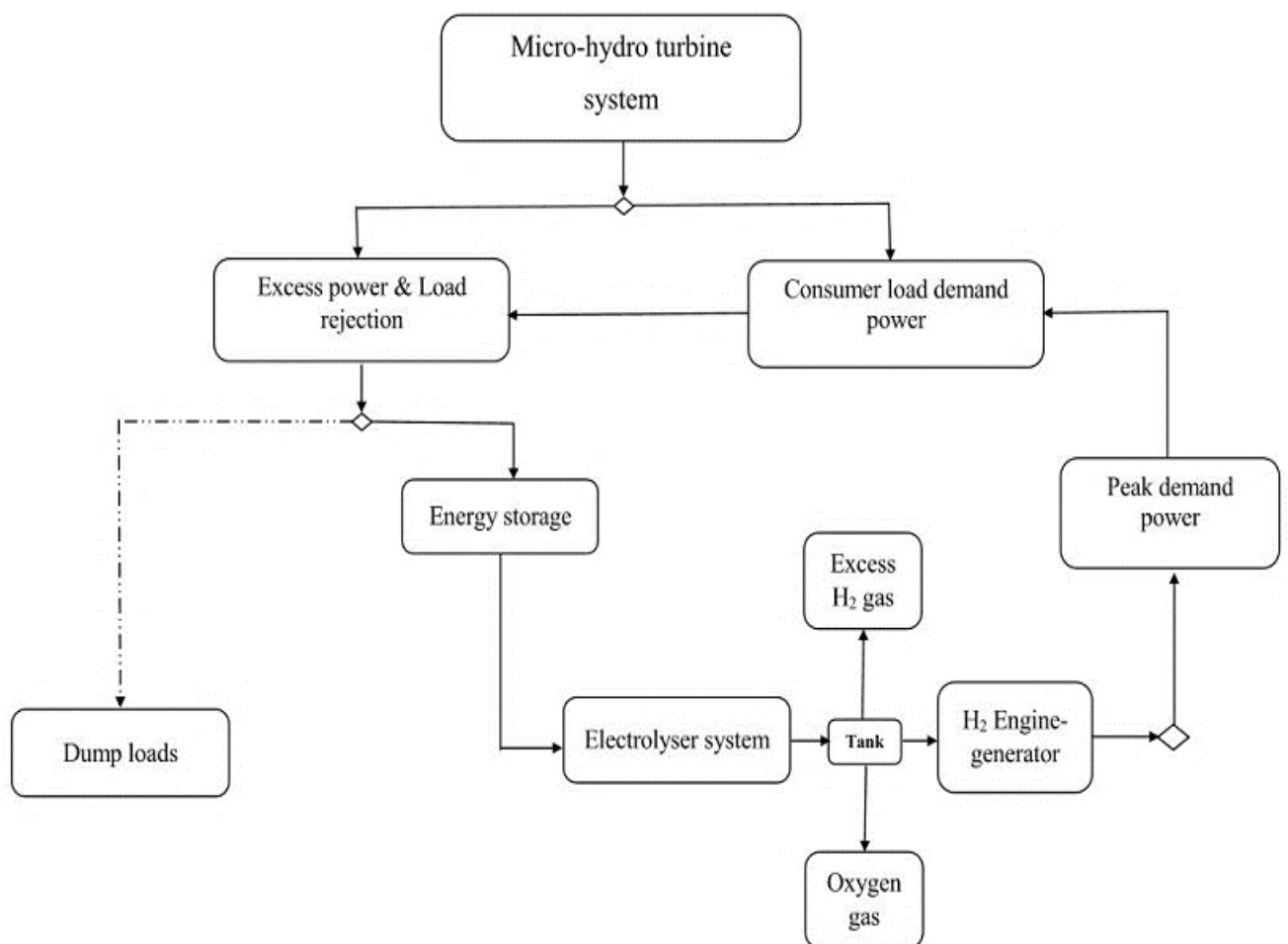


Figure 7.32: Optimized system model layout

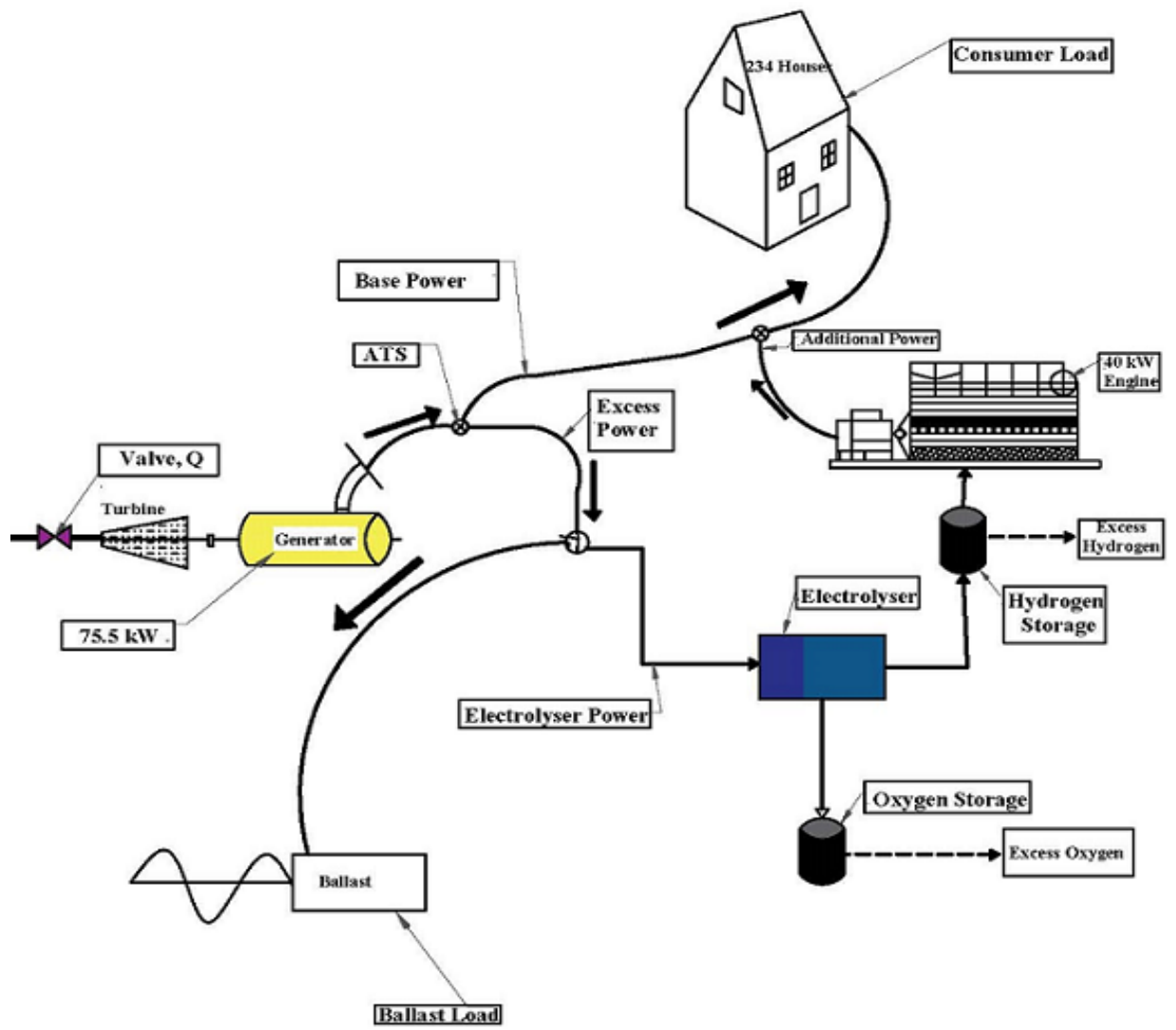


Figure 7.33: Optimised system design layout

Chapter 8 Results and discussion

8.1 Operational variables

In this Chapter, the developed hydro turbine model has been simulated to see the results of its performance and stability under different loading conditions. Based on the model input values, the maximum output power capacity for the hydro turbine system is 75.5 kW with a system frequency of 50 Hz. In order to obtain this power output, water flow discharge should be flowing through the penstock pipe to the turbine. This is called the hydraulic system and involved water flow discharge Q , head H and mechanical power P_m . In the hydraulic system, water flow discharge through the penstock pipe has been simulated based on the model transfer functions. The simulation results show that the stability of water flow through the penstock is influenced by the length of the penstock pipe. Longer penstock pipes tend to have longer stability time for the water flow inside the penstock. This is also valid in this research study because the length of penstock is around 162m. The water stability in the penstock is not very much influenced by the velocity of the water in the penstock because the speed of water flowing in the penstock pipe should be set to below 3m/s. In hydropower system, the power output generated power from the turbine-generator system depends on two main parameters that are mostly site specific. The two site parameters are the amount of water flow discharge to the turbine (Q) and the site head (H). In the relation, the turbine-generator power output is proportional to the amount of water flow discharge (Q) and head (H). However, there is a third variable of turbine-generator efficiency (η) which must be included in the mathematical model during simulation in order to obtain the correct power output value. Therefore, the above determining variables formulate the relationship between the input parameters to the turbine system with the power output from the generator system.

But experience have shown that, in hydropower plants design the value of head, H is kept at constant value and also most of the turbine-generator system nowadays have a fixed efficiency operating range. Thus, the only parameter that can very much influence the power output in a hydro turbine system is the water flow discharge, Q . In this case, water flow Q is used as one of the inputs parameters for the turbine in order to generate electricity. On the other hand, this research project is based on off-grid micro-hydro turbine system which is supplying power to the local community and due to that, the power supply has to operate close to the load demand power curve. But this usually brings problems to the

turbine-generator system stability because the load demand power is always fluctuating. Therefore, the load demand power from the consumer is also variable and affects the power output from the turbine-generator system.

In the simulation, the operational variables are operated as signal values of the turbine-generator system that are simulated to show the system performance in terms of power output (P_e), rotational speed (ω_r), frequency (Hz) and also system stability and response time (t). The initial system design is based on two step power supply phase which includes a 40 kW power supply capacity during the low power demand of the day that is mainly at night hours and 75.5 kW power supply capacity during the high power demand hours of the day which is mostly during the day time hours. In order to supply the two power steps, the water flow discharge to the turbine needs also to be regulated in to two steps on which in the simulated values it is 0.24 m³/s during low demand and 0.45 m³/s during the high demand hours.

In order to simulate the turbine and generator system correctly, there is a need to consider the dumping coefficient which takes care of the system inertial during the turbine rotation. In the turbine system, the dumping coefficient changes with the changes in water flow discharge and during the low power demand step with low water flow, the turbine dumping coefficient value is 0.00205 which seems to be very minimal. On the other hand, when the turbine power increases to maximum, the simulation results show that the turbine dumping coefficient decreases to 0.00110 which is 46.34% reduction.

On the generator system, the simulated values represent the generator power output, generator speed and frequency. In this case, the generator power (power output) represents the sum of the load demand power and the dumping power value. The generator system dynamics also include the dumping coefficient and in this case, its value depends on the amount of power produce at that particular hour. The results also show that during the low demand hours of the day the dumping coefficient is at its highest value which is around 1.63 while during the low demand hours the dumping is lower to a value of 0.05. But when simulating the power capacities at full load and no load for the generator system, two dumping coefficient values have been obtained at 0.045 and 2.030 respectively which also shows reduction characteristics when load power is increased to the turbine system. Therefore, from these results, it is conclusive evidence that the dumping coefficient of a turbine and generator system decreases with an increasing power output or load demand power.

8.2 Turbine performance

In penstock pipe, the water volume has a flow discharge value of $Q(s)$ as input which is influenced by $H(s)$ in order to produce a power output of $P(s)$. In this case, when considering the input value for the $Q(s)$ in relation to the response of $H(s)$ from the transfer function block diagram, the results show a smooth non-linear curve relation with $H(s)$ which initially become unstable and start to stabilize at around 0.7 seconds. The higher stability value of $H(s)$ represent the effects of pressure wave when water volume starts to flows into the penstock pipe and in normal applications, this pressure wave effect needs to be minimized. The pressure wave in the penstock is due to air trapped inside the penstock when there is no water flow and this causes longer system stability time as shown on Figure 8.1 below which represent the relation of $H(s)$ signal response value to the input signal $Q(s)$ value.

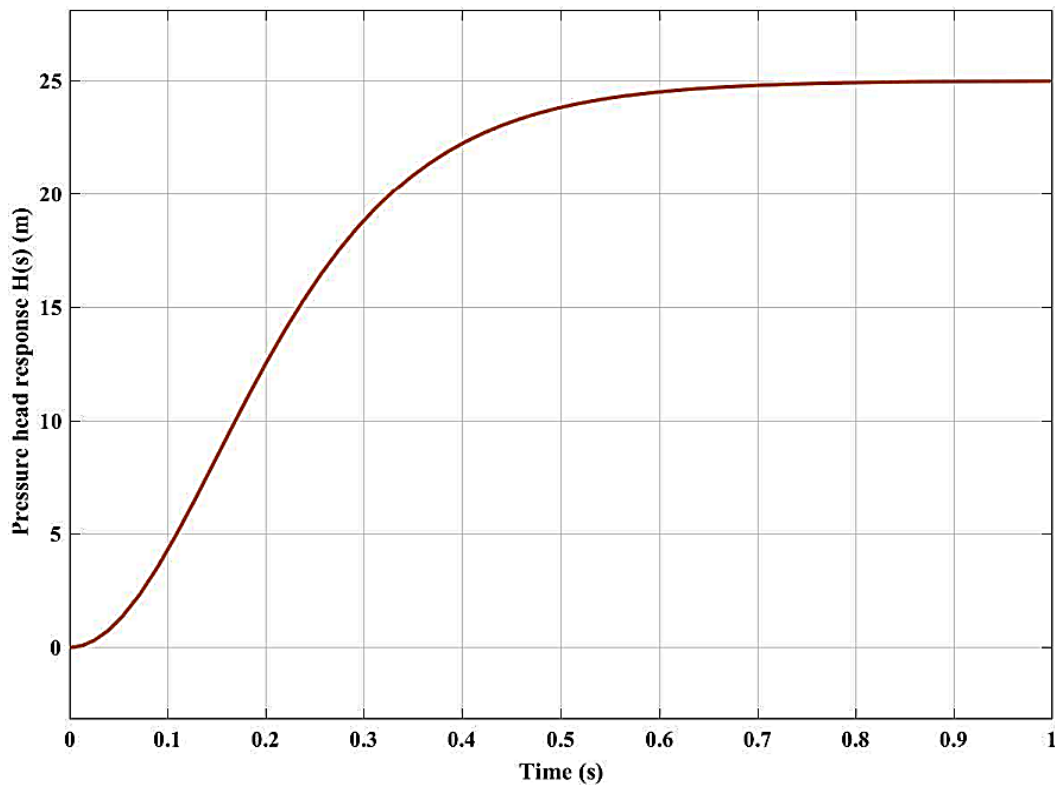


Figure 8.1: Signal response for input discharge $Q(s)$ with the output pressure head $H(s)$

When considering the water flow velocity in the penstock in relation to pressure head, the step signal response pressure head can be visualised when plotted and analysed. The relationship is also non-linear and it is noted that in this case, the system takes longer to stabilise at around 10 seconds. This means that the initial water flow velocity in the penstock influences the pressure head in the penstock pipe to a certainly point until the

system stabilises. Also, the water flow velocity signal as the input increases the pressure head value as output to a maximum point on which it becomes stable at the value of 1 p.u. The simulation results also show that the input step signal from water flow velocity to the pressure head seems to be stable at around 10 seconds which is much higher for a system of micro hydropower. This effect is due to the higher value of water starting time ($T_w = 1.79$ seconds) for the designed micro hydro turbine system and the contributing factor is the long penstock pipe of 162 m in length for the Hhaynu micro hydro-turbine project.

From the transfer function block diagram of water flow velocity signal with the power output response, it is noted that the power output signal took very short time to stabilize and this is because the velocity of the flowing water in the penstock pipe does not cause much effect on the power output on most of the micro hydro turbines. In this case, the water flow velocity signal $U(s)$ is the component of flow discharge signal $Q(s)$ which is influenced by gate valve signal $G(s)$ for the hydro turbine system.

On the other hand, water flow discharge $Q(s)$ can be influenced by water flow velocity $U(s)$ in the penstock pipe. In this case, when the velocity signal $U(s)$ is high it also increases the water flow discharge $Q(s)$ on the system. From the simulation results, the water flow signal value stabilises at around 0.7 seconds which is similar to the other system design stability time. The simulation results also shows that at 50% rated water flow discharge capacity ($0.225 \text{ m}^3/\text{s}$), the turbine performance is affected by the power stability condition due to reduced water flow until the water discharge is increased and reached at least 88% of the rated capacity ($0.396 \text{ m}^3/\text{s}$) and this effect is due to transient state of the water flow in the penstock pipe as shown in Figure 8.2 below against simulation time.

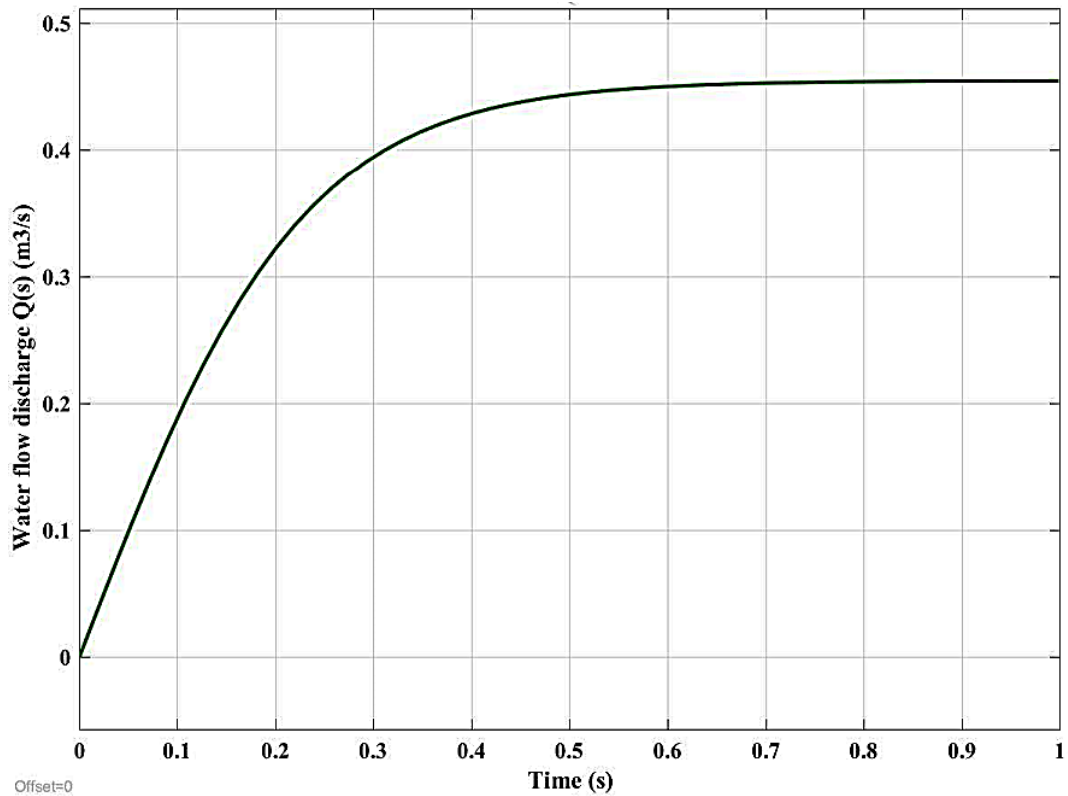


Figure 8.2: Signal response for the input pressure head $H(s)$ to the output discharge $Q(s)$. On the other hand, the power output signal $P(s)$ is also influenced by water flow discharge $Q(s)$ signal input and in this case, the signal response for $Q(s)$ and $P(s)$ with transfer function includes a turbine gain factor K_t of 0.005. This gain value is used to correct the signal error due to pressure wave and the results show that the response signal also behaves as a non-linear smooth curve with similar time on the system stability curve. In addition to that, the simulation result values have also incorporated a feedback loop which is the same as the flow discharge value, $Q(s)$ and in this case, the Power output signal $P(s)$ stabilises at around 0.8 seconds which is the same as the previous results for the pressure head. Theoretically as the flow discharge $Q(s)$ increase in the penstock pipe, the Power output $P(s)$ also increase as stipulated in Figure 8.3 below for the power output signal response.

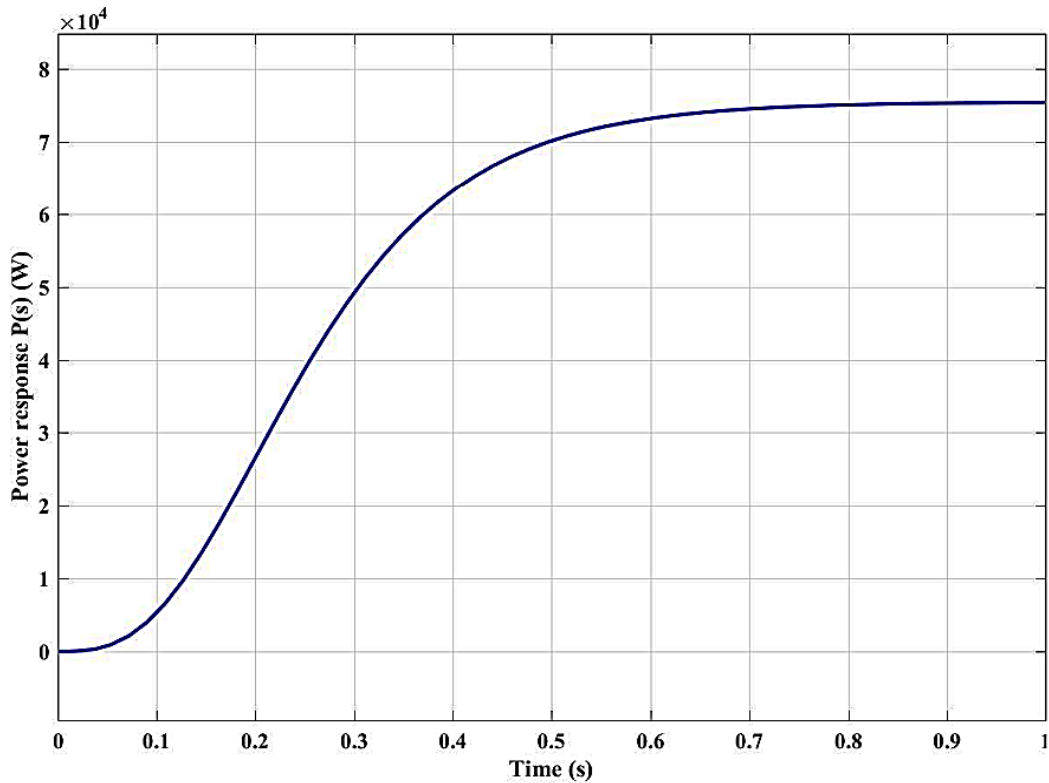


Figure 8.3: Signal response for the input discharge $Q(s)$ with the output Power $P(s)$

Another parameter that influences the power output of a micro-hydro turbine is the gate position denoted by $G(s)$ which acts as a valve that allows a certain amount of water to flow through a penstock pipe to the turbine. The gate position $G(s)$ can be simulated as signal input with other turbine parameter $Q(s)$ and $H(S)$ in order to stipulate the signal response at different gate position. When considering water flow in the penstock pipe with step input gate position signal of 1 p.u. (max opening), simulation results show that the change in pressure head ΔH of 4.39×10^{-4} p.u. while the change in water flow discharge ΔQ of 1.389 p.u., with the dumping value of K_{Dt} of 0.72 (flow discharge dumping coefficient) and turbine power P_m of 0.9994 p.u. as shown on Figure 8.4 below. The flow discharge dumping coefficient is the feedback loop factor for the flow discharge $Q(s)$ that accounts for flow losses. With time response, for the gate position signal input (p.u.values) to mechanical power signal output and 72% turbine efficient (gain), the penstock hydraulic model stabilizes after 55 seconds (< 1 minute) which is within the stability time for the micro-hydro turbine systems.

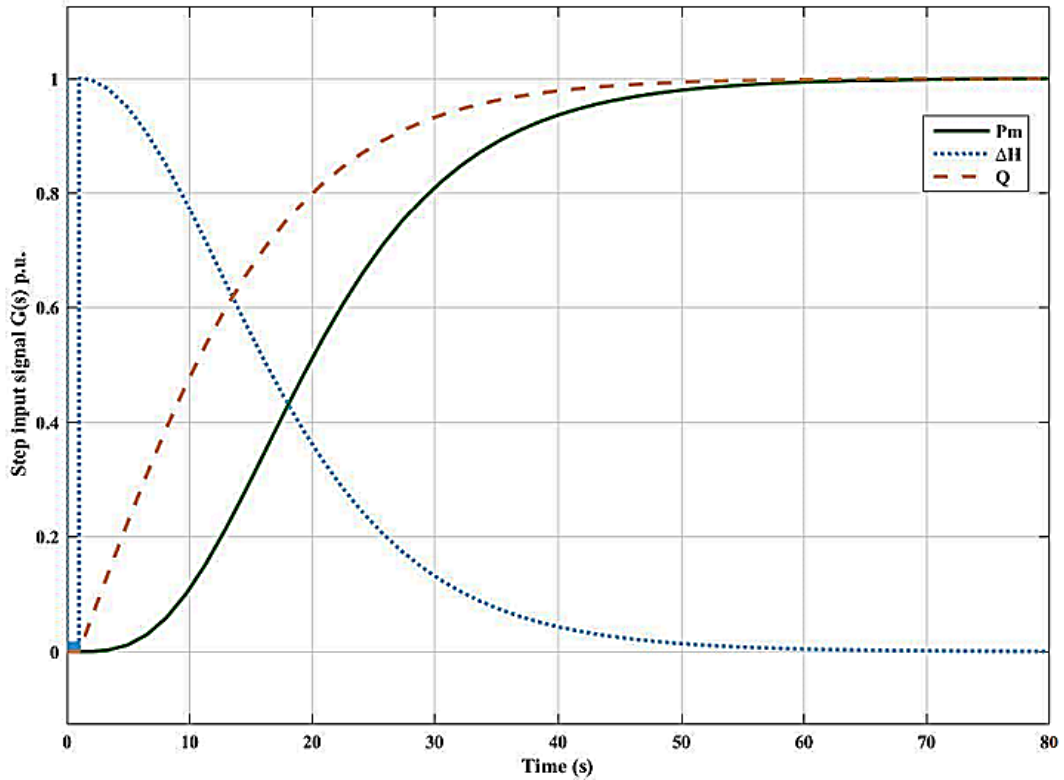


Figure 8.4: Step signal response for gate position $G(s)$ with turbine Power P_m , pressure change ΔH and flow discharge $Q(s)$

The results also show that, the gate valve opening has an effect on the stability of the hydraulic system and the results from the simulation shows that the changes on the gate position from fully closed (0 signal value) to fully open (1 signal value) increases the pressure head ΔH to a maximum signal value just after the opening of the gate valve. This is due to the fact that water flow discharge started passing through the penstock pipe. But soon after the initial gate opening position this pressure change, ΔH starts to decrease until it stabilizes after 55 seconds of the gate opening. On the other hand, the gate opening also increases the flow discharge to the turbine, Q and hence mechanical power value, P_m . The effects of pressure change ΔH cause the system to stabilize at around 55 seconds for both water flow discharge and also mechanical power P_m . Both the flow discharge signal $Q(s)$ and the mechanical power signal P_m increases with the opening of the gate valve position to a stability value while the pressure head $H(s)$ signal decreases from the initial gate opening position. From these results, it is noted that the effect of pressure wave due to changes in head value ΔH , is higher during the initial gate opening and reduces to zero when the system stabilises. The signal input values for the gate position are in p.u. on which 0 is the initial position and 1 is the maximum position.

In the power output p.u. values from Figure 8.5 below, it is also noted that the power output value, P_m is initially dropped from 0 to -2 p.u. at the first initial seconds and then in a few seconds later the power starts to increase non-linearly to a maximum value at P_m equals to 1 p.u. When continuing opening the gate valve position further, the power output signal starts to stabilise after 4 seconds to the P_m value of 1 p.u. The initial changes of mechanical power P_m to a negative value is due to the transient condition when water is introduced to the turbine through a penstock pipe on which changes in mechanical power $\Delta P_m(at t = 0) = -2$. At a later stage the turbine system becomes stable and in this case the steady state mechanical power value $\Delta P_m(at t = \infty) = 1$ which means the input signal is the same as the output signal. These are the special characteristics of the micro-hydro turbines as shown in Figure 8.5 below for more details.

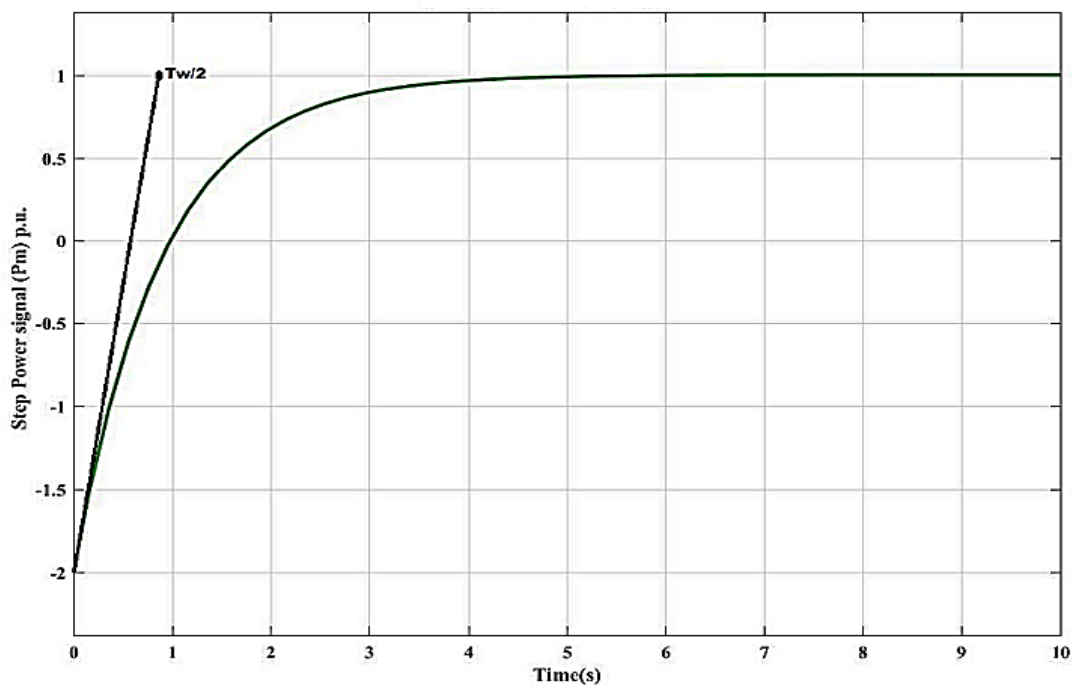


Figure 8.5: Changes in mechanical power (P_m) with gate valve position (G_v)

In these special characteristics the power output signal, P_m from the micro-hydro turbine is characterised by a non-linear system on which when a straight line is drawn from $\Delta P_m(at t = 0) = -2$ a straight line is obtained which has the value of $\frac{T_w}{2}$ i.e 0.895 seconds. This line represents the linear characteristics behaviour of the turbine system as an approximated value. In order to reduce this linear characteristic behaviour of the turbine system, the gain correction factors are introduced on the system which include an integrator and a feedback loop as a result it reduces the transient effects on the system and make the system more stable during the initial water flow stage as compared to the previous system block diagram

on which ΔP_m (at time = 0) was -2. In this case, the system stabilises at around 35 seconds which is a 36% improvement to the original block results.

In the graphical representation of the signal responses of the transfer function for the change in gate opening $\Delta G(s)$ to the change in mechanical power $\Delta P(s)$ based on the updated formulated signal response diagram is shown in Figure 8.6.

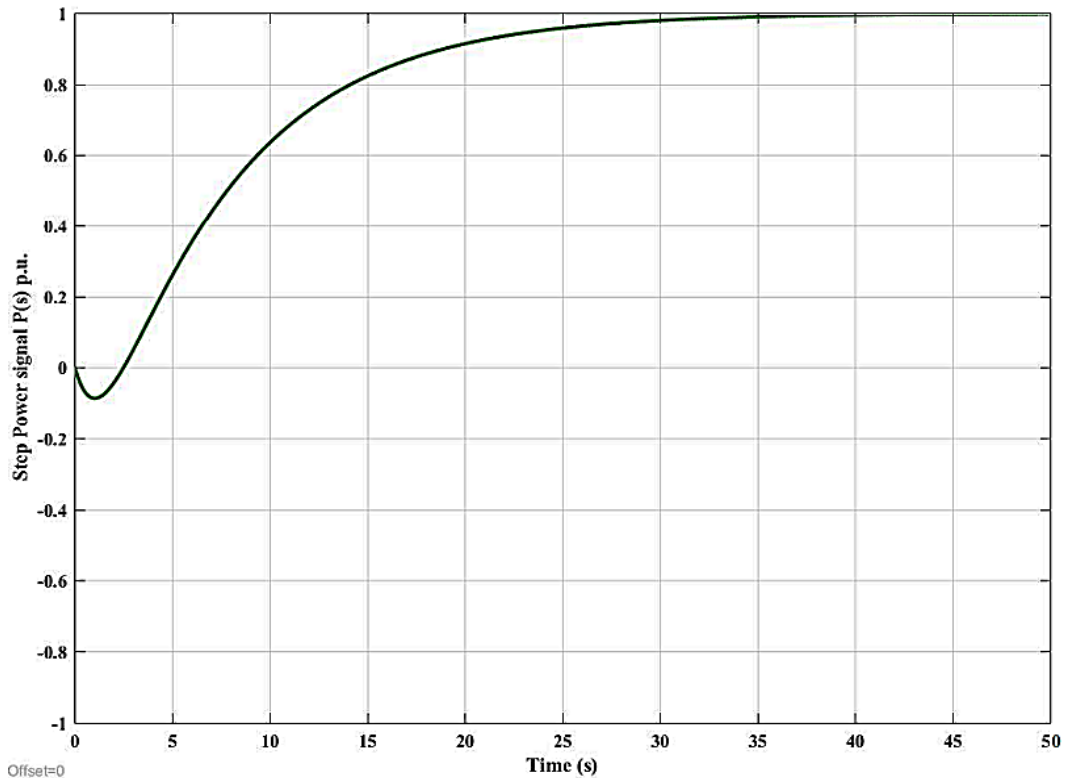


Figure 8.6: Improved signal responses for the power output in relation to the gate position

The results of the above improved simulation graph show p.u. values of power response output signal to the gate opening input signal with a typical non-linear characteristics line graph for the power output of a micro hydro turbine system. In this case when the gate position input signal is activated (gate is opened), it increases the water flow discharge to the turbine through the penstock pipe, thus increase the turbine power (mechanical) and hence the generator power (electrical power), this is valid for most of the micro hydro power systems like Hhaynu micro hydro turbine (present study).

As for comparison, the system input signals with water flow velocity signal $U(s)$ takes shorter time of around 1.4 seconds to stabilize as compared it to power output signal $P(s)$ which took around 35 seconds as compared to the pressure head signal $H(s)$ and flow discharge signal $Q(s)$ on which the system stabilises at around 0.7 seconds which is much quicker than power and gate position signals.

In a nut shell and from design and simulation perspective, the changes in power output signal is mostly influenced by the gate position value $G(s)$ value and also water flow discharge $Q(s)$ value and as the flow discharge and head increases, the turbine power output also increases as shown in Figure 8.7 below for the rated values of $0.45\text{m}^3/\text{s}$ water flow discharge, head of 25m and power output of 75kW.

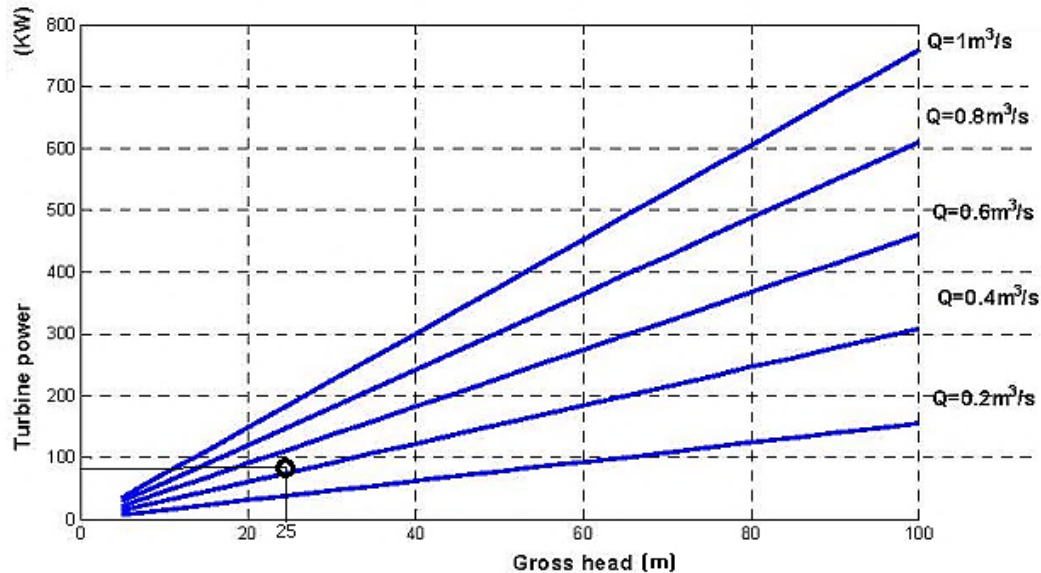


Figure 8.7: Turbine power and gross head variation at different water flow rate

8.3 Generator system

In the generator system model, load power, P_L may be varied to obtain different simulation results for the generator performance and characteristics. Many scenarios have been developed for example when considering the generator system supplying 80% load power demand at the particular time of the day then the other 20% remaining power set as excess. The simulation results from the generator system show that the p.u. speed values drop at the beginning for few milliseconds before the system stabilises below 1 second and this is due to the loading conditions on the generator during the transient state. This is the general characteristics of most of the micro-hydro turbine generator system during the start-ups as shown in Figure 8.8 with the simulation results in power output based on the designed generator model with a rated power capacity. Both mechanical and electrical power output stabilise at around 0.8 seconds. The characteristics of power output from the simulation results are a non-linear graph which is applicable to the micro-hydropower system due to the nature of the transfer functions used.

In the system design, the mechanical power (turbine power) is rated at 79.5 kW and the electrical power (generator power) at 75.5 kW which are in the micro hydropower category.

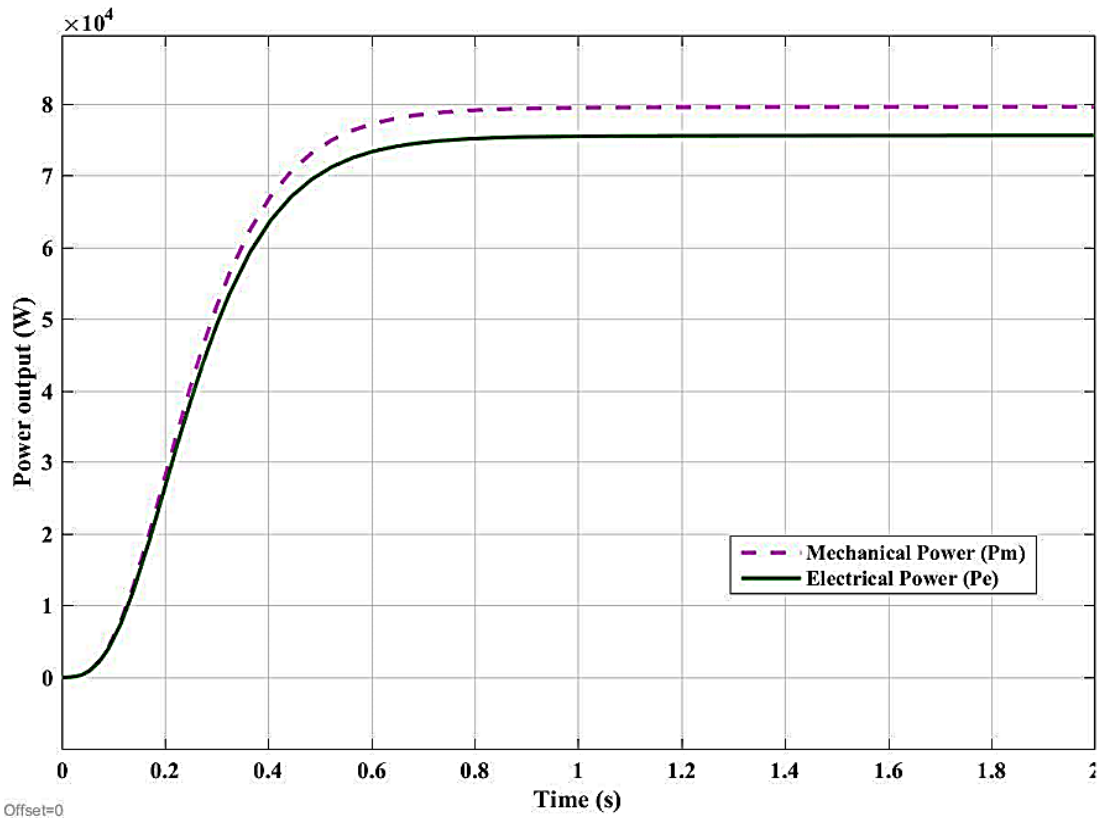


Figure 8.8: Mechanical and electrical power output stability response time

On the other hand, when considering the signal response by adding different load power to the generator start up to full load, the generator response time takes a long time to stabilise, this is due to the fact that during increased loading of the generator system, the system experience transient response which has un-stable condition caused by changes in load power. During the condition with a full load, the generator dumping coefficient, K_D is at its very minimal and the generator system become un-stable between the load power and electrical power. This is mostly applicable to islanding micro-hydropower system conditions like that of Hhaynu in Mbulu Tanzania. In additional to that, the results of the generator response time have also been simulated with the step input signal p.u. value and the results show that when you start the generator with full load power its speed decreases sharply and the system becomes un-stable and due to this, it is advisable to power the generators in stages at a time, starting with the minimum available load then increase after a while to full load.

In order to reduce this effect of instability on the generator system during loading condition, the step signal response of the generator system needs to be modelled and simulated at different amount of load conditions and when considering at 50% load power, the system took 12 seconds to stabilize, while at 20% load power, the stability time decreases to 8 seconds and without any load power (0% load power) the system stability time is much

reduced to 6 seconds. This result shows that the stability response of the generator system is mostly affected by the loading condition with more stability time during high or maximum loading condition and less time during minimum or no-load condition.

With no load power, means all the electrical power produced from the generator system goes to dumping, so there is no much load to the generator windings which affect the system stability due to winding inertia. The problem with this set up of the generator system with no load condition is that it needs to take control of the effect of generator overspend due to excess power produced and this is taken care by the generator governor controls. The comparison between 50% load power and no-load power (0%) is the difference in generator speed and time taken to stabilise the system.

When load power decreases, the generator rated speed, w_r and system stability improve as can be seen from the two scenarios. At 50% load power, the generator speed dropped to 10% rated value while at no load power the generator speed dropped to 30% rated value. The speed drop in hydro generators when they are starting is due to their inertial condition which has to be overcome by mechanical torque. Figure 8.9 below shows a more detailed generator speed response due to different loading conditions on which at no load condition the generator speed rises to just above 1580 RPM which make it unstable. This is normally called run-away speed of the turbine-generator system and it should be set or known from the turbine-generator characteristics.

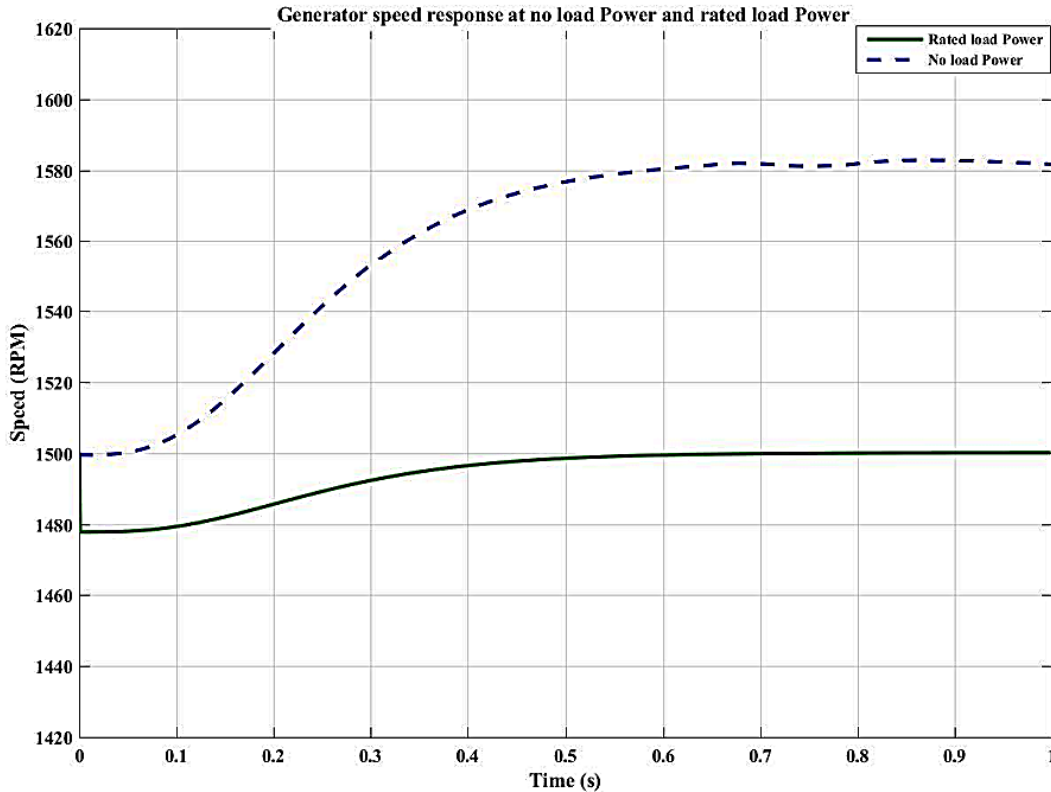


Figure 8.9: Generator speed response to rated load power capacity and no-load power

The general performance characteristics results show that, when reducing the load power on the generator system, the dumping coefficient increases while the stability system response time decreases and from this relationship, we can say that the load power P_L is

inversely proportional to the dumping coefficient i.e. $P_L \approx \frac{1}{K_D}$

In terms of generator rated speed response at the two generator power steps and in comparison with stability time response, the simulation results also show that the generated power at 40 kW which is 53.3% rated capacity stabilise at 0.3 seconds while the generator power at the rated value of 75.5 kW the generator stabilises at 0.6 seconds. It is also noted that the stability time response at rated capacity is twice as compared to that at 53.3% power capacity. This is true for all micro-hydro turbine system, thus is why it is not safe to operate the generator system at its rated capacity in most of the time.

In terms of speed drop at the generator start up due to inertial on which high loading power increases the inertial of the generator system and hence more time for the generator system to stabilise. From the simulation results, it is also noted that the generator speed dropped to around 1478 RPM which 1.5% speed drop from the nominal value. Most small-scale isolated generator system can tolerate a speed drop of up to 2% without and problem. Figure 8.10 below shows the generator signal response at the two steps power rated capacity.

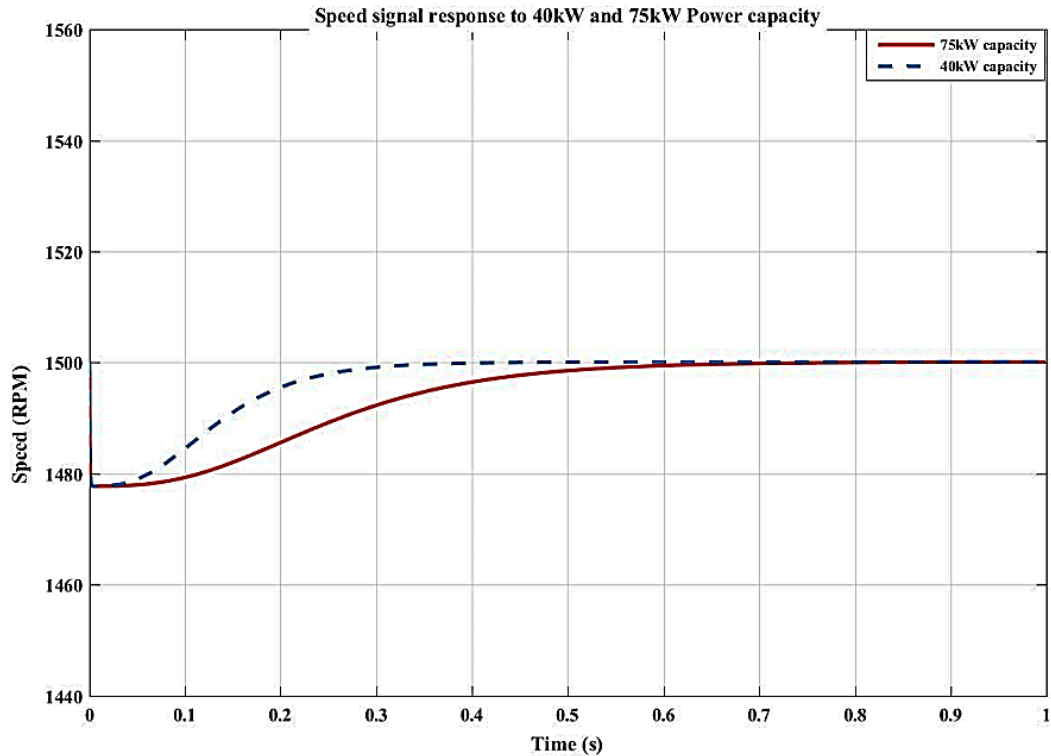


Figure 8.10: Generator speed stability response time at the two power supply steps

In actual operation of the micro-hydro turbine-generator system, the load demand is usually fluctuating during the time of the day between the minimum and maximum values and this changes in load demand affects the generator internal resistance and hence the speed. In modelling, this effect is demonstrated by the introduction of so called dumping coefficient, K_D in generator systems that represent the internal resistance of the generator system.

In p.u. values the simulation results show that when a generator is started to pick up the load, its rotational speed is reduced to a certain value for a short period of time before the system stabilise. Based on the loading condition with the average load power demand of 46.36 kW in the first scenario, the generator speed initially drops to below its rated value for 0.1 seconds before it rises and stabilises at around 0.3 seconds. On the other hand, when considering the rated condition and in comparison to the stability response time, the simulation results of the generator power response at rated values show that the stability value (steady state) is attained at 0.8 seconds which is below 1 second as shown on Figure 8.11 below.

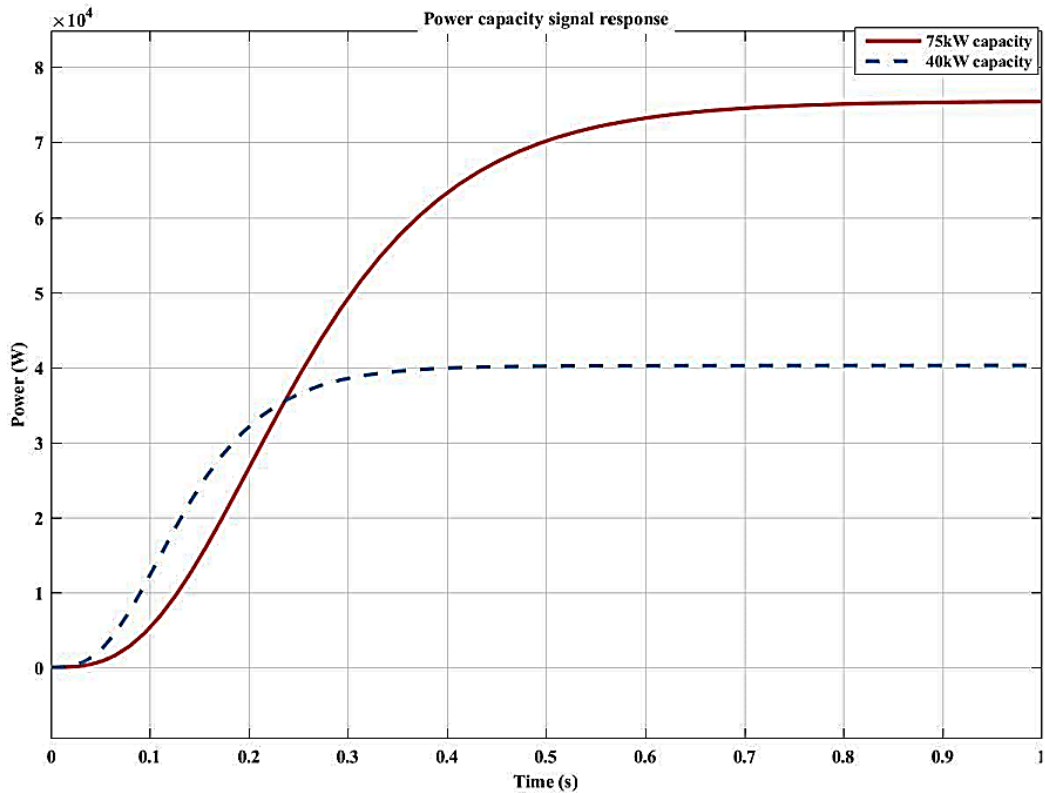


Figure 8.11: Generator power stability response time at the two power supply steps

The generator performance can also be measured by frequency in Hz on which 50 Hz is the rated value and the simulation results show a similar stability response time of 0.8 seconds with the generator frequency measurements which is similar to the power response time. It is also noted that when the generator is loaded, its frequency value dropped and based on the results the lowest initial frequency drop is 49.25 Hz which is 1.5% frequency drop and took only a few seconds at this value. From literature, this value is within the recommended frequency drop for most micro-hydro turbine generators which is around 4% speed droop value [192]. Figure 8.12 below shows the simulation results of the generator frequency response to two power supply steps.

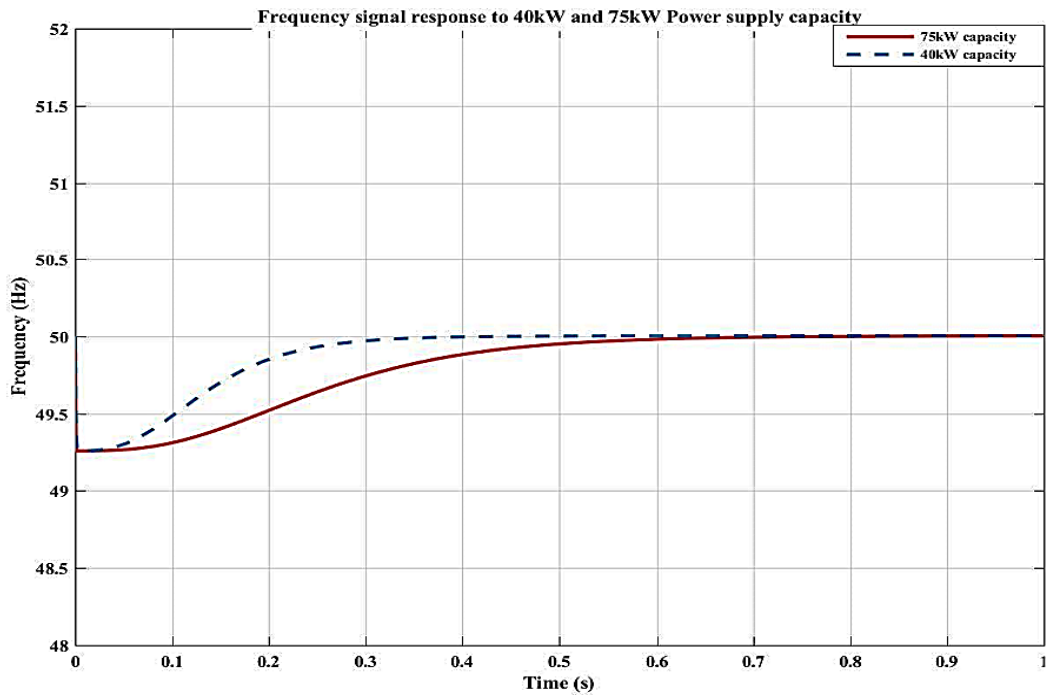


Figure 8.12: Generator frequency stability response time at the two power supply steps

From the design point of view, the generator output speed is influenced by the turbine power which depends on the water flow discharge to the turbine and also available head. In this case, in order to increase the generator speed, more water flow discharge is supplied to the turbine to increase its power output which will eventually cause the generator power increase and hence make it spin faster. The relationship between speed, head and water flow discharge in the turbine-generator system is linear incremental on which the increase in water flow leads to an increase in turbine-generator speed and vice versa. At the rated speed value of 1500 RPM, the water flow discharge is 0.45 m³/s and the head value of 25m which is represented by a constant water flow discharge line graph as shown in Figure 8.13 below. This is only valid in small river water flow discharge of up to 1m³/s which is also applicable to Hhaynu micro hydropower plant for this research project.

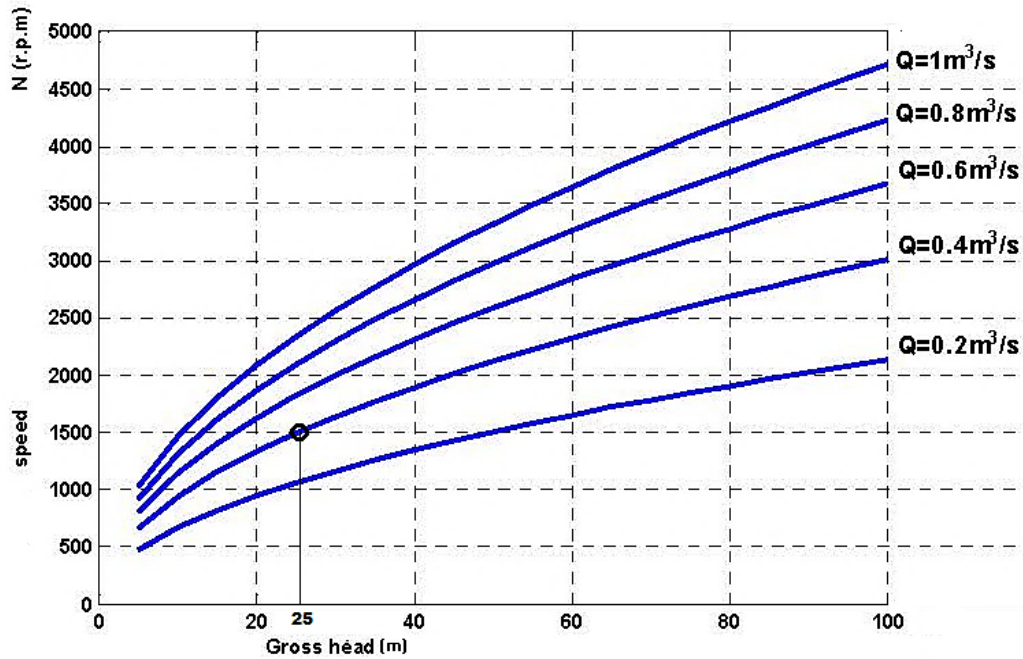


Figure 8.13: Speed variations at a different water flow rate and head values

The above relation in Figure 8.13 can be used to standardise generator speed value of a different turbine-generator system with known water flow discharge Q and head H for micro hydro turbine system and can be applied to the local turbine and generator system manufacturers.

8.4 Control action

In turbine-generator system control, there are three main control modes that need to be applied when operating a hydro turbine system. The initial control mechanism is the primary frequency control which is mostly due to system inertial and is usually a few seconds. During this stage, the generator frequency drops sharply to a below nominal value in few seconds after which it then starts to re-cover in seconds later which usually takes up to 20 seconds.

On the other hand, after the primary frequency control, action from the governor is applied, the generator frequency may still be lower than the nominal value despite several minutes elapses after the primary control action. In this case, a secondary frequency control needs to be applied to the turbine-generator system which involving generation control action. The secondary frequency control mechanism is sometimes called supplementary control which is necessary to drive frequency back to the nominal value of 50 Hz. In this control action process, the gate valve which controls the amount of water flow to the turbine is commanded to open in order to allow more water to flow to the turbine to produce more

power which will eventually increase the generator power output hence the generator speed. Figure 8.14 below shows the generator control modes on which the first two control actions are the most applicable to isolated micro-hydro turbine system like Hhaynu micro-hydro for this research study project.

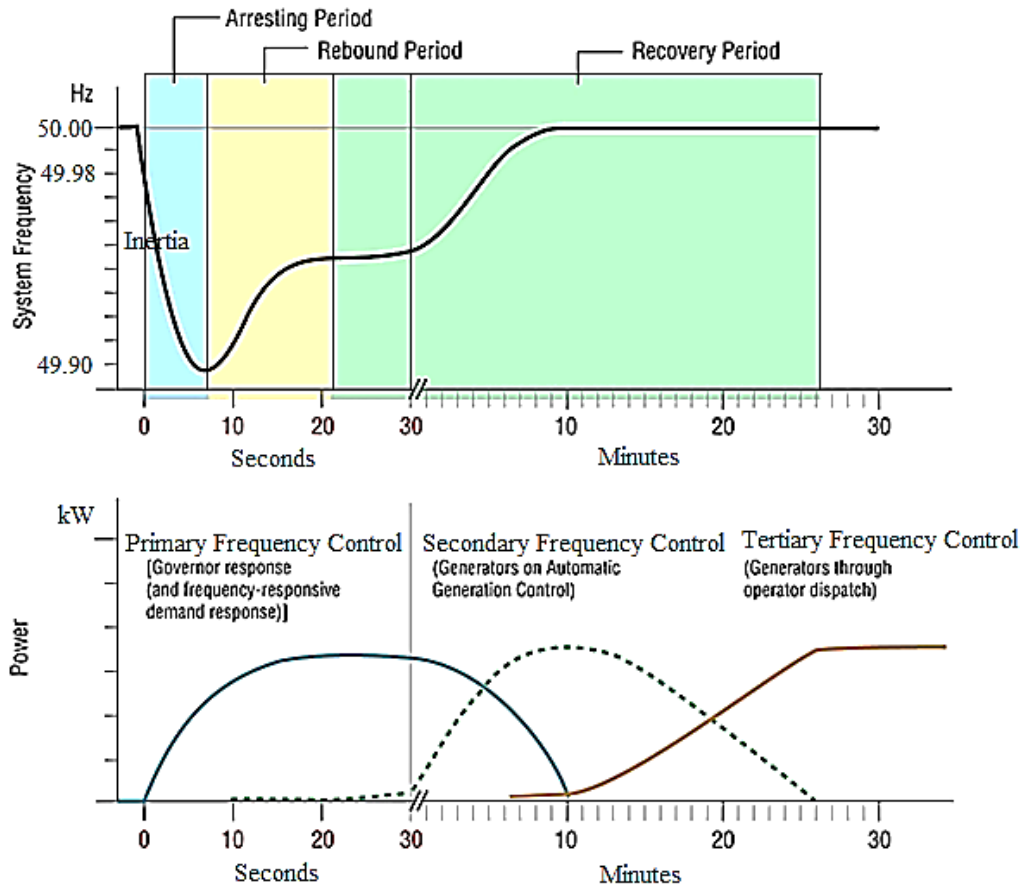


Figure 8.14: Turbine-generator system control modes of operation [193]

In the primary control mechanism, the generator system is very un-stable because of transient condition due to its loading and at this stage, the primary frequency control action is needed to be applied that includes governor control action. There are several governor systems used in hydro turbine system but in this research, four (4) main types of governor control systems have been studied and analysed in detail. These are Mechanical control governor, *PID* control governor, *PDF* control governor and Load control governor.

From modelling and simulation results, the following parameters have been obtained and have been used throughout the control action.

$$T_G = 0.05 \text{ seconds}$$

$$K_G = 5$$

$$T_T = 1.79 \text{ seconds } (T_w)$$

$$K_T = 0.005$$

$T_p = 8$ seconds ($2 \times J$)

$K_p = 0.085$

Inertia (J) = 4 seconds

The above values have been used to form Laplace transform function for individual control equations for the governor, turbine and generator system as follows:

$$\text{Governor control} = G_G(s) = \frac{K_G}{1+ST_G} = \frac{5}{1+0.05s} \quad (8.1)$$

$$\text{Turbine control} = G_T(s) = \frac{K_T}{1+ST_T} = \frac{0.005}{1+1.79s} \quad (8.2)$$

$$\text{Power system} = G_P(s) = \frac{k_p}{1+ST_p} = \frac{0.085}{1+8s} \quad (8.3)$$

8.4.1 Mechanical control governor response

In turbine control system modelling, four (4) types of turbine control governors have been simulated and analysed. The first control governor system is the mechanical governor on which the input signal error value which is the different between the speed reference and actual generator speed is fed to mechanical governor system that consists of a pilot valve and servo motor that drive the gate valve. The pilot valve and servo have been modelled using a transfer function with a time constant of 0.05 seconds and also it includes a gain value of 5. In the mechanical governor model system, there are usually two types of feedback loop systems, permanent droop with the time gain value of 0.224 seconds for this design. The permanent droop deals with steady state error corrections, while the other feedback loop is called the temporary droop and deals with the transient error correction during system starting and loading changes. Temporary droop is modelled using the transfer function with a reset time of 8.95 seconds and temporary droop gain of 0.56 seconds.

The response of the gate opening signal $G(s)$ from the step input signal ($\omega_{ref} - \omega_r$), shows that the gate valve full open after seven (7) seconds i.e. < 10 seconds, which is higher than most of the turbine control governor's action in today's micro-hydropower plant standards [194] Figure 8.15 below shows the simulation results of a mechanical governor control action to the gate opening with linear characteristics for the p.u. values.

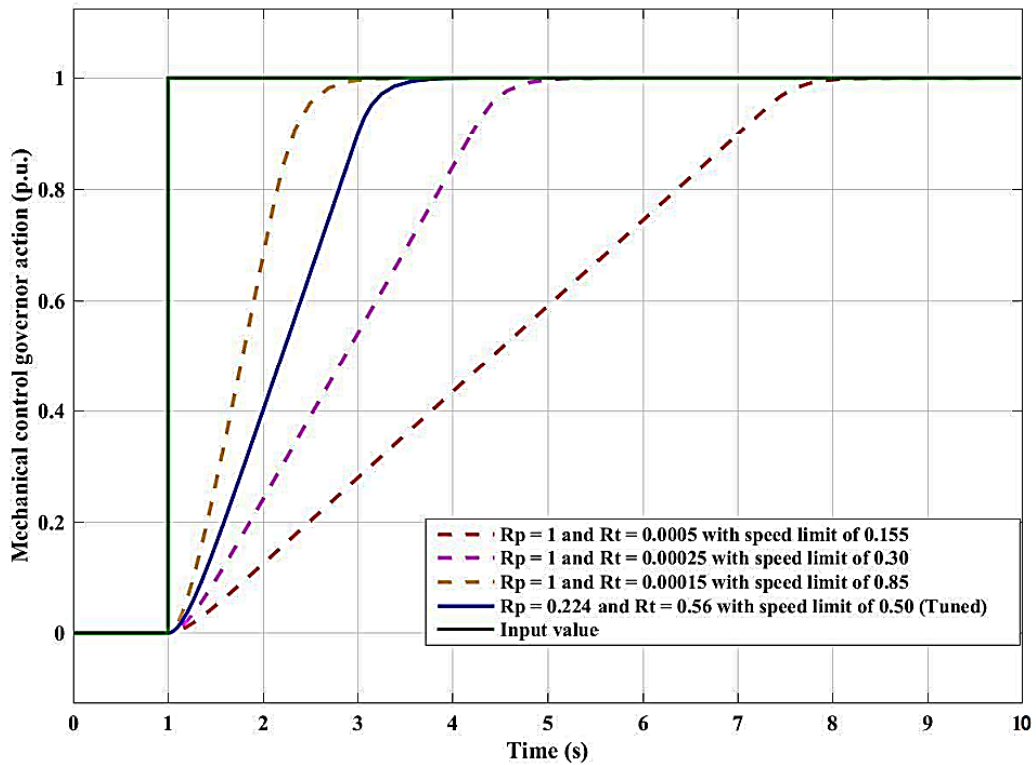


Figure 8.15: Mechanical governor action for the step signal input p.u. value

During the modelling process, the signal response of the mechanical governor in Figure 8.15 has been simulated based on the following constraints [195]:

- (i) Maximum limit gate position = 1.0 and Minimum limit gate position = 0
- (ii) Maximum gate opening rate, $G_v = 0.15$ p.u./s and Maximum gate closing rate, $G_v = 0.15$ p.u./s based on the simulation results.

In the mechanical governor control action, the two feedback signal loops, permanent droop and transient/temporary droop sometimes known as dashpot are the two feedback signals and their main function is to counterbalance as a feedback signal from the input error signal in order to correct the input error based on the reference parameter value as an input and desired value as an output. The value of permanent droop depends on the hydraulic turbine system and need to be calculated on each micro-hydro turbine system but as default value, it is usually set to 5% (0.05) [196]. Two operating conditions do exist in a micro hydraulic turbine system, a dynamic condition when the hydraulic system is in transient and unstable and also instead state condition when the hydraulic system is stable. The dashpot feedback signal will only be available when the system is in dynamic condition (speed responses during loading and unloading conditions) and when the hydraulic system is in steady state condition (stable operating condition) the net droop will be determined by the permanent droop signal only.

On the other hand, when tuning the mechanical governor parameters, the above two considerations need to be optimised based on the steady state (stable) operating condition. It should also be noted that the optimum choice of the temporary droop, as well as reset time, need to be determined using the following relation:

$$R_T = [2.5 - (T_w - 1.0)0.15] \frac{T_w}{T_m} = 0.5329 \text{ seconds [Compared to the previous calculated value of } R_T = 0.54 \text{ seconds]}$$

where $T_w = 1.79$ seconds and $T_m = 8$ seconds

and

$$T_R = [5.0 - (T_w - 1.0) 0.5] T_w = 8.24 \text{ seconds [Compared to the previous calculated value of } T_R = 8.95 \text{ seconds]}$$

The above values for temporary droop (R_T) and reset time (T_R) are the optimum choice parameters under stable (steady state) turbine operation with a long re-setting time [197]. But when a micro hydro-turbine system is operating under the dynamic (transient) operating condition the above values will result in a slow system response because of fast frequency deviation that requires fast speed control mechanisms. So, in this case, the satisfactory dynamic operating condition of the mechanical governor should have a low gain and the reset time T_R which should be less than 1.0 seconds for fast speed response (preferably value close to 0.5 seconds) [195]. This condition of slow response during dynamic (transient) operating condition and fast response during the stable (stead state) operating condition is the special characteristic feature of most micro hydro-turbine mechanical governor control systems and these conditions are usually optimised by the introduction of a dashpot feedback bypass loop that allows both conditions to operate at the same time.

8.4.2 PID control governor response (PD controller)

The turbine control action using PID was initially simulated with the p.u. values for the proportional, integral and derivative values. In this case, the K_p value was set to be one (1) while the K_i value to be zero (0) and the K_d value set to be zero (0). Using these initial values to simulate the PID control system for the gate position response with 1 minute simulation time. The initial results show that with K_p value of 1, the system becomes unstable at this simulation time. In this case, other values of K_p gain need to be determined in order for the system to obtain the system stability.

Due to the nature of the *PID* controllers as fast response control governors, this effect of system instability will affect the performance of the micro hydro turbine system. In order to reduce this effect, the *PID* governors need to be tuned so as to obtain the optimised *PID* values for system stability and reduce the overall system error. The tuned *PID* control values based on simulation results for the step input signal systems with transfer functions on the control equations with *PID* parameters are $K_p = 2.1$, $K_i = 0$ and $K_d = 0.08$. These values are set to be the tuned *PID* control governor gains with step input value (set point) and when simulated it resulted into a stable steady state system condition with quick system response time of around 0.2 seconds which is better compared to the un-tuned values. From these results, it is also noted that $K_i = 0$ which means that there is no integral for the tuned *PID* controller gain and the system error, in this case, is corrected by a proportional gain and derivative gain. The following diagram on Figure 8.16 shows per unit values of the results of the *PID* controller response on which the system stabilises at around 0.2 seconds of simulation time.

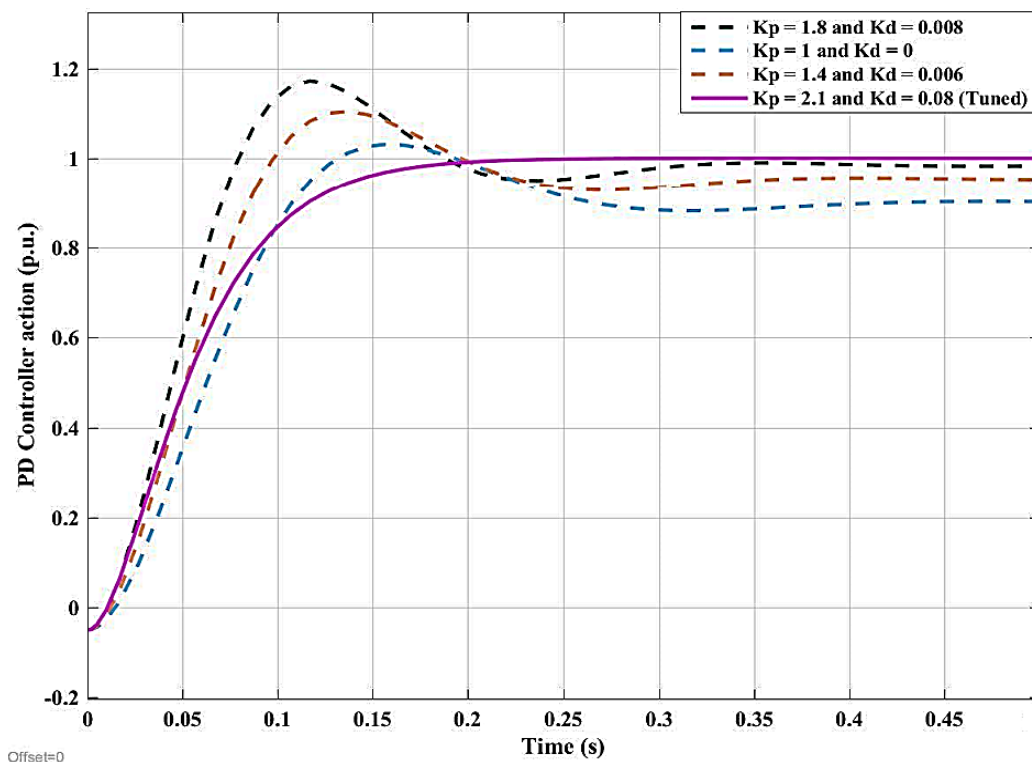


Figure 8.16: PD controller action for the step signal input p.u. value

From the simulation results, it is also noted that *PID* control systems are very quick in control response and takes very short time below 0.5 seconds to stabilize the system as compared to the mechanical governor system which takes at least 3 seconds. The results also highlight the fact that in most micro-hydro turbine system control mechanisms, *PID*

controls are the mostly widely used in stand-alone system mini grid system due to their advantages of very short response time for stability control during load changes or disturbances [198].

In the actual system design of the *PID* controller, governor tuning has been done in order to suit the dynamics of the hydro turbine-generator system that needs to be controlled. The initial design for the micro-hydro turbine system uses the default *PID* control gains which in principal will not give the desired turbine performance and may also lead to system instability and control performance problems. In order to obtain the best system performance and eliminate the instability problems, the *PID* controller for the system design need also to be tuned using the trial and error method. In this method, the tuning is done when the system is running by first setting K_i and K_d values to zero and increase the K_p until the system reaches the oscillating behaviour. After that, the K_i value is adjusted to stop oscillations and then the K_d value is adjusted to obtain the fast response time.

Based on the simulation results of the tuned *PID* control governor with p.u. values for the designed micro-hydro turbine system, the following Table 8.1 shows the final tuned simulation values for the proportional gain, integral gain and derivative gain for system design *PID* control governor.

Table 8.1: *PID* Controller gain values with permanent droop and response time

Proportional gain (K_p)	Proportional band (PB) %	Integral gain (K_i)	Derivative gain (K_d)	Permanent droop (R_p)	Stability response time(s)	Control action
Per unit initial values (p.u)						
2.1	47.62	0	0.008	0.9	0.2	<i>PD</i> Controller
System design values						
0.025	4,000	1.588	0	0.494	1.8	<i>PI</i> Controller

Based on the above results of Table 8.1, it is noted that the initial system control with p.u. values resulted in a *PD* control action (*PD* controller) while the tuned control system design resulted in a *PI* control action (*PI* controller). In the *PD* controller, the control action will increase the stability of the system without affecting the steady state error. On the other hand, the use of *PI* controller on the system design control action has many advantages compared to the *PD* controller. The function of the *PI* controller is to decrease the steady state error without affecting the stability of the system hence improve the transient response of the system but may lead to an oscillating response.

From this result, it is also noted that the principle aim of the proportional gain in *PI* Control action is to control the process as the condition change and the small or narrow K_p gain value will cause less stable process but with minimum offset. Therefore, the tuned K_p gain value of 0.025 in this system design is the smallest acceptable proportional band that will always keep the process stable with minimum offset. But in most processes, the offset cannot be avoided on the system due to load changes. So, in this case, the Integral gain K_i is used to compensate for the offset due to the effects of load changes on the system. The *PI* Controllers are widely used to control processes that are characterised by offset error due to load changes and this is common to micro hydro turbine systems.

Figure 8.17 below shows the *PI* control action for the different values of integral gain with the tuned K_p and K_i values at 0.025 and 1.588 respectively.

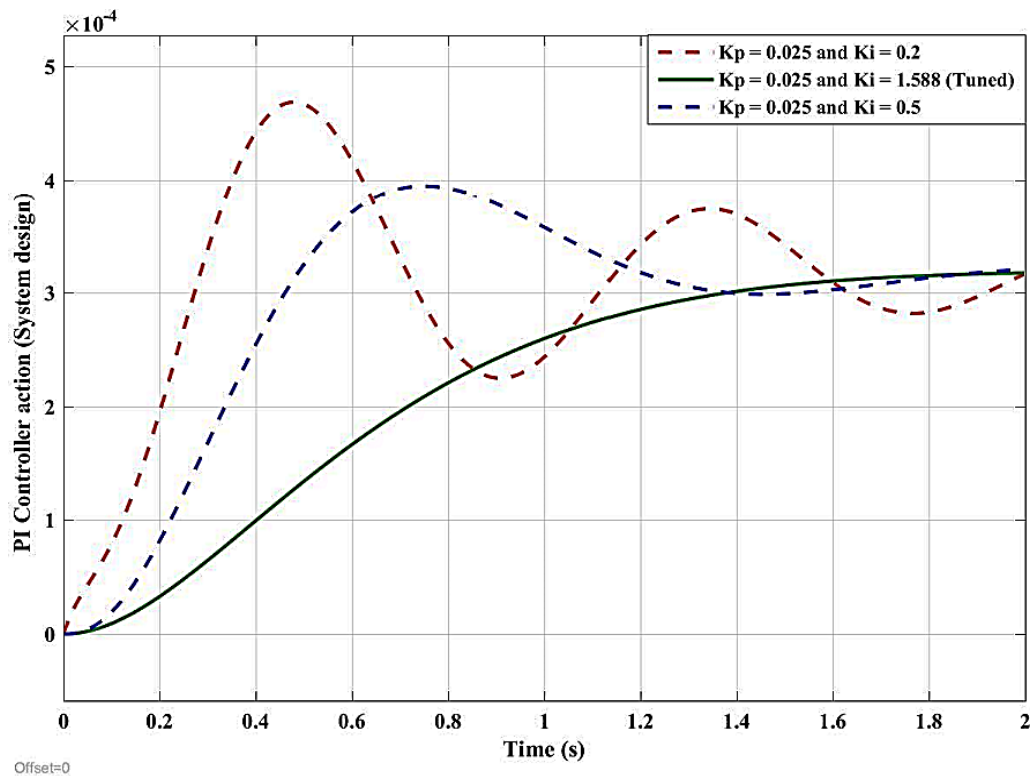


Figure 8.17: PI control governor response for the micro hydro turbine system design

8.4.3 PDF control governor response

In order to obtain the simulation results for this governor, the *PDF* control system has been initially simulated with the step input signal and 5% disturbances to reflect the noise signal that the system may encounter.

Initial simulation results with p.u. values show that the *PDF* control system with the designed transfer function and step signal input stabilise the system at around 0.8 seconds. When compared to the *PID* control system, the *PDF* control system response is a bit slow

by a few fractions of seconds. This implies that when considering the fast response of a hydro turbine system control, Both *PDF* and *PID* control system could be utilized because both control governors provide zero steady state error under loading condition although the *PID* control system provides the fastest response with zero overshoot to a step input signal [188]. The difference in orientation for *PID* and *PDF* control systems is that the *PDF* uses integral plus pseudo-derivative feedback system while the *PID* used proportional, integral and derivative feedforward system and it is a widely common type of control application in the hydropower system. The p.u. values for the step input signal of a *PDF* controller simulation shows that the best stable results are obtained with $K_i = 1.588$ and $K_{pd} = 0.008$ which is similar to the *PID* control gains. This means that the integral control gain which limits the speed of system response is the main control parameter and in this case, the speed of system response is increased by decreasing integral gain K_i while the steady state error value is decreasing as shown in Figure 8.18 for the *PDF* controller response under step input simulation value.

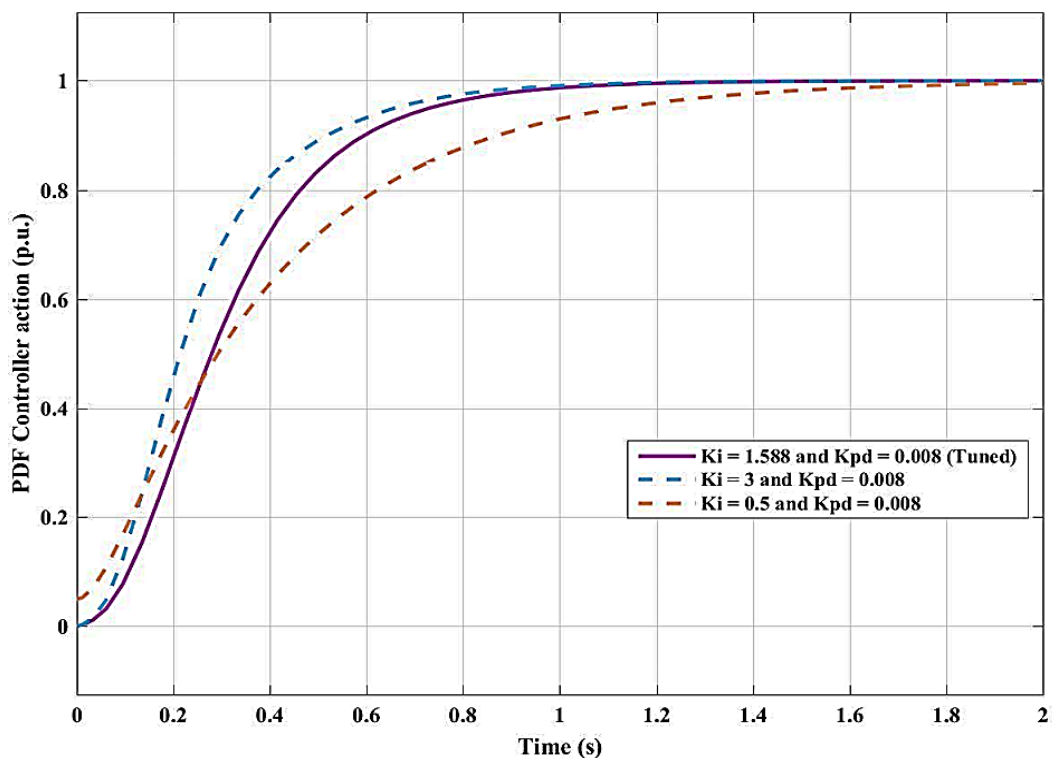


Figure 8.18: PDF control governor response with step input p.u. value

In controlling the turbine-generator system using the *PDF* control governor the initial *PDF* gain values should be applied and then tuned to obtain the best system stability response. Different gain values have been applied for tuning the system design and based on the simulation results the tuned integral gain is less than the p.u. value with K_i of 0.5 but the

derivative gain has increased to 0.09. The advantage of the *PID* and *PDF* control action is that using the derivative control mode in these controllers has made the control loop to respond faster. In this case the more the derivative time setting, the more derivative action is produced from the controller. This is shown between the tuned *PDF* control gain parameters on p.u. values and system design on which the stability time for the system design took twice (1.6 seconds) as compared to p.u. values (0.8 second). In this case, the K_{pd} value on the system design needs to be set high for the high derivative time in order to reduce the error changes at a faster rate as shown in Figure 8.19 below.

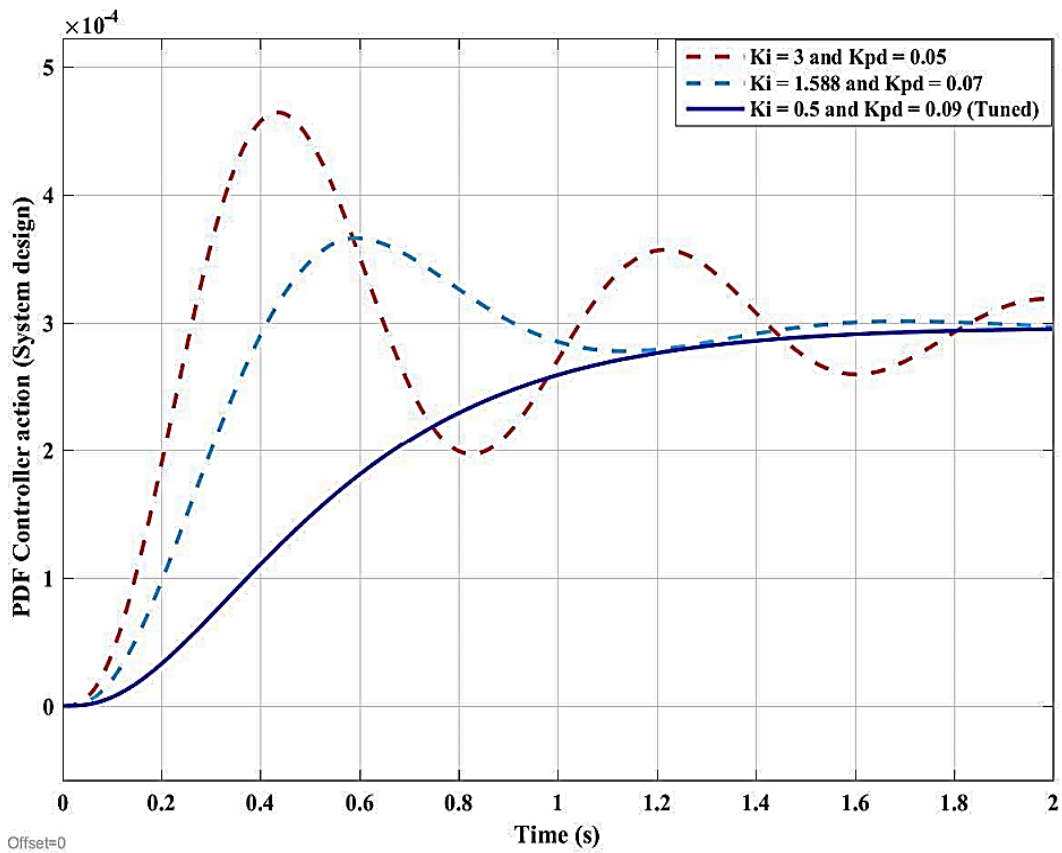


Figure 8.19: PDF control governor response for the micro-hydro turbine system

8.4.4 Load control governor system

In most small and micro hydro turbine system with small water flow capacity, the type of control governor used which is economical is called a shunt load governor system which basically uses electronic load controller (*ELC*) system to balance between the produced power supply and the available load demand. The working principle of the load control governor system is based on balancing the power supply (generator power) with the load demand power in order to stabilise the system. In this case, the turbine power is kept at a constant value which also makes the generator power to be at a constant value by supplying

a constant load demand power. Now, due to the fluctuations on the load demand in most cases and in order to maintain the system stability, an additional dump load is connected at the generator terminals. The function of a dump load is to divert excess power produced during low demand hours in order to balance the generator power output and the instantaneous consumer load for the purpose of keeping the generator speed and frequency at a constant value.

High power demand hours have the lowest dumping coefficient and low demand hours have the highest dumping coefficient. This result implies that the dumping coefficient is determined by the amount of load power demand value during the time of the day. In addition to these results, the dumping coefficient also affects the generator stability in such a way that when a generator system is loaded it takes a long time to stabilise and in this state, the dumping coefficient is reduced. So, at low dumping coefficient of a generator system which is during supplying high load power demand, the generator system stability is affected and in most cases the generator stability response time takes longer time as shown in Table 8.2 below Thus why it is advisable to load electrical generator by starting with the lowest available load power then step by step change to the next and finally to the highest load power in order to reduce the stability response time.

Table 8.2: Relationship between load power, dumping coefficient and stability response

Load Power, P_L (%)	Dumping, K_D (%)	Stability response time, t (seconds)
99	1	450
80	20	25
50	50	12
20	80	8
0	100	6

From the above Table 8.2, the results also show that the load power P_L is inversely proportional to the generator dumping coefficient K_D on which at no load power, the dumping coefficient is at 100% (K_D max. and with a short stability time response of 6 seconds. This is also valid during high load demand on which the dumping is at its lowest value at 1% but the system takes a long time to stabilise as shown in Figure 6.20 below. This effect is mostly applicable to the off-grid turbine-generator system on which load power demand changes regularly at different hours of the day. In order to reduce this effect of long stability response time on islanding micro hydro turbine system, the available load power demand needs to be connected in load phases at a time starting with low demand

power phase at the beginning, then to intermediate power phase and finally the high demand power phase at the end. Loading generators to full load capacity in a few seconds will cause the stability problem to the generator system. Therefore, in order to operate the generator at its best performance, there is a need to balance between power supply and power demand with the system stability and find the optimum operating conditions and in this research, these values have been obtained as shown in Figure 8.20 below.

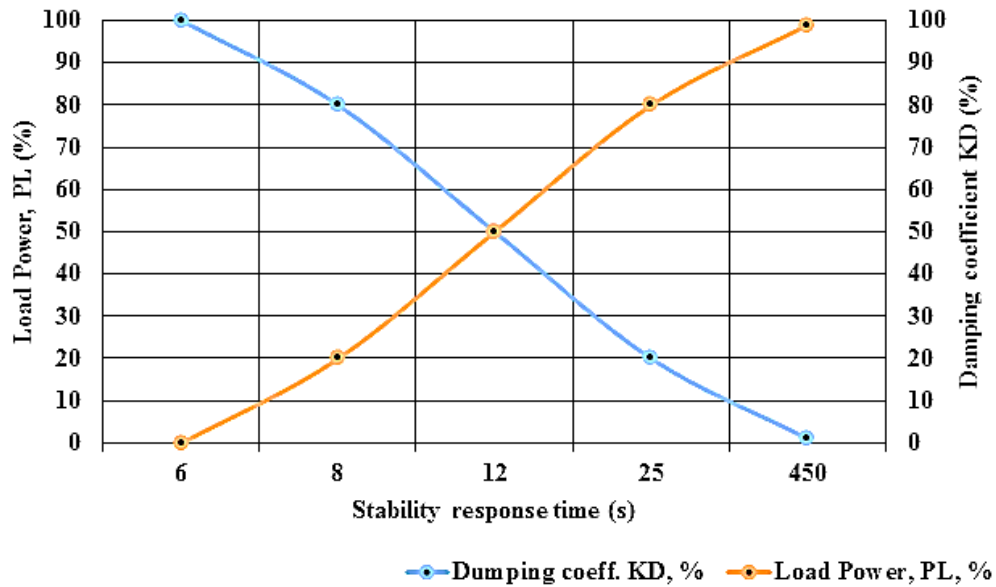


Figure 8.20: Relationship between the load power and dumping coefficient

In comparing the power output with consumer load power, P_L and produced dumping power, P_{Dump} for the following relation is applicable:

$$P_O = P_L + P_{(Dump)} \quad (8.4)$$

where, P_O = power output, P_L = consumer power and $P_{(Dump)}$ = dumping power

Based on the above relation in equation 8.4, it is noted that the output power needs to be in a balance such a way that when P_L is low as in the most cases when the electrical generators are starting up then the $P_{(Dump)}$ value is at the highest. This is caused by the inertial of the turbine winding system on which it has to be overcome by the balancing power supply.

On the other hand, the dumping power $P_{(Dump)}$ depends on the damping coefficient as well as the consumer load power PL and change in generator speed $\Delta\omega r$ as follows:

$$P_{(Dump)} = P_L \cdot K_D \cdot \Delta\omega r \quad (8.5)$$

In this case, for the system to stabilise at the rated power values, then the dumping power must be reduced to zero on which the power output will only supply to the consumer i.e. $P_{(output)} = \text{consumer load power } (P_L)$ load as shown in Figure 8.21 below.

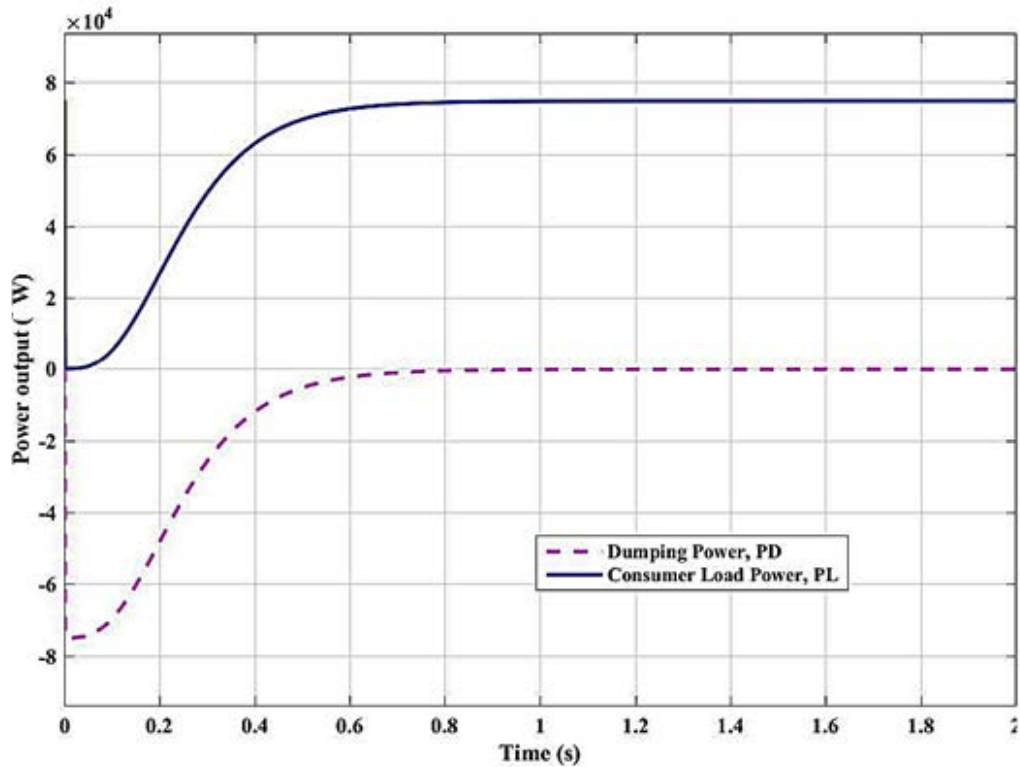


Figure 8.21: Responses of consumer load power in relation to dumping power

8.5 Control governor choice for the system design

Choices for selecting a particular type of control governor system for the designed turbine-generator system depend on many factors but the most applicable factor is the response time that the governor will take to stabilize the turbine-generator system. In micro-hydro turbine systems, which are mostly off-grid and stand-alone systems, a quick response time governor system is needed in order to avoid the risk of generator speed changes from nominal value because of abrupt changes in consumer load demand.

In most hydro power systems, the initial governor control parameters are set to default values when operating the system and in this setup, it is called un-tuned control governor. When simulating this kind of system, the effect is that there is a predominant amount of steady state error produced which makes the system unstable as shown in Figure 8.22 below. Different control action will produce different steady state error value and based on the present research study, un-tuned *PDF* control action have the highest steady state error value while the mechanical control governor does not produce any steady state error but took longer time to stabilize of about 3.5 seconds which is similar time with the *PDF* control governor to stabilize. Steady state error for *PID* control governor system is lower than the *PDF* control governor but in comparison with the input value and short stability time, *PID*

control governor system shows good results as shown on Figure 8.22 below for the un-tuned control governor choices.

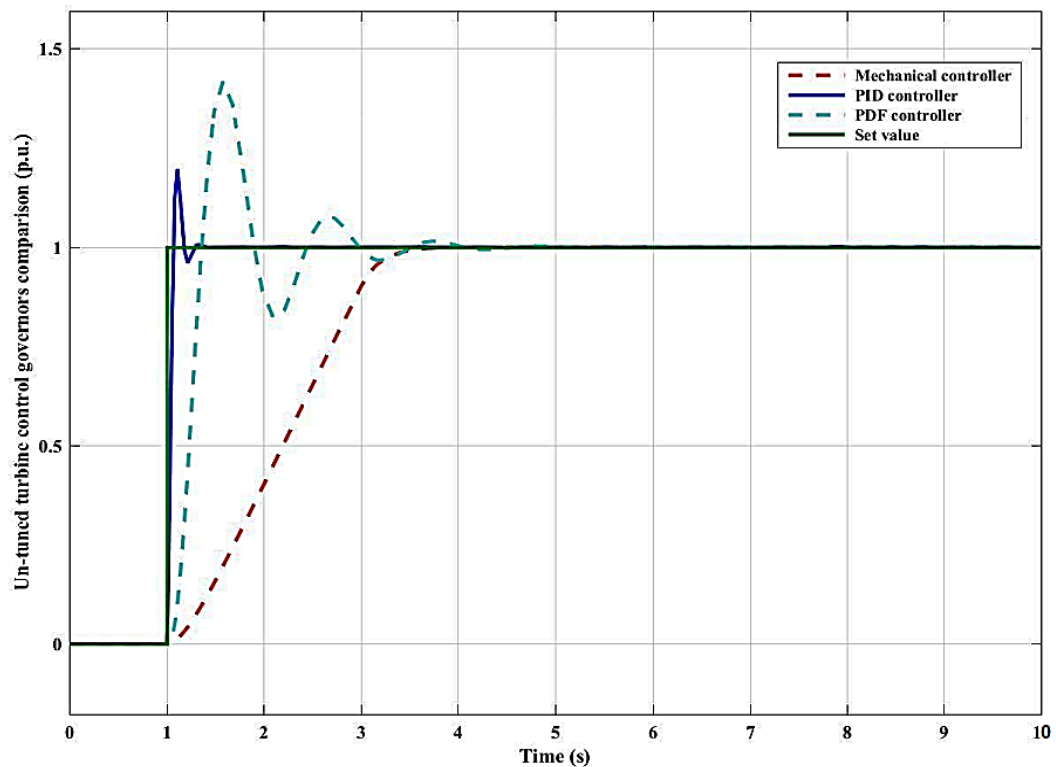


Figure 8.22: Un-tuned control governor's responses to input set value

In order to reduce or eliminate the steady state error in the governor control action, the initial selected (defaults) governor parameters need to be tuned in order to stabilize the turbine-generator system. In the present study, the three control governors tuning has been done manually and the simulation results of the tuned control system show that mechanical governor took a long time to stabilise for about 3 seconds, followed by the *PDF* controller at about 2 seconds, while the *PID* controller has a quick response and took around 1.25 seconds. Also, the results show that the *PID* controller output values are very close to the input values which means the system error has been very much reduced as compared to the *PDF* and mechanical control governor systems. On the other hand, in terms of permanent droop value R_p , the *PID* control governor *PDF* control governor has a permanent droop of 0.9 (gain of 1.1) while the mechanical control governor has a droop of 0.224 (gain of 4.5) which is 4 times higher. This is because the mechanical control governor contains a secondary feedback loop called transient droop with a temporary droop gain of 0.56 seconds. The other noticeable results are that the derivative gain K_d values for *PID* and *PDF* control governor are of the same value of 0.008 which is very close to 0. Despite very close similarities in many aspects between the *PID* and *PDF* control governors, the *PID*

controller seems to perform better and close to the input values as compared to the *PDF* controller and the Mechanical control governor. Therefore, due to its good performance in terms of control action, the *PID* control governor is suitable for control action in this research project and is recommended for use in the designed micro-hydro turbine system as the main control governor system. Figure 8.23 below shows the simulation results in comparison of the three control governor systems with step input value (p.u.) and 10 seconds of simulation time.

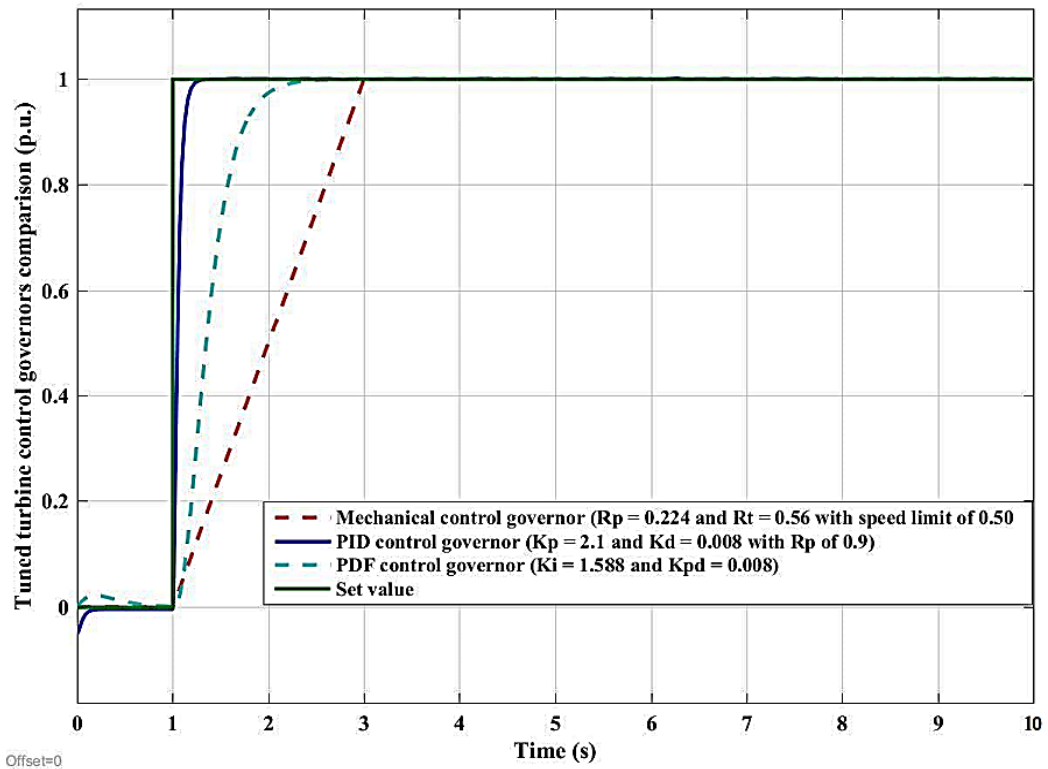


Figure 8.23: Tuned control governor comparison based on response to step input value

8.6 Power supply and load demand optimization

The main power supply in the system design mainly comes from the micro-hydro turbine system. The micro-hydro turbine system has the nominal capacity of 75.5 kW on which the average output power is 70.1 kW which gives the yearly energy production of 614,284 kWh/year with the capacity factor of 92.9%. On the other hand, due to changes in load demand phases between low and high demand hours, the micro-hydro turbine system can also operate in two power phases which are 40 kW power supply during low demand and 75.5 kW power supply during the high demand hours of the day on which the available power capacity is supplied to the consumers throughout the day. The micro-hydropower is

the main source of power on the system design and covers around 70% of the total load power which is mainly consumer load demand.

But during the peak hours of the day, this power supply capacity is not enough to supply the required high load power demand and in this case, the additional power supply is required. During most times of the day except peak hours, excess power is produced from the hydro turbine source and in the original design, this power is wasted as shunt loads (water heaters). From the simulation, more excess power is produced during the night hours on which up to 60 kW each hour could be available between 1 AM to 4 AM. On the other hand, the maximum peak power that is needed during high demand hour is 101.8 kW as shown on Figure 8.24 below which is 25.8% more than the rated capacity which must be provided by other renewable energy sources and one of the best option is to use or store energy from the excess electricity and use it during the peak hours of the day.

The use of 40 kW power supply during the low power demand times of the day has some disadvantages in terms of getting less excess electricity. So, in order to maximize the production of excess electricity, the power supply from the micro-hydro turbine-generator system must be operated close to its rated capacity most times of the day on which from simulation results the mean power output from the generator system should be at 70.1 kW as shown on Figure 8.24 below.

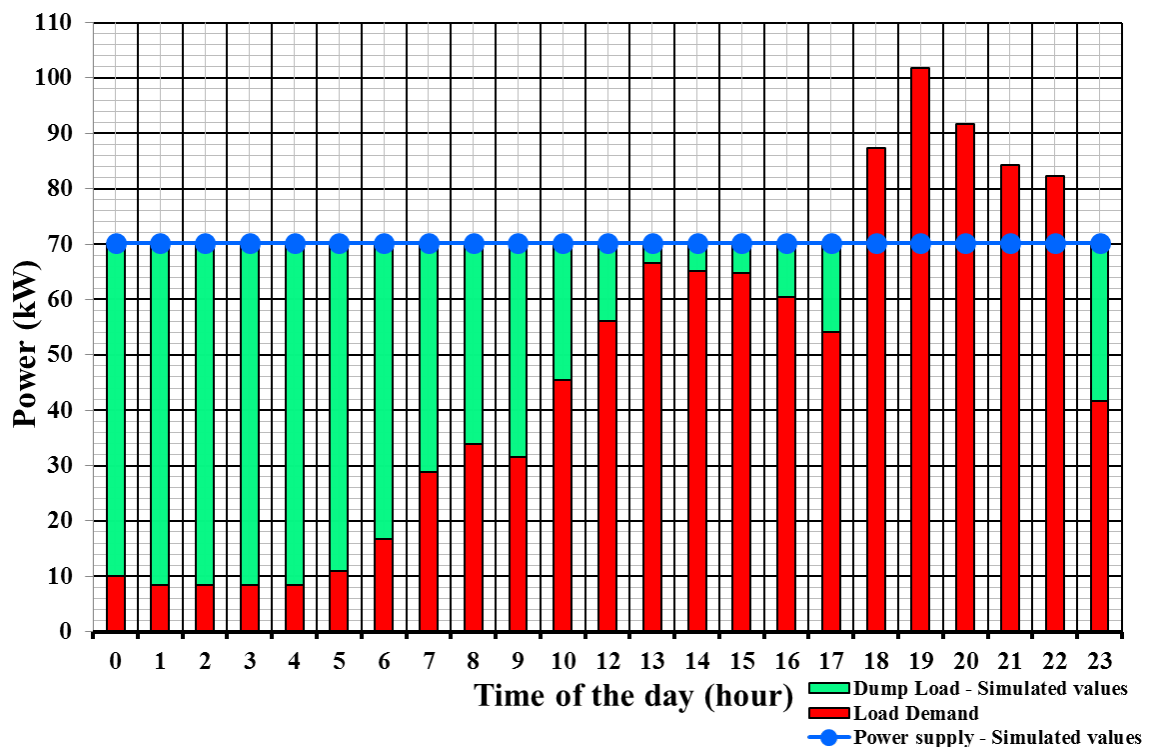


Figure 8.24: Simulated values for the power and load demand

The cumulative excess electricity production is also shown on a monthly basis and the results show that high power values during the night hours of the day. In this case, during the low demand phase which is between midnight hours to around 6 AM, the monthly average cumulative excess electrical production could reach up to 60 kW. The results also show that, during the morning hours when the load demand starts to increase, the monthly average excess electrical production ranges between 50kW (after 6 AM) to 25kW (before 12 noon). Due to high load demand power during the peak hours of the day, there are few hours in a day where there is no excess electrical production which includes the time between 13:00 hours to 15:59 hours and also between 18:00 hours to 22:59 hours. These times of the day have the highest peak values for the load demand and are mainly during the lunch hour and dinner time respectively.

Despite the availability of excess electrical production in most hours of the day, the results also shows that there is a capacity shortage during the peak hours of the day. This is because there is no energy storage component which will store most of the available excess electricity produced. This capacity shortage is mostly noticed on each day between 18:00 hours to 22:00 hours because at this time of the day is the peak hours on which power supply above rated capacity is required to supply to the high load demand. In this case, the capacity shortage ranges between 8kW to 26.8kW (10.6% to 35.5%) of the nominal power capacity which is equivalent to 328.32 kWh/d on average (19.5% average).

From the above simulation results it has been considered in the system design that instead of wasting excess electricity produced from hydro turbine system as a dump load, it may be effectively used to supply power during the high demand hours and one of the innovative options that have been applied in this research study is the additional of another renewable energy source. In this case, excess electricity produced on each hour is optimised to supply power to other renewable energy systems and in this research study, two additional systems have been selected. The main system design has an electrolyser which uses available excess electricity to produce hydrogen and oxygen gas. The hydrogen gas produced by the electrolyser is used as a fuel gas to power the hydrogen *ICE* engine-generator system that produces electricity to supply power during the peak demand hours of the day and because more hydrogen is produced, the excess hydrogen gas that is produced is sold to the local industries. The system design setup will lead to two energy production sources on which the hydro turbine system will have a yearly average energy production capacity is 614,284 kWh/year (95% of the total energy) and the engine-generator system yearly average energy

production capacity is 35,374 kWh/year (5% of the total energy). The two power supply sources have been optimised based on the available excess power from the hydro turbine and also hourly load demand from the consumer. The *ICE* engine-generator power supply system only works during the peak hours of the day which is about 5 hours between 18:00 hours to 22:00 hours.

On the other hand, the engine-generator system will have a rated capacity of 40 kW with maximum electrical output of 36.2 kW which is mostly supplied during the highest peak hours of the day (19:00 hour to 20:00 hour), while the minimum electrical output of 16.6 kW is supplied during the low peak hours (18:00 hour and between 21:00 hour to 22:59 hour) and the average electrical output of 23.9 kW is supplied when the average excess power is required which is between 20:00 hour to 21:00 hour as shown on Figure 6.28 below with the monthly average electrical output values. The engine-generator system power production gives a capacity factor of 10.1% with a fuel energy input of 69,120 kWh/year and the electrical energy production of 35,374 kWh/year which gives the mean electrical energy efficiency of 51.2%.

The engine-generator system will be powered by hydrogen gas (which is renewable energy source) produced from the electrolyser system at the rate of 2,074 kg/year which gives specific fuel consumption of 0.059 kg/kWh that is equivalent to 16.95 kWh/Kg as compared to petrol fuel at 6.6 kWh/Kg.

The produced power from hydro turbine system and engine-generator system together with the excess electricity available are used to supply to the consumer load power demand and other load demand power facilities. From the system design layout in the present study, there are three main types of load power demand systems that need to be supplied by the power produced from the hydro turbine and engine-generator system which include A/C primary load power and electrolyser load power. In this case, it should be noted that the additional system design layout will be powered by the available excess electricity produced from the micro-hydro turbine system and the results show that the excess power after system optimization has been reduced significantly to a very minimum value.

8.6.1 AC primary load

The AC primary load is the main load demand from the consumers that is supplied by the micro-hydro turbine system and it includes household energy demand, small business and small industries and accounts for about 406,269 kWh/year which is 63% of the total annual energy consumption. In general, the AC primary load have been divided in to three main

categories based on the consumer type. These include domestic use which accounts for about 778.78 kWh/d which is 69.88% of the total AC primary load demand, productive use that accounts for about 257.8 kWh/d which is 23.13% of the total AC primary load demand power and social infrastructure with the value of 77.80 kWh/d that gives 6.98% of the total AC primary load demand power. The above values give the total average daily energy consumption for the AC primary load to be 1,114.38 kWh/d. In terms of hourly power demand on each day, the maximum instantaneous value of load power demand per month that need to be supplied to the consumers during the high demand hours is 101.8 kW while during the low demand hours, the minimum power demand value is 8.42 kW.

Based on the system design values, the hourly primary load demand power is not constant and changes every hour. This changes in load power demand can significantly affect the rotation speed of the turbine-generator system and hence the system frequency. In the system design the local grid operates at 50 Hz frequency and the maximum load demand power (peak hours) in the community is around 101.80 kW (19:00 hour) on which the micro hydro turbine system can only produce a maximum power of 75.5 kW on which this capacity will not be sufficient to supply enough electricity to the local community. In this case, there is a load deficit of 26.5 kW to the system during the peak hours of the day which in this analysis have to be supplied by other energy source or obtained from the energy storage system as explained in the previous sections.

The Figure 8.25 below, shows the simulated values for the hourly load demand values in the case study area on which low demand hours are during the night hours and the high demand hours are in the day time with morning peak, afternoon peak and evening peak which is the maximum.

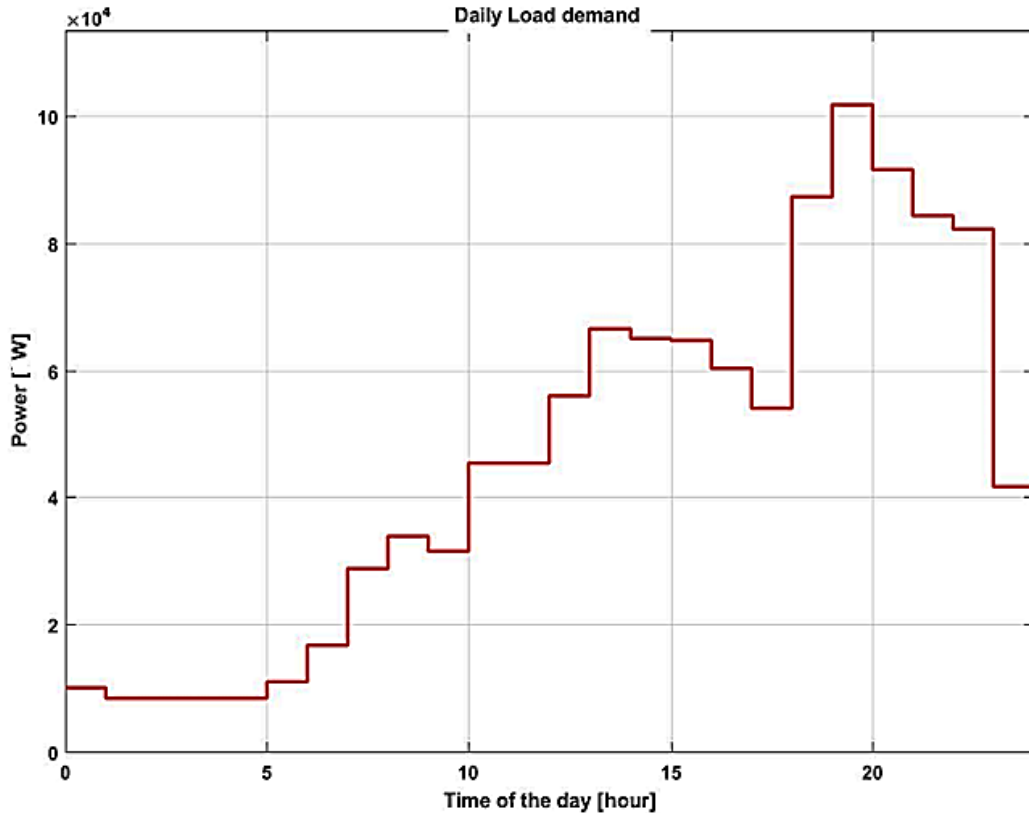


Figure 8.25: Hourly AC primary load demand – Simulated values

The characteristics of the daily load demand profile on Figure 8.25 with peak demand power which is higher than that of the available power supply, then lets analyse the changes in generator frequency and hence the system frequency at these peak load demand hours when the power is supplied by the micro -hydro turbine-generator system.

In this case, let's consider the designed micro-hydro turbine with the following operating set conditions:

Maximum demand (P_{max}) = 110.80 kW (Peak load Power)

Minimum demand (P_{min}) = 8.42 kW (Overnight)

Nominal operating load (P_D^0) = 75 kW

Operating frequency (f) = 50 Hz

System droop = 5.44% (Actual)

System Inertia (J) = 4 seconds

Now, if the micro hydro turbine is the only power source that is used to supply all the load demand to the community then the power supply to the load must increase by $\Delta P_D = 26.5$ kW and consider frequency Response Coefficient - β .

8.6.1.1 Generator frequency at peak demand (75.5 kW power supply)

In relation to changes in load demand, the changes in frequency response coefficient (β) need to be analysed for the turbine-generator system.

Mathematically:

$$\beta = R + \left(\frac{1}{R_{(pu)}}\right) \text{ and } \Delta f_s = - \left(\frac{Droop}{\beta}\right) \quad (8.8)$$

Also, from actual dumping D value = $\frac{(P_D)}{f_0} = 1.5 \text{ kW/Hz}$

where $P_D = 75 \text{ kW}$ and $f_0 = 50 \text{ Hz}$

When considering Droop value in p.u. = $\frac{\text{Actual value (D value)}}{\text{Max. load power (Pmax)}} = 0.02 \text{ p.u. kW/Hz}$

where Droop value = 1.5 kW/Hz and $P_{\text{max}} = 75 \text{ kW}$

Then, the value of $R = \text{Droop} R \times \frac{f}{Pr} = \frac{R}{100} \times \frac{f}{Pr} = 0.03627 \text{ Hz/kW}$

where $f = 50 \text{ Hz}$, $Pr = 75 \text{ kW}$ and Droop $R = 5.44\%$

Then p.u. values for $R = 0.03627 \times P_D = 2.72 \text{ Hz/p.u. kW}$

Then from the equation 8.8;

$$\beta = R + \left(\frac{1}{R_{(pu)}}\right) \text{ and } \Delta f_s = - \left(\frac{Droop}{\beta}\right)$$

Frequency response coefficient value;

$$\beta = \left[R + \frac{1}{2.72}\right] = 0.4039 \text{ p.u. kW/Hz}$$

where $R = 0.03627 \text{ Hz/kW}$ and $R_{(pu)} = 2.72 \text{ Hz/p.u. kW}$

This is the frequency response coefficient value which is given in p.u. kW/Hz

Then from the corresponding equation $\Delta f_s = - \left(\frac{\Delta P_D}{\beta}\right)$

Change in frequency $\Delta f_s = - \left(\frac{Droop}{\beta}\right) = -0.0495 \text{ Hz}$

where Droop = 0.02 and $\beta = 0.4039$

Now the frequency of the system can be obtained as follows;

$$f_s = f_0 + \Delta f_s \quad 8.9$$

Therefore, using mathematical equations, the system frequency value at the peak demand hours,

$$f_s = 49.95 \text{ Hz}$$

8.6.1.2 Generator frequency at low power demand (40 kW power supply)

In relation to changes in load demand at a minimum value power supply, the changes in frequency response coefficient (β) need to be analysed for the turbine-generator system.

using equation 8.8.

In this case the actual damping D value = $\frac{(P_D)}{f_0} = 0.8 \text{ kW/Hz}$

where $P_D = 40 \text{ kW}$ and $f_0 = 50 \text{ Hz}$

When considering D value in p.u. = $\frac{\text{Actual value (D value)}}{\text{Min. power (Pmin)}} = 0.02 \text{ p.u. kW/Hz}$

where Droop value = 0.8 kW/Hz and $P_{\max} = 40 \text{ kW}$

Then, the value of $R = \text{Droop } R \times \frac{f}{Pr} = \frac{R}{100} \times \frac{f}{Pr} = 0.068 \text{ Hz/kW}$

where $f = 50 \text{ Hz}$, $Pr = 40 \text{ kW}$ and Droop $R = 5.44\%$

Thus p.u. values for $R = 0.068 \times 40 = 2.72 \text{ Hz/p.u. kW}$

Then the frequency response coefficient value can be obtained as follows;

$$\beta = [R + \frac{1}{2.72}] = 0.4356 \text{ p.u. kW/Hz}$$

where $R = 0.068 \text{ Hz/kW}$ and $R_{(pu)} = 2.72 \text{ Hz/p.u. kW}$

This is the frequency response coefficient value which is given in p.u. kW/Hz

Then from the equation $\Delta f_s = - (\frac{\text{Droop}}{\beta}) = - 0.0459 \text{ Hz}$

where Droop = 0.02 and $\beta = 0.4356$

Then the frequency of the system using equation 8.9 gives

$$f_s = 50.05 \text{ Hz}$$

which gives the system frequency value at off-pick demand hours.

So, based on mathematical calculations, the changes in frequency $\Delta f(s)$ are -0.03736 Hz during peak load demand and $+0.0459 \text{ Hz}$ during low demand respectively which led to the system frequency to drop to 49.95 Hz and frequency increase to 50.05 Hz which is equivalent to 0.1% frequency droop and does not reflect the actual frequency droop. But in comparison with the simulation generator frequency values it shows some differences on which the frequency has increased up to 52.72 Hz (max) during the low demand hours and reduced to 49.89 Hz (min) during the high demand hours which is equivalent to a frequency droop of 5.44% as shown on Figure 8.26 below. The difference in values between the calculated frequency using formula and the simulated frequency value is that the simulation values have been obtained based on dynamic system condition while the use of mathematical formula only implies static system condition.

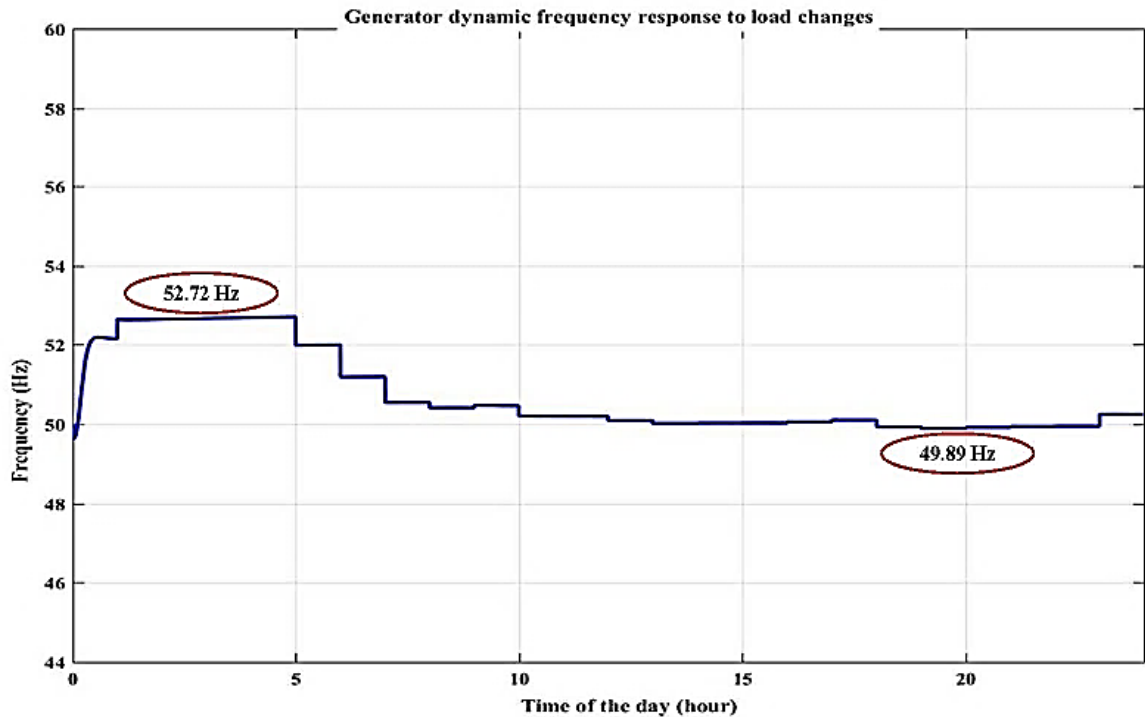


Figure 8.26: Dynamic values of generator frequency during a typical day

The dynamic simulation results also obtained the following values for the generator dumping coefficient $K_D = 12.6$ as compared to the static simulation value of $K_D = 0.045$ which is a very small value. The reasons for low dumping coefficient value for the static condition is that the power value used in the simulation is set to the maximum value, as a result, the dumping coefficient is reduced.

The other simulation aspects that have been looked at, is the hydro turbine system loading conditions on which both static and dynamic loading have been studied. The static condition has been based on the constant load conditions and in this case three load conditions have been analysed which are at full load, 53.3% load and no-load condition. The initial simulations result for the static loading was based on the rated values for the hydro turbine on which the flow discharge of $0.45 \text{ m}^3/\text{s}$ was allowed to pass through the gate valve to produce a mechanical power of 79.5 kW which drives the generator to produce a power output of 75.5 kW. In this scenario, the load power is matched with the generator output power and the results show close values for the design and simulated values. This is the maximum power that can be supplied by the micro-hydro turbine-generator system. During this phase, almost all the available power production is used to supply to the consumer load, so there is very minimal power available as dumping which is around 0.438 kW and this amount is only used to supply the auxiliary turbine components. Because most

micro hydro turbine operates close to the consumer load demand values, therefore no much power is lost which is shown by the results from the present study in Table 8.3 below.

Table 8.3: Static simulations results at rated capacity/Full load condition

Full rated capacity				Remarks
Turbine = 79.5 kW		Generator = 75.5 kW		
Head	24.94 m	Frequency, f	50 Hz	Supplying auxiliary power
Friction head, ΔH	0.01894 m	Speed	1500 RPM	
Flow discharge, Q	0.450 m ³ /s	Generator Power, P_e	75.44 kW	
No load flow discharge, Q_{nl}	0.00460 m ³ /s	Load Power	75 kW	
Turbine Power, P_m	79.41 kW	Damping Power	438 W	
Turbine damping coeff., K_D	0.00110	Generator damping coeff., K_D	0.045	

Note: Simulation time: 1 second

On the other hand, when reducing the amount of water flow through the gate valve it affects the stability of the system due to changes in power output and this reduces the available power significantly. One scenario is when supplying 53.3% of the rated power capacity and this is specifically during the low demand hours. In this case, the water flow has been reduced to 0.24 m³/s which gives the turbine power value of 42.36 kW and generator power output of 40 kW. To maintain the load power demand at this value the results shows that the auxiliary power value has reduced to 0.245 kW (reduced by 43.97%) which is valid due to power reduction as shown on Table 8.4 below.

Table 8.4: Static simulations results at rated capacity/Full load condition

53.3% Rated capacity				Remarks
Turbine = 42 kW		Generator = 40 kW		
Head	25 m	Frequency, f	50 Hz	Supplying auxiliary power
Friction head, ΔH	0.01894 m	Speed	1500 RPM	
Flow discharge, Q	0.240 m ³ /s	Generator Power, P_e	40.25 kW	
No load flow discharge, Q_{nl}	0.00420 m ³ /s	Load Power (53.33% Load)	40 kW	
Turbine Power, P_m	42.36 kW	Damping Power	245.4 W	
Turbine damping coeff., K_D	0.00205	Generator damping coeff., K_D	0.045	

Note: Simulation time: 1 second

In order to maintain the required water flow discharge and also power output from the generator system, the turbine system uses control governor to regulate the amount of water flow discharge through the penstock pipe into the turbine by using gate valve. In this research study, four types of control governors have been simulated and analysed based on their stability response time. The studied governors include mechanical control governor, *PID* control governor, *PDF* control governor and load control governor. The first three governors use control gain to correct the error signal from the process plant and from the simulation results, the mechanical governor seems to have a very slow response time with a gain of 4.5. These types of control governor systems use mostly mechanical components thus why they are slow to respond and hence are not widely used in today's hydro turbine control technology. On the other hand, both *PID* control governor (for this research study *PD* controller) and *PDF* control governor shows some similarities in terms of the gain value of 1.588 with a derivative factor of 0.008. But in terms of p.u. value response time, *PID* controller outperforms the *PDF* controller and the mechanical governor with less stability response time below 1.25 seconds as compared to *PDF* controller which is at 2 seconds and mechanical governor above 3 seconds. The general performance of a *PID* controller in terms of quick response time has recently increased their industrial application in terms controller choice, specifically in hydro turbine systems and for this reason, the *PID* controller is the choice for the present research study of Hhaynu micro hydro-turbine system [199].

The other consideration in the power supply and demand optimization is when the available power output from the generator is not supplied to any load demand and this may be during the local grid disconnect or breakdown. In this case, the available power output is not consumed or supplied to the load, hence it will be dumped. Due to the availability of unused power output from the generator, the results show that this effect will cause the generator speed and frequency to increase by 5.44% which creates system stability problems as noticed on the change in pressure head value (-ve value) and this is due to the droop characteristics of the hydro turbine generator system for the speed and frequency values as shown on Table 8.5 below for the no load condition.

Table 8.5: Static simulations results at no load condition

No load condition				Remarks
Turbine = 79.5 kW		Generator = 75.5 kW		
Head	25.17 m	Frequency, f	52.72 Hz	Supplying auxiliary power
Friction head, ΔH	-0.1714 m	Speed	1582 RPM	
Flow discharge, Q	0.4457 m ³ /s	Generator Power, P_e	75.29 kW	
No load flow discharge, Q_{nl}	0.00460 m ³ /s	Load Power (No load)	450 W	
Turbine Power, P_m	79.24 kW	Dumping Power	74.84 kW	
Turbine dumping coeff., K_D	0.0010920	Generator damping coeff., K_D	2.030	

In the third scenarios for the static loading condition and power optimization is based on supplying constant power though out the day to the consumer load in order to maintain generator frequency at the optimum value of 50 Hz as it is shown on the results by varying the amount of water flow through the gate valve. In theory, this operation is comparing and matching the power supply and demand with constant power value (static condition), but in practical application in hydro turbine systems, this is not possible because the consumer load demand is always fluctuating throughout the day and cannot be in a constant value throughout the time.

So, due to the nature of the consumer load demand, the static simulation will not provide very correct simulation results, therefore there is a need to analyse the dynamic simulation whereby the actual hourly consumer load demand power in a day is used instead of only rated values for the load power. This kind of simulation represent the actual system dynamics by which every hour the load demand value changes and this represent the actual operation of a micro-hydro turbine-generator system. From the simulation results for the dynamic loading condition, the noticeable feature is the substantial increase in dumping power as compared to the static loading condition. This is because the consumer load demand has two phases, low power demand phase and high power demand phase on which during the low demand hours more power is available as excess (dumping power) because the hydro turbine system usually supplies a constant power value as shown on Table 8.6 below.

Table 8.6: Dynamic simulations results at rated capacity/Full load condition

Dynamic condition				Remarks
Turbine = 79.5 kW		Generator = 75.5 kW		
Head	25 m	Frequency, f	50 Hz	Supplying auxiliary power
Friction head, ΔH	0.019 m	Speed	1500 RPM	
Flow discharge, Q	0.4518 m ³ /s	Generator Power, P_e	75.0 kW	
No load flow discharge, Q_{nl}	0.00472 m ³ /s	Load Power (Dynamic)	Hourly	
Turbine Power, P_m	78.94 kW	Dumping Power	4.9 kW	
Turbine damping coeff., K_D	0.001105	Generator damping coeff., K_D	12.6	

Note: Simulation time: 24 seconds

In both static and dynamic loading conditions, it is also noted that the dumping power produced is related to the so called dumping coefficient on which at rated power values where by when the load power demand is high, the dumping coefficient is at the lowest and at no load condition, the dumping coefficient is high. This gives the relationship between the load demand power and dumping coefficient on which $P_L \propto \frac{1}{K_D}$, where K_D = dumping coefficient of the generator system

In dynamic loading condition, the simulation results show that the dumping coefficient is very high as compared to static loading condition and this implies that the loading power used is below rated capacity as compared to the static loading condition. Therefore, due to the nature of the simulation results for the dynamic loading condition, the load power demand was based on the daily total average load demand value of 70.1 kW while the hydro turbine-generator system can supply power at the rated value of 75.5 kW.

To highlight this effect, the relationship between the dumping coefficient and the load power demand have been simulated during the 24 hours period based on the actual load demand power (dynamic loading condition). The results confirm with the daily profile of the load power demand which shows that during low demand hours of the day (night hours), the dumping coefficient is at its highest while during the high demand and peak hours of the day (evening time), and the dumping coefficient is at its lowest value as shown on Figure 8.27 below.

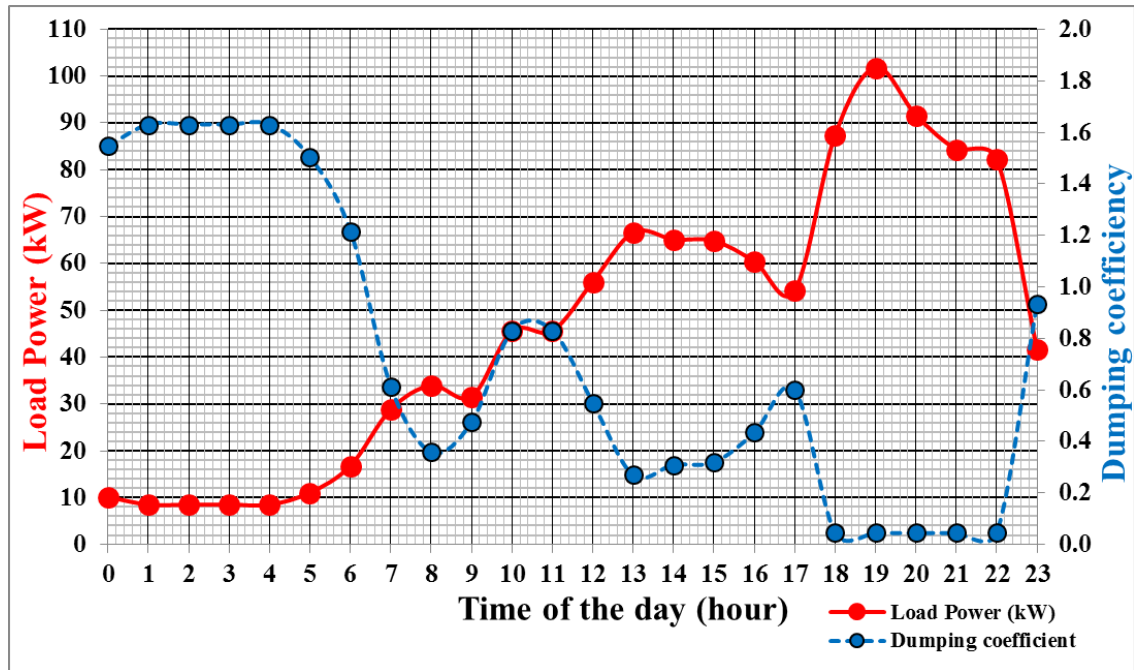


Figure 8.27: Response of dumping coefficient with load Power changes

Note: Dumping power (P_{Dump}) = Load Power (P_L) x Dumping coefficient (K_D)

In order to fully optimize the available power from the micro hydro turbine system for hydrogen production, the turbine system must be operated at its full capacity all the time. From the system design the rated capacity of the turbine-generator system is 75.5 kW but based on the simulation results this cannot be achievable due to the capacity shortage. So, based on this and in order to fully maximize the available power output, the use of simulation software have resulted to obtain an average power output from the turbine-generator system of 70.1 kW that must be supplied throughout the day in order to benefit with the max excess electricity production to supply to the electrolyser system. This resulted to the power supply from the micro-hydro turbine system being properly optimized to supply energy to the AC load demand and electrolyser system that produce hydrogen gas which is the fuel to power engine-generator system that supplies peak power as shown in Figure 8.28 below.

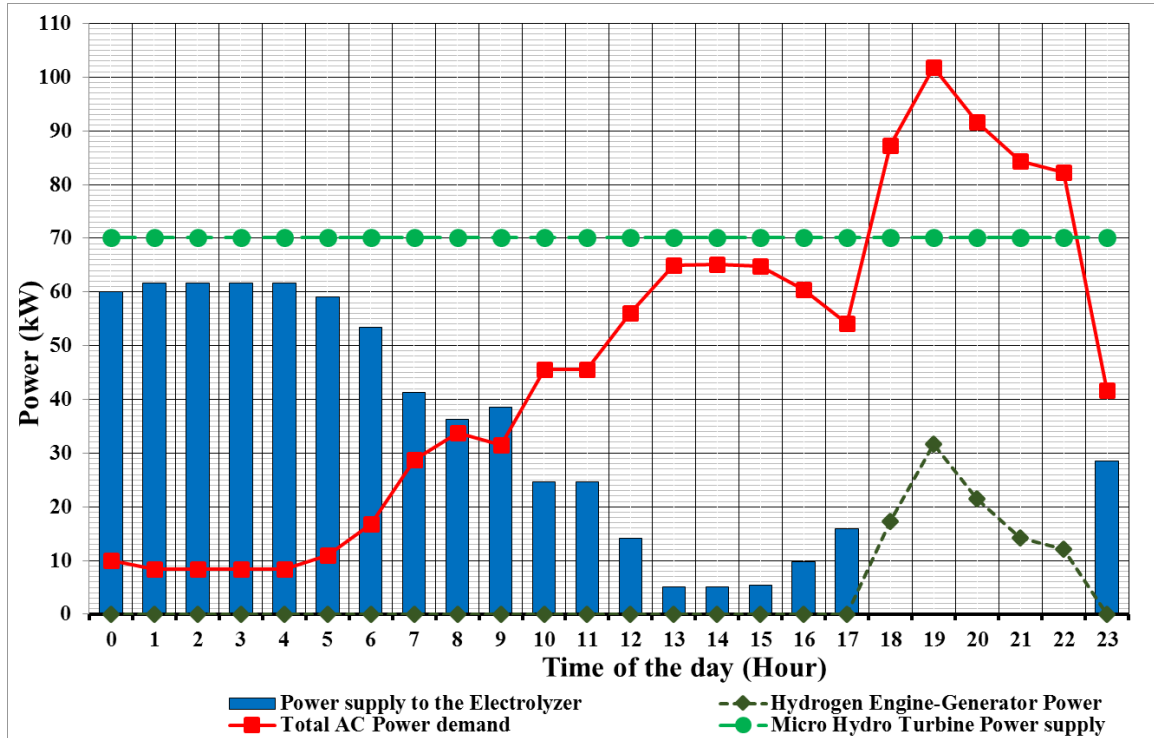


Figure 8.28: Optimized power supply and demand from micro-hydro and engine

From simulation results, it has also been noted that the generator frequency changes are only applied to a certain limit values of the generator speed drop and this is a special characteristic for most of the hydropower generator system that is related to speed/frequency changes and is called droop.

8.6.1.3 Generator Droop Characteristics

Using the obtained simulation values, droop can be calculated using the following formula:

$$\text{Droop} = \frac{\text{No load frequency} - \text{Full load frequency}}{\text{Full load rated frequency}} = 0.0544 \quad (8.10)$$

No load frequency = 52.72 Hz and Full load frequency = 50 Hz

Therefore, the speed droop = $0.0544 \times 100\% = 5.44\%$

This droop value is almost the same as the calculated droop value of R_2 which is 5.99% and from the literature, the normal recommended percentage range of droop value is between 3% to 5% and the theoretical commonly used droop value is 4% [200]

The interpretation of this this droop value is that, the drop of 5.44% is set at 100% load which is 75 kW Power capacity and this means that the droop governor will decrease or increase the frequency reference set point by 5.44% of the nominal value from no load condition to full/rated load condition as shown on Figure 8.29 below.

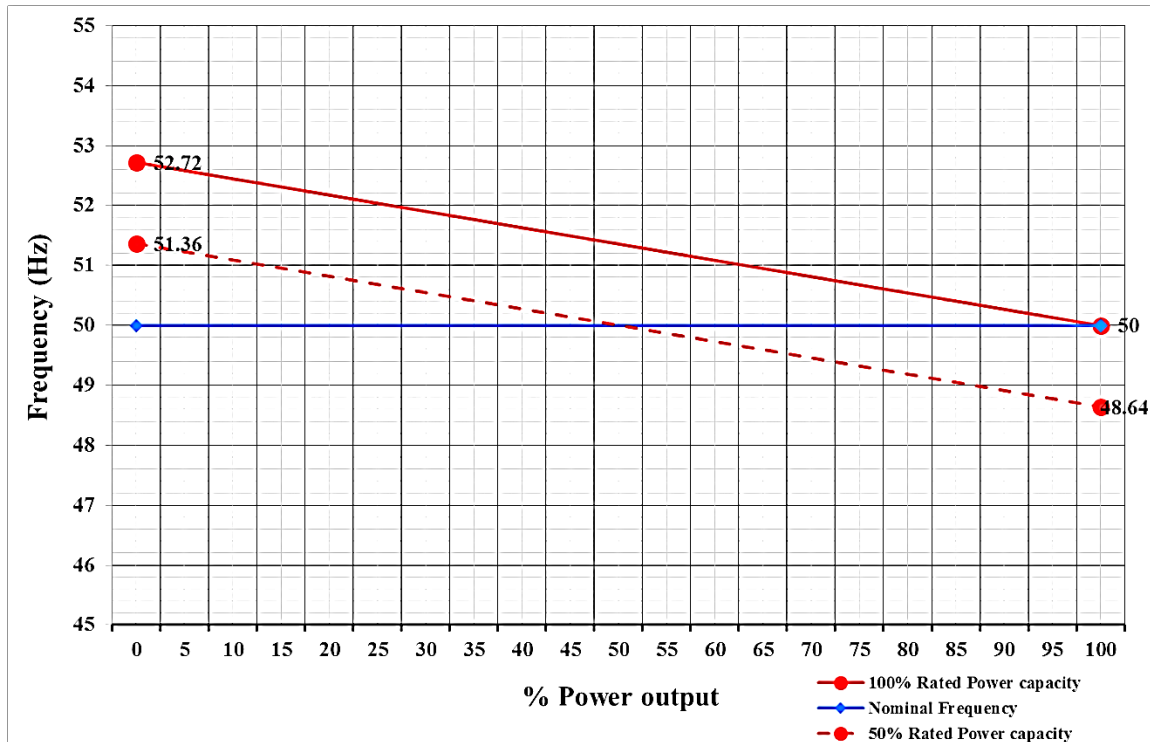


Figure 8.29: Simulated generator characteristic at 100% and 50% rated Power capacity with 5.44% speed droop

When the load power demand values changes, the droop line shift back and forth in order to maintain the required power output and also adjust the frequency back to 50Hz nominal value. In one scenario is when considering the turbine-generator system supplying low power output of 40kW, the appropriate droop is given as follows:

- (a) For droop of 5.44% at 100% load with 75kW rated power capacity
- (b) The percentage of Power output is given as: $\frac{40\text{kW}}{75\text{kW}} = 53.33\%$
- (c) So, with the same droop value for 40kW rated power capacity, the percentage of power output is equivalent to 53.33% of the rated power

The application of speed droop in the generator system is utilised when the turbine-generator system has been operated to a fully capacity and the system frequency value dropped from the nominal value which resulting in the system become unstable and in this case it is recommended to reduce the percentage power output of the turbine-generator system through droop value to the safe operating range and in most condition the range between 100% to 50% power output is mostly recommended range for use in micro hydro turbine system. On the other hand, if this is not possible due to the type of load to be supplied, then the turbine-generator system must be integrated with another energy source or include an energy storage system that will supply the excess energy demand in order to stabilise the system generator frequency to nominal value.

8.6.2 Electrolyser system

The electrolyser system will have a rated capacity of 70 kW with the average input power capacity of 33.53 kW. Maximum power consumption for the electrolyser is during the low demand hours of the day which is in the midnight hours. This is the time when most of the excess electricity is produced from the micro-hydro turbine due to the low availability of demand power. During the peak hours of the day less excess electricity is available, hence the electrolyser is supplied with less electricity of up to 9.16 kW as minimum power value. The system operates when excess electricity is available and on average the electrolyser can operate at 19 hours per day which gives yearly hours of operation to be 6,935 hours/year. Based on the average input power and hours of operation, the electrolyser will also consume an equivalent of 243,385 kWh/y as total input energy which is 37% of the total annual energy consumption. It is also noted that the electrolyser system consumes electricity in order to produce hydrogen gas, so the main electrolyser output is the amount of hydrogen produced at a specified period of time. Based on the simulation results, the electrolyser system can produce hydrogen gas to a maximum value of 0.938 kg/hr with the average value of 0.423 kg/hr which gives the daily average value of 10.15 kg/d and the annual total production of 3,702 kg/year.

The amount of daily hydrogen production is first stored in a pressurised hydrogen tank which has a storage capacity of 30 kg and is equivalent to the energy storage capacity of 1,000kWh. In terms of average hydrogen content inside the tanks, the amount at the beginning of the year (January) is 15kg (50%) while at the end of the year (December) the average content increased to 19.3kg (38.6%) which gives the tank autonomy of 19 hours. In terms of tank level with the frequency of occurrence, it is noted that the full capacity hydrogen tank level has not been reached. The maximum tank level capacity that hydrogen could reach is around 27kg (90%) capacity which occurs at only 1% of the time while the minimum tank level is at around 15kg (50%) which occurs at the very minimum level of only 0.5% that gives the tank level range of 12kg. On the other hand, the highest occurrences of tank level capacity are at 23kg which occurs at 15.4% of the time.

In this system design, the produced and stored hydrogen gas is mainly used in two main ways. The first main use is to power the engine-generator system that is used to supply electricity during the peak hours of the day and this accounts for 56.02% of the total hydrogen production. The remaining excess hydrogen that is available which amount to 1,628 kg/year (43.98% of the total hydrogen production) is used as a raw material for the

local oil and fertilizer industries. In addition to hydrogen as a raw material for the local industries, the electrolyser system also produces oxygen at the rate of 0.469 kg/h as the maximum value and 0.212 kg/h as mean output which gives the total oxygen production of 1,851 kg/year. The produced oxygen from the electrolyser system is sold at a reduced price to the local health centre as a contribution to the health care support and also some other amount will be supplied to the local science secondary schools to be used in science laboratories. The contribution of supplying locally manufactured hydrogen gas to the industries and also oxygen to the health centres and schools have added the value of this project to the local community which made the project viable and sustainable.

8.7 Summary

The power output and system stability from the micro-hydro turbine system is influenced by the gate valve position. The function of the gate valve is to allow water to flow through the penstock pipe to the turbine and the simulation results shows that when the gate valve is initially opened, the system becomes unstable due to its transient state. The initial water flow through the penstock pipe causes pressure changes which affect the power output at the initial stage. The initial pressure signal becomes high at full gate valve opening which caused the system to be unstable for the water flow discharge and also power output. This phenomenon is also related to the so called water starting time (T_w) in micro-hydro turbine system which is the time required for the water to flow through the penstock pipe to reach to the turbine unit on which in this system design it is 1.79 seconds.

In comparing to stability studies during the transient stage, it is noted that the micro-hydropower system takes longer time to stabilise under the influence of gate valve position G_v of around 6 seconds as compared to other signal values of flow discharge Q , pressure head ΔH and power signal P_m which took around 0.7 seconds. This effect is due to the long penstock pipe for the Hhaynu micro-hydropower plant. In conclusion is noted that the biggest influence of turbine stability in micro-hydropower system is the changes in the gate valve position, G_v .

Chapter 9 Conclusions and Recommendations for further work

9.1 Introduction

Many rural villages in Tanzania are not connected to the national grid because of low population density and also no proper access roads to these areas which makes grid connection projects un-economical. This made the local communities to be isolated from the rest of the neighbouring villages with access to electricity. As a result, most of the people in these areas became poor and less developed due to limited economic activities. In comparison to other developed nearby villages in the region, it has been noted that there are some key elements that trigger and facilitate the rapid growth and development of those local communities. One of the main elements that has been found to speed up this local community development and improve people's life is the introduction of electricity in the local villages. Rural electrification has a huge impact on village development by increasing economic activities and reduces poverty in those areas, thus why my research study has been focusing on this area of study that is related to rural electrification.

There are many rural electrification technologies that could be applicable to off-grid villages, but due to the nature of low population density in many villages in Tanzania, small scale and specifically at micro level energy technologies have proven to be suitable for village electrification. This is because the energy supply systems at the micro-scale can be easily adapted to the local rural settings, have no effects to the environments and also can be installed at the fraction of the cost which makes them more economical and sustainable. In areas where water resources from small rivers are available, micro-hydropower technology can be developed to supply the required electricity demand to the local villages. This is evidenced by Kwermusl village in Mbulu district, northern Tanzania on which there is no grid-connection but in the local area there is a small river called Hhaynu which have been proven to provide the required water volumetric flow to develop a micro hydropower plant in the area and this idea has been the main focus of this research study.

9.2 Summary of the findings and the resulting conclusions

In order to execute this concept and implement the idea, this research study has been conducted with the aim of designing and developing a community based micro-hydro turbine system to supply electricity to off-grid villages in Mbulu – Tanzania. The local villages in the study area will be used as a case study on which all site information will be

obtained. To achieve this aim of designing and developing the micro-hydro turbine system in the area, three main objectives have been formulated as follows:

- To assess and gather site information and river volumetric flow in order to obtain the design data
- To design and develop a micro-hydro turbine system with increased energy utilization and minimum energy losses using an integrated energy storage system
- To analyse the project costs for the designed micro-hydro turbine system in order to determine the economic and environmental feasibility of the system

The above three objectives form the basis of doing this research study and on the implementation of the first objective, detailed field work and site measurements have been conducted in the case study area to determine the required site information. Among the data that has been analysed in the area are river hydrology and water flow volume, site elevation, energy potential and demand assessment.

Because of the availability of Hhaynu river in the local area, the field work and site measurements results show that there is an availability of water flow from the local river which is proven to develop a micro-hydro turbine system. This was done by two different water flow velocity measurements methods of the floating method (use the floating object) and current meter method (use the instruments). Both methods produce very close values despite the fact that the current meter velocity measurement method claimed to be the accurate method and this outcome answers one of the research questions.

Based on the river flow velocity and cross-section area measurements, the results from the hydrological analysis have shown that the river has an average flow rate of $0.9 \text{ m}^3/\text{s}$ on which during the dry months of the year the river flow dropped to $0.6 \text{ m}^3/\text{s}$ as the minimum value. Therefore, to make use of the available water flow throughout the year and also consider the environment flow with water provisional for irrigation due to farming activities in the area, the results from the flow duration curve (FDC) gives the value of the water flow discharge that can be supplied to the turbine throughout the year to be $0.45 \text{ m}^3/\text{s}$ which is about 50% of the average river volumetric flow. This is based on the type of scheme called run-of-river that takes water directly from the river through an intake weir, canals and penstock to the turbine unit. But, due to food shortages in recent years, most of the local farmers in the area have introduced the new concept of irrigation farming along the river banks and nearby farms. In many parts of the country where water resources are available, this new concept of small-scale irrigation farming has brought some conflicts on

water use priorities. Depending on the economic activities of the area, it is noted that in some areas people prefer water usage for farming rather than hydro power production. Also, in recent years in Tanzania, small towns and villages population have increased which lead to an increased demand in water supply which resulted to the development of new water supply projects that consume a significant volume of water from local rivers hence reduce significantly the river flow volume for micro-hydropower development. So, in order to accommodate the current irrigation farming activities with environmental flow and also avoid the water usage crises in the near future, the use of 50% of the available water flow volume ($0.45 \text{ m}^3/\text{s}$) as a flow discharge for the Hhaynu micro-hydro turbine will sustain the water capacity to the turbine for long period of time. Studies have shown that many small-scale hydropower plants in Tanzania have reduced their power production due to the reduction in water flow volume from rivers which led to grid instability and load shading. Using the case study site measured water flow discharge of $0.45 \text{ m}^3/\text{s}$ and also measured site elevation of 25m as a site head value, the turbine power has been determined to be 79.5 kW using the turbine efficiency of 72%. There are several turbine technologies that can be used on a micro-scale but based on the turbine selection chart which use the design flow discharge and site head, the cross-flow turbine technology fits all aspects of the design and has been selected for this research study. Cross flow turbines have a wider application of head and flow discharge and have been used in Asians countries in micro-scale application for many years in supplying electricity to rural and off-grid areas. Its technology is robust and can be installed locally in the village settings with the local experts hence reduce the project costs on materials and labours (no need for experts).

Most of the cross-flow turbines are connected to the electrical generator by the pulley and belts on which the turbine (mechanical) power is transferred to electrical power. Based on the above turbine mechanical power value, the constant power output produced by the generator system is 75.5 kW with the generator efficiency of 95%. On the other hand, when looking into the in hydropower class for this power output range, it falls under micro-hydropower scale which ranges from 5 kW to 100 kW and can supply electricity from few houses to more than 100 houses in the local village area.

In terms of energy potential the designed micro-hydro turbine system in the case study area is able to produce a maximum of 1,812 kWh/day of renewable and sustainable energy and based on the assessment of the consumer load demand in the area, the daily average energy demand is around 1,114.38 kWh/day which is based on the following categories, 778.78

kWh/day for the domestic use, 257.80 kWh/day for the productive use and 77.80 kWh/day social infrastructure. In the domestic use, 234 households will be provided by the electricity for lighting and power at an average value of 140 Watt (maximum 500 W) per household on standardised tariffs of 4 cents per kWh. This power capacity that is supplied to the households will be quite enough for most the households because, during the initial energy demand analysis, few houses own few number of electrical equipment's which can be accommodated by the supplied power capacity and this outcome answers one of the research questions. But, based on studies from other parts the country, the introduction of electricity in the households will significantly increase the economic activities of the people which in turn more standard electrical equipment's will be own by families and hence this will lead to an increase in the consumer load demand in the near future which will need to be considered.

In terms of energy demand per household per day, the results show that each household will consume an average of 3.3 kWh/day which is much lower compared to the UK at an average of 12.6 kWh/day (almost 4 times higher) while the global average is around 9.6 kWh/day. Most of the developed countries like the UK have higher household energy consumption and this is because of almost 100% of the houses have electricity and also the family size is limited to few people as compared to less developed countries like Tanzania on which the national electrification rate is less than 40% (mostly in urban areas) and also an average household size of at least 5 people.

In the productive energy demand category, shops and small businesses together with the village offices, schools and health centres for the social infrastructure will be supplied with electricity on a commercial basis at the rate of 5 cents per kWh and this will create an income to the project revenues and hence make the project sustainable. When looking on the daily load demand profile, it is noted that there are two power demand phases on a day, low power demand hours and high power demand hours. During most times of the day hours, the power demand is relatively high with peak demand during the evening hours from 18:00 hours to 22:00 hours on which the maximum load power demand is 101.8 kW at around 19:00 hours. The changes in power demand during most time of the day is caused by the nature of the activities in the area whereby most people in the households go for farming and grazing animals during hours of the day and return home during the evening hours when they start using electrical equipment and switch on lights. On the other hand, the low demand hours of the day are observed during the late-night hours on which the load

demand dropped to around 8.42 kW. This very low demand power at this time of the day is because most of the electrical equipment in the households are switched off and the majority of the people have gone to sleep.

From the energy potential calculation results, the micro-hydro turbine system will produce a constant power output of 75.5 kW throughout the day but based on the energy supply and energy demand analysis, the micro-hydro turbine power capacity will not provide enough power during the peak hours of the day while during the low demand hours, more power is produced than it can be consumed. This situation causes un-balancing between the power supply and load demand, as a result, five hours power deficit is observed during the peak hours of the day and excess power during the low demand hours of the day. In order to overcome this effect, the option of energy storage has been considered because the excess power production have reached up to 60 kW during the low demand hours. In order to reduce this effect of excess power, two power supply phases have initially been implemented. In this initial setup, a 40 kW power supply capacity (53% of rated capacity) have been used during the low demand hours and full rated power capacity with the stored energy during the high demand and peak hours. In this setup, the produced excess electricity is not constant and in some hours of the peak demand phase it reduced to zero which resulted to the reduction in the amount of stored power.

The turbine-generator system operational conditions have been simulated in order to show the performance and stability characteristics under difference loading condition. The simulation results show that in the generator static loading condition with a full load, the generator dumping coefficient, K_D is at its lowest value close to zero ($K_D = 0.045$) while during static no load condition, the generator dumping coefficient increased to a maximum value ($K_D = 2.030$). The changes in the generator dumping coefficient during static loading from a minimum value at full load condition to a maximum value at no load condition is related to the load power demand value in such a way that the generator dumping coefficient is inversely proportional to the load power, i.e. $K_D \propto \frac{1}{P_L}$. But in the actual operation of a micro-hydro turbine systems, the generators are operated under dynamic conditions ON which the load demand power changes every hour. So, when applying this kind of condition to the generator system, the simulations results shows that the dumping coefficient is much higher than in static loading conditions, i.e. $K_D = 12.6$. The reason for this increased K_D value is that, in dynamic loading condition the total hourly load demand

power has been estimated based on the optimized average power supply value of 70.1 kW which is lower than the rated capacity.

From the system design and simulation results for power supply and demand values, it is noted that there is a power deficit of five hours each day. In order to supply this power deficit during the peak hours of the day, an energy storage system has been considered integrated with the micro-hydro turbine system. Several energy storage options have been studied and analysed in this research project which includes, micro-hydro turbine with battery energy storage and micro-hydro turbine with hydrogen storage. In all these energy storage options, the available excess electricity is stored in a form of chemical energy for the battery or hydrogen gas for the hydrogen system respectively. When evaluating the above storage options in terms of storage capacity, conversion efficiency, response time and energy content, the hydrogen energy storage system outperform the other option of battery storage despite its lowest usage in today's small scale energy storage technologies and based on these advantages it has been selected as a means of energy storage in this research study.

In order to produce the hydrogen energy storage with the micro-hydro turbine system, the excess electricity produced is supplied to an electrolyser system of 70 kW capacity which produce hydrogen gas at an average rate of 10.15 Kg per day and oxygen gas at an average rate of 5.08 Kg per day. The produced hydrogen gas of about 56.02% is used as fuel gas to power the 40kW hydrogen internal combustion engine-generator (H₂ - ICE) which produces electricity to supply the required power deficit during the peak hours of the day. The remaining 43.98% of the produced hydrogen gas is sold to the local oil and fertilizer industries for the production of fertilizer and oil products. On the other hand, the produced oxygen gas is supplied to the local health centre to save lives and also to the local secondary school's laboratories for supporting scientific experiments.

System design has shown that, in order to fully maximize the hydrogen gas production to run the hydrogen engine-generator system to produce the required 35% additional power required during the peak hours of the day, the micro-hydro turbine system has to produce the maximum excess electricity possible, so in this case, it should be operated close to its rated capacity. Also, results from the simulation and power optimization shows that the micro-hydro turbine needs to be operated at an average power capacity of 70.1 kW (92.9% capacity factor). This will produce enough excess electricity to power a 70 kW electrolyser system and also additional power to supply to other auxilliary renewable energy systems.

In terms of investments cost, the designed and developed micro-hydro turbine system has one of the least costs of energy for rural and off-grid electrification. The results from the economic analysis and environmental study which is based on material and labour cost as well as energy saving and pollution reduction show that the cost of an investment for the project is very low at 1,656.67 £/kW for the 75.5 kW installed power capacity. It is also noted that the cost is below the standard value for the most similar power capacity micro-hydropower project investment cost. The reason for this is that there is no fuel involved in the system design, so revenues are obtained from selling electricity to the consumers and also additional revenue is obtained from selling hydrogen and oxygen gas and this increased the benefit to cost ratio of the project to 1.31 which answers one of the research questions. So, based on the research study results, it is now clear that the final optimized system design for this project work is comprised of a micro-hydro turbine system which will supply the required base power, the electrolyser system which produces hydrogen and oxygen gas and hydrogen engine-generator system which supplies power deficit to the load demand. The designed micro-hydro turbine system optimization has increased energy utilization and minimizing energy losses which makes it different from other micro-hydro systems and satisfies the project objectives by answering all the research questions.

The general outcome of this research study and the developed project is that the availability of electricity in rural and off-grid area of Tanzania have shown a significance improvement in people's life in terms of improvement in local schools academic performance due to the increased study hours, improvement in the local health services, introduction of small business and agro-processing industries which have raised the incomes of the people and hence resulted to a significant poverty reduction in the village communities.

9.3 Recommendations for further work

In doing this research work and according to the research objectives there are few recommendations that are worth mention on which some of them are related to the current work and some for the future work as follows:

- (a) The first thing is related to the development of community projects like micro-hydro in rural areas. Experience has shown that many small electrification projects have failed to continue operating because of the lack of integrating the local economic activities with the project development and also involving the local community. To

reduce this drawback and make the rural projects sustainable, it is recommended to involve the local people during all phases of the project execution.

- (b) During the initial feasibility study of most hydropower projects development, there is an involvement of a large number of data sets for the river hydrology and site information. But some of these data may be inaccurate or missing, which may lead to the incorrect design of system parameters. In order to avoid this when developing a micro-hydropower project, it is recommended to do a pilot study with sample data sets and form the basis for the system design.
- (c) When doing field work and site measurements for the river flow velocity measurement with limited resources, a simple and yet accurate means of river flow measurement called the floating method can be used
- (d) In micro-hydropower system design and development, there is a need to do modelling and simulation in order to obtain system performance characteristics. In most system design, static simulation is conducted which does not reflect the actual operational characteristics of micro-hydropower systems. So, in order to obtain the true performance characteristics values for the micro-hydropower system, there is a need to do more dynamic simulations in order to reflect the turbine and generators performance due to load demand changes or load rejection.
- (e) The introduction of the hydrogen engine-generator on the system maintains the renewable energy fraction due to the zero emission of pollutants from the engine. But due to the available high temperature from the engine exhaust system, an additional system like an absorption chiller (absorption refrigeration) could be added on the engine system to increase energy efficiency.
- (f) The initial investment costs for a micro-hydropower projects seems to be high for most private investors to afford and also these small projects do not attract support from the local governments. So, in order to reduce this and acquire the required financial support for the implementation of micro-hydropower projects, it is recommended to use the private-public partnership (PPP) model for the projects funding support and execution.

9.4 Contributions to the knowledge

In rural electrification projects, the micro-hydro turbine systems are one of the technologies that are suitable to supply electricity to the off-grid areas where water resources are

available. The design configuration of micro-hydro turbine systems consists of a water intake system, turbine system and generator system. The power of the water drives the turbine to produce mechanical power that drive the generator to produce electrical power that is supplied to the load demand. In off-grid areas where the population density is low, the load demand power is changing most times of the day. Using the results from the present research study, it is noted that load demand power is high during peak hours and low during off-peak hours. This phenomeno produces excess electricity especially during low demand hours due to the condition that power from the micro-hydro is always supplied at a constant value. It is also noted that on each day there is a load power deficit of around 5 hours which have to be supplied from other energy sources. From literature, a number of publications have described the designs of a number of micro-hydro turbine system to include a dump loads or battery energy storage system to make use of the excess electricity produced from the micro-hydro turbine. In this case, the battery energy storage stores excess electricity in order to supply to the the peak hours load demand power deficit while the dump loads consume all the excess electricity as ballast loads (air or water heaters). In the current system design, the peak load demand hours (power deficit) is supplied by the diesel electrical generators that run together with the micro-hydro turbine.

The reasons as to why most micro-hydro turbines are installed with the diesel electrical generator or battery energy storage that is integrated with dump loads and this is because of the local availability of the lead acid batteries and diesel fuel and air/water heating elements in the rural areas which resulted to the reduction in project initial investments costs which attracts most of the local project investors. But studies from this research revealed that the use of diesel electrical generators or battery energy storage and dump loads in a micro-hydro turbine system can be replaced. This is because these systems don't add value to the so called "green integrated micro-hydro turbine system" on which the battery energy storage system has limitations on storage capacity, conversion efficient and limited energy content hence need more space (bulk) while the diesel generator system pollute the environment by producing toxic exhaust gases and the dump loads system waste power as thermal loads to the ballast which could be used to supply power to the other renewable energy systems.

In order to bridge this gap with the existing micro-hydro turbine system design, new knowledge on energy storage technologies need to be studied. This is demonstrated in this research project by using hydrogen storage. The available excess electricity instead of

stored it into the batteries or send it to the dump ballast loads, it is used to power the electrolyser system that produces hydrogen gas which is stored as energy. This new energy utilization concept has proven to increase energy storage capacity by eliminating 68.37% of excess energy to the dump load and also increase excess energy storage from 31.63% for the battery system to 100% for the electrolyser system. In this case, during the daily peak hours and power deficit, instead of using battery energy storage or diesel electrical generator to supply the required electricity, a hydrogen fuel engine-generator system is used. Hydrogen has proven to have more energy content than most of the fuels and also when supplied to an engine (gas engine) does not produce pollution when operating and hence the hydrogen energy storage is the energy storage technology for the future especially at the micro scale.

References

1. IEA, I.E.A., *IEA energy statistics, electricity generation by fuel in Tanzania*. 2017.
2. TANESCO, *Tanzania Electric Supply Company*. 2018.
3. URT, U.R.o.T., Ministry of Energy and Minerals:, *Energy Sector (Tanzania, 2016)*. 2016.
4. Bank, T.W., *World Bank National Accounts Data: Country Profile - Tanzania, 2018*. 2018.
5. C. Kaunda, C.K., T. Nielsen, *Potential of small-scale hydropower for electricity generation in Sub-Saharan Africa, A Review article*. *Renewable Energy*, 2012. 132606 ((2012b)).
6. ADB, A.D.B., *Renewable Energy in Africa: Tanzania country profile (Ivory Coast, 2015)*. 2015.
7. URT, U.R.o.T., Ministry of Energy and Minerals, *Power System Master Plan. 2016 Update (Dar Es Salaam, Tanzania, 2016)*. 2016.
8. Chiyembekezo S. Kaunda, C.Z.K., and Torbjorn K. Nielsen, *Hydropower in the Context of Sustainable Energy Supply: A Review of Technologies and Challenges*. *Renewable Energy*, 2012. vol. 2012 (Article ID 730631).
9. C.S. Kaunda, C.Z.K., T.K. Nielsen, *A technical discussion on micro-hydropower technology and its turbines*. *Renewable and Sustainable Energy Review* 2014. 35: p. 445–459
10. O. J. Mdee, T.K.N., Cuthbert Z. K. and J. Kihedu, *A review article on Assessment of hydropower resources in Tanzania*. *Renewable Energy and Environmental Sustainability* 2018. 3(4).
11. K. Kabaka, F.G.o., *Challenges in Small hydropower in Tanzania, renewable energy perspective*. International Conference on Small Hydropower, 2007: p. pp. 22-24.
12. GIZ, D.G.f.I.Z., *Tanzania's Small – Hydro Energy Market, Target Market Analysis*. 2009.
13. C. S. Kaunda, C.Z.K.a.P.M.N., *The Development of Micro Hydro for Rural Energy Supply in Tanzania*. *International Journal on Hydropower and Dams* 6, 2012a. 19(No. 6): p. 60-67.
14. Chhetri, A.B., Pokharel, G. R., & Islam, M. R., *Sustainability of Micro-Hydrosystems – A Case Study*. *Energy & Environment*, 2009. 20(4): p. 567–585.
15. UNIDO-GEF, U.R.o.T., *Mini-grids Based on Small Hydropower Sources to Augment Rural Electrification in Tanzania* 2015: Vienna.
16. Canada, N.R., *Micro-hydropower systems: A buyer's guide. Cat. no. M144-29/2004E*. 2004.
17. Ayeng'o, S.a.N., P M, *Development of small hydropower plant in Tanzania: Challenges and Opportunities*. International Conference on Future Electrical Power and Energy Systems. *Lecture Notes in Information Technology*, 2012: p. 255-262.
18. Hans H, E.B., Wycliff J and Florian L, *Advanced Scoping for Technical Capacity Building on Small Hydropower in East Africa – Final Report*. 2015, Hydrophil.
19. Tanzania, T.U.R.o., *Ministry of Agriculture, Food Security and Cooperatives*. 2012.

20. Plas, P.M.a.R.J.v.d., *Innovative Private Micro-Hydro Power Development in Rwanda*. Energy Policy 2009. 37(11): p. 4753-4760.
21. Kusakana K, M.J.L.a.J.A., *Economic and Environmental analysis of micro hydropower system for rural power supply*. Proceedings of the 2nd IEEE Power and Energy Conference, 2008: p. 441-4.
22. Kusakana, K., *Survey of innovative technologies increasing the viability of micro-hydropower as a cost-effective rural electrification option in South Africa*. Renewable and Sustainable Energy Reviews 2014. Renewable and Sustainable Energy Reviews (37): p. 370-379.
23. H. Ahlborg, L.H., *Drivers and Barriers to rural electrification in Tanzania and Mozambique grid extension, off-grid and renewable energy technologies*. Renewable Energy, 2014. 2014(61): p. 117-124
24. IMF, I.M.F., *Poverty Reduction Strategy Paper for the United Republic of Tanzania*. 2006.
25. URT, U.R.o.T., *Ministry of Energy and Minerals - National Energy Policy*. 2015: Dar Es Salaam.
26. REA, R.E.A.T., *Annual Report 2013/2014*. 2014.
27. Michael, J.W.a.E.G., *Increasing sustainability of rural community electricity schemes, A Case study of small hydropower in Tanzania*, in *International Conference on Sustainable Energy and Technologies*. 2009: Aachen, Germany.
28. Kassana L., e.a., *Small-scale hydropower for rural development in Tanzania*. 2005.
29. Ramadhani Wakati, e.a., *Design and Fabrication of Cross Flow Turbine*. Nile Basin Capacity Building Network, 2010.
30. Koç, C., *A study on operation problems of hydropower plants integrated with irrigation schemes operated in Turkey*. International Journal of Green Energy, 2018. 15(2): p. 129-135.
31. P. Lemsomboona, T.P., K. Bhumkittipich, *Performance Study of Micro Hydro Turbine and PV for Electricity Generator, Case Study: Bunnasopit School, Nan Province, Thailand*. Energy Procedia, 2013. 34: p. 235-242.
32. Chiyembekezo S. Kaunda, C.Z.K., and Torbjorn K. Nielsen, *Potential of Small-Scale Hydropower for Electricity Generation in Sub-Saharan Africa*. Renewable Energy, 2012. 2012(ID 132606).
33. al, W.J.e., *Sustainability of rural community electricity schemes - Case study of small hydropower in Tanzania*. 2010.
34. V Kashore, D.J.a.N.G., *Rural Electrification Through Decentralised Off-grid Systems in Developing Countries*. 2013, London Springer-Verlag
35. Prakash, V.I.K.B.a.R., *Life Cycle Analysis of Run-of-River Small Hydro Power Plants in India*. The Open Renewable Energy Journal, 2008(1): p. 11-16.
36. S, W.D.a.G.R., *Instantaneous wind energy penetration in isolated electricity grid: Concepts and review*. Renewable Energy 2005. 30(8): p. 1299-308.
37. K, K.J., *Investigation of Greek wind energy market time-evolution* Energy Policy 2004(32): p. 865-79.

38. Shafiqur Rehman, L.M.A.-H.a.M.M.A., *Pumped hydro energy storage system, A Technology review*. Renewable and Sustainable Energy Reviews, 2015(44): p. 586 – 598.
39. Weblink1, *REN21-Renewable Energy Policy Network for the 21st Century*. 2013.
40. Omer, A.M., *Sustainable renewable energy resources, their development and applications*. Journal of African Studies and Development 2010(2.2): p. 035-057.
41. (2012c), I., *Energy Technology Perspective 2012*, OECD/IEA.
42. IHA, I.H.A. IHA: United Kingdom.
43. Ulgiati, M.T.B.a.S., *Understanding the global economic crises: A biophysical perspective*. Ecological modelling, 2011. 223(1): p. 4 - 13.
44. Manoj, K., *Overview of small hydro power development in Himalayan region*. 2006, Himalayan Small Hydropower Summit Dehradun.
45. NHA, N.H.A. USA.
46. Brown A, M.S.a.D.Z., *Renewable Energy – Markets and Prospects by Technology*. 2011, OECD/IEA: Paris.
47. Locker, H., *Environmental Issues and Management for Hydropower Peaking Operations*. 2004, United Nations, Department of Economic and Social Affairs UN-ESA.
48. Roth, E., *Why thermal power plants have relatively low efficiency*. Sustainable Energy for All (SEAL) Paper, 2005(February 2005).
49. Agency, I.E., *Renewable Energy Essentials: Hydropower*. 2010, International Energy Agency.
50. Dams, I.J.o.H.a., *World Hydropower Atlas & Industry Guide*. International Journal of Hydropower and Dams, 2010.
51. R, B., *Energy storage: A non-technical guide*. 2006, PennWell, Tulsa, OK.
52. Francis, T.a., *The Future of Large Dams: “Dealing with Social, Environmental, Institutional and Political Costs*. 2012.
53. Dams, I.C.o.L. ICOLD.
54. Cernea., M., *Hydropower dams and social impacts: A sociological perspective*, in *Social Development Papers*. 1997, World Bank Paper
55. S., M., *Behaviour and operation of pumped storage hydro plants*, in *PhD thesis*. University of Wales, Bangor.
56. J, Y., *Pumped hydroelectric storage. accedido a 20*. 2010.
57. Economist, *Energy storage-packing some power*. 2012.
58. Rigway S L, D.J.L.a.H.R.P., *Large energy storage systems for utilities*. Applied Energy 1980(6): p. 133-42.
59. Katsaprakakis D A, C.D.G., Zervos E A, Papantonis D and Voutsinas S, *Pumped storage systems introduction in isolated power distribution systems*. Renewable Energy 2008(33): p. 467-90.
60. EPRI, *Electric Energy Storage Technology Options: A White Paper Primer on Application, Costs and benefits*. 2010: Palo Alto, CA.
61. Turbine, *Turbine*. A New Zealand journal of New Writing, 2013.

62. A, D.B.a.B., *The contribution of wind hydro pumped storage systems in meeting Turkey's electric energy demand*. Renewable Sustainable Energy Revision 2010(7): p. 1979-88.
63. Ma T, Y.H., Lu L and Peng J. , *Pumped storage based stand-alone photovoltaic power generation system: modelling and techno-economic optimization*. Applied Energy 2015(137): p. 649-59.
64. H, H.C.E.a.R.I., *Solar and Wind resource complementarity: Advancing options for renewable electricity integration in Ontario, Canada*. Renewable Energy 2011(36): p. 97-107.
65. G., L., *Pumped Hydro electric energy storage and spatial diversity of wind resources as methods of improving utilization of renewable energy sources*. 2007, University of Colorado.
66. T., K., *Basic planning analysis of pumped storage*. 1989.
67. D, B., *Evaluation of Integration of pumped storage units in an isolated network*. 2006, University of Porto: Faculty of Engineering, Department of Electrical and Computer Engineering.
68. W, S.S.a.H., *Long vs short term energy storage technology analysis – a life cycle cost study*, in Sandia report, SAND2003-2783. 2003.
69. T., J., *Pumped Storage in Switzerland-An Outlook beyond 2000*, in *The Economics* 2014, Stucky Consulting Engineers Ltd: Post Box 1000 Lausanne 6, Switzerland.
70. G., L.a.J., *Pumped hydro-electric energy storage and spatial diversity of wind resources as methods of improving utilization of renewable energy sources page 6*. December 2007, University of Colorado.
71. Chi-Jen, Y., *Pumped hydroelectric storage*. 2012, Duke University.
72. Company, E.S.H.E., 2012.
73. Caralis G, R.K.a.Z., *On the market of wind with hydro pumped storage systems in autonomous Greek islands*. Renewable Sustainable Energy Revision 2010(14): p. 2221-6.
74. M, T.A.a.O.M., *Pumped storage in systems with very high wind penetration*. Energy Policy 2011. 39(4): p. 1965-74.
75. Sivakumar N, D.D., Padhy N P, Senthilkumar ARc, and Bisoyi N, *Status of pumped hydro storage schemes and its future in India*. Renewable Sustainable Energy Review, 2013(19): p. 208-13.
76. Yin J I, W.D.Z., Kim Y T and Lee Y H. , *A hybrid energy storage system using pump compressed air and micro-hydro turbine*. Renewable Energy 2014(65): p. 117-22.
77. D, L.B.a.G., *Massive electricity storage*. An AIChE paper, June 2008.
78. A, K.S.a.K., *Small hydro power – A review*. International Journal of Thermal Technologies December 2011. 1(1).
79. Yi C S, L.J.H.a.S.M.P., *Site location analysis for small hydropower using geo-spatial information system*. Renewable Energy 2010. 35(4): p. 852-61.
80. A, K.J.K.a.K.K., *Optimal wind-hydro solution for Aegean Sea Islands Electricity-demand fulfilment*. Applied Energy 2001. 70(4): p. 333-54.

81. Ardizzon A, C.G.a.P.G., *A new generation of small hydro and pumped-hydro power plants: Advances and future challenges*. *A renewable and Sustainable Energy Reviews* 2014(31): p. 746-761.
82. Agency, I.R.E., *Renewable Energy Technologies: Cost Analysis Series*. Hydropower, June 2012. 1(3/5).
83. Chiaramonti, G.a.D., *Small hydro in Europe helps meet CO2 target*. *International Water and Dam Construction*, 1999: p. 36-40.
84. A, H.A.a.B., *Micro hydro Design Manual*. 1992: ITDG Publishing.
85. Pokharel, G.R., A. B. Chhetri, M. I. Khan and M. R. Islam, *Decentralized Micro-Hydro Energy Systems in Nepal: En Route to Sustainable Energy Development, Energy Sources Part B*, in *Economics, Planning and Policy* 2008. p. 144-154.
86. REA, R.E.A.n.d., *Annual Report 2009/2010*, REA: Tanzania.
87. Adhau, S.P., *Economic Analysis and Application of Small Mico/Hydro Power Plants*, in *International Conference on Renewable Energies and Power Quality 2009*, ICREPQ'09: Valencia (Spain).
88. P. Maher, N.S.a.A.W., *Assessment of Pico hydro as an option for off-grid electrification in Kenya*. *Renewable energy*, July 2003. 28(9): p. 1357-1369.
89. Marie-Louise Barry, H.S.a.A.B., *Selection of Renewable Energy Technologies for Africa: Eight case studies in Rwanda, Tanzania and Malawi*. *Renewable Energy*, 2011(36): p. 2845-2852.
90. Gwang'ombe, K.T.K.a.F., *Challenges in small hydropower development in Tanzania: Rural electrification perspective*, in *International Conference on Small hydropower-Hydro 2007*: Sri Lanka. p. 24.
91. Klunne, W.J., *Small Hydropower Development in Africa*. *ESI Africa*, 2007(2).
92. Klunne, W., *Micro and Small hydropower for Africa*. *ESI Africa*, 2003. 4: p. 22-23.
93. Michael, K.W.J.a.E.G., *Increasing sustainability of rural community electricity schemes - Case study of small-scale hydropower plants in Tanzania*. July 2010.
94. Barnes, D.F.a.W.M.F., *Rural Energy In Developing Countries: A Challenges for Economic Development*. *Annual Review of Energy and the Environment*, 1996. 21(1): p. 497-530.
95. Cruickshank, Y.A.a.H., *The Value of Cooperatives in Rural Electrification*. *Technology Policy* 2010. 38(6): p. 2941-2947.
96. Meghan Bailey, J.H., John Holmes and Ruch Jain, *Providing village-level energy services in developing countries*. October 2012, Malaysian Commonwealth, Studies Centre.
97. Kruti Gupta, K.K.S.a.B.S. *Standalone and Hybrid Systems: A Survey*. in *IJCA Proceedings on National Conference on Advancements in Alternate Energy Resources for Rural Applications* December 2015. AERA 2015.
98. G, M.K.a.S.M.M., *Dynamic behaviour of a stand-alone hybrid power generation system of wind turbine micro turbine, solar array and battery storage*. *Applied Energy*, October 2010. 87(10): p. 3051 – 3064.
99. al, E.G.M.e., *Sustainability of off-grid rural community electricity schemes in Tanzania*.

100. Wind, I., *Integration of wind and hydropower systems*, in *Tasks 24 final technical report*. 2011.
101. Kaldellis, J., *Stand-alone and Hybrid Wind Energy Systems, Technology Energy Storage and Applications*. 1 ed. 2010: Woodhead publishing.
102. Daniel Akinyele, J.B.a.Y.L., *Battery Storage Technologies for Electrical Applications: Impact in Stand-Alone Photovoltaic Systems*. *Energies*, 2017. 10(11): p. 1760.
103. al, S.A.e., *Micro hydro energy resources in Bangladesh: A review*. *Australian Journal of basic and Applied Sciences*, 2008. 2(4): p. 1209-1222.
104. Penche, C., *Guide on how to develop a small hydropower plant*, *European Small hydropower Association*. 2004, European Renewable Energy Council.
105. M. T. Gatte, R.A.K., *Hydropower*. 2012, INTECH. p. 95-124.
106. Tanzania, U.-U.R.o., *Mini-grids based on small hydropower sources to augment rural electrification in Tanzania*. 2015.
107. E. L. B. Kassana, N.G., D. Mashauri, Z. Hailu, D. J. Chambega, S. K. Makhanu et al, *Small scale hydropower for rural development in Tanzania*. 2005.
108. al, M.E.G.e., *Sustainability of rural community small hydropower schemes in Tanzania*.
109. Adhau, S.P. *A comparative study of micro-hydropower schemes promoting self-sustained rural areas*. in *Proceedings of the 1st International Conference on Sustainable Power Generation and Supply*. April 2009. SUPERGEN.
110. S. P. Adhau, R.M.M.a.P.G.A. *Reassessment of irrigation potential for micro-hydropower generation*. in *Proceedings of the IEEE International Conference on Sustainable Energy Technologies*. December 2010. Kandy, Sri-Lanka: ICSET.
111. ADAMA, I.J.e.a., *Agricultural Production in Rural Communities: Evidence from Nigeria*. *Journal of Environmental Management and Tourism*, September 2018. 9(3): p. 428-438.
112. Kaldellis, J.K., *The contribution of small hydropower stations to the electricity generation in Greece: Technical and economic considerations*. *Energy policy* 2007. 35(4): p. 2187-2196.
113. S. J. Williamson, B.H., Stark, J. D. Booker, *Low head pico hydro turbine selection using a multi-criteria analysis*, in *Hydropower Application*. May 2011: Linkoping, Sweden. p. pp 1377-1385.
114. F, C.G.a.Z., *Small-scale hydroelectric power for developing countries: methodology of site-selection based on environmental issues*. *Environmental Conservation*, 1982(9): p. 329.
115. Croockewit, J., *Development Micro Hydro in British Columbia*. 2004, BC Hydro Engineering.
116. Paish, O., *Small hydropower: technology and current status*. *Renewable Sustainable Energy Review*, 2002. 6(6): p. 537-556.
117. Borota, M., *Mini Hydro Power Plants, Green Power for Users*. 2008, Directorate for Water Management, Ministry of Agriculture, Forestry and Water Management: Merita Borota, Serbia.

118. <http://www.microhydropower.net/basics/intro.php>.
119. Oliver, P., *Micro-hydro Power: Status and Prospects. Journal of Power and Energy*. 2002: Professional Engineering Publishing.
120. F. S. Javadi, B.R., M. Sarraf, O. Afshar, R. Saidur, H. W. Ping et al, *Global policy of rural electrification*,. *Renewable and Sustainable Energy Review* 2013(19): p. 402-416
121. EWURA, E.a.W.U.R.A., *The Electricity Standardised Small Power Projects Tariff, Tanzania*. 2015.
122. Harper, G.D., *Planning and Installing Micro Hydro Systems: A Guide for Installers, Architects and Engineers*. December 2011: Earthscan Publications Ltd,.
123. Cernea, M.M., *Hydropower dams and social impacts: a sociological perspective*. 2012: The World Bank.
124. C, D.B.a.G., *The role of hydroelectric power and contribution of small hydropower plants for sustainable development in Turkey*. *Renewable Energy* 2011(36): p. 1227–35.
125. G.o.K.T.e., *Challenges in small hydropower in Tanzania*, in *Renewable energy perspective*. 2007, Conference on small hydropower. p. 22 - 24.
126. Review, I.T., *UNIDO projects for promotion of small hydropower for productive use*. 2010, UNIDO evaluation group Vienna.
127. Ombeni J. Mdee1, T.K.N., Cuthbert Z. Kimambo, and Joseph Kihedu, *Assessment of hydropower resources in Tanzania, A review article*. *Renewable Energy and Environmental Sustainability*, 2018. 3(4).
128. A, M.A.W.a., *Ahmed. Micro-hydro energy resources in Bangladesh: A review*. *Australian Journal of Basic and Applied Sciences*, 2008. 2(4): p. 1209-1222.
129. Shrestha, S.M.a.R., *Technical problem analysis of micro hydropower plants, a case study at Pokhari Chauri of Kavre district*.
130. Tong, J., *Small Hydro on a large scale, challenges and opportunities in China*. *Renewable Energy World* 2006. 6: p. 93.
131. Tong, J., *Small Hydropower: China's Practice*. 2004: China.
132. Chris, G., *Small is pitiful, Micro-hydroelectricity and the Politics of Rural Electricity Provision in Thailand*. 2003, Energy and Resources Group: UC Berkeley, USA.
133. Hino T, L.A., *Pumped storage hydro power developments*. *Compare Renewable Energy*, 2012(6): p. 405-34.
134. R., K.G.a.C., *Reserving judgement: perception of pumped hydro and utility-scale batteries for electricity storage and reserve generation in New Zealand*. *Renewable Energy*, 2013(57): p. 249-61.
135. Blaabjerg F, C.A., Ferreira J, van Wyk J, *The future of electric power processing and conversion*. *IEEE Trans Power Electron* 2005. 20(3): p. 715-20.
136. L, M.M.W.a.A.C., *Contribution of pumped hydro storage to the integration of wind power in Kenya: An optimal control approach*. *Renewable Energy* 2014(63): p.:698-59.
137. USBR, *Reclamation managing water in the west*. 2016.

138. Tylee, J.L., *Chaos in a real system*. Simulation, 1995(64): p. 176-183
139. B. J. Lewis, J.M.C., A. M. Wouden, *Major historical developments in the design of water wheels and Francis hydro turbines*. IOP Conference Series: Earth and Environment Science 2014: IOP Publishing.
140. R. E. Horton, *Turbine Water-wheel tests and Power Tables* 1906: Washington.
141. J. L. Chukwunke, C.H.A., M. C. Nwosu, J. E. Sinebe, *Analysis and simulation on the effect of head and bucket splitter angle on the power output of a Pelton turbine*. International Journal of Engineering Applied Science 2014(5): p. 1-8.
142. Harvey, A., *Micro-Hydro Design Manual: A Guide to Small-Scale Water Power Schemes*. 1993: Practical Action.
143. Pandey, V., *Research Report on Feasibility Study of Micro Hydropower in Nepal*. 2011, Nepal Engineering College: Bhaktapur.
144. Pandey, B., *Micro Hydro System Design*. 2006.
145. Sanchez, T.a.R., L., *Designing and Building Mini and Micro Hydro Power Schemes, in A Practical Guide*. June 2011.
146. Kumar, R.a.S., S.K., *Penstock material selection in small hydropower plants using MADM methods*. Renewable and Sustainable Energy Reviews, 2015(52): p. 240-255.
147. O.J. Mdee, C.Z.K., T.K. Nielsen and J. Kihedu, *Measurement methods for hydropower resources: A review*. Water Utility Journal 2018(18): p. 21-38.
148. Singhal M. K., A.K., *Optimum Design of Penstock for Hydro Projects*. International Journal of Energy and Power Engineering, 2015. 4(4): p. 216-226.
149. A. C. Menezes, A.C., R. A. Buswell, J. Wright and D. Bouchlaghem, *Estimating the energy consumption and power demand of small power equipment in office buildings*. Energy and Buildings, June 2014. 75: p. 199-209.
150. Statistics, N., *Energy consumption in the UK*. UK.
151. Herschy, R., *Streamflow measurement*. 2009: London.
152. Smart., G.M., *Turbulent Velocity Profiles and Boundary Shear in Gravel Bed Rivers*. Journal of Hydraulic Engineering, February 1999. 125(2).
153. Morlock, G.T.F.a.S.E., *Discharge Measurements in Shallow Urban Streams Using a Hydroacoustic Current Meter*, in *Hydraulic Measurements and Experimental Methods Specialty Conference*. 2002, HMEM: Colorado, United States.
154. Sign., D., *Micro Hydropower Resources Assessment Handbook*. An Initiative of the Asian and Pacific Centre for Transfer of Technology. September 2009.
155. Binayak Bhandari, S.R.P., Kyung-Tae Lee and Sung-Hoon Ahn, *Mathematical Modelling of Hybrid Renewable Energy System: A Review on Small Hydro-Solar-Wind Power Generation*. International Journal of Precision Engineering and Manufacturing-green Technology April 2014. 1(2): p. 157-173.
156. Tanzania, U.R.o., *Hydrological Field Report*. 2010/2016, Ministry of Water, Internal Drainage Basin Water Board.
157. AHEC-IITR, *1.3-Project hydrology and installed capacity” Standard/manual/guideline* August 2013, Ministry of New and Renewable Energy: Roorkee.
158. Annual, E.P., in *Table 5.2*. 2009.

159. IFM. 2016; Available from: https://ifm.org.uk/wp-content/uploads/2017/01/Guidance-for-run-of-river-hydropower-development-LIT4122-747_12-version-5-May-2016.pdf.
160. Association, B.H., *A guide to UK Mini-Hydro Development v3.0*. 2012.
161. Laboratory, N.R.E., *Energy Efficiency and Renewable Energy*. 2008: USA.
162. Efficiency, E.C.f.R.E.a.E., *HOMER Software for Renewable Energy Design*. 2013, ECREEE.
163. Energy, H., *Getting Started Guide for HOMER Legacy (Version 2.68)*. 2011, Homer Energy and National Renewable Energy Laboratory: Colorado.
164. 01:2011, R.I.-P.T.-. *World-wide overview of design and simulation tools for hybrid PV systems*. 2011.
165. Laboratory, N.R.E., *Technology Brief: Analysis of Current – Day Commercial Electrolyser*, in *A national laboratory of the U.S Department of Energy*.
166. M. Eikerling, Y.I.K., A. A. Kornyshev, Y. M. Volkovich, *Phenomenological theory of electro-osmotic effect and water management in polymer electrolyte proton-conducting membranes*. *Journal of the Electrochemical Society*, 1998. 145(8): p. 2684-2699.
167. D. M. Bernardi, M.W.V., *A mathematical model of the solid polymer electrolyte fuel cell*. *Journal of the Electrochemical Society*, 1992. 139(9): p. 2477-2491.
168. V. Gurau, F.B., H. T. Liu, *An analytical solution of a half cell model for PEM fuel cell*. *Journal of the Electrochemical Society*, 2000. 147(7): p. 2468-2477.
169. T. Thampan, S.M., J. X. Zhang, R. Datta, *PEM fuel cell as a membrane reactor*. *Catalysis Today*, 2001. 67(1): p. 15-32.
170. S. H. Chan, Z.T.X., *Polarization effects in electrolyte/electrode supported solid oxide fuel cells*. *Journal of Applied Electrochemistry*, 2002. 32(3): p. 339-347.
171. T. Loroi, K.Y., Z. Siroma, N. Fujiwara, Y. Miyazaki, *Thin film electro-catalyst layer for unitised regenerative polymer electrolyte fuel cells*. *Journal of Power sources*, 2002. 112(2): p. 583-587.
172. P. Millet, F.A., R. Durand, *Design and performance of a solid polymer electrolyte water electrolyzer*. *International Journal of Hydrogen Energy*, 1996. 21(2): p. 87-93.
173. Centre, P.E., *Hydrogen Electrolyser*.
174. Frano Barbir, A.B.a.T.N.V., *Compendium of Hydrogen Energy*, in *Hydrogen Energy Conversion*. September 2015.
175. Gomes Antunes JM, M.R., Roskilly AP, *An experimental study of a direct injection compression ignition hydrogen engine*. *International Journal of Hydrogen Energy* 2009. 34(15): p. 6516-6522.
176. Gomes Antunes JM, M.R., Roskilly AP, *An investigation of hydrogen-fuelled HCCI engine performance and operation*. *International Journal of Hydrogen Energy*, 2008. 33(20): p. 5823-5828.
177. Centre, A.F.D., *Fuel properties comparisons*, in *Energy Efficiency and Renewable Energy*, U. S. Department of Energy.
178. NREL, *Small hydropower systems*. 2001, Department of Energy, USA: National Renewable Energy Laboratory.

179. C, G., *Assessment of the Effect of Hydraulic Power Plants Governor Settings on Low-Frequency Inter-area Oscillations*. 2010, Middle East Technical University.
180. report, I.C., *Dynamic Models for Steam and Hydro Turbines in Power System Studies*, in *Power Apparatus and Systems*. Nov/Dec 1973. p. 1904 – 1915.
181. Larock, B.E., Jeppson, R. W. and Watters, G. Z, *Hydraulics of Pipeline Systems*. 1999: CRC Press.
182. Chaudhry, M.H., *Applied hydraulic transients*. 2nd ed. 1987, New York.
183. Kundur, P., *Power System Stability and Control*. 1994, New York: McGraw-Hill.
184. R. A. Naghizadeh, S.J.a.B.V., *Modelling Hydro Power Plants and Tuning Hydro Governors as an Educational Guideline*. International Review on Modelling and Simulations (I.RE.MO.S.), 2012. 5(4).
185. K., S.C., *Accurate low order model for hydraulic turbines-penstock*. IEEE Trans Energy Conversation, 1987(2): p. 196-200.
186. IEEE, *Guide for the Application of Turbine Governing Systems for Hydroelectric Generating Units*, in *IEEE Standard* November 2004. p. 1207 - 2004.
187. Skooglund, D.G.R.a.J.W., *Detailed Hydrogovernor Representation for System Stability Studies*. IEEE Trans. on Power App. and System, January 1970. PAS-89(1): p. 106 - 112.
188. Phelan, R.M., *Automatic Control Systems* 1977, Ithaca - New York, USA: Cornell University Press.
189. al, G.A.M.-H.e., *Modelling and Controlling Hydropower Plants*. Advances in Industrial Control. Vol. 1. 2013, London Springer-Verlag.
190. R.A. Naghizadeh, S.J.a.B.V., *Modelling Hydro Power Plants and Tuning Hydro Governors as an Educational Guideline*. International Review on Modeling and Simulation (I.R.E.M.O.S.), August 2012. 5(4).
191. ELEC0047, T.V.C., *Power system dynamics, control and stability. Turbines and speed governors*. November 2015, University de Liege.
192. Hansen, A.D., Sørensen, P. E., Zeni, L. and Altin, M, *Frequency Control Modelling - Basics*. 2016, DTU Wind Energy E.
193. Kerdphol, T.R., Fathin & Watanabe, Masayuki & Mitani, Yasunori & Turschner, Dirk & Beck, Hans-Peter, *Enhanced Virtual Inertia Control Based on Derivative Technique to Emulate Simultaneous Inertia and Damping Properties for Microgrid Frequency Regulation*. IEEE Access, 2019. 1-1.
194. IEEE, *Hydraulic turbine and turbine control models for system dynamic studies*. IEEE Transactions on Power Systems, February 1992. 7(1): p. 167-179.
195. IEEE, *IEEE guide for the application of turbine governing systems for hydroelectric generating units*, in *IEEE Std 1207-2004*. 2004. p. 1—121.
196. Woodward, J.M.U.a.J.L., *Nonlinear hydro governing model and improved calculation for determining temporary droop*. IEEE Transactions on Power Apparatus and Systems, PAS, April 1967. 86(4): p. 443--453.
197. Group, I.W., *Prime Mover and Energy Supply Models for System Dynamic Performance Studies, Hydraulic Turbine and Turbine Control Models for System Dynamic Studies*. IEEE Trans. Power Systems, February 1992. 7(1): p. 167-179.

198. A. Khodabakhshian, R.H., *A new PID controller design for automatic generation control of hydro power systems*. International Journal of Electrical Power & Energy Systems, 2010. 32(5): p. 375-382.
199. Hasmaini M, H.M., Halim A. B, Hew Wooi P, *A review on islanding operation and control for distribution network connected with small hydro power plant*. Renewable and Sustainable Energy Reviews, October 2011. 15(8): p. 3952-3962.
200. WeijiaY., J., Wencheng G., Per Norrlund, *Response time for primary frequency control of hydroelectric generating unit*. International Journal of Electrical Power & Energy Systems, January 2016. 74: p. 16-24.
201. EWURA, E.a.W.U.R.A., *The Electricity Standardized Small Power Projects Tariff 2015*: Tanzania.
202. Action, P., *Small-scale hydro power: small hydro an economic option. Technical information by Practical Action*. 2013, Charitable Organisation headquartered in Rugby, United Kingdom.
203. EU, T., *China Small Hydro Industry Guide*. 1999, IT Power LTD: Chineham.
204. (IPCC), I.P.o.C.C., *Special Report Renewable Energy Sources and Climate Change Mitigation*, in *Working Group III-Mitigation of Climate Change*. 2011.
205. O, P., *Small hydropower, Technology and current status*. Renewable and Sustainable Energy Reviews, 2002. 6(6): p. 537-56.

Appendices

Appendix A: Economic analysis

A.1 Introduction

Hydropower is one of the least expensive sources of power since the cost of hydropower is dominated by the initial capital cost of building the facility while the ongoing operating and maintenance (variable) costs are low. Moreover, since hydropower generation does not require burning fuels, the operations costs are not vulnerable to fuel price fluctuations like those from thermal and coal power plants. Existing hydropower facilities are very cheap to operate and they can operate for 25 years or more without major replacement. The cost of hydropower is highly site-specific and depends on different factors which including hydrological characteristics that is the nature of flowing river and possibility of a dam, site accessibility due to terrain and distance of transmission which contribute to a significant cost increase.

In small and micro hydro power plant category, the cost of developing a hydropower plant is even lower as compared to the large-scale hydro power plants. This is because most small scale and micro-hydro power plants operate as a run-of-river scheme on which no huge civil construction is undertaken like the construction of a dam or water storage reservoir. In micro hydropower scale, the cost of developing a hydropower plant is comparable small due to the small constructions that these micro scale plants are developed. Most of the costs in the micro-hydropower plants are related to civil works for the construction of intake/weir, canal, settling basing, forebay and power house and also on the areas of distribution power lines from the power house to the consumers. In order to determine the project total costs, the economic analysis of the project has to be conducted which aims at choosing the best financial decisions to be taken for the project to be profitable.

A.2 Methodology

The methodology used in the project economic analysis is basically relies on costing and financial data that have been provided, i.e. investment cost (material costs, labour costs and overheads), interests rates and project life time. In the financial analysis, using the annual interest rates, most project costs can be compounded to the future values of year “*n*” using the following formula:

$$F = P(1 + i)^n \quad (\text{A.1})$$

Where:

F = Future value

P = Initial investment (Present value)

i = Interest rate

n = Number of compounded years

The usefulness of this formula is that it is also possible to find the present value when future payment for the project is made for compounding years using provided interest rate. Future payments for the project costs can also be related to a loan which is a common practice in financing micro-hydropower. So, in order to determine the amount of loan payment as a function of interest rates and a number of years then the following formula is used.

$$L = P \sum_{t=1}^n (1 + i)^t \quad (\text{A.2})$$

Where:

L = loan payment

P = present value (loan amount)

i = monthly interest rate

n = months of the loan

t = time

For each individual year of the loan payment, the following term is used to determine the amount of loan compounded to “ n ” years with “ i ” value as the interest rate.

$$\sum_{t=1}^n \frac{1}{(1+i)^t} \quad (\text{A.3})$$

Based on the above initial financial analysis by looking on the loan as an investment cost, then the detailed economic analysis of the project needs to look into the net cash flow values of the project life time. In this case, it should be noted that the net cash flow is always taking into account the savings (positive values) as well as the costs (negative values) of the project cash flow.

So in order to analyse the net cash flow and to make the best economic choice, four (4) measures need to be determined, i.e. Payback period, Net Present Value, Return on Investment and Benefit-Cost Ratio.

(a) Payback period

In the project economic analysis, the payback period is the time taken for the cash flow to recover the capital costs of the initial project investment. This is done by taking the capital cost divided by the payments on each month or year of the project life time.

$$\text{Payback period} = \frac{C_c}{C_p} \quad (\text{A.4})$$

Where:

C_c = capital costs or a loan amount

C_p = cash payments or monthly payments

In the project cash flow analysis, the less the payback period the better the project in terms of value for money and profitability.

(b) Net Present Value (NPV)

The net present value is the amount of money obtained when all the future cash flow amounts are brought to the present time using discounted rate and subtracting the capital costs. The assumptions in this method are that at the end of this discounted period all the cash flow will appear.

$$NPV = \sum_{t=1}^n \frac{C_f}{(1+i)^t} - C_c \quad (\text{A.5})$$

Where:

C_f = cash flow

i = discounted rate (%)

t = time

In the cost-benefit analysis, the interest rate used is termed as discount rate because it makes the future discounted factor smaller than the present factor due to the increased number of years.

$$\text{Discount factor} = \frac{1}{(1+i)^t} \quad (\text{A.6})$$

(c) Return On Investment (ROI) or IRR

The return on investment is the interest rate at which the NPV is becoming zero on which the NPV formula can be used by setting it to zero and solve for (i). When setting the NPV to zero means that the cash flow is equal to the capital cost and no profit or loss for the project. So, the value of interest rate (i) for the cash flow at this time must be used in order to return the investments cost.

$$NPV = 0 = \sum_{t=1}^n \frac{C_f}{(1+i)^t} \quad (\text{A.7})$$

In this, the total present value of the benefits (cash flow) must be equal to the total present value of the costs (capital cost)

$$C_c = \sum_{t=1}^n \frac{C_f}{(1+i)^t} \quad (\text{A.8})$$

(d) Benefit-Cost Ratio (B/C ratio)

In this measure, it represents the size of the present value cash flow costs and benefits and calculated by dividing the net present value of the cash flow (benefits) with the capital costs. It is a very useful indicator of project cash flow analysis but the downside of it is that it does not give an indication of the scale of investment as the value only indicates positive values (profit) or negative values (loss).

$$B/C = \frac{NPV}{C_c} \quad (A.9)$$

A.3 Results and discussion

In the determination of the total cost of the designed and developed micro-hydropower plant, all the individual costs of the plant components have been worked out taking into consideration the availability of local construction materials and labour. In addition to that, the rates for skilled and unskilled manpower have also been based on the local practices available in the village community. So, in this case, the rate of electro-mechanical equipment is taken from the current quotation prices of the manufacturer/installer and are subjected to change. Thus, these costs estimates show only an indicative and close approximation values hence, they should be used only for budgetary and evaluation purposes. Due to the changes in turbine material prices, the cost of electro-mechanical equipment may vary according to change in the market price in the given time. All the costs of the materials are included VAT.

In the cost analysis, each system design section has been analysed separately starting with the micro-hydro turbine system and the generator system in the areas of civil, electrical and mechanical components. In this section, most of the mechanical components are locally manufactured in order to transfer knowledge to the local people so as to insure the project sustainability. The civil materials are also purchased locally while the electrical components like cables switch gears, transformer and generator are sourced from abroad. Based on the optimized system design, the micro-hydro turbine system will also be integrated with an electrolyser system and hydrogen engine-generator system which their cost will also be analysed, although most of the equipments are commercially available on the market.

A.3.1 Capital costs

A.3.1.1 Cost of civil components and works

The main civil components consist of intake structures for diverting the water from the river then the canal to carry water from the intake to the settling basin that allows water to settle before they pass to the forebay which is a water storage tank that is connected to the penstock pipe. Down the line, there are other civil components which include support piers and anchor blocks for the penstock pipe, power house building and also tailrace canal.

Based on current material prices, the total cost of the civil components of the project is £16,496.40. It is 13.19 % of the sub-total project cost. The rates and analysis have been done on the basis of local material costs and also norms adopted in Tanzania, taking into consideration the current rates and practices for the civil materials. The total cost has been quoted in British pounds.

Note: The low cost in civil components is due to the simple designs of the civil structures, i.e. intake, canal and power house

A.3.1.2 Cost of electrical components and works

The cost estimation for the electrical components consists of the generator system, cables and conductors, transformers, poles and other electrical components. Most of the electrical items are purchased locally but some are ordered from abroad. Due to the long distance in the transmission line, the total cost of the electrical conductors has been significantly high.

Based on the current market prices, the electrical component cost of the project is £26,759.33. It is 21.39 % of the sub-total project cost on which a significant portion of it includes the cost of a generator, governing system, control and protection system, transformer and earthing. These costs are based upon quotations from the local suppliers and are quoted from local currency. The higher cost in electrical components is because of the long transmission lines of around 5km from the power house to the load centre.

A.3.1.3 Cost of mechanical components and works

The mechanical components of the project cost £18,960.75. It is 15.16% of the sub-total project cost. It includes the cost of the micro hydro turbine and its fittings, power/torque transmission, penstock pipe and its fittings and trash rack etc. The cost is based on a quotation from local manufacturers/suppliers. There is a possibility of manufacturing the turbine system locally if the manufacturer becomes available otherwise it has to be purchased abroad. In this section, the turbine system and the penstock pipe have the highest

percentage of the cost in mechanical components section because the turbine unit is the main mechanical item and also the penstock pipe length is a bit longer of about 162m.

A.3.1.4 Cost of the electrolyser system

The power capacity of 70 kW for the designed electrolyser unit is available on the market as explained in the previous Chapters. In this design, the Proton Exchange Membrane (PEM) electrolyser system is selected which produce pure hydrogen and oxygen gas at the rate of 99.99%. The electrolyser cost based on the current market price is a bit higher because electrolyser systems are new technology, so limited researches and development have been conducted to reduce the energy intensive electrolysis process and hydrogen storage technologies. But based on the price from Beijing CEI Technology Co. Ltd in China, the cost of the selected HGPS-10 electrolyser system is around £32,500.50.

A.3.1.5 Cost of engine-generator system

The designed engine-generator size of 40 kW is also available commercially and this type of gas engine uses hydrogen fuel gas as an input to produce electricity. The cost of the selected gas engine-generator is similar to other IC engines of same power capacity and based on Weifang Ronsum Power Technology Co. Ltd in China the cost of the of the selected LS-40GFT hydrogen gas engine-generator system is around £16,250.25.

A.3.1.6 Cost of tools and spare parts

In order to operate and maintain a micro hydro power system with trouble free services for a long period of time, plant maintenance is very crucial because it increases the plant capacity factor. In addition to that and in order also to properly maintain the micro-hydro power plant to reach its lifetime, tools and spare parts need to be purchased, supplied and stored. In the present project, the cost of tools and spare parts are amounting to £4,467.30 which are required for the annual basis. It accounts for around 3.57 % of the combined sub-total cost of civil, electro-mechanical, electrolyser and engine-generator.

A.3.1.7 Cost of transportation and packing

Most of the project materials and components need to be transported to the site area from different parts outside the site location. The main transport process for the materials is through the roads by big trucks that need to be hired and due to the remoteness of the project site location, it has increased the transportation cost significantly. But despite this elevated cost effect, the material transportation works creates a kind of local opportunity for the local people who are contributing and share their time by involving in the transportation of construction materials, components and some equipment as well. In this section the total

transportation cost for the project materials and equipment is £5,019.49 and it accounts for about 4.01 % of combined civil, electro-mechanical, electrolyser and generator-engine cost.

A.3.1.8 Cost of installation, testing & commissioning

Installation, testing and commissioning cost of the project is proposed, as £4,623.39. It is 3.70% of the combined civil, electro-mechanical, electrolyser and generator-engine cost.

A.3.1.9 Contingency cost

Due to price changes for the project materials and equipment and consideration of the project execution period, the cost contingency needs to be considered based on the total costs of the sub-sections. In this case, the contingency cost is amounting to **£12,507.74** which is **10%** of the sub-total project cost.

A.3.2 Summary of project capital cost

The total material and equipment cost of the project is the sum of costs from civil, electro-mechanical, electrolyser and engine-generator individual costs. The results show that the cost of the electrolyser system has the highest cost value which is 25.98% while the Tools and spare parts cost has the lowest cost of 3.57%. The higher value of the electrolyser system also increases the overall project cost as shown in Table A.1 below.

Table A.1: Summary of total capital cost

Description of works	Amount (£)	% of Sub-Total
Civil works	16,496.4	13.19
Electrical works	26,759.33	21.39
Mechanical works	18,960.75	15.16
Electrolyser system	32,500.50	25.98
Engine-Generator system	16,250.25	12.99
Tools and Spare Parts	4,467.30	3.57
Transportation	5,019.49	4.01
Installation and Commissioning	4,623,39	3.70
Sub - Total	125,077.41	100

A.3.3 Financing and costing

Several sources of finance have been approached for financing the development of this projects scheme and Rural Energy Agency - Tanzania (REA) is the main financing supporter by providing a grant for the development of the project. Some other financial institutions may also provide support for the project in a form of financial aid and other forms like loans. Different sources of funds for the project have also been approached in the local community, which some include community contributions in cash and materials/labour and also some from the local district and regional council support. Beneficiaries from members of community organizations are committed to volunteer labour, construction of the canal, powerhouse and other necessary civil works. In addition, members of the community collect and contribute cash as well. The community contributions will be in a form of works that include the local labourer, local cash contribution and bank loan payments. The financial analysis is carried out such that the total financing source that covers project costs may be taken as a bank loan and hence the bank loan is £125,072.41. From the cost analysis, it is noted that additional materials and equipment cost for the optimized system design components increased the project cost by £48,750.75.

A.3.3.1 End use energy supply capacity and revenues

Feasibility study report indicated that members of the local community in the project area need electricity for facilitating the economic activities. Micro-hydro power electricity is an important alternative source of energy because the existing sources are unreliable and also not available in the project case study area. Currently, the people use fire wood, charcoal and kerosene as their major source of energy for cooking and lighting. The end-use available energy include lighting for local households and shops which will replace kerosene lamps. Other uses involve electricity for business which includes a power supply for saloons, phone charging stations, maize mills, agricultural products processing factories and social/religion centres etc. The total project revenue collected from the consumers that are supplied by electricity is amounting to £1,519.73 per month.

A.3.3.2 Additional project revenues

The excess hydrogen gas produced from the electrolyser will be sold to the nearby industries like the fertilizer factory and increase the project revenue. The amount of hydrogen gas produced depend on the amount of electricity available during that day but on average the hydrogen production capacity is 0.343 Kg/hour which is equivalent to 8.23

Kg/day. In addition to hydrogen gas, the electrolyser system also produces oxygen gas half the capacity of hydrogen and this gas is supplied to the local health centre to save lives. The revenues generated by hydrogen and oxygen gas are shown in Table A.2 below.

Table A.2: Revenue from hydrogen and oxygen production

S/N	Type of Business	Daily quantity (Kg/d)	Monthly quantity (Kg/m)	Price per Kg (£)	Monthly income (£)
1	Hydrogen gas	10.15	304.5	1.2	365.4
2	Oxygen gas	5.08	152.4	0.6	91.44
TOTAL per month (£)					456.84

A.3.3.3 Expected annual revenue

For the Hhaynu Hydropower Scheme, the tariff is fixed in terms of energy use in kilo-watt per month for lighting and power system in the households. However, for other uses, the tariff is being designed on the unit basis. The tariffs are calculated by considering aspects as follows [201]

- Demand for the services
- Purchasing capacity of the consumer
- Tariff from EWURA
- Income from end uses
- Total Project Cost
- Operating cost of the scheme

Table A.3: Proposed tariff

Service	Tariff (£)
Household Lighting and Power	4 pence per kWh
End Users	5 pence per kWh

The above tariff's values are to be reviewed and revised periodically as the price levels change based on the economy of the area. The estimated value of £1,519.73 and £456.84 are the monthly revenue collected from the end use. If you consider annually (12 months period), the annual revenue can also be calculated by multiplying the monthly revenues with 12 months.

Thus, the total annual expected income is **£23,718.84**. The exact locations of some of the end users in terms of businesses and small industries locations have not been identified and

it is expected that the other demands will be running together with the households lighting and power demands.

7.2.3.4 Estimated annual costs

The total annual expenses of the Hhaynu hydropower scheme is £ 8,222.85 as shown in Table A.4 below.

Table A.4: Total annual costs

Component	Qty.	Monthly salary/expenses each (£)	Month in year	Annual cost (£)	Remarks
Hydro Power Plant	3*	82.05	12	2,953.8	
Operators/Technicians					
Plant Manager	1	98.42	12	1,181.04	
Accountant	1	88.62	12	1,063.44	
Office attendant	1	55.80	12	669.6	
Repair & Maintenance	LS			1,644.57	2.5% of the Sub-Total Cost
Office Expenses	LS	32.80	12	393.6	
Miscellaneous	LS	26.40	12	316.8	
TOTAL ANNUAL EXPENSES				8,222.85	

* Civil, Electrical and Mechanical Technicians

A.3.3.5 Investment cost

The project investment cost has been calculated after deducting all the applicable VAT and Taxes from the total project cost. So, investment cost, in this case, is calculated as follows:

Investment Cost = Total project cost – VAT (18%) and Contingencies (10%)

$$= \text{£ } 162,350.48 - \text{£ } 37,273.07$$

$$\text{Investment Cost} = \underline{\text{£ } 125,077.41} \text{ (optimised system)}$$

When considering the original system design without the electrolyser and hydrogen engine-generator system, then the cost is calculated as follows:

$$\text{Investment Cost} = \text{£ } 125,077.41 - \text{£ } 48,750.75 = \underline{\text{£ } 76,326.66} \text{ (original system cost excluding electrolyser system and engine-generator system)}$$

Therefore, when considering the capacity of the micro-hydro power plant of 75.5 kW, the investment cost per kW of the project is estimated to be 1,656.67 £/kW (2,200 US\$/kW)

for the optimised system design which is within the recommended range for project cost estimation for this kind of micro-hydropower project [202] as shown on Figure A.1 below.

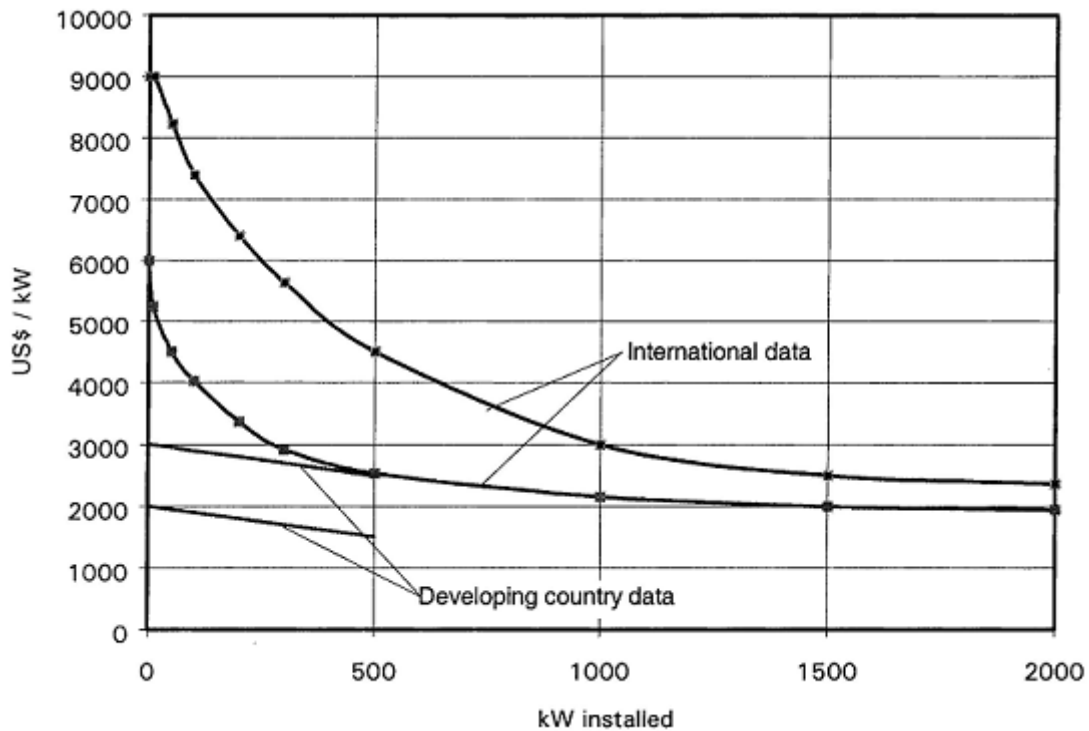


Figure A.1: Micro-hydro power plants project cost estimation [203]

A.3.4 Financial and economic measures

The financial and economic analysis of the scheme indicates the validity of the project in terms of its capital/investment cost. It focuses on the sources of funding for the project, annual income, annual expenditure and financial indicators of the project such as Net Present Value (NPV), Benefit Cost Ratio (B/C) and Internal Rate of Return on the Investment (IRR). The financial and economic analysis of the scheme indicates that the Hhaynu micro-hydropower project is viable both financially and economically based on below financial indicators.

A.3.4.1 NPV, B/C ratio and IRR

Based on the estimated income and expenditure and considering the standard discount rate of 7% (6% - 9% for run-of-river schemes) [204], the net present value (NPV) for the project is £45,033.75. This positive results NPV value indicates that the project has a better return on investments (profitable) which means that the project earnings exceeds the anticipated project expenses. It is also considered that the project investment cost has been taken as a loan and from the analysis results, it is shown that the payback period is 6.3 years which is OK for renewable energy projects. Based on the average economic life time of the plant

which is 25 years [205] the salvage value of the plant is £25,014.48 which is the re-sale value at the end of the estimated project life time. The financial analysis also shows that the internal rate of return (IRR) is 15 % which is the interest rate at which the NPV of all the cash flow from the project investment is equal to zero. From the result, it is also noted the value of the IRR falls above the required rate of return, then the Hhaynu micro-hydropower project is desirable. Another analysis that has been considered is the cost analysis called the benefit cost ratio (B/C) and the analysis shows that project B/C value is 1.31. This B/C value of above 1.0 indicates that the project has positive NPV value and also the IRR value is above the discounted rate used in the cost analysis which makes the project economical. The financial analysis has been done considering total project cost including taxes and contingency. Using the NPV value with the selected discount rate, the project cost can also be evaluated for the undiscounted and discounted values as shown in Table A.5 below.

Table A.5: Cost-benefit analysis results

S/N	Discounted factor for $i = 7\%$	Undiscounted		Discounted	
		Costs	Benefits	Costs	Benefits
1	1 ^a	45,033.75	0	45,033.75 ^b	0
2	0.71	10,840.21	20,841.83	7,696.55	6,044.13
3	0.51	9,539.38	23,342.85	4,865.09	11,438.00
4	0.36	8,394.66	26,143.99	3,022.08	16,732.15
5	0.26	7,387.30	29,281.27	1,920.70	21,668.14
6	0.18	6,500.82	32,795.02	1,170.15	26,891.92
Total		87,696.13	132,404.96	63,708.31	82,774.34
Net Benefit		44,708.84		19,066.03	
B/C ratio		1.51		1.30	
$a = \frac{1}{(1+(\frac{7}{100}))^0}$		$b = a \times C_p$			

A.3.4.2 Cost of energy

Based on the above financial analysis results and looking into economic point of view, it is evidence that the development of Hhaynu Micro-hydropower plant in Mbulu Tanzania for the purpose of electricity generation with the designed power capacity of 75.5 kW and

energy demand optimization to meet the available load demand, the project is feasible and will bring economic benefits to the local community by transforming people's lives through income generation and providing the required services. The cost analysis also shows that the equivalent cost of energy for the micro-hydropower project is 5 cents per kWh which is lower than the cost of energy for fossil fuel sources. This is based on the subsidised cost for the available power supply from the micro-hydropower on which the electricity price for lighting is sold at 4 cents per kWh which is mostly for households use while electricity for power is sold at 5 cents per kWh which is mostly for business use.

A.3 Summary

From the preceding analyses and discussions, it is found out that the project is technically and financially feasible. The implementation of the project will provide high quality lighting for household purpose as well as reliable and environmentally safe power for end-use applications. An installed capacity of the scheme will be 75.5 kW comprising of a unit cross-flow turbine, operating at a rated gross head of 25 m and design flow of 450 l/s. Based on the financial analysis, this scheme is considered beneficial from all aspects of economic and environmental with the following features that answers one of the research questions.

Financial Features

Total Cost of Scheme	: £ 125,077.41 (Excluding VAT and Contingency)
Cost per kW	: 1,656.67 £/kW
Revenues	: 23,718.84 £/year
Expenses	: 8,222.85 £/year
IRR	: 15%
NPV	: £45,033.75
B/C Ratio	: 1.31
Payback Period	: 6.3 Years
Annuity Payment	: £20,840.21

The project finances will come from various sources and the majority of the funds will come in a form of a grant as a contribution to rural electrification while other sources will be provided by the local government, local community villages and also another amount in a form of a bank loan. During the project implementation, some of the project activities will be implemented by the local people as their contribution to the project implementation. These include some of the building materials and also part of the labour during construction as shown in Table A.6 below.

Table A.6: Sources of Finance

S/N	Source of finance	Amount (£)	Share (%)	Remarks
1	REA Grant/Fund	62,538.71	50	
2	Local government contribution	31,269.35	25	
3	Local Labour & Materials	2,501.55	2	Items 3, 4 and 5 are to be collected by the local community
4	Community cash contribution	3,752.32	3	
5	Bank Loan by the Community	25,015.48	20	
Total		125,077.41	100	

Note: The total project cost includes the optimized system design

The assessment of economic benefits covers quantifiable and non-quantifiable, direct as well as indirect benefits. Calculations, in this case, involve Economic Rate of Return on quantifiable non-incremental benefits. Benefits have been assessed based on the avoided cost of diesel generation in the case of supply to productive end uses and the avoided cost of on kerosene use for lighting purposes in the households and also the cost of dry cell battery use.

(a) Benefits from kerosene replacement

The average use of kerosene in the project area is 10 litres per household per month. After the introduction of electricity, it is assumed that a household would require less than 2 litres of kerosene per household per month. Therefore, the micro-hydro scheme will replace 8 litres of kerosene per month in turn £96 will be saved annually in each household. (8 litres x £1 x 12 months). The calculation is based on the cost of kerosene at £1 per litre.

(b) Benefits from diesel replacement

It is envisioned that each maize and timber mills will use three litres of diesel per operating hour on average. So, annually 5,940 litres of diesel will be saved on each system (3 litres x 5.5 hours/day x 30 days/month x 12 months/year), equivalent to £5,049 that will be saved based on the unit cost of £ 0.85 per litre of diesel (5,940 litres x £0.85). In addition to

diesel replacement, the new system will protect the environment by eliminating the pollution of the diesel-powered engines and generators systems.

(c) Benefits from dry cell battery replacement

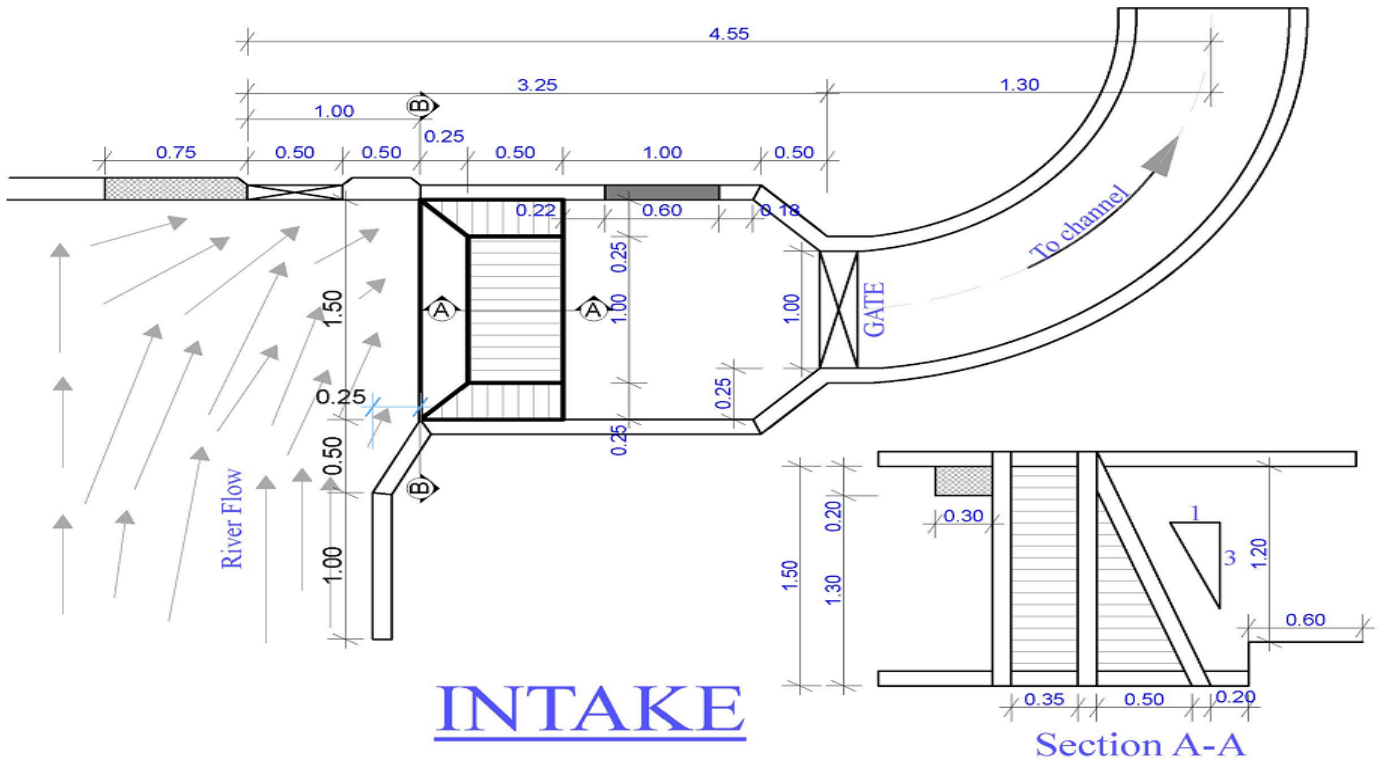
It has been revealed that the beneficiary households use about three pairs of dry cell batteries per day on average. The micro-hydropower scheme will save two pairs of dry cell batteries per household per day, which will make 1,440 pairs of dry cell batteries (4 batteries x 30 days/month x 12 months/year), will be replaced per year. Therefore, £720 will be saved per year by replacing dry cell batteries based on the cost of a pair of dry cells as £0.5 (1,440 pairs x £0.5).

(d) Incremental benefits

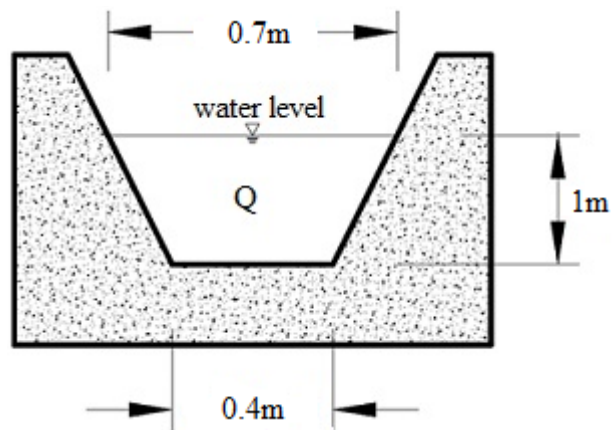
The benefits, which are not included in the analysis but could be worth mentioned, are the incremental benefits. The incremental benefits are the benefits, which come from the increase in modernity from the electricity uses due to the low prices of available electricity. The benefits include direct improvement in the quality of education as a result of the availability of electricity. In addition to that, educational benefits due to the availability of electricity which include extended reading hours and better quality lighting facility. Members of the community will also use electricity for media like TV, radio and computer operations. The availability of electricity will also make members of the community to get the opportunity to engage in income generating activities, especially during evening hours and dawn. The other benefit worth mentioning is the improved indoor air quality and reduction of air pollution due to the elimination or reduction of firewood, charcoal and kerosene usage which will bring the health and environmental benefits to the community.

Appendix B: Detail drawings

B.1: Intake



B.2: Canal sections



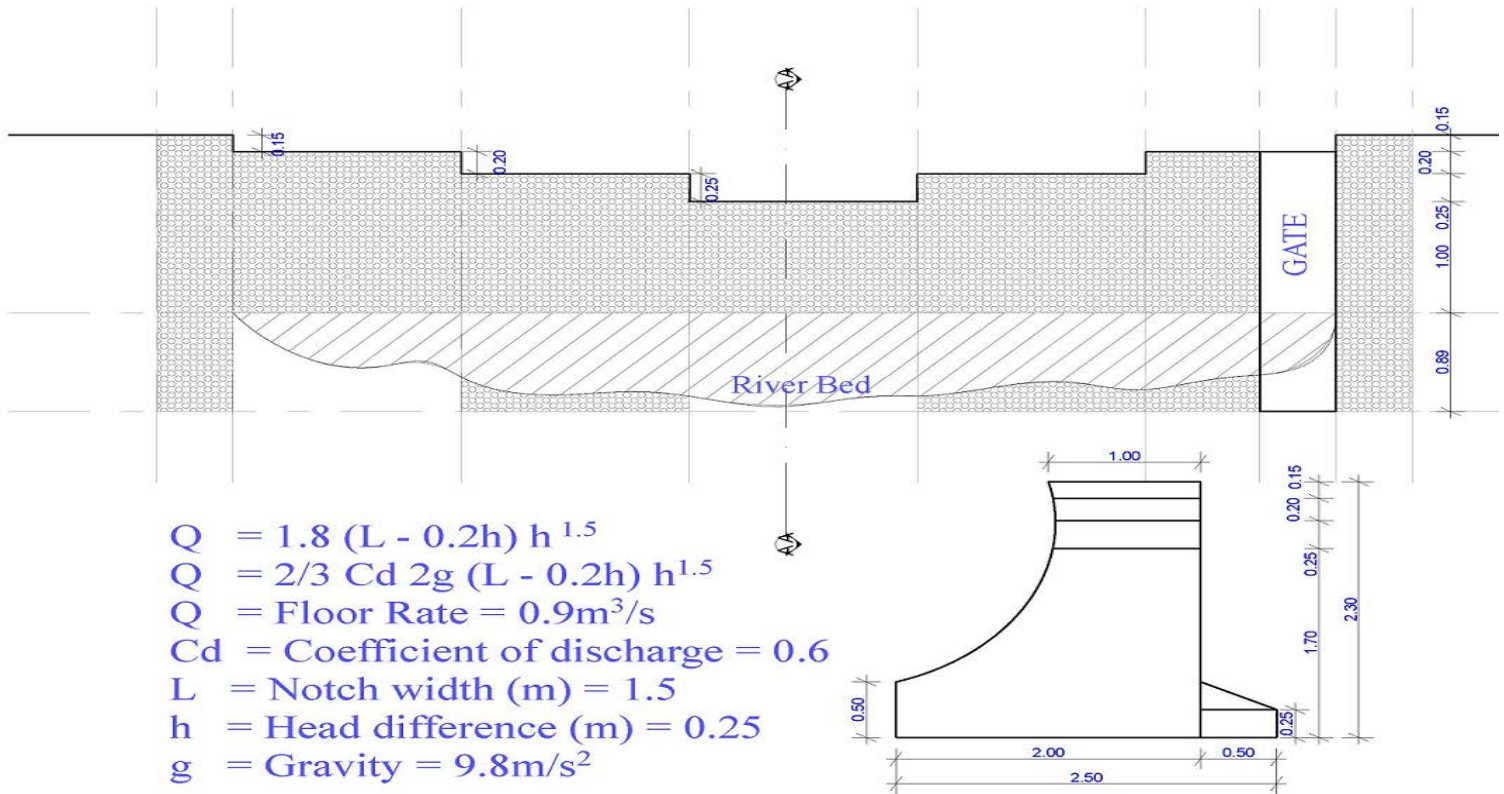


Canal construction

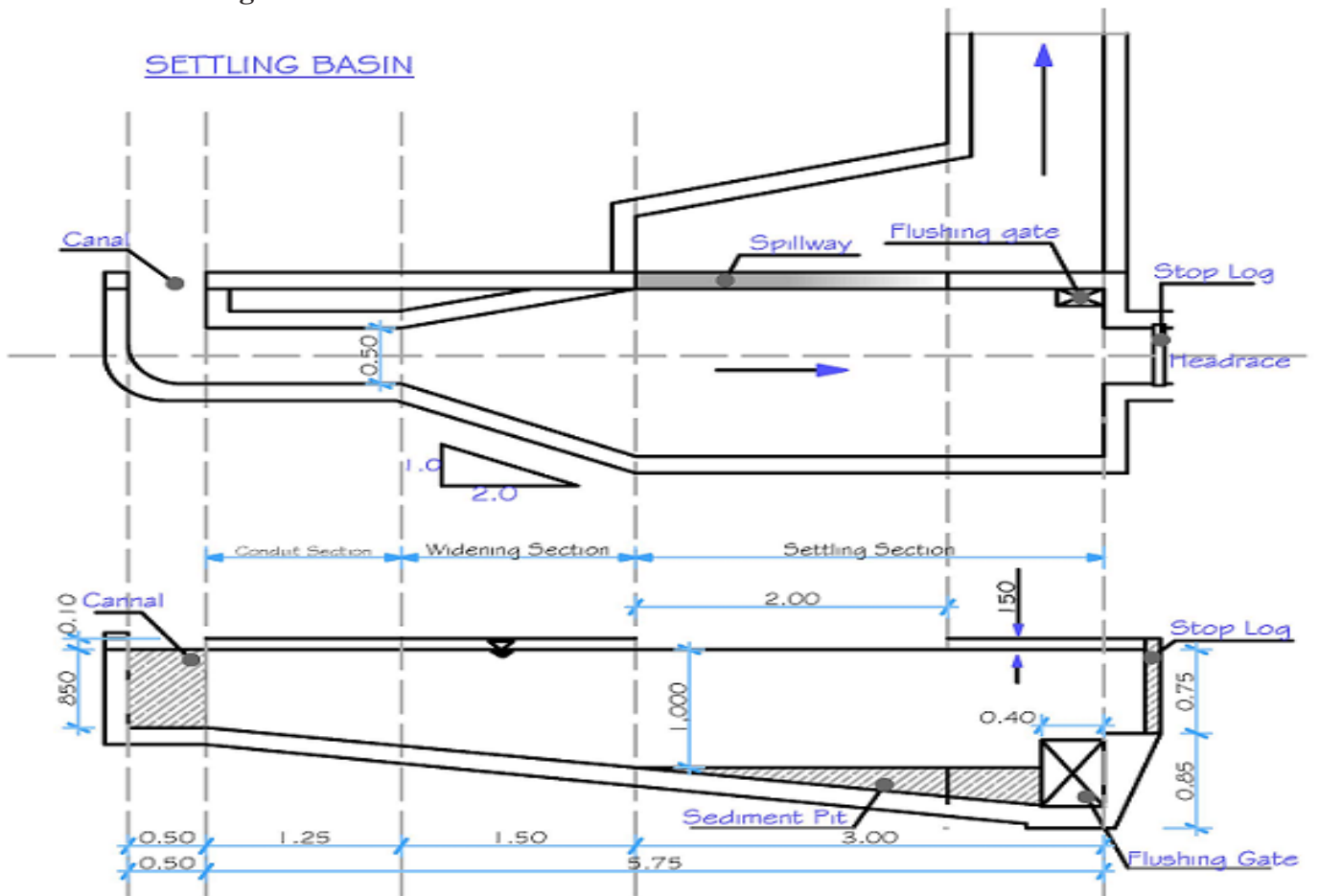


B.3: Weir structure

Front view - Weir

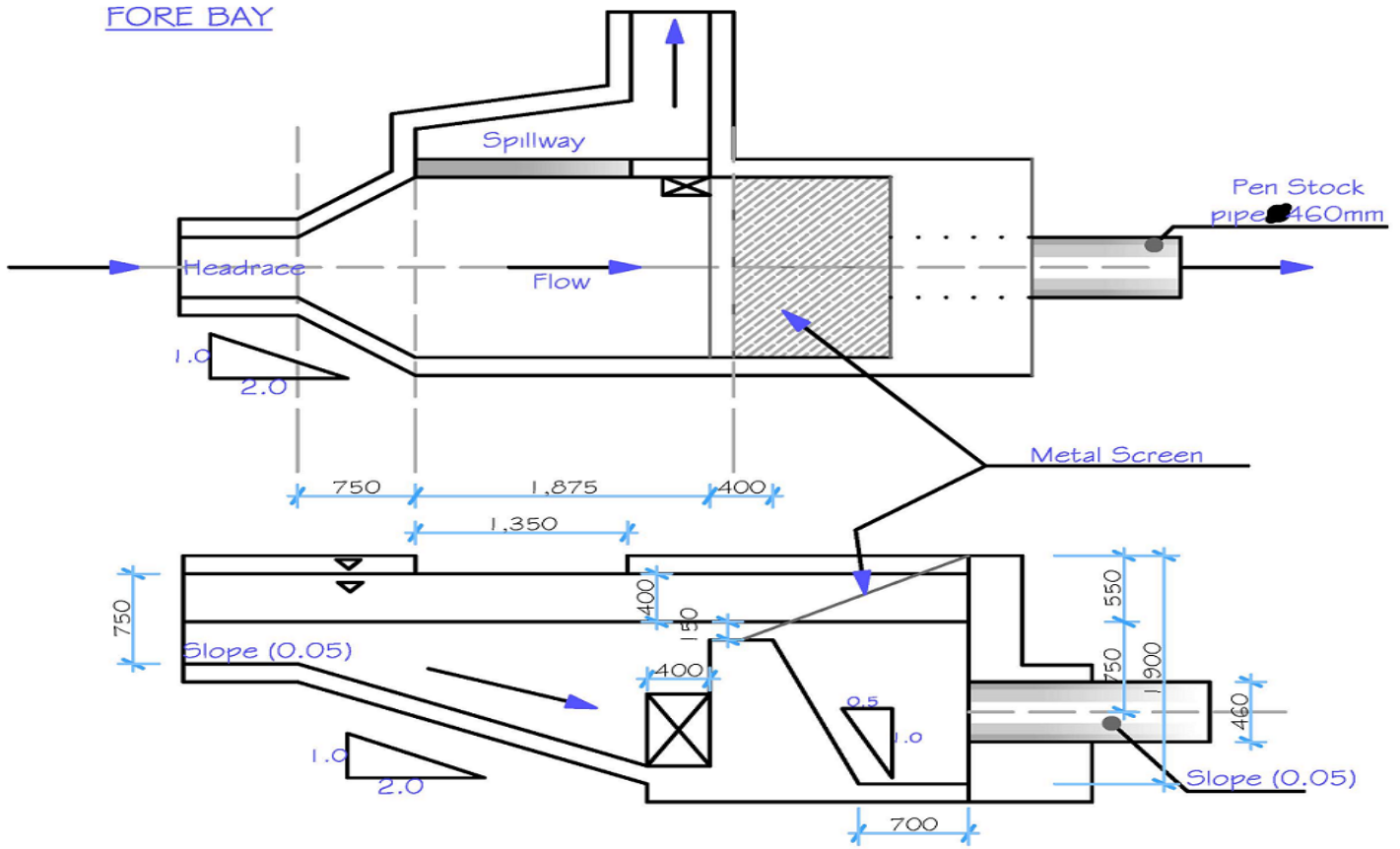


B.4: Settling basin

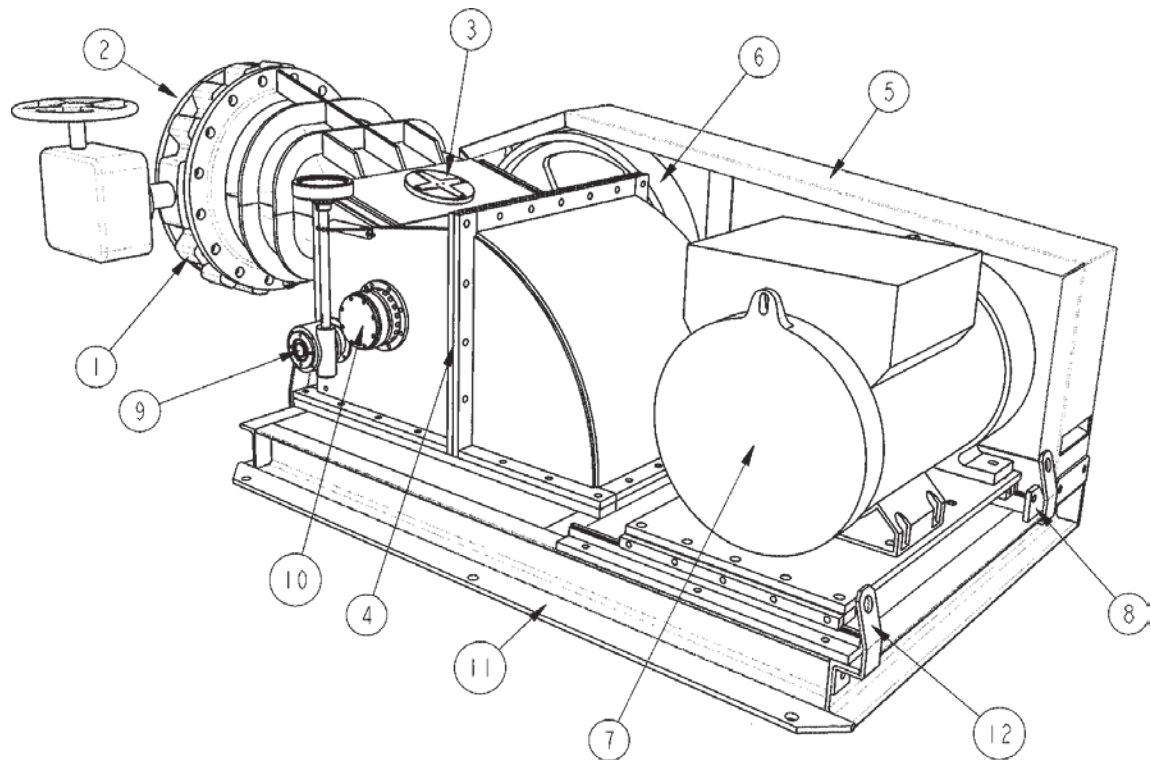


B.5: Fore bay

FORE BAY



B.6: Turbine unit

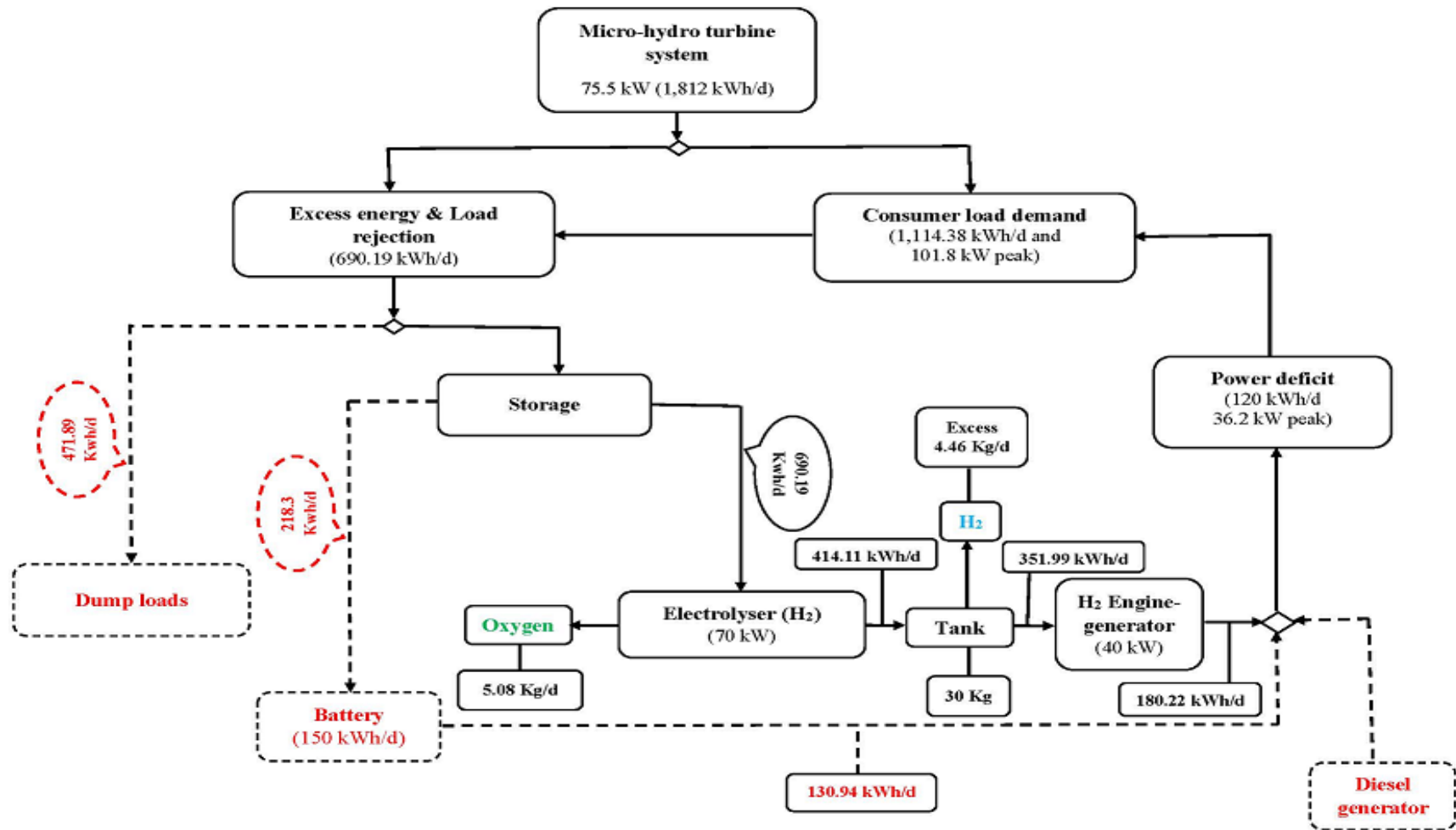


1. Manual / semi-automatic floodgate
2. Connection to the penstock
3. Inspection door
4. Turbine case
5. Guard for pulley and belt
6. Pulleys with a cogged driving belt
7. Generator
8. Generator fixing slide with belt tightening pulley
9. Flow regulation (manual or automatic)
10. Bearing
11. Frame
12. Lifting points



Fabricated turbine unit

Appendix C: Optimized energy utilization block diagram



Appendix D: Electrolyser system

PEM small pure water electrolysis hydrogen production equipment

We provide a series of Technology leading and mature PEM small pure water electrolysis hydrogen production equipment. The hydrogen capacity is from 1Nm³/h-100Nm³/h, the purity of hydrogen is $\geq 99.999\%$, the dew point is $\leq -50^{\circ}\text{C}$, and the pressure is up to 3.2MPa. This series of products integrate the world's leading and mature PEM electrolyser and optimized process treatment and electronic control system (pressure differential system and balance system), to ensure that customers have excellent performance indicators and cost-effective products and services.



Advantages

1. Super pure hydrogen

- The purity of the hydrogen is up to 99.999%

2. Product structure

- Importing from the US DuPont, ionic membrane pure water electrolysis to produce hydrogen, without any alkaline solution
- Zero polar distance, highly active SPE (PEM) catalytic electrode pairs
- Structure of repolarization multicomponent electrolyser with excellent mass transfer, heat transfer and chemical process performance

- Material selection of repolarization multicomponent electrolyser with electrochemical properties, corrosion resistance, passivation resistance, etc. superior performances

3. Product features

- Pure water electrolysis (no alkaline addition) to produce hydrogen, no corrosion, no pollution, high hydrogen purity
- The unit electrolyser voltage is low, the internal resistance of the electrolyser is small, no heat, the desiccant replacement cycle is long, and the hydrogen purity is high.
- The electrolysis current is small, but the gas production is sufficient and the pressure rise is fast (3-5 minutes).
- Hydrogen steady pressure, steady flow output, and automatic tracking with the change of gas consumption with load, automatic protection technology is complete and reliable.
- Steady pressure with high precision, water shortage, over-pressure, waterproof etc. automatic protection technologies are complete and reliable.
- Low noise (the user is using, the fan does not start basically)
- Low power consumption and High efficiency of electrolysis.
- Good sealing performance

4. Product application

- GC (gas phase) gas and carrier gas
- ELCD (conductivity detector) reaction gas
- AED (Atomic emission spectroscopic detector) reaction gas

5. Custom design

We can provide the customized design of hydrogen production equipment to optimize and integrate the existing factory facilities.

6. Safe operation

The system can monitor the security, performance and automation of the system, and allow remote monitoring and fault diagnosis.

Model	Hydrogen capacity	Hydrogen pressure	Hydrogen purity	Power
HGPS-1	1m ³ /h	≤3.2MPa	99.999%	5KW
HGPS-2	2m ³ /h	≤3.2MPa	99.999%	10KW
HGPS-5	5m ³ /h	≤3.2MPa	99.999%	25KW
HGPS-10	10m³/h	≤3.2MPa	99.999%	50KW
HGPS-15	15m ³ /h	≤3.2MPa	99.999%	75KW
HGPS-20	20m ³ /h	≤3.2MPa	99.999%	100KW

Beijing CEI Technology Co. Ltd in China

<https://bjzdfy.en.alibaba.com/?spm=a2700.details.cordpanyb.1.344470c0SxsZn6>

10Nm³/h Onsite hydrogen production electrolysis

Main Features & Options Available

- Water purification system
- 50L Purified water buffer storage tank
- Alkaline electrolysis system
- Integrated Hydrogen purification system
 - Deoxygenation to achieve up to 99.995%
 - Drier to achieve up to -45°C average dew point
- Power conditioning and control
- Multipoint active hydrogen detection
- Integration into complete turn-key solution

TECHNOLOGY & SYSTEM LAYOUT

Hydrogen is produced using state of the art alkaline electrolysis of water to produce hydrogen & oxygen gases through the use of electricity. Equipment is provided with all necessary auxiliary items to provide safe reliable onsite hydrogen production

ELECTROLYSIS TECHNICAL SPECIFICATIONS

Maximum Hydrogen Production	<i>10.66 Nm³/hour</i>
Maximum Electricity consumption / supply	<i>58 kW @ 400VAC 50Hz</i>
Transformer position	<i>Internal</i>
Control panel position	<i>Internal</i>
Production variation range	<i>20% to 100% of maximum capacity</i>
Deionised water consumption at full power	<i>9 litre/hour</i>
Hydrogen purity (before purifier)	<i>99.3%-99.8%</i>
Outlet gas dew point (before drier)	<i>Saturated at ambient temperature</i>
Outlet gas Pressure	<i>up to 12 bar</i>
Environment temperature range	<i>5-35°C</i>
Valves actuation	<i>Pneumatic</i>
Cooling system	<i>Air or Liquid</i>
Dimensions (Length X Depth X Height)	<i>950 mm X 2000 mm X 2000 mm</i>
Weight	<i>1600 kg</i>
Certification	<i>CE approved</i>
Additional Configuration Options	
<i>Parallel connection of several units to increase production capacity</i>	
<i>remote surveillance control system through Internet</i>	
<i>full service contract</i>	
<i>compression & buffer storage allowing for flexible supply independent from production</i>	
<i>purchase of 'green' electricity to eliminate CO2 emissions from the production process</i>	

Appendix E: Hydrogen gas Internal Combustion Engine

GGW50G | **5.4L** | **50kVA**
INDUSTRIAL SPARK-IGNITED GENERATOR SET
PRAMAC | Power Engineering Division



*Assembled in the USA using domestic and foreign parts

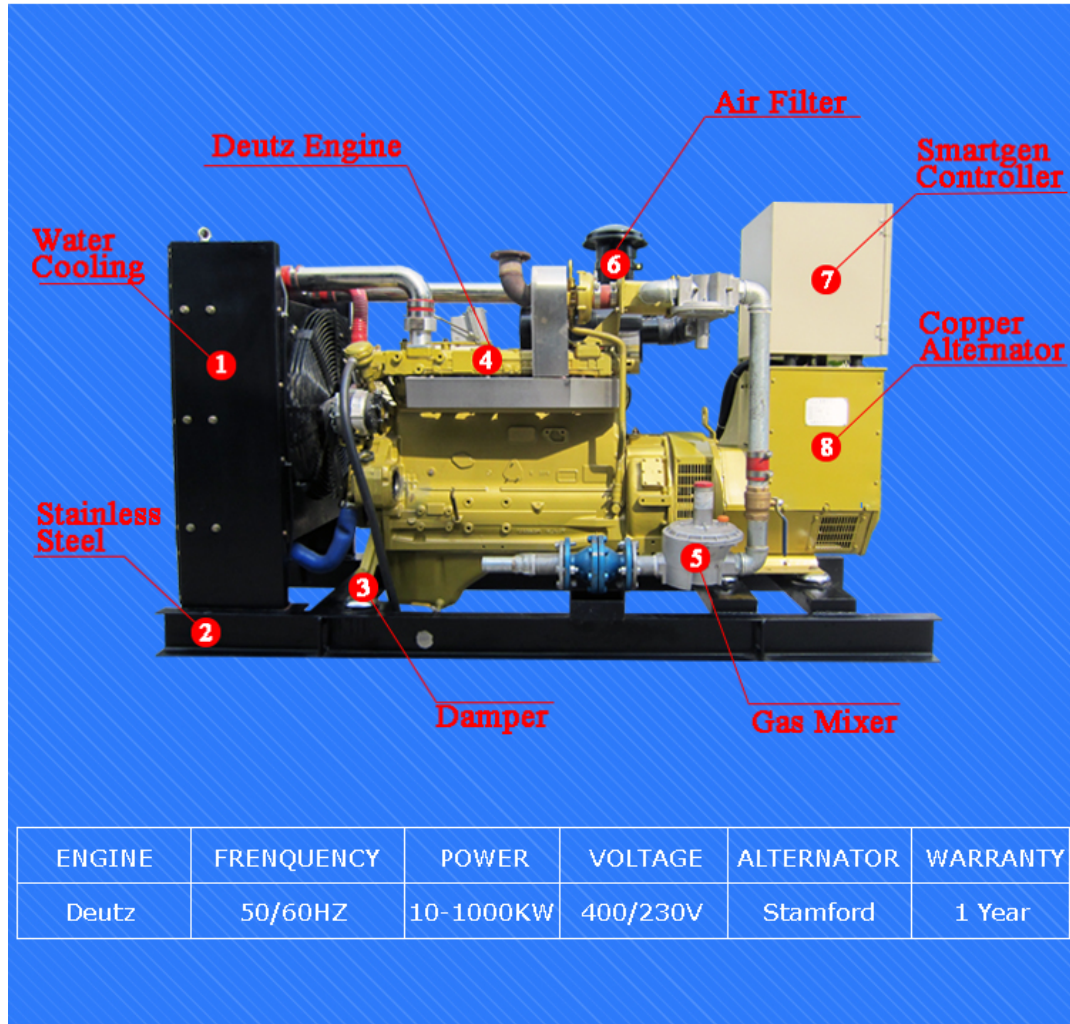


Image used for illustration purposes only

Power Ratings		
GGW50	Standby	50 kVA/40 kW
	Prime	45 kVA/36 kW

Hydrogen Gas Generator

Product Description



ENGINE	FREQUENCY	POWER	VOLTAGE	ALTERNATOR	WARRANTY
Deutz	50/60HZ	10-1000KW	400/230V	Stamford	1 Year

Product Type		Gas generator
Genset Model		LS-40GFT
Rated Power		40KW
Rated Frequency		50/60Hz
Phases Arrangement		3P4W
Rated Voltage		400V/230V
Rated Current		72A
Rated Power Factor		0.8
Engine	Engine Series	Deutz
	Engine Model	LS48-65G

	Engine Power	40kw
	Rated Speed	1500rpm/1800rpm
	Cylinder Qty	6
	Bore*Stroke	105*125mm
	Displacement	6.5L
	Air Intake Method	Natural Aspirated
	Speed Regulation	Electronic Governor
	Start Method	Electrical Starting
Alternator	Brand	Stamford
	Model	UCI224D
Dimension(L*W*H)		1850*770*1350mm
Net Weight		920kg

Weifang Ronsum Power Technology Co. Ltd

<https://ronsunpower.en.alibaba.com/?spm=a2700.details.cordpanyb.1.7b9f56a61hUqvJ>

Appendix F: Typical electrical equipment's power capacities

Typical Rated Power Capacity for Electrical Equipment's

Item	Rated Power
Mill (maize, rice etc.)	2 - 4 kW
Grain thresher (maize, sorghum, etc.)	3 - 4 kW
Huller (rice, wheat)	3 - 5 kW
Oil expeller	5 - 8 kW
Kapok mill (50 Kg/hr)	2.5 kW
Planer	0.5 - 0.75 kW
Angle grinder	0.5 kW
Drilling machine	~0.5 kW
Circular saw (200mm diameter)	0.75 kW
Band saw wheel (300mm diameter)	0.75 kW
Centre lathe (medium duty, 160mm)	0.3 - 0.4 kW
Soldering iron	0.07 kW
Battery charging	0.1 - 2 kW
Electric oven (bread, cakes etc.)	1 -25 kW
Blender/Juicer	0.3 - 0.4 kW
Mixer	0.3 - 0.4 kW
Refrigerator/Freezer	0.3 -0.4 kW
Ironing	0.3 - 0.8 kW
Incandescent bulb (25 - 100 W)	0.025 - 0.1 kW
Energy efficient lamp (brightness of a 100 W bulb)	0.012 kW